**CPUC-1000**

**Blade Report**

**I.19-06-016**

**ALJs: Hecht/Poirier**

**Date Admitted: 3/24/2021**

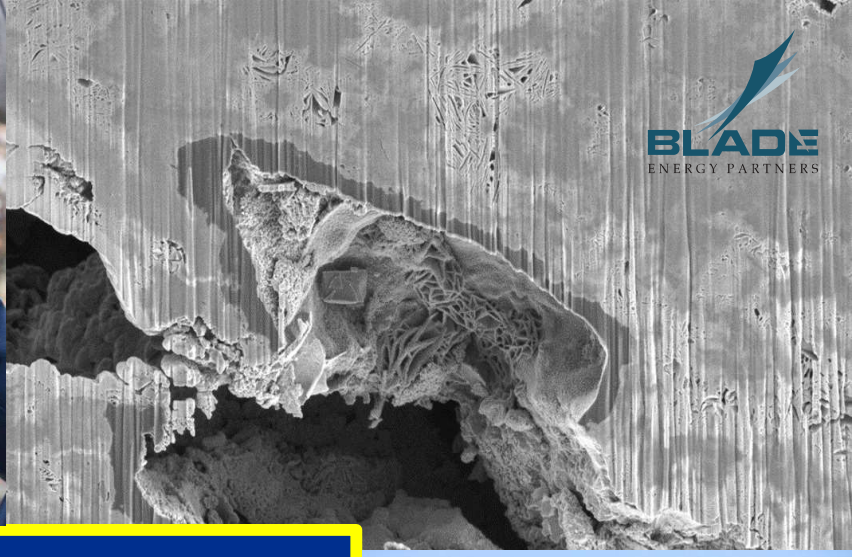

BLADE ENERGY PARTNERS

# Root Cause Analysis of the Uncontrolled Hydrocarbon Release from Aliso Canyon SS-25

May 16, 2019

# MAIN REPORT

The RCA work necessitated a substantial amount of testing, analyses, modeling, and interpretations. All of the technical details and discussions are provided in four volumes of supplementary reports. The integrated work is reflected in this Main Report.

# MAIN REPORT

**Root Cause Analysis of the Uncontrolled Hydrocarbon Release from Aliso Canyon SS-25**

# SUPPLEMENTARY REPORTS

## Volume 1: Approach

- Phase 0 Summary
- Phase 1 Summary
- Phase 2 Summary
- Phase 3 Summary
- Phase 4 Summary

## Volume 2: SS-25 Well Failure Causes

- SS-25 Casing Failure Analysis
- SS-25 7 in. Speedtite Connection Testing and 11 3/4 in. STC Assessment
- SS-25 Analysis of Microbial Organisms on 7 in. Production Casing
- SS-25 7 in. Casing Internal Corrosion Assessment
- SS-25 Inspection Log Analyses
- SS-25 Temperature, Pressure, and Noise Log Analysis
- Aliso Canyon Field: Hydrology
- SS-25 Geology Summary
- SS-25 7 in. Casing Load Analysis
- SS-25 Tubulars NDE Analyses
- SS-25 Annular Flow Safety System Review

## Volume 3: Post-SS-25 Leak Events

- SS-25 Nodal Analysis with Uncontrolled Leak Estimation
- Aliso Canyon Injection Network Deliverability Analysis Prior to Uncontrolled Leak
- Analysis of the Post-Failure Gas Pathway and Temperature Anomalies at the SS-25 Site
- SS-25 Transient Well Kill Analysis

## Volume 4: Aliso Canyon Casing Integrity

- Analysis of Aliso Canyon Wells with Casing Failures
- Aliso Canyon Shallow Corrosion Analysis
- Aliso Canyon Surface Casing Evaluation
- Review of the 1988 Candidate Wells for Casing Inspection
- Gas Storage Well Regulations Review
- Aliso Canyon Field Withdrawal/Injection Analysis
- Aliso Canyon: Regional and Local Seismic Events Analysis

# SS-25 RCA Main Report

# Root Cause Analysis of the Uncontrolled Hydrocarbon Release from Aliso Canyon SS-25

**Purpose:**
Root Cause Analysis Report

**Date:**
May 16, 2019


**2600 Network Boulevard, Suite 550**
**Frisco, Texas 75034**

**+1 972-712-8407 (phone)**
**+1 972-712-8408 (fax)**

**16285 Park Ten Place, Suite 600**
**Houston, Texas 77084**

**1-800-319-2940 (toll free)**
**+1 281-206-2000 (phone)**
**+1 281-206-2005 (fax)**

**www.blade-energy.com**

# Executive Summary

The Standard Sesnon 25 (SS-25) well was shut in at 3:30 PM on October 23, 2015; a leak was discovered at 3:15 PM. The 7 in. production casing had axially ruptured and circumferentially parted. This resulted in a blowout and gas release into the atmosphere, which lasted for 111 days, until the well was eventually killed via a relief well on February 11, 2016.

SS-25 was drilled as an oil well in 1954. After the oil was considered depleted, SS-25 was converted to a gas storage well in 1973. Operationally, there were some key differences between the use of SS-25 in oil production mode and in gas storage mode. As an oil well, the oil was produced through a tubing string; the primary mechanical barrier to the oil was the tubing, and the secondary one was the casing; the pressure load decreased through the life of the oil well due to depletion of the oil. As a gas storage well, the gas was injected and withdrawn through the tubing and the casing, making the casing the primary barrier for the gas during gas storage operations. Operating pressure loads remained the same or at similar levels despite annual and seasonal variations caused by gas demand through the life of the well.

Pressure tests were conducted on the SS-25 casing in 1973 during the well's conversion from oil production to gas storage. The well's integrity was monitored using yearly temperature logs and occasional noise logs. If a leak in the casing had occurred, then the casing would have locally cooled, and consequently the temperature would have deviated at the leak location. The SS-25 temperature and noise logs had never shown an anomaly related to casing integrity. Pressure measurements, which were collected at SS-25 weekly, had not indicated a leak or failure prior to the incident. Well integrity issues went undetected until the leak event of October 23, 2015.

The Aliso Canyon storage wells had numerous casing leaks. Blade reviewed 124 gas storage wells and identified 63 casing leaks, 29 tight spots, 4 parted casings, and 3 other types of failures. Based on the data available to Blade, no details regarding the nature or cause of these leaks and failures were available because no failure analyses were done. Forty percent of the gas storage wells reviewed by Blade had casing failures with an average of two casing failures per well. The FF-34A well file mentioned a study of the possible external casing corrosion problems in the southeastern portion of the field, but Blade was not able to locate any documentation related to this study [1].

In addition, two Aliso Canyon wells had underground blowouts from casing leaks: Frew-3 in 1984 and FF-34A in 1990. These wells were successfully killed by pumping fluid down the tubing, and the consequences of a larger leak or a near-surface casing rupture were not anticipated until the SS-25 event.

Southern California Gas Company (SoCalGas) had a two-year plan in 1988 to determine the mechanical condition of the casing in 20 wells originally completed in the 1940s and 1950s. The wells, including SS-25, were prioritized based on gas deliverability, operational history, and length of time since their last workover. SS-25 was given a low priority. Of the 20 wells, SoCalGas ran inspection logs in 7 wells within the 2 year plan window. The inspection logs showed metal loss indications on the outside diameter (OD) of the casing ranging from 20% to 60% of wall thickness in 5 of the 7 wells logged from 1988 to 1990. Some of the wells had indications above the surface casing shoe, and many had indications below the casing shoe. Blade found no documentation indicating that investigations into the causes of external corrosion on any of these wells were ever conducted. SS-25 was never logged as part of this 1988 program or at any other time.

The approach to well integrity at Aliso Canyon had been reactive rather than proactive. The data collected by Blade supports this assessment, which was also SoCalGas's conclusion in the General Rate Case (GRC) submission in 2014. SoCalGas proposed a six-year Storage Integrity Management Program (SIMP) in 2014

to "proactively identify and mitigate potential storage well safety and/or integrity issues before they result in unsafe conditions for the public or employees [2]."

Based on Blade's Root Cause Analysis (RCA), a direct cause of the SS-25 incident was outside surface corrosion of the 7 in. production casing. The injection gas was of pipeline quality and dry, and the withdrawn gas was undersaturated (that is, water never condensed); therefore, no significant internal corrosion in the 7 in. casing had occurred; the casing was corroding from the outside as a result of contact with groundwater.

Surface runoff water permeates the ground and follows fractures and faults to various depths. At the SS-9 location (approximately 600 ft away from SS-25) groundwater was observed at depths above 400 ft and below 900 ft. Except for runoff water, there are no other sources of groundwater at Aliso Canyon.

In the SS-25 well, the groundwater displaced the drilling fluid over a period of time and caused the 7 in. production casing to corrode from the outside. This groundwater and microbes—likely methanogens, a form of Archaea—caused the corrosion. Some of the 7 in. casing connections were seeping gas to the outside of the casing. The carbon dioxide in the gas was likely a nutrient for the methanogens. The corrosion patch at 892 ft was 9.25 in. in length and contained grooves from tunnels created by the microbes that coalesced over a period of time. The corrosion removed 85% of the wall thickness in a smaller patch of 2.13 in. within the larger 9.25 in. corroded region.

The shallow groundwater above 400 ft accessed the poorly cemented 11 3/4 in. surface casing and caused localized corrosion on the surface casing OD.

On the morning of October 23, 2015, SS-25 started injecting gas between 3 and 4 AM, and the pressure slowly climbed as gas was being injected. The injection pressure at the wellhead was around 2,700 psi. Sometime after the injection had started, the 7 in. casing bulged and then ruptured axially. The grooves within the corrosion patch acted as stress concentrators, resulting in the axial rupture. At this point, Blade estimates that around 160 MMscf/D gas, originating from both the injection network and the storage reservoir, was flowing through the axial rupture region. The gas flowing through the axial rupture on the 7 in. production casing caused an increase in pressure on the 11 3/4 in. surface casing. This caused several of the surface casing corroded regions to fail, creating holes and thus providing a pathway for gas to escape. Over 50 such holes provided a pathway for the gas to surface.

As the gas continued to expand through the axial rupture, the temperature continued to decrease locally, reducing the casing material toughness. Within hours of the axial rupture, the 7 in. casing circumferentially cracked adjacent to the axial rupture region, which then connected with the axial rupture and then parted. This circumferential parting likely occurred between 7 and 8 AM on October 23, 2015, when the injection gas temperature was the coldest that day. The leak was detected at 3:15 PM of the same day, October 23, 2015.

SS-25 was shut in at 3:30 PM, and it was realized that the well was still flowing gas. Using the immediately available production and surface casing annuli and tubing pressure measurements, Blade estimated the flow rate to be at 91 MMscf/D at the time. Subsequently, Blade used a more sophisticated model to estimate the flow rate from the historical SS-25 flow test data, and arrived at 93 MMscf/D.

On October 24, 2015, the first kill attempt (kill attempt #1) was performed by pumping down the tubing but was unsuccessful. SoCalGas contracted a well-control company to provide technical and operational support for the subsequent six kill attempts in November and December, 2015, which were also unsuccessful.

Based on the data reviewed by Blade, the well-control company appeared to have designed the kill attempts solely by calculating a kill fluid density that was higher than the static bottom hole pressure [3]. Kill operations where a fluid is being pumped into a well while the gas is escaping at a high rate requires a detailed transient model to define the operational parameters.

Blade conducted detailed modeling and used the more accurate estimate of flow rate and concluded that a fluid weight of 12 ppg or higher at pump rates of 10 bpm or higher would have successfully controlled the well as early as November 13 or 14, 2015. Instead, a variation of the same kill attempt design with the fluid densities of around 9.4 ppg and pump rates of around 5 to 13 bpm were utilized for kill attempts #2 through #6. Meanwhile, the well site deteriorated with the continued flow of gas. Blade reviewed all the available data and concluded that no transient modeling was done when designing these kill attempts, contributing to the lack of success in the kill attempts. The data indicated that the well flow rate had been significantly underestimated. Finally, for kill attempt #7, transient modeling was conducted, the density was increased to 15 ppg and the well appeared to be briefly under control. However, there were operational issues that required this kill attempt to be terminated early.

The uncontrolled release of hydrocarbon gas for 111 days resulted from many different causes. To evaluate these causes, upon completion of the technical analyses, the root cause was investigated in a structured fashion using the Apollo RCA Methodology.

Direct causes, including contributing ones, are those that, if identified and prevented, would eliminate the occurrence of an SS-25 type of incident (or similar). Root causes are those that, if identified and prevented, would avert an SS-25 type of incident and all other types of well integrity incidents through the use of procedures, best practices, design, management systems, and regulations. The investigation of the SS-25 incident identified direct causes and root causes.

The direct causes for the uncontrolled release of hydrocarbons for 111 days from SS-25 were:

- Axial rupture due to external microbial corrosion on the 7 in. casing OD caused by the groundwater.
  - Groundwater accessed the 11 3/4 in. x 7 in. annulus and provided an environment conducive to microbial corrosion.
  - Carbon dioxide, a component of natural gas, seeped through the 7 in. casing connections and was likely a nutrient for the microbes.
- Unsuccessful top-kills because of insufficient kill fluid density and pump rates.
  - Transient kill modeling was not performed for the first six kill attempts.
  - Gas flow rates from the well were not estimated or used in engineering the kill attempts.

The root causes for the uncontrolled release of hydrocarbons for 111 days from SS-25 were:

- The lack of detailed follow-up investigation, failure analyses, or RCA of casing leaks, parted casings, or other failure events in the field in the past. There had been over 60 casing leaks at Aliso Canyon before the SS-25 incident, but no failure investigations were ever conducted. Furthermore, external corrosion on production casing had been identified in several wells. Based on the data reviewed by Blade, no investigation of the causes was performed, and, therefore, the extent and consequences of the corrosion in the other wells were not understood.
- The lack of any form of risk assessment focused on wellbore integrity management. This included assessment of qualitative probability of production casing leaks or failures. By extension, the potential consequences of production casing failures or surface blowouts had not been assessed.

- The lack of a dual mechanical barrier system in the wellbore. The 7 in. OD production casing was the primary barrier to the gas.
- The lack of internal policy and regulations that required production casing wall thickness inspections. The existing regulations were inadequate at the time. Annual temperature logging and weekly pressure measurements are adequate to detect leaks and fix them only after an event has occurred. In SS-25, the corrosion patch was large (around 9.25 in. in length), and due to the microbial nature, the grooves within the corrosion patch acted as stress concentration locations. Consequently, when the corrosion region failed, it resulted in a rupture that was about 2 ft long. The trailing indicators of these failures were not adequate to manage the failures. Methodologies such as periodic wall thickness measurements were necessary.
- The lack of a well-specific, well-control plan that considered transient kill modeling or well deliverability. There was no quantitative understanding of well deliverability, although data were available, and well-established industry practices existed for such analysis.
- The lack of understanding of groundwater depths relative to the surface casing shoe and production casing, until the two groundwater wells were drilled at SS-9 in 2018.
- The lack of systematic practices of external corrosion protection for surface casing strings. The consequences of corroded surface casings and uncemented production casings were therefore not understood.
- The lack of a real-time, continuous pressure monitoring system for well surveillance. This prevented an immediate identification of the SS-25 leak and accurate estimation of the gas flow rate.

The roles of safety culture, operational and technical resources, and other organizational issues were also investigated as part of the RCA. Information about the SoCalGas's historical organizational structures and departmental and job function roles and responsibilities was limited. The lack of data and evidence prevented Blade from making any direct correlation to causes of the SS-25 incident. However, the approach to well integrity management, GRC submissions, and other information gleaned during this investigation allows one to infer a possible impact from the organizational structure and resources.

The histories of 124 gas storage wells were analyzed, and 40% of them evidenced wellbore integrity issues. The relevant operations standards related to gas storage were assessed with respect to wellbore integrity. The integrity procedures were reactive and were not updated.

Blade reviewed the 2007 testimony for SoCalGas's 2008 GRC [4]. Costs and details were outlined related to reservoir engineering studies, additional personnel, technological advances, and well expenses. SoCalGas cited that over a 15-year period, the number of gas storage specialists reduced from 10 to 4 for unspecified reasons, and the company "experienced a significant decline in its ability to assess the performance of individual wells due to the lack of recent data." In 2007, SoCalGas requested two additional specialists. Unlike robust transmission pipeline integrity and distribution pipeline integrity programs, there was no such focus on well integrity. This was also supported by the SoCalGas's GRC submission in 2012 [5]. SoCalGas was perhaps inadequately resourced to manage Aliso Canyon prior to the 2015 incident, but because detailed data on resourcing was not available, the lack of resources was not identified as a root cause.

The current SoCalGas well integrity practices and regulations from the Division of Oil, Gas, and Geothermal Resources (DOGGR) address most of the root causes identified during this investigation. SoCalGas has adopted the SIMP and operationally executed it for the Aliso Canyon field following the SS-25 incident. Further, DOGGR has adopted regulations that address many of the root causes.

# Table of Contents

# List of Figures

# List of Tables

# 1 Background and Approach

At 3:15 PM on October 23, 2015, a leak was discovered in SS-25. Following the discovery of the leak, the injection header valve was closed, and the well was shut in at 3:30 PM. The casing pressure dropped to 270 psi, and the surface safety valve (SSV) on the casing automatically closed. The SSV low set point was at 300 psi. The sound of gas flow was observed at the wellhead. The initial cause had been thought to be a leak in the wellhead seal between the 7 in. production casing and the 11 3/4 in. surface casing. The well was leaking gas somewhere below the wellhead. The pressures recorded then were: tubing pressure—1,700 psi, production casing pressure—270 psi, and surface casing pressure—140 psi.

On October 24, 2015, kill attempt #1 was undertaken—11.8 bbl of 10 ppg polymer brine were pumped down the tubing. The pressure rose to 3,500 psi. The pumping through the tubing was shut down. Eighty-nine bbl of 8.6 ppg brine were pumped down the 7 in. production casing annulus, and operators observed that fissures had begun to form in the ground around the wellhead site and that gas was venting at the surface. This kill attempt was shut down.

A well-control company arrived onsite on October 25, 2019. Kill attempt #2 was undertaken on November 13, 2015. At a maximum pump rate of 8 bpm, 6 bbl of 10.8 ppg $CaCl_2$ and approximately 703 bbl of 9.4 ppg $CaCl_2$ were pumped down the tubing, upon which a vent opened 20 ft from the wellbore and shot debris nearly 75 ft in the air. Gas leaked around the surrounding hillside. The DOGGR notes state that on November 13, 2015, “the well blew out in a conventional sense [6].” The consideration of drilling a relief well began at this point.

Kill attempt #3 occurred on November 15, 2015, and kill attempt #4, on November 18, 2015. These kill attempts included 18 ppg barite pills. The pump rates ranged from 8 to 9 bpm. Gas rate from the fissures on the surface appeared to have increased on November 15, 2015. On November 18, 2015, the gas rate appeared to have further increased from fissures, and barite at the surface was reported for the first time.

A crater started forming during kill attempt #3. Gas and brine flow from surface fissures increased during these kill attempts. The crater increased in size during subsequent kill attempts.

Kill attempt #5 was undertaken on November 24, 2015. The 9.4 ppg fluid was pumped at 5 bpm; however, 8.34 ppg fresh water was pumped at rates approaching 13 bpm, followed by an 18 ppg barite pill. Gas flow continued to increase from the crater. Kill attempt #6 on November 25, 2015, was similar in nature to kill attempt #5, with a lost circulation material pill (LCM) instead of a barite pill. As the crater size increased, gas flow rates also appeared to increase.

Kill attempt #7, which was distinctly different from the other kill attempts, was executed on December 22, 2015. A much heavier density fluid was used: 15 ppg water-based drilling fluid at pump rates approaching 5.8 bpm. This kill attempt appeared to have briefly controlled the leak; however, the wellhead was rocking, and the kill attempt was stopped. The crater grew wider and deeper.

The drilling of a relief well was started on December 04, 2015. The relief well successfully controlled SS-25 on February 11, 2016.

SS-25 had flowed uncontrollably for 111 days, and approximately 6.6 BCF of natural gas had leaked.

## 1.1 Report Structure

This RCA report is broken into four major sections:

- SS-25 Well Failure Causes—This section focuses on the cause of the failure of the well. The various factors that contributed to the failure of the wellbore as well as the sequence and timing of all the failure events are identified here.
- SS-25 Post-Leak Events—This section focuses on the events following the discovery of the leak on October 23, 2015. The well deliverability is quantified just prior to and after the leak until the well was under control. The pathway of the gas after the failure is delineated. The kill attempts are modeled and analyzed for their effectiveness, and alternative options are quantified.
- Aliso Canyon Casing Integrity—This section focuses on analyzing casing failure history during the storage operational period of the field. The internal memos that discussed casing inspection and the rate case data on casing integrity are reviewed and analyzed. Post-2016 inspection log data are reviewed for the extent of shallow corrosion in the field. Gas storage regulations that existed during the SS-25 operations and their impact on integrity are discussed.
- Root Cause: Approach and Results—This section focuses on identifying root causes and mitigations by using Apollo RCA, a structured causal analysis process, and the results of this study.

This RCA work necessitated a substantial amount of testing, analyses, modeling, and interpretations. The integrated work is reflected in this Main Report. Additionally, all the technical details and discussions are provided in supplementary reports—the source documents for this RCA report—in four volumes as follows:

Volume 1: Approach

a. Phase 0 Summary
b. Phase 1 Summary
c. Phase 2 Summary
d. Phase 3 Summary
e. Phase 4 Summary

Volume 2: SS-25 Well Failure Causes

a. SS-25 Casing Failure Analysis
b. SS-25 7 in. Speedtite Connection Testing and 11 3/4 in. STC Assessment
c. SS-25 Analysis of Microbial Organisms on 7 in. Production Casing
d. SS-25 7 in. Casing Internal Corrosion Assessment
e. SS-25 Inspection Log Analyses
f. SS-25 Temperature, Pressure, and Noise Log Analysis
g. Aliso Canyon Field: Hydrology
h. SS-25 Geology Summary
i. SS-25 7 in. Casing Load Analysis

j. SS-25 Tubulars NDE Analyses

k. SS-25 Annular Flow Safety System Review

Volume 3: Post-SS-25 Leak Events

a. SS-25 Nodal Analysis with Uncontrolled Leak Estimation

b. Aliso Canyon Injection Network Deliverability Analysis Prior to Uncontrolled Leak

c. Analysis of the Post-Failure Gas Pathway and Temperature Anomalies at the SS-25 Site

d. SS-25 Transient Well Kill Analysis

Volume 4: Aliso Canyon Casing Integrity

a. Analysis of Aliso Canyon Wells with Casing Failures

b. Aliso Canyon Shallow Corrosion Analysis

c. Aliso Canyon Surface Casing Evaluation

d. Review of the 1988 Candidate Wells for Casing Inspection

e. Gas Storage Well Regulations Review

f. Aliso Canyon Field Withdrawal/Injection Analysis

g. Aliso Canyon: Regional and Local Seismic Events Analysis

## 1.2 Aliso Canyon SS-25

SS-25 is a gas storage well located in the Standard Sesnon lease of the Aliso Canyon field. Figure 1 shows the location of the Aliso Canyon field relative to the Porter Ranch neighborhood. The field is located in the foothills of the Oat Mountain northwest of Porter Ranch, which is a neighborhood in Los Angeles County approximately 30 miles northwest of downtown Los Angeles.

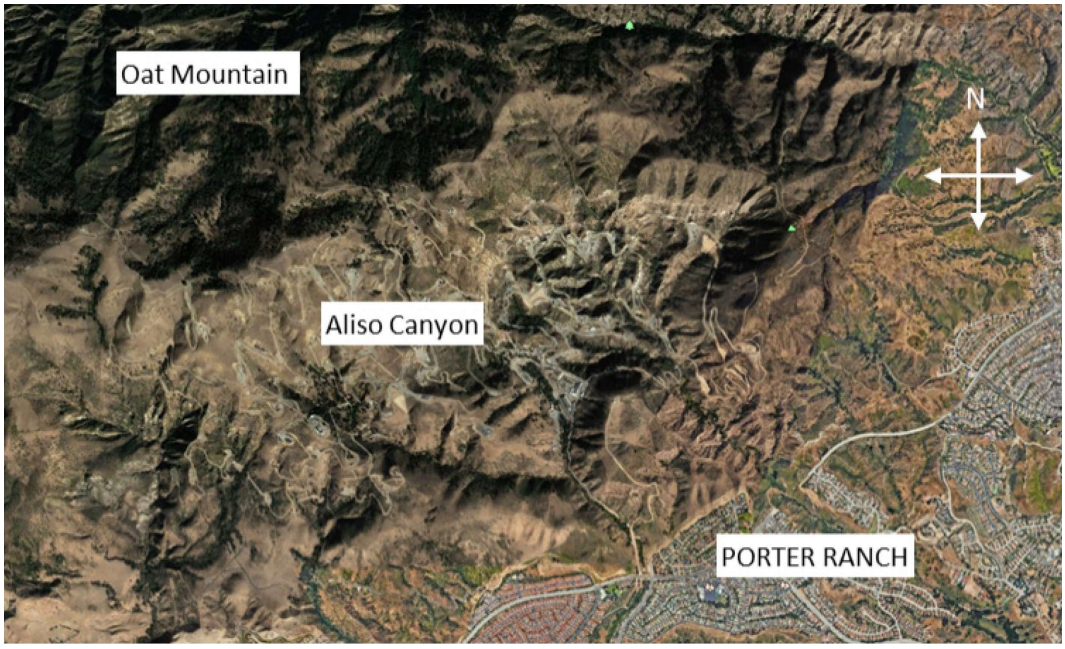


**Figure 1: Aliso Canyon Gas Field Location**

Aliso Canyon had approximately 119 active or idle gas wells at the time of the blowout. Figure 2 shows a map of the SS-25 well site and surrounding wells. The white box in Figure 2 identifies the SS-25 well site location. The area immediately surrounding SS-25 contains wells from the Porter (P), Porter Sesnon (PS), and Standard Sesnon (SS) leases; the yellow dots are SS wells, and the green dots are P wells. The SS-25 well site contains three wells: SS-25, SS-25A, and SS-25B. These wells are located in close proximity to one another on top of a knoll.

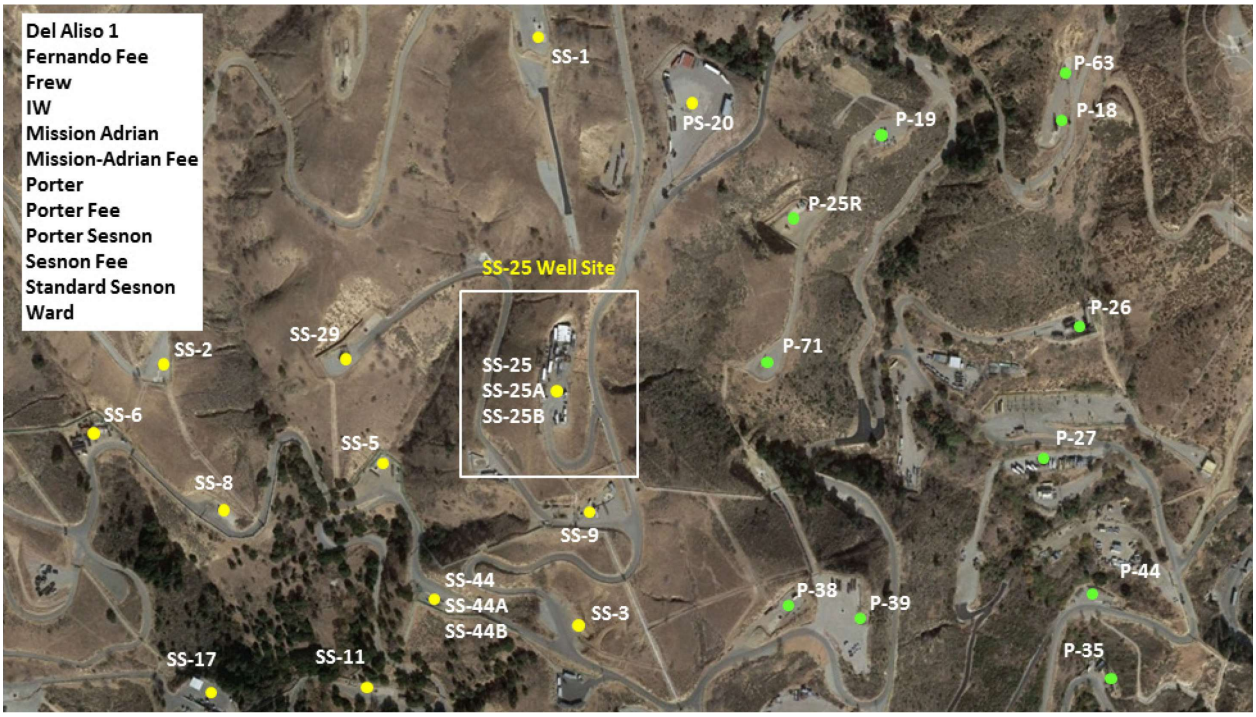


**Figure 2: 2D Map Showing the SS-25 Well Site and Surrounding Wells**

Gas storage operations in Aliso Canyon are conducted only by SoCalGas. During injection, gas is injected into the Sesnon-Frew zone through injection wells. During withdrawal, gas is withdrawn (produced) through withdrawal wells.

SoCalGas has divided the field into east, central, and west sectors based on the injection and withdrawal facility networks (Figure 3) [7]. SS-25, the incident well, is located in the west sector.

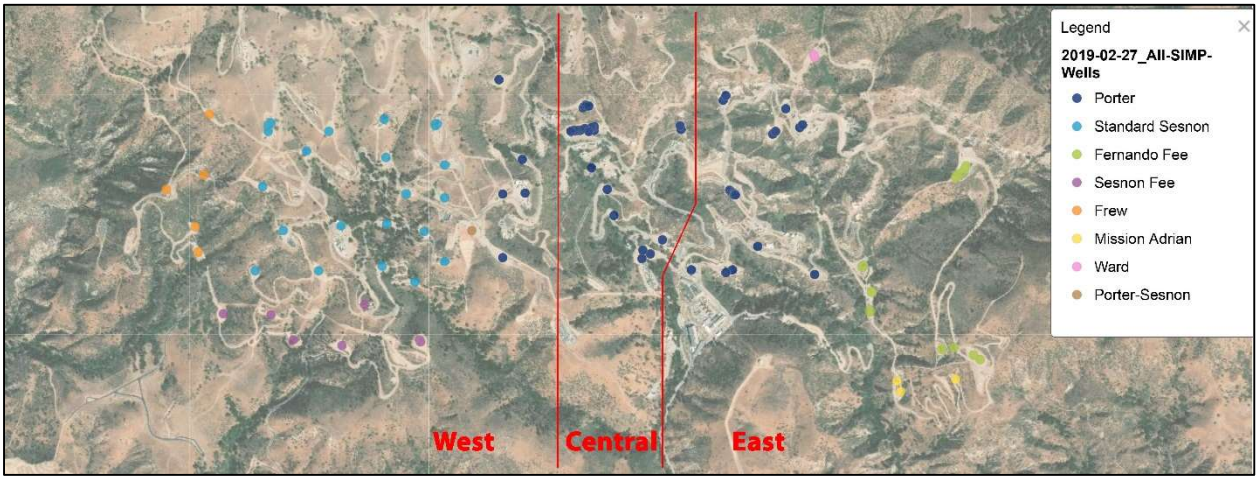


**Figure 3: Aliso Canyon Field (with East, Central, and West Sectors)**

There were 119 active or idle and 12 plugged and abandoned (P&A'd) gas storage wells (Table 1) in October 2015. In addition, there were nearly 65 conventional and 12 water injection wells. The gas storage wells were mainly of two vintages:

- Wells drilled between 1938 and 1955, when the Aliso Canyon field was first developed
- Wells drilled between 1971 and 1985, when the Sesnon-Frew zone was converted from conventional oil operations to gas storage (Figure 4)

A few newer wells were drilled in the 1990s and 2000s. (Figure 4)

**Table 1: Ages of Wells (in Years) to October 2015 in the Aliso Canyon Field**

| Wells | Gas Storage | Conventional Production | Water Injection |
|---|---|---|---|
| **Active/Idle Wells** | | | |
| Count (number) | 119 | 65 | 12 |
| Median Age (years) | 43 | 63 | 65 |
| Oldest Age (years) | 77 | 78 | 76 |
| **P&A Wells** | | | |
| Count | 12 | 17 | 0 |
| Median Age at P&A | 41 | 41 | - |
| Youngest Age at P&A | 33 | 2 months | - |
| Oldest Age at P&A | 48 | 61 | - |

The median age of the gas storage wells is 43 years, and the oldest gas storage well is 77 years old (Table 1). For the P&A'd wells, the age at abandonment ranged from 33 to 48 years, with a median value of 41 (Table 1, Figure 5). SS-25 was spudded in October 1953 and was 62 years old at the time of the incident in October 2015.

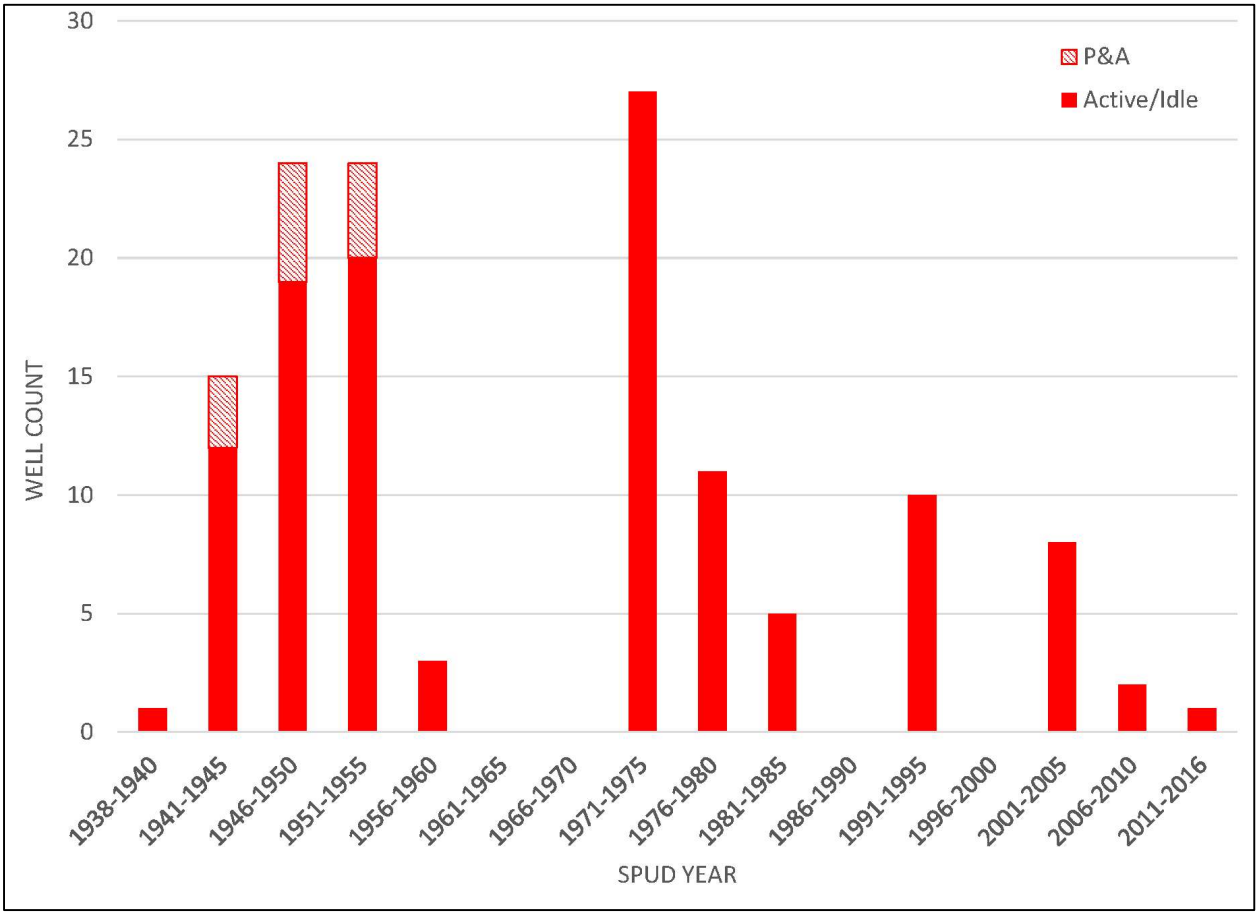


**Figure 4: Drilling History of Gas Storage Wells**

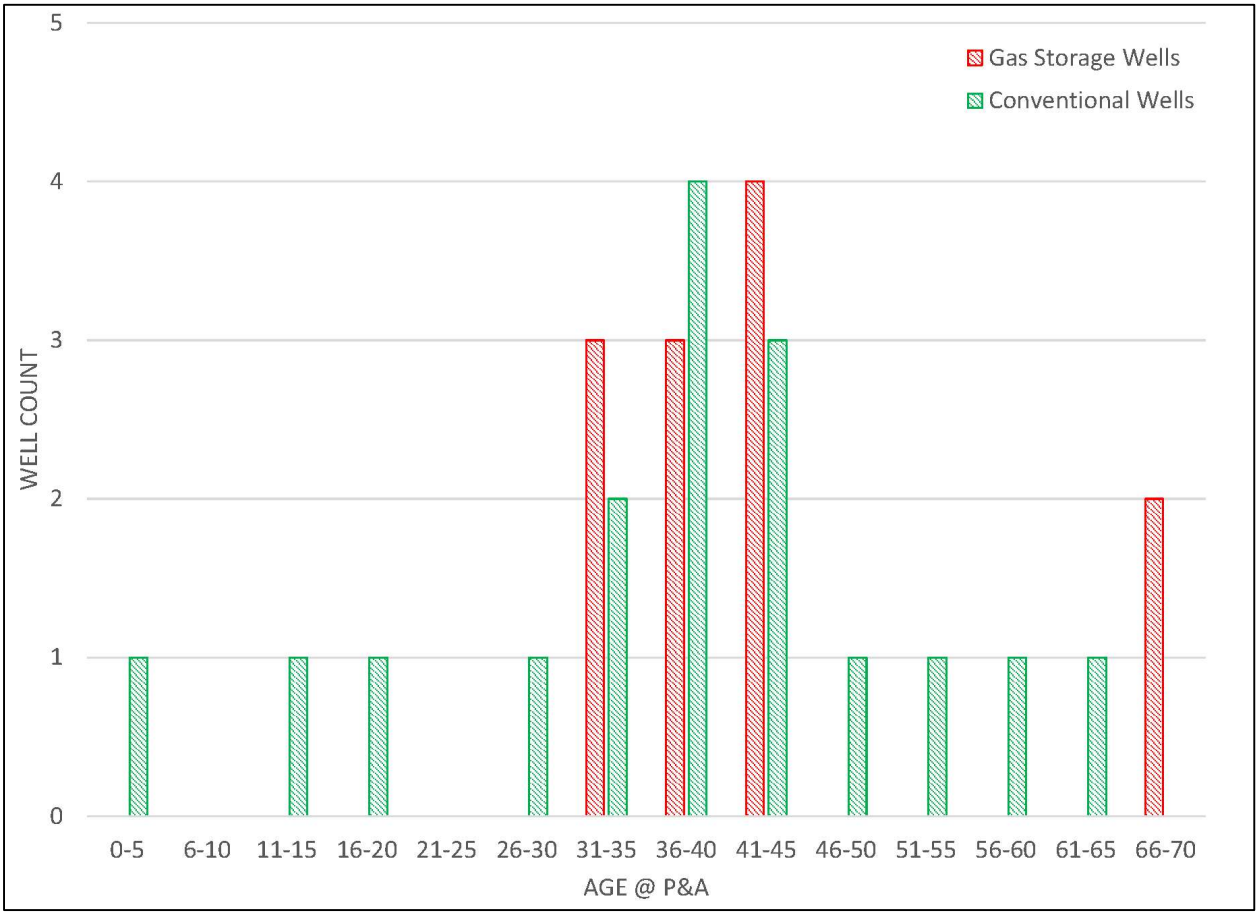


**Figure 5: Plug and Abandon History of Wells**

Over the life of Aliso Canyon Gas Storage field, the number of wells used for gas storage had varied between 83 and 108, with a median value of 99 (Figure 6). On average, about 60% of the wells were used for both injection and withdrawal, and 40% were used for withdrawal only. Except for 1977, at the beginning of the gas storage operations, very few wells were dedicated to injection. The number of active and inactive wells fluctuated through the life of the field. The number of wells discussed in various sections of this report may vary and reflect the timing of the source data and the source itself.

As Figure 6 shows, for a given year, a well is designated as:

- *Injection Only* if its injected gas volume is greater than zero and its withdrawn gas volume is zero for that year.
- *Withdrawal Only* if its injected gas volume is zero and its withdrawn gas volume is greater than zero for that year.
- *Injection & Withdrawal* if both its injected and withdrawn gas volumes are greater than zero for that year.
- *Idle/Unused* if both its injected and withdrawn gas volumes are zero for that year (not shown in Figure 6).

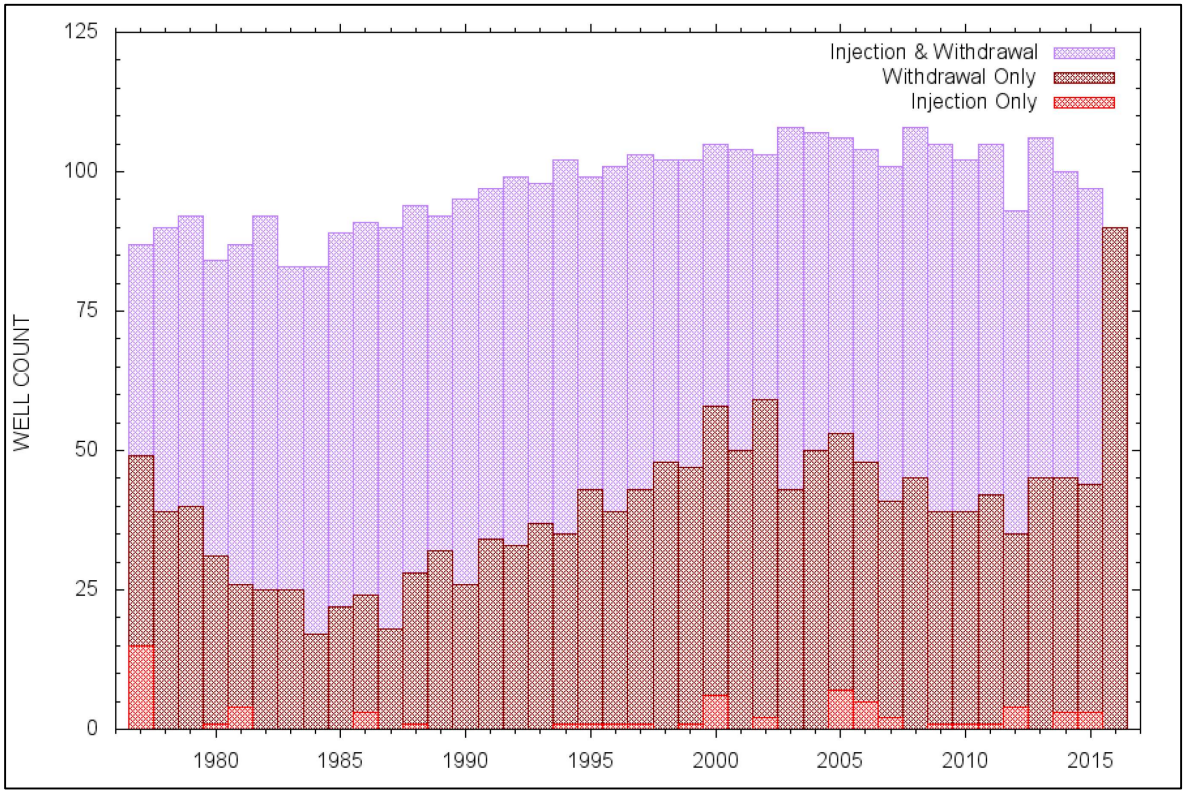


**Figure 6: Gas Storage Well Types**

A well's designation may change from year to year. At the time of the incident, 1,895 Bscf (billion standard cubic feet) of gas had been injected, and 1,805 Bscf of gas had been withdrawn from the gas storage zone since 1977 (Table 2). In addition, 4.04 MMstb (million standard barrels) of oil and 4.67 MMstb of water had been co-produced along with the withdrawn gas, resulting in an overall oil-to-gas ratio (OGR) of 2.24 stb/MMscf and an overall water-to-gas ratio (WGR) of 2.58 stb/MMscf.

The data indicate an imbalance between the geographical distribution of injection and withdrawal volumes. The gas is mostly injected in the east and central sectors, which account for 50% and 33% of the total injection, respectively. The east, central, and west sectors account for 40%, 20%, and 40% of the withdrawn gas volumes, respectively; therefore, gas is withdrawn more evenly. This suggests that a net migration of gas from the east to the west occurs within the storage zone.

In addition, the data indicate that OGR and WGR increase from the east to the west.

**Table 2: Gas Storage Injection and Withdrawal Volumes (January 1977–October 2015)**

| Sector | Totals | | | | | OGR (stb/ MMscf) | WGR (stb/ MMscf) |
|---|---|---|---|---|---|---|---|
| | Injected Gas (Bscf) | Withdrawn Gas (Bscf) | Net Injection (Bscf) | Oil (MMstb) | Water (MMstb) | | |
| East Sector | 937.3 | 705.2 | +232.1 | 0.89 | 1.19 | 0.76 | 0.84 |
| Central Sector | 639.6 | 393.8 | +245.8 | 0.30 | 0.33 | 1.27 | 1.69 |
| West Sector | 318.5 | 706.2 | –387.7 | 2.85 | 3.15 | 4.04 | 4.45 |
| **Field Total** | **1,895.4** | **1,805.2** | **+90.2** | **4.04** | **4.67** | **2.24** | **2.58** |

Figure 7 shows the annual injection-withdrawal cycle. Gas is injected for about 8–9 months (February to October) and withdrawn for 3–4 months (October to February). This pattern varies slightly from year to year, which presumably depends on the weather.

Year-to-year gas inventory increased between 1995 and 2010 and has since remained steady. Since 2005, every third winter has seen higher withdrawal volumes than the previous two.

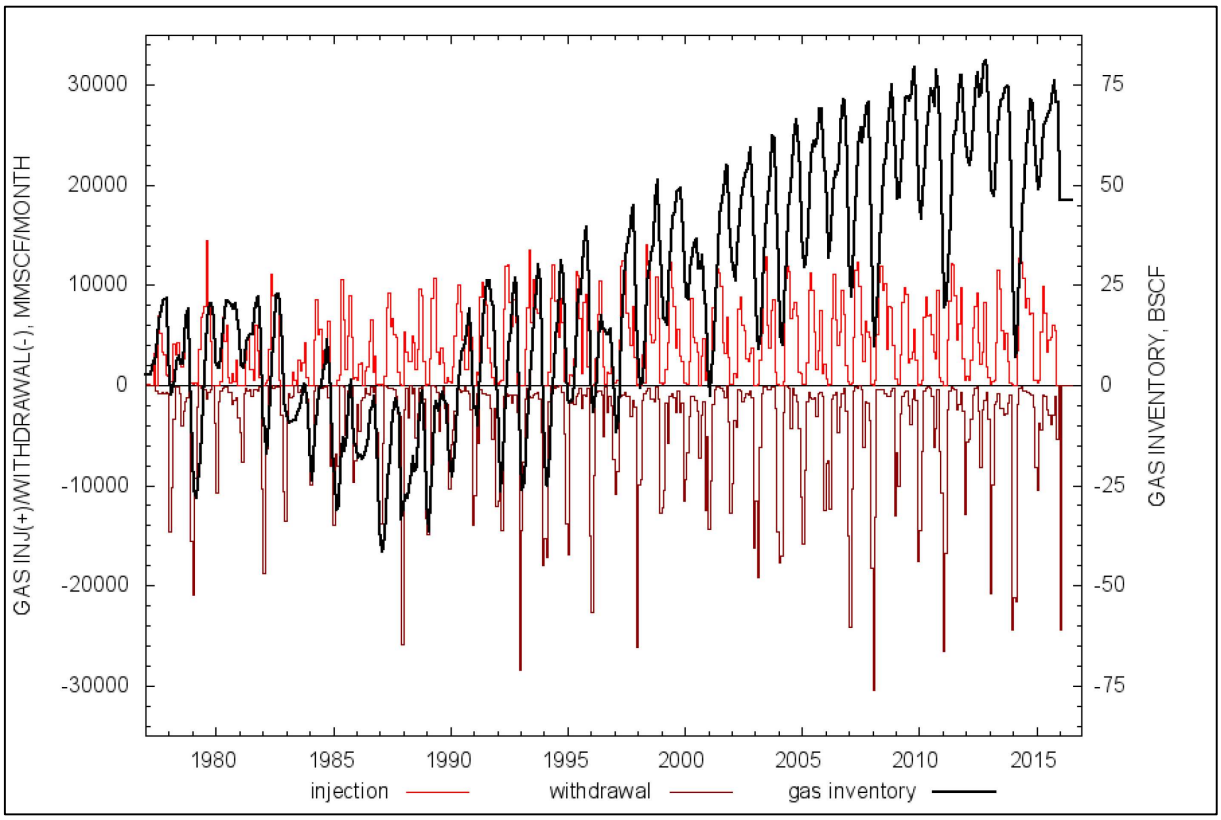


**Figure 7: Gas Storage Operations (1977–2016)**

The SS-25 incident occurred during the end of the injection season, on October 23, 2015. Estimated working inventory in the field was 75 Bscf (Figure 8). This was close to, but below, the highest historical working inventory of 81 Bscf recorded in December 2012.

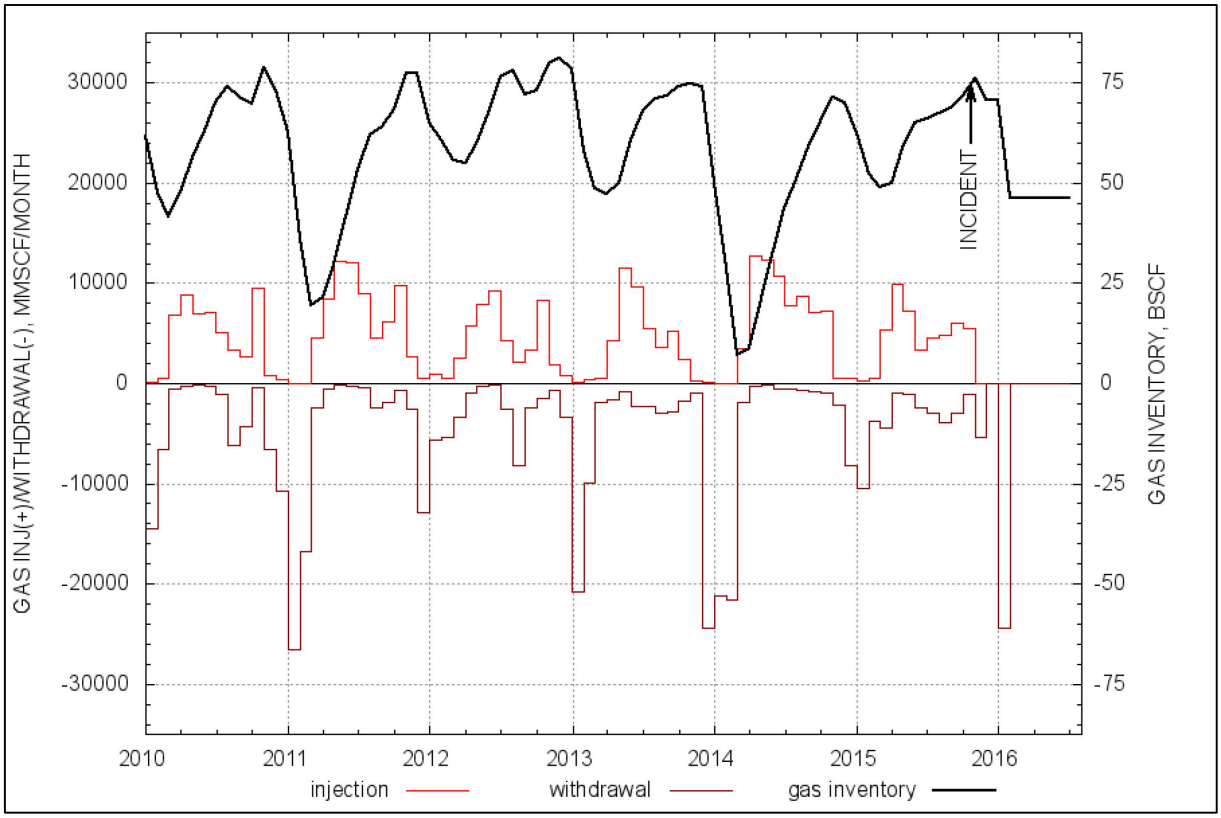


**Figure 8: Gas Storage Operations (2010–2016)**

## 1.3 Root Cause Analysis Approach

The RCA began on January 29, 2016. Prior to the successful intervention by means of the relief well, gas samples were collected from SS-25 on February 04, 2016, and assessed for carbon dioxide and hydrogen sulfide concentrations.

An RCA is a systematic process for identifying the root causes of problems or events and defining methods for responding to and preventing them. A major incident or failure rarely derives from one single cause; therefore, a systematic process that is supported by data, evidence, and technical analysis is necessary to identify the true underlying problems that contributed to the event, rather than just the symptoms.

An RCA requires two critical pieces of evidence: historical data and records and physical evidence. Historical data and records were obtained from SoCalGas and the regulatory agencies. Physical evidence was extracted, while avoiding damage, for analysis and interpretation. The location and type of failure were unknown when the RCA began. Consequently, the approach had to be deliberate and thorough, requiring a structured approach. The RCA was conducted in phases on the basis of the scope of the work activity.

Brief descriptions of the phases selected for this RCA with the approximate timeframes for each phase are as follows:

- **Phase 0—Well and Field Data Collection, Collation, and Analyses**

  February 2016–May 2019

  Well and field records were collected through data requests and public access through the DOGGR website. Data were reviewed and catalogued in a secure database with controlled access. The data included historical drilling and completion records for the wells along with internal memos and discussions regarding decisions, workover data, reservoir test data, integrity monitoring data, and other data of the kind. In addition to historical data, the recently completed kill and relief operations provided insight into the failure and its causes. This part of the RCA extended through the entire phase of the project and was an iterative process as analysis was completed. These data resulted in modeling the deliverability, kill effectiveness, thermal simulation, identification of the failure timing and causes, and several other aspects of the overall operation of the field.

- **Phase 1—SS-25 Site Evidence Collection and Documentation**

  February 2016–May 2016

  This phase included a physical search of the area surrounding the SS-25 well site to locate and document any physical evidence that may have been associated with the leak. The west and east sides of the SS-25 site were also examined for evidence. Liquid samples were collected from the surface and within the crater. Through-tubing logging was also conducted during this phase in an attempt to assess the condition of the casing. By end of Phase I, the failure had been tentatively located through logging.

- **Phase 2—Site Restoration to Rig Readiness**

  June 2016–October 2016

  The gas leak and subsequent flow of gas to the surface resulted in a large crater that formed around the wellhead of SS-25. Phase 2, which was coordinated by SoCalGas, included removing well fluids and contaminated soil from the crater and the surface location surrounding the well site. The crater was then filled in, a new cellar was added for work around the wellhead, and a concrete pad was poured in preparation for moving a rig over the well for the Phase 3 work.

- **Phase 3—Tubing, Casing, and Wellhead Extraction**

  April 2016–December 2018

  Phase 3 covered all of the downhole-related operations conducted for the RCA. It included working with SoCalGas and the regulatory agencies to obtain approval and permits to extract and collect well equipment from SS-25 for the RCA. The operations consisted of extracting the tubing, casing, and wellhead; preserving the equipment; and properly P&A'ing the well. The production casing failure samples were extracted while minimizing and eliminating any extraction-related damage. After the equipment was extracted, the casing left in the well was evaluated using wireline logs. Protecting critical pieces included wrapping, coating, and bolstering the tubing and casing and crating them as required. All equipment extracted was treated as *evidence* and required special handling and documentation. Additional Phase 3 activities included evaluating several offset wells similar to SS-25, conducting a shallow geophysical investigation of the SS-25 site, and conducting operations on well SS-25A. Finally, the well was P&A'd.

- **Phase 4—Nondestructive Evaluation and Laboratory Metallurgical Examination**

  February 2018–April 2019

  Nondestructive evaluation (NDE) and laboratory metallurgical examination were used to evaluate appropriate samples of the equipment extracted. This included visual examination, physical measurements, micro-fractographic and metallographic examination, mechanical and chemical testing, and corrosion and cracking evaluation.

- **Phase 5—Integration, Interpretation, and Final Reports**

  October 2018—May 2019

  Data collected and results from the previous phases were integrated and interpreted to determine the root cause of the leak and failure. The data and analysis were compiled into final reports to document and present the RCA work.

# 2 SS-25 Well Failure Causes

The process of failure examination started on February 20, 2016, after SS-25 was under control. A detailed examination of the SS-25 site was undertaken as part of Phase I with the intent of locating failure pieces. The extent and location of the failure were unknown in February 2016. Minimization or elimination of any damage during extraction and the consequent handling were the focus of Phase 3 of the RCA investigation. All the physical data collected during Phase 3 were analyzed and interpreted. The examination process and results are discussed in the following order:

1. Background of the SS-25 construction and operations
2. Key results from Phase I and Phase 3 operations
3. Casing failure sequence and events
4. Connection test results
5. Location of the groundwater and its chemistry
6. Outside diameter corrosion on the 7 in. casing and the possible mechanisms of the corrosion
7. Material properties analysis of the 7 in. casing
8. 11 3/4 in. surface casing corrosion
9. Interpretation of all the results and summary of the failure causes

## 2.1 Introduction

### 2.1.1 SS-25 Well Construction

The SS-25 well was originally drilled, starting October 01, 1953, by Tidewater Associated Oil Company as an oil producer. The 11 3/4 in. surface casing was cemented at 990 ft on October 18, 1953. Returns were lost at 169 ft, 741 ft, and at 990 ft, and a top job was done to bring cement to the surface. The 11 3/4 in. surface casing was logged as part of the RCA. Good cement was observed only in short, isolated portions of the 11 3/4 in. annulus, specifically at 606–660 ft and 950–985 ft. Cement was not observed above 400 ft.

SS-25 was drilled and cored to 8,585 ft, and the 7 in. OD production casing was cemented at 8,585 ft on February 10, 1954. The cement top was at 7,000 ft, and this was confirmed by the logging conducted during the RCA. A 6 in. hole was drilled to 8,749 ft, and a 5 1/2 in. slotted liner was set on February 15, 1954. The well was completed as an oil producer with gas lift in 1954.

SS-25 was later converted to a gas storage well. The process of conversion started on May 24, 1973. The tubing was pulled, and the 7 in. casing was pressure tested in the following stages:

- 1,500 psi from 8,525 ft to surface
- 2,000 psi from 6,000 ft to surface
- 2,400 psi from 4,500 ft to surface
- 2,800 psi from 3,000 ft to surface
- 3,100 psi from 2,000 ft to surface

- 3,400 psi from 1,000 ft to surface

These pressure tests were higher than the anticipated differential pressure loading that the 7 in. casing would experience as a storage well.

SS-25 started operations as a gas storage well in 1977. There was a workover in February 1979 to remove, repair, or replace and reinstall the annular flow safety system. The tubing and completion equipment were run back in the well. Figure 9 shows the condition of the wellbore in February 1979. The rig was released February 20, 1979. This was the last reported rig work on SS-25 until after the casing leak on October 23, 2015.

Other wireline work included running and pulling bottomhole chokes and running and pulling the valve and pack-off that were part of the annular flow safety system. On January 07, 1980, wireline work started to service the annular flow safety system. The valve would not stay set in the nipple profile. Tools were stuck and recovered. The pack-off was set and tested. Problems continued with pulling and running the safety system, and the system failed to test. On January 28, 1980, Camco pulled the valve and pack-off. The report stated “System apparently bad [8].”

The well had operated since 1980 without the valve and pack-off, and this resulted in the 2 7/8 in. tubing and 7 in. × 2 7/8 in. annulus to be in communication through the annular flow safety system ports.

Records from SoCalGas and DOGGR show that approximately 65 temperature, 8 noise surveys, and 41 pressure surveys were run between 1974 and 2014.

In summary, the SS-25 well was drilled and completed in the 1950s and converted to gas storage in the 1970s. The leak event occurred in 2015. The SS-25 well required no intervention work other than the routine noise and temperature logs from around 1980 until the leak event in October 2015.

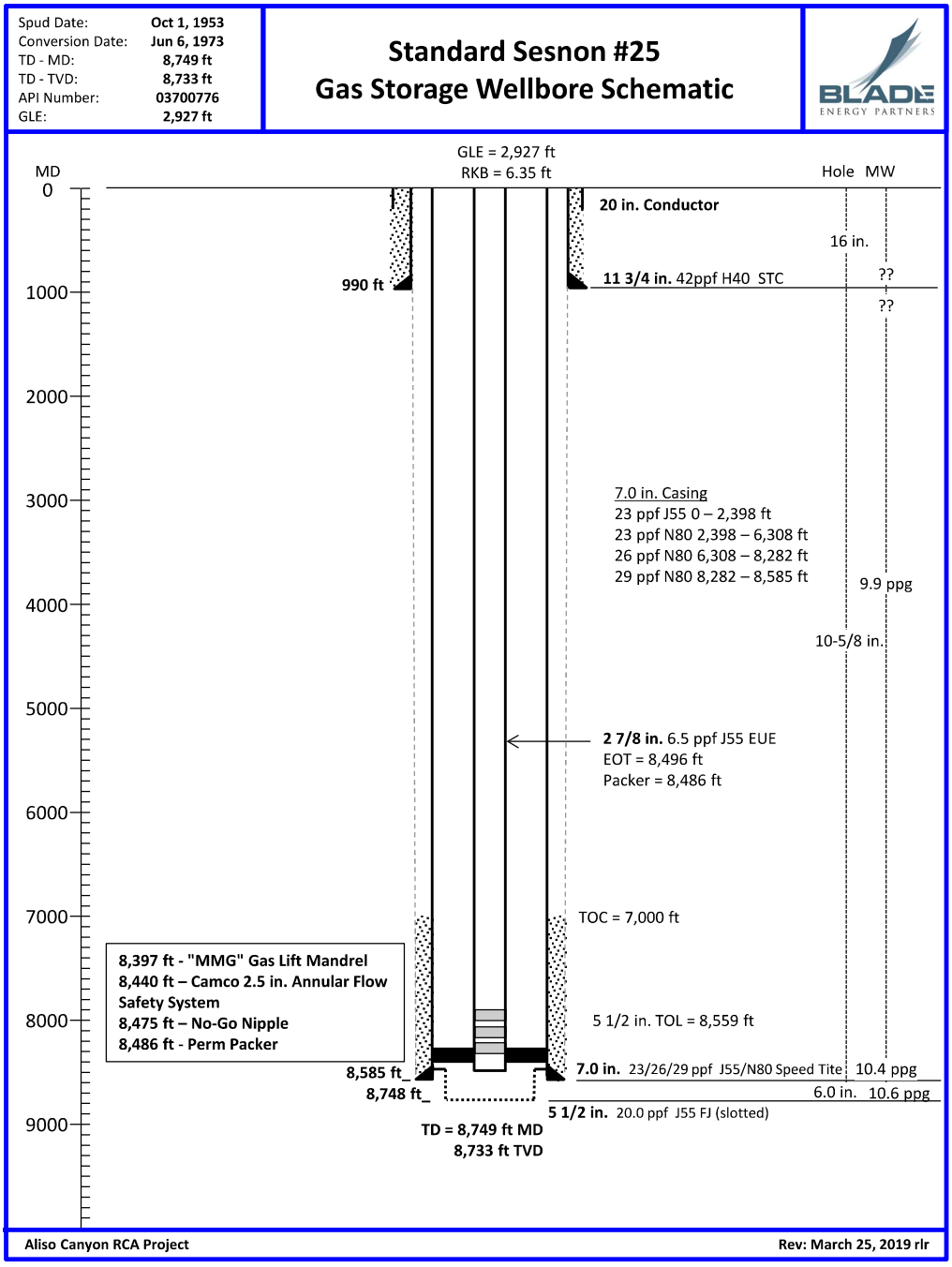


**Figure 9: SS-25 Wellbore Schematic in February 1979**

## 2.1.2 SS-25 Injection and Withdrawal Operations

The review of injection and production data for the SS-25 incident well and the other two wells on the same site (SS-25A and SS-25B) showed that all three wells were used for both injection and withdrawal; however, the injection volumes were higher than the withdrawal volumes. All three wells are located in the west sector, and had a lower OGR than the field and the sector values (Table 3). Although all three wells had a WGR below the sector average, SS-25A had produced more water than its two neighbors and had a WGR above the field average.

However, during this period SS-25 was operated as a gas storage well; that is, it operated as an injector and a producer. From 1977 to 2015, the injection volume was 33 Bcf while the withdrawal volume was 31 Bcf.

**Table 3: Gas Storage Injection and Withdrawal Volumes for Incident Well, SS-25A and SS-25B (January 1977–October 2015)**

| Sector | Totals | | | | | OGR (stb/ MMscf) | WGR (stb/ MMscf) |
|---|---|---|---|---|---|---|---|
| | Injected Gas (Bscf) | Withdrawn Gas (Bscf) | Net Injection (Bscf) | Oil (MMstb) | Water (MMstb) | | |
| SS-25[1] | 33.0 | 31.0 | +2.0 | 0.033 | 0.030 | 1.053 | 0.959 |
| SS-25A | 25.7 | 16.9 | +8.8 | 0.019 | 0.053 | 1.110 | 3.134 |
| SS-25B | 45.8 | 24.9 | +20.9 | 0.016 | 0.021 | 0.632 | 0.844 |
| **Pad Total** | **104.5** | **72.8** | **+31.7** | **0.067** | **0.103** | **0.922** | **1.424** |

[1] Incident well

The injection and production period for SS-25 over the history of the well is summarized in Figure 10. The well withdrew gas for 1,451 days over its history—approximately 10% of its life. This well was predominantly an injection well for over 5,253 days—approximately 36% of its life—and idle (in a shut-in condition) for the remaining period.

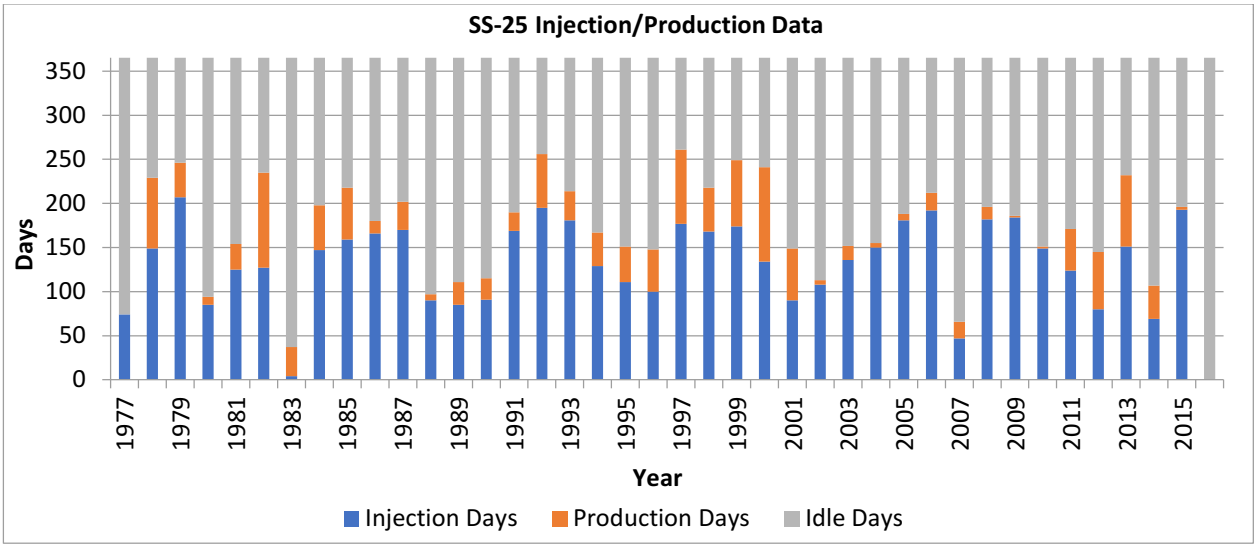


**Figure 10: SS-25 Injection/Production data from 1977 to 2015**

A more detailed assessment of the well in the year 2015 revealed it to be primarily an injection well. There was a negligible period of time SS-25 was in withdrawal mode; the well was predominantly in injection mode (Figure 11), starting in March 2015 until October 2015.

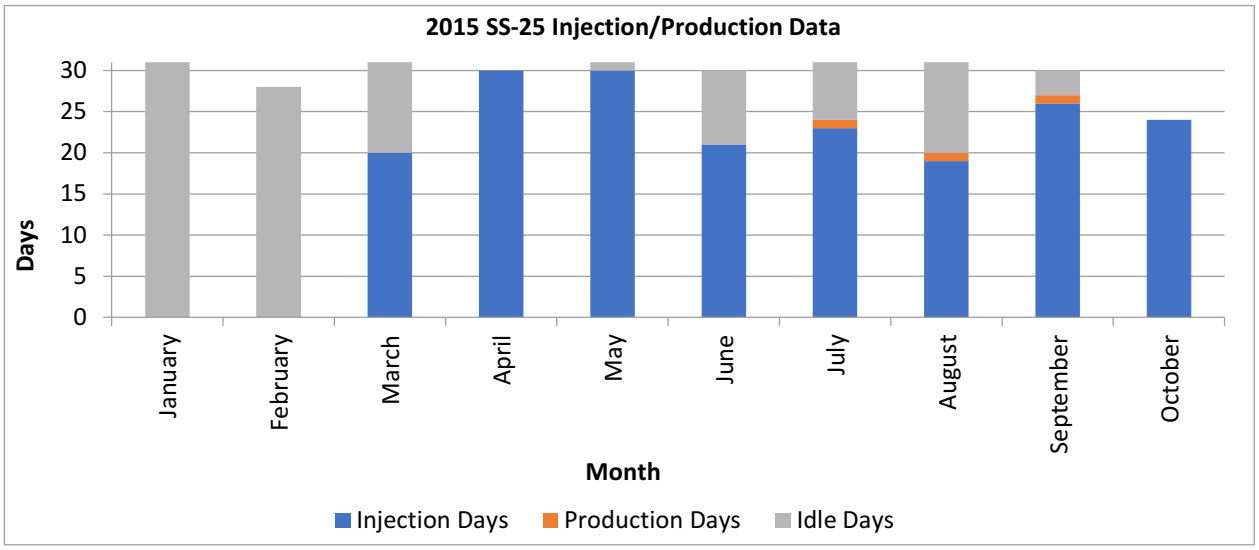


**Figure 11: SS-25 Well Injection/Production days in 2015**

Consistent with the long periods of injection, the casing pressure increased to 2,595 psi over the months leading to October 15, 2015. The final reported pressure was 2,700 psi; just prior to the leak event on October 23, 2015. Early on in the year, the pressure was around 1,930 psi, with the lowest measurement being 1,790 psi. The pressure was at its highest during the leak event. The pressure measurements in Figure 12 are the weekly shut-in pressure measurements.

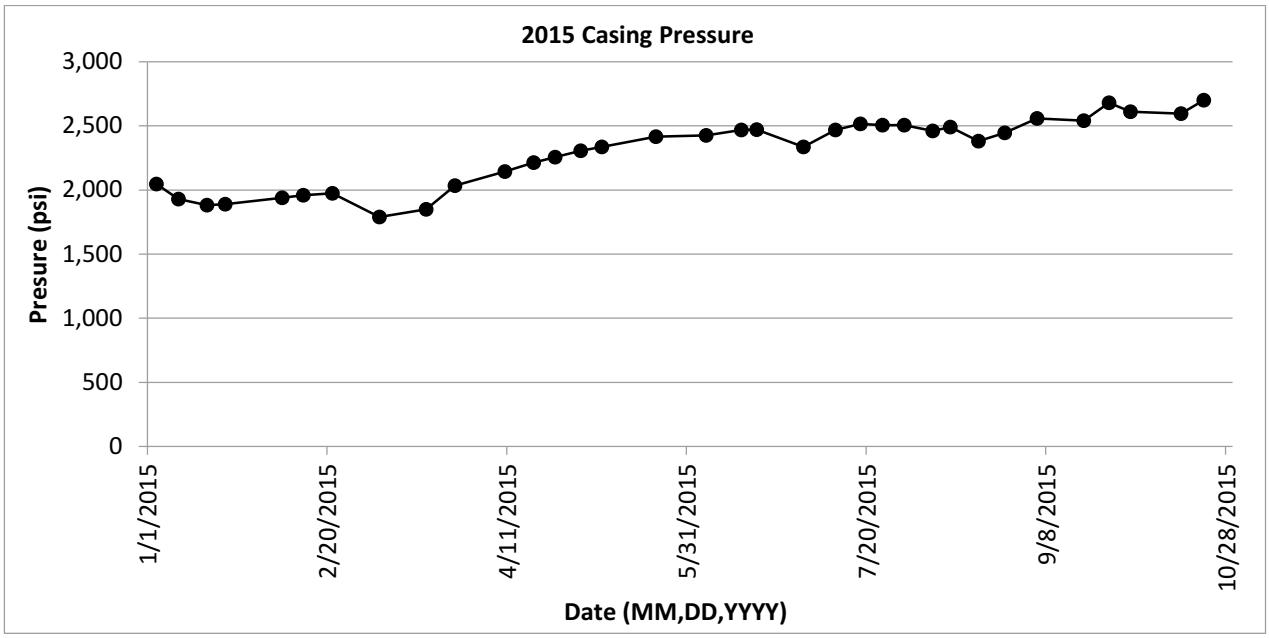


**Figure 12: Casing Pressure change in 2015**

### 2.1.3 SS-25 Temperature and Noise Logs

Figure 13 shows the dates of the temperature, pressure, and noise surveys performed in SS-25 from 1974 to 2015 (41 years). The numbers of surveys were approximately:

- 65 temperature surveys
- 8 noise surveys
- 41 pressure surveys

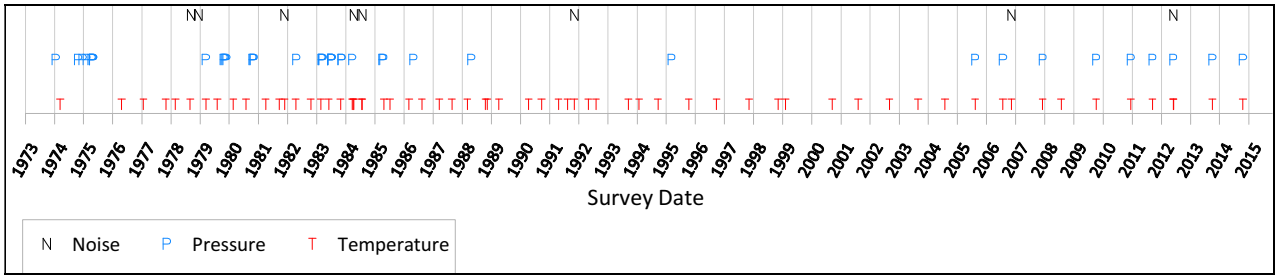


**Figure 13: Dates of Pre-Incident Temperature, Pressure, and Noise Surveys**

No anomalies were ever recorded during the measurements.

Figure 14 shows the temperature survey from October 21, 2014, the *last* survey before the incident of October 23, 2015, and shows no anomalies related to casing integrity. A cooling feature was found below approximately 8,200 ft related to gas injection and withdrawal, but it was not related to a casing integrity issue.

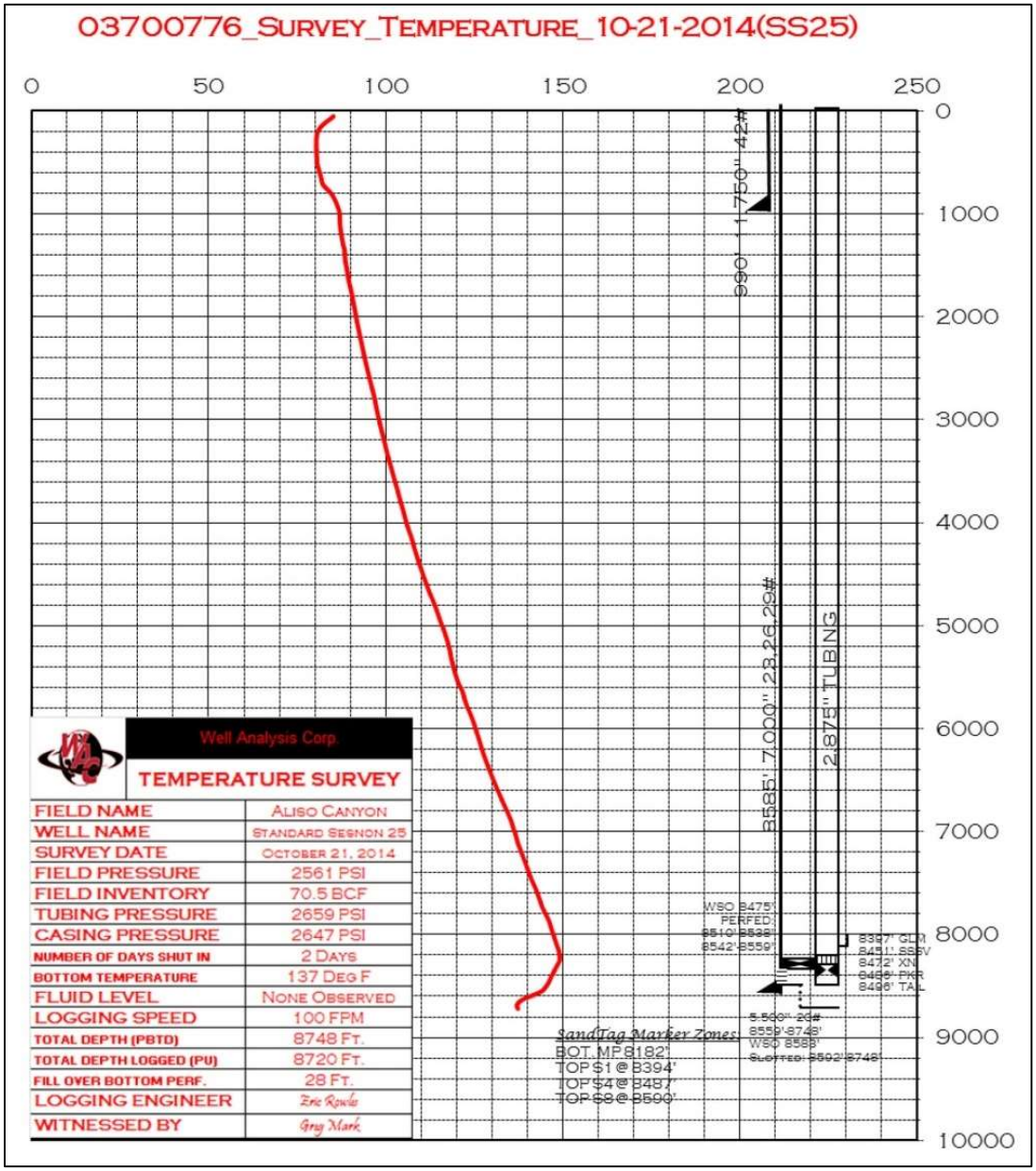


**Figure 14: Temperature Survey on October 21, 2014**

No temperature, pressure, or noise anomalies in the surveys indicated a preexisting casing failure before the incident of October 23, 2015. Additionally, no physical observations from well inspections and weekly pressure measurements indicated an existing casing integrity problem.

## 2.2 SS-25 Site Evidence Search and Through Tubing Logging

After successfully controlling the SS-25 well through the P-39A relief well, Phase I of the RCA began in February 2016. The objectives of Phase 1 were to identify, collect, and document any evidence associated with the failure. The SS-25 site was examined in detail with the primary objective of locating any failure samples, even though the possibility of finding any was considered to be remote. The location of the failure was an unknown but, based on all the data, it was believed to be the 7 in. production casing.

Oil and soil samples were collected from the surface as part of Phase 1. Logging was also a key aspect of Phase I and was expected to provide an insight into failure location.

Phase 1 was the first opportunity for the Blade team to observe and document the SS-25 well site. Figure 15 shows one of the initial images taken after the well site was opened to the Blade team. The image shows the SS-25 tree, crater, bridge spanning the crater, SS-25A and SS-25B heat shields, and piping for SS-25, SS-25A, and SS-25B. The majority of the non-permanent items shown in the image were removed throughout Phase 1 or during Phase 2. These items included the trailer, bridge, heat shields, sand bags, cones, and concrete beam.

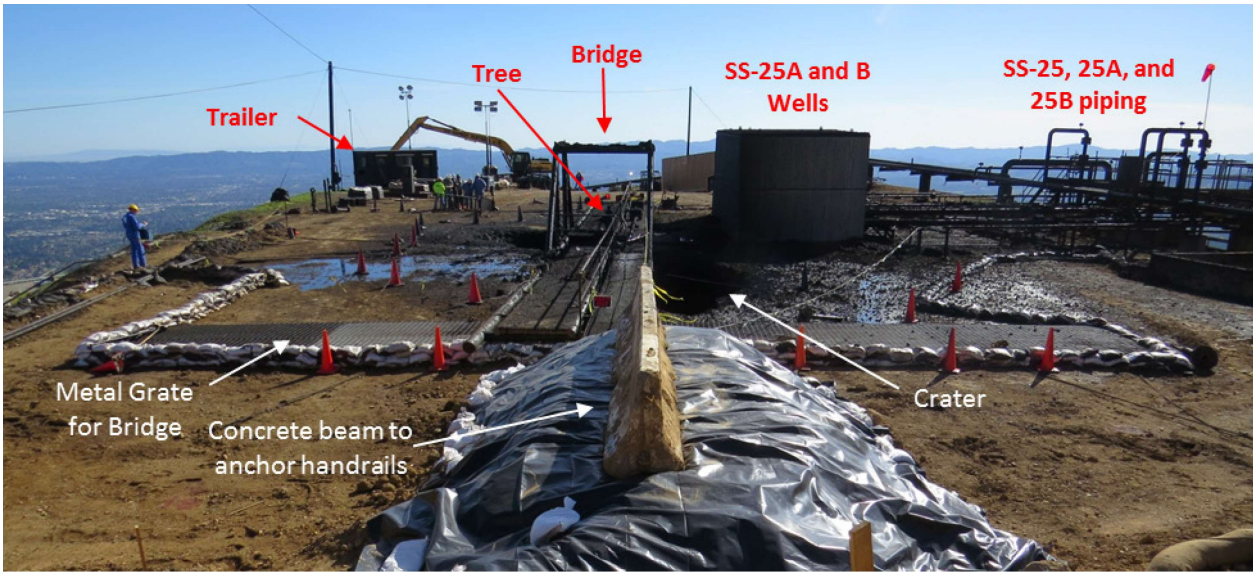


**Figure 15: SS-25 Well Site Condition on February 25, 2016**

Formation of the crater occurred during various periods of the blowout. Figure 16 and Figure 17 show aerial photographs of the crater looking down and west, respectively. The images also show the SS-25A and SS-25B wellheads after removing the heat shields. The bridge and concrete beam were installed during the kill operations to provide access to the wellhead. The bridge provided a platform for personnel to connect lines and operate valves. The concrete beam was used to anchor a steel cable handrail.

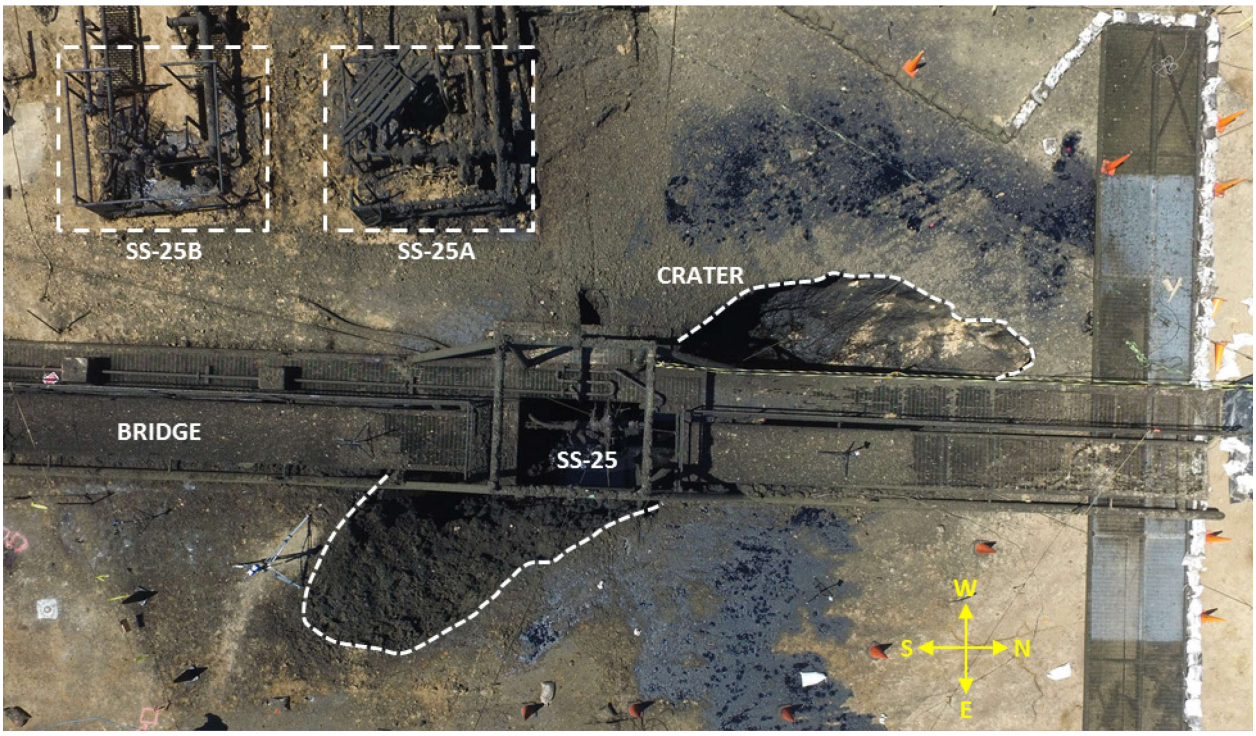


**Figure 16: SS-25 Well Site Top View Aerial Photograph Post Blowout Taken on April 01, 2016**

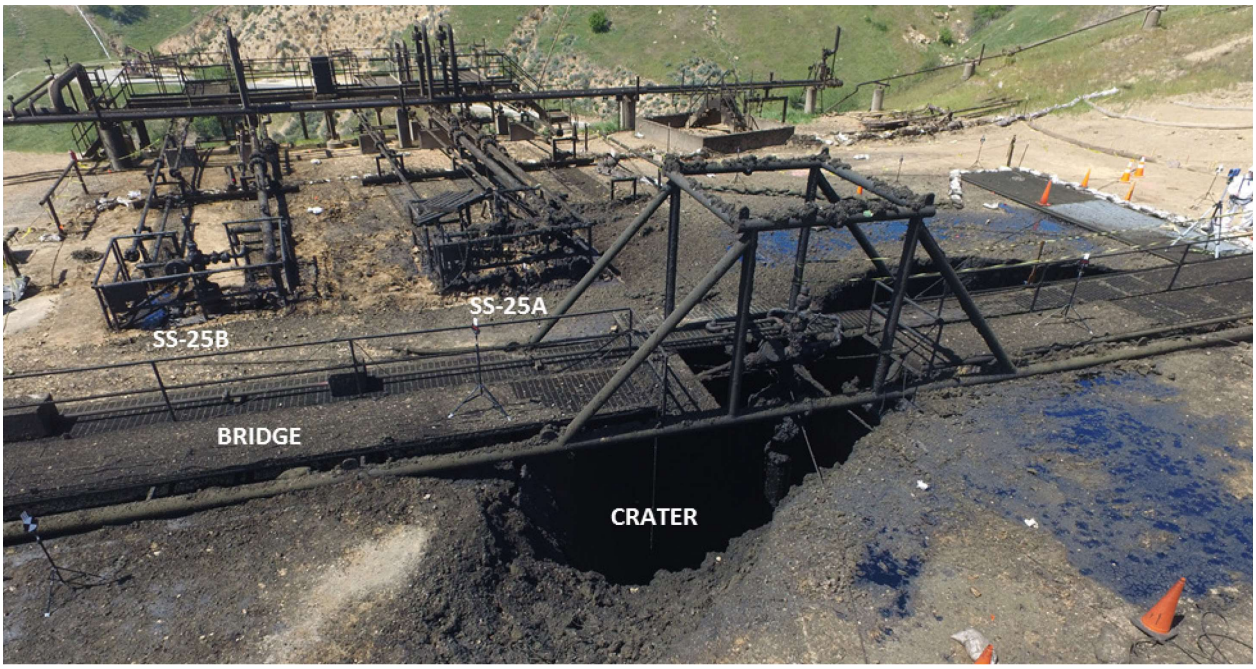


**Figure 17: SS-25 Well Site West View Aerial Photograph Post Blowout Taken on April 01, 2016**

Figure 18 shows an image of the location of the missing 11 3/4 in. casing annulus valve. The valve backed off during the kill attempts and was not located during the Phase 1 evidence search. The valve most likely ended up at the bottom of the crater with the SS-25 cellar. The cellar collapsed to the bottom of the crater during its formation. A portion of the concrete pad that was attached to the cellar was hanging

from the south side of the crater. The details of the Phase I activities are described in the *Phase I summary* report [9].

**Figure 18: Photos of Missing 11 3/4 in. Casing Valve Taken on February 25, 2016**

During Phase 1, a Magnetic Imaging Defectoscope (MID) logging tool was used. This tool is designed to record the time response to electromagnetic pulses to detect metal loss or gain in up to three barriers. The MID tool was run within the 2 7/8 in. tubing (first barrier) to identify anomalies in the 7 in. casing (second barrier) and 11 3/4 in. casing (third barrier). The MID detected metal loss at several locations along the length of the 7 in. casing—the most notable one at 895ft MID log depth. Figure 19 shows the MID results at a depth of 895 ft. The well schematic in Figure 19 shows a 38% metal loss feature on the 7 in. casing, suggesting significant metal loss at that depth.

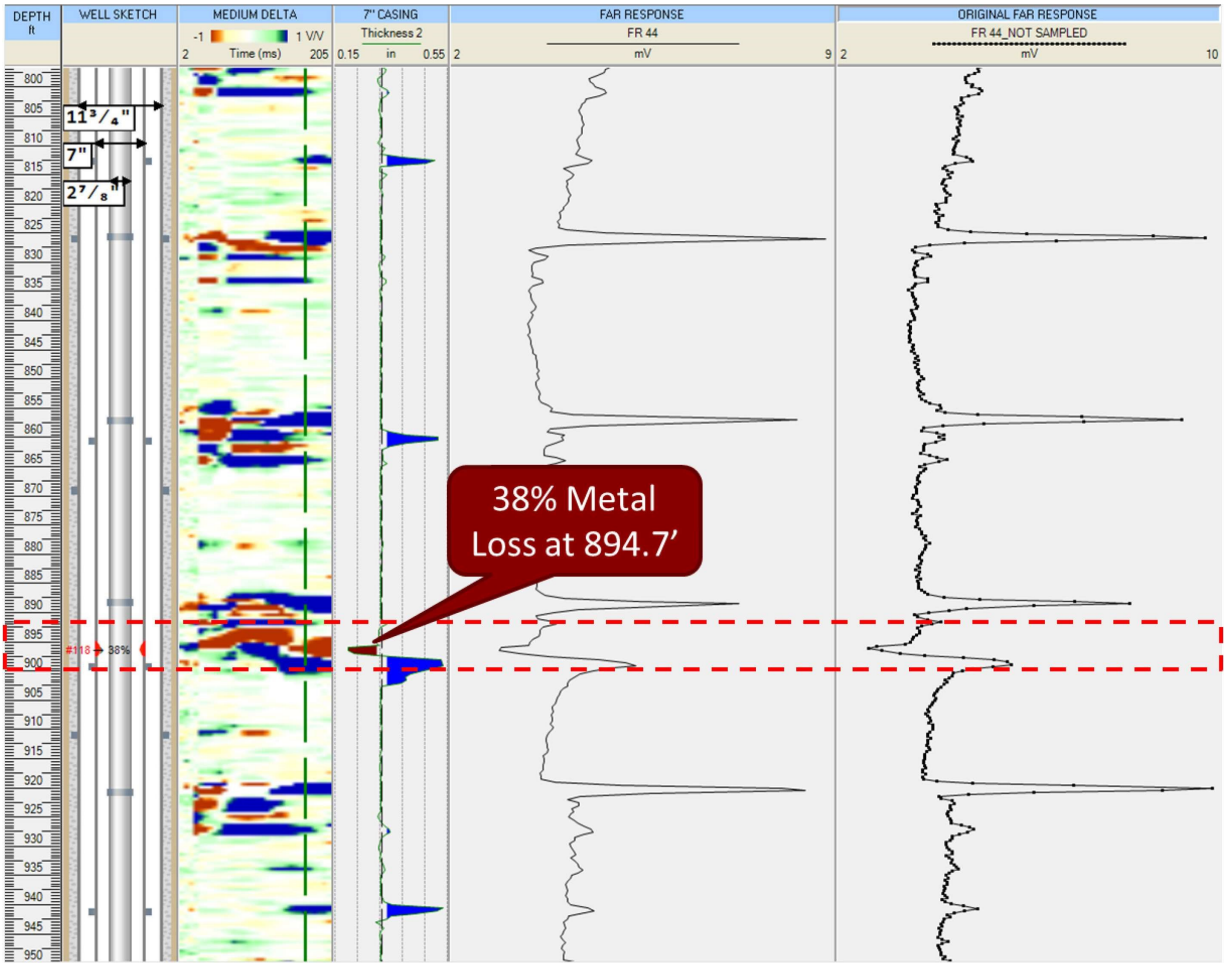


**Figure 19: MID Results Showing 38% Metal Loss at Approximately 895 ft**

Logging tools were also run through the 2 7/8 in. tubing with the intent of confirming tubing integrity and identifying noise and temperature anomalies.

The magnetic flux leakage logging tool MicroVertilog (MVRT) was run through the 2 7/8 in. tubing to assess its integrity, but did not identify any features of interest. However, it did identify a metal gain at approximately 890 ft of MVRT log depth. The MVRT is a single barrier tool, which means that it cannot detect beyond the string it is run in. It can detect metal gain if the first barrier is in contact with the second barrier, though. The metal gain detected at 890 ft was interpreted as the 7 in. casing making contact with the OD of the 2 7/8 in. tubing. This data, along with the MID results, contributed to the working theory that the 7 in. casing was parted at this depth and was in contact with the tubing.

These tubing logs were important and influenced the decisions during the extraction operations. For the first time, the location of the failure was identified with some degree of confidence. The MID and MVRT data taken together suggested that the 7 in. casing behind the tubing might have been parted. These assumptions were used during the planning stages of Phase 3 to plan casing extraction, and also minimize the risk of damaging the 7 in. casing.

Figure 20 shows a 3D map and a 3D model of the SS-25 well site topography. The 3D model was generated using Light Detection and Ranging (LIDAR) data collected during Phase 1. LIDAR is a method of

measuring distances to the earth using light in the form of a pulsed laser. The SS-25 well site is small and has limited access, which had to be factored into any well operations.

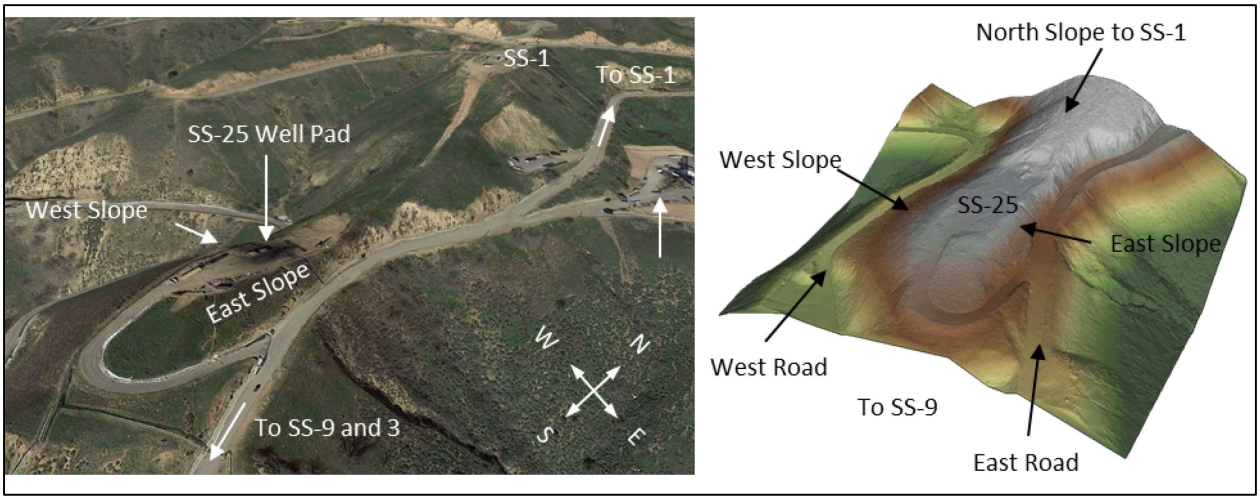


**Figure 20: SS-25 Well Site Shown with 3D Map and LIDAR Data**

Figure 21 shows aerial photographs taken from a drone during Phase 1. The images show the sloping terrain surrounding the SS-25 well site. The neighborhoods at the base of the Aliso Canyon field can be seen in the background. The SS-1, SS-9, and PS-20 well sites were used throughout the RCA to assist with the investigation.

SS-1 is located north of SS-25 on top of the northern slope. SS-1 served as the initial vantage point during the blowout due to its higher elevation and proximity to SS-25. The initial photos provided to the Blade team were taken from SS-1. SS-9 is south of SS-25 at the bottom of the south slope.

SS-9 served as a staging area for equipment and vehicles and was the first location for the Phase 1 evidence trailers. Eventually, the borehole Test Hole 1 (TH-1) was drilled at the SS-9 site.

PS-20 initially served as a staging area for equipment and a turnaround area for large vehicles. It later became the staging area for the metallurgical investigation. Trailers, pipe racks, sea containers, and other equipment were brought to PS-20 to assist with the Phase 3 pipe inspection. PS-20 was chosen due to its size and proximity to SS-25 and was a key well site during Phase 3. Figure 22 shows a 3D map of SS-25 and the surrounding wells. The image includes a list of the primary RCA operational functions for each well site.

**Figure 21: SS-25 Well Site Drone Aerial Photographs Taken on April 01, 2016**

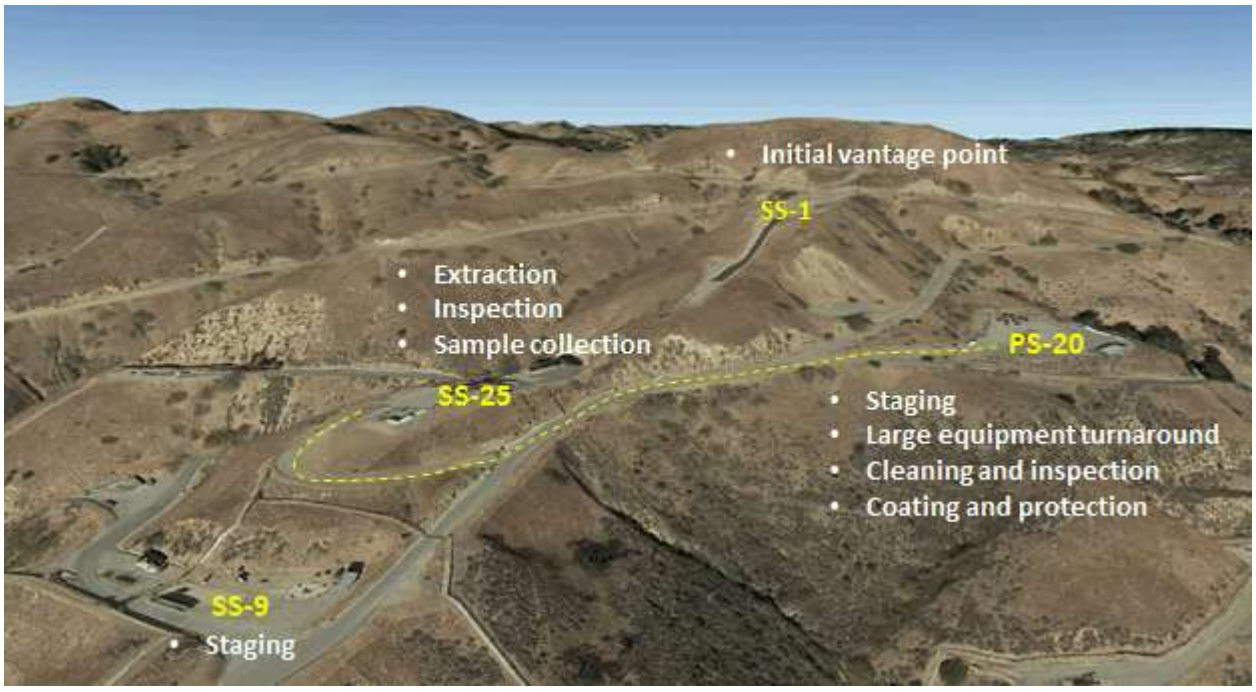


**Figure 22: SS-25 RCA Tubular Handling Locations**

## 2.3 Tubing and Casing Extraction

The tubing, casing, and wellhead were extracted and examined during Phase 3. The objective was to extract the physical evidence from the SS-25 well with minimal damage. The key operations that were conducted to meet this objective were to:

- Confirm the failure location with logs and downhole camera.
- Extract and visually examine all of the 2 7/8 in. tubing.
- Extract and visually examine the 7 in. casing to a depth below the shoe including the failed joint.
- Inspect the remaining 7 in. and 11 3/4 in. casings with logs and downhole camera.

- Determine the condition of the annuli with logs.

The SS-25 site was restored for rig readiness during Phase 2 in preparation for the Phase 3 operations. The Phase 2 operations are discussed in the *Phase 2 Summary* supplementary report [10].

The *SS-25 Phase 3 Tubing, Casing, Wellhead Extraction Protocol* [11] was drafted to document the planning for Phase 3. It includes a summary of the SS-25 well history, geologic information, offset well data, expected equipment and service requirements, summary steps, contingency steps, and the overall operational concept for the tubular extraction and P&A process. This document served as a design basis and provided the foundation on which the detailed operational work plans were developed. Phase 3 preparation, planning, discussions, and activities started in April 2016 and were completed in December 2018.

Phase 3 operations required extensive regulatory oversight and approvals. Witnesses representing various parties were present on the SS-25 site during the operations. Phase 3 also included partial abandonment of the SS-25A well due to a suspected casing patch repair leak. Consequently, the extraction operations in SS-25 started in late July 2017. All the activity details from Phase 3 are summarized in a supplementary report [12].

### 2.3.1 Tubing Extraction

The Phase 3 operations at SS-25 began on July 31, 2017. The tree was nippled down after successful pressure tests and fluid sampling. The blowout preventer (BOP) and diverter were nippled up and tested on August 19, 2017. The tree was transferred in one piece to PS-20, where it was dissembled into its individual components and then cleaned, inspected, and crated in accordance with the Tubulars Handling Protocol [13] procedures.

A total of 244 joints identified as T001 through T244 were extracted from the SS-25 well. The final joint was extracted on September 01, 2017.

Blade observed an occasional low-magnitude but sharp increase in tension (i.e., overpull) on the rig weight indicator during the extraction of the 2 7/8 in. tubing. The overpull was spaced in roughly 31 ft increments. Some of the tubing connections were observed to have a 1/2–1 in. area of shallow deformation at the bevel on the upper side of the connection. Blade interpreted this as a probable full circumferential parting of the 7 in. casing and that the tubing connections were momentarily hung up as they passed through the parted area. This needed to be visually examined to plan future operations. The tubing extraction was stopped when the base of the tubing reached 953 ft.

A Baker Hughes wireline was rigged up and used to run the EV downhole video camera through the tubing and into the 7 in. casing. Figure 23 shows a schematic of the well configuration for the video camera work. With the video camera positioned at the end of tubing, the tubing was slowly raised while simultaneously pumping clear 8.5 ppg KCl fluid. Pumping continued while the ID of the 7 in. casing was observed with the camera.

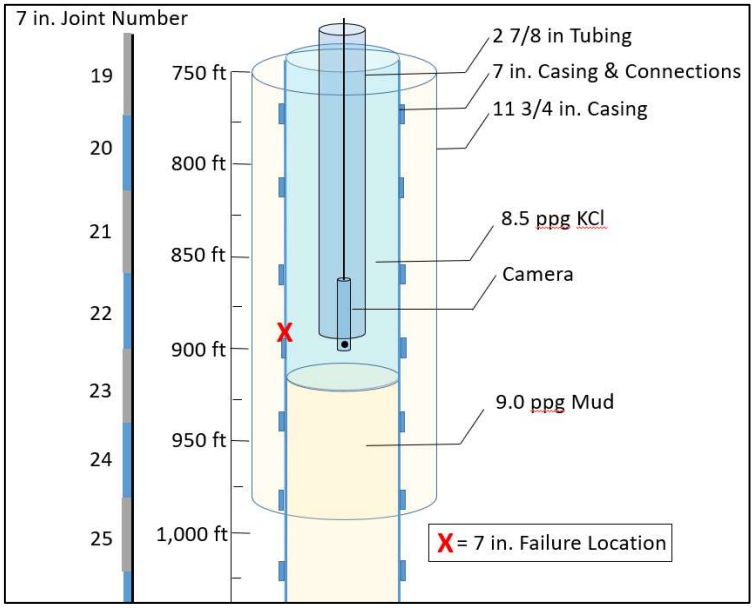


**Figure 23: Well Configuration for Through-Tubing Camera Run to View 7 in. Failure Area**

Figure 24 shows images extracted during the camera run. Figure 24 (a) shows the end of the tubing, which was set at approximately 885 ft. Figure 24 (b) shows the camera inside the upper 7 in. casing string after exiting the tubing. Figure 24 (c) shows the end of the upper 7 in. casing string. This was the location of the parted 7 in. casing. The camera exited the upper string and looked down at the lower string. Figure 24 (d) shows the lower 7 in. casing string offset from the camera. The lower string was sitting approximately 5 in. below the upper string. The camera runs confirmed that the 7 in. casing was parted and that the lower fish was offset from the upper string.

In general, a fish is an object or equipment that is left in the wellbore during drilling or workover operations. In this case, the fish was the lower portion of the parted 7 in. casing.

Understanding the misalignment of the upper and lower parted casing was important to the fishing operations. A custom-built pawl tool was designed and manufactured for the recovery of the fish.

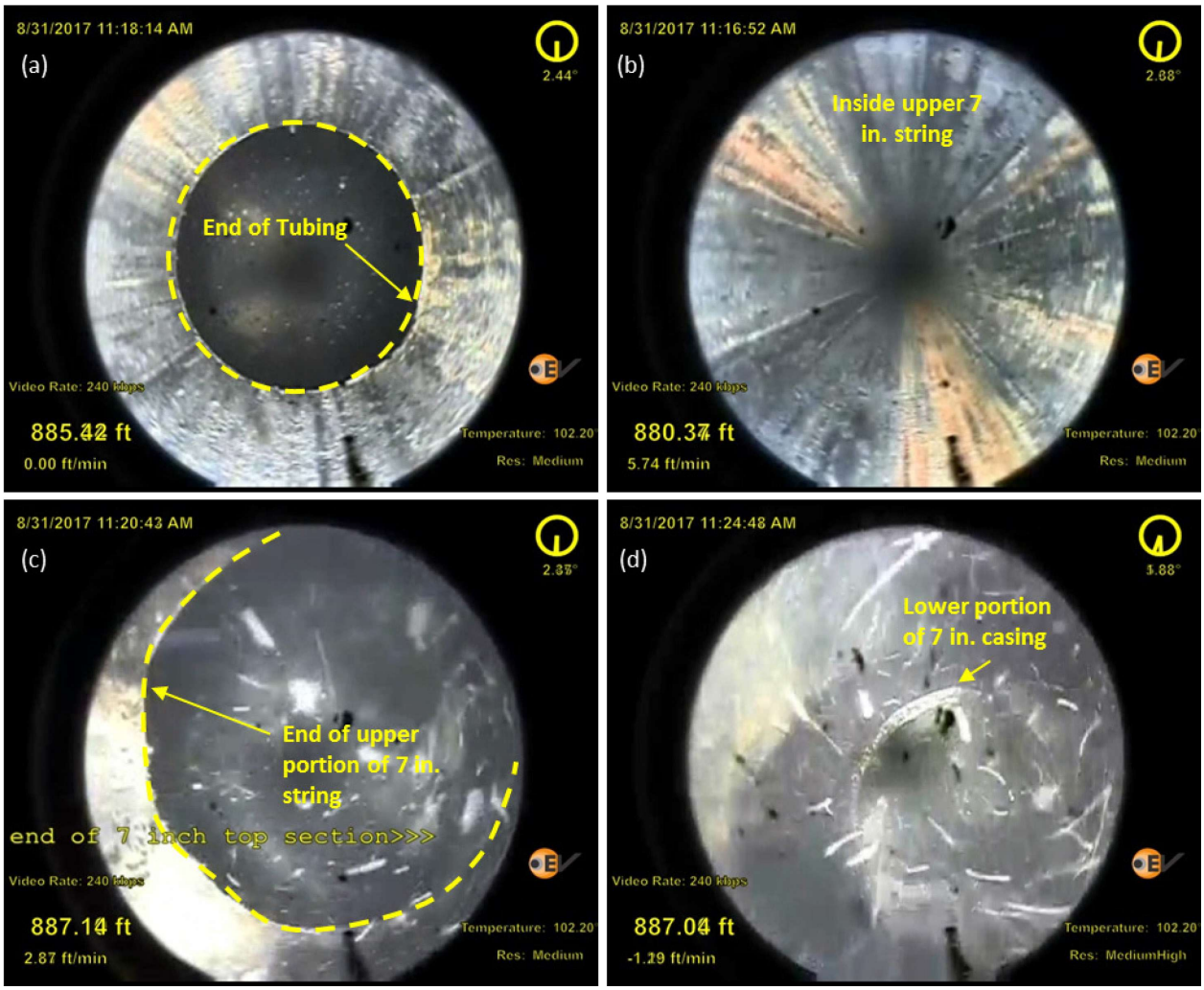


**Figure 24: EV Lower Camera Snapshots from August 31, 2017 Showing the Parted 7 in. Casing**

### 2.3.2 7 in. Casing Extraction

The downhole camera confirmed that the 7 in. casing was parted at Joint 22. Retrieval of the upper parted casing and the extraction of the lower fish were required to collect the upper and lower portions of the circumferential parting. A total of 25 casing joints were extracted from the SS-25 well. Casing joints were given Joint Sequence Numbers (JSN) per the Tubulars Handling Protocol [13]. JSNs refer to individual sections of the casing that were cut and extracted from the string and do not directly correspond to the joint numbers because the casing was cut below each connection. The cuts were made to preserve the connections for gas pressure integrity testing. Figure 25 shows the typical correlation between JSNs and joint numbers.

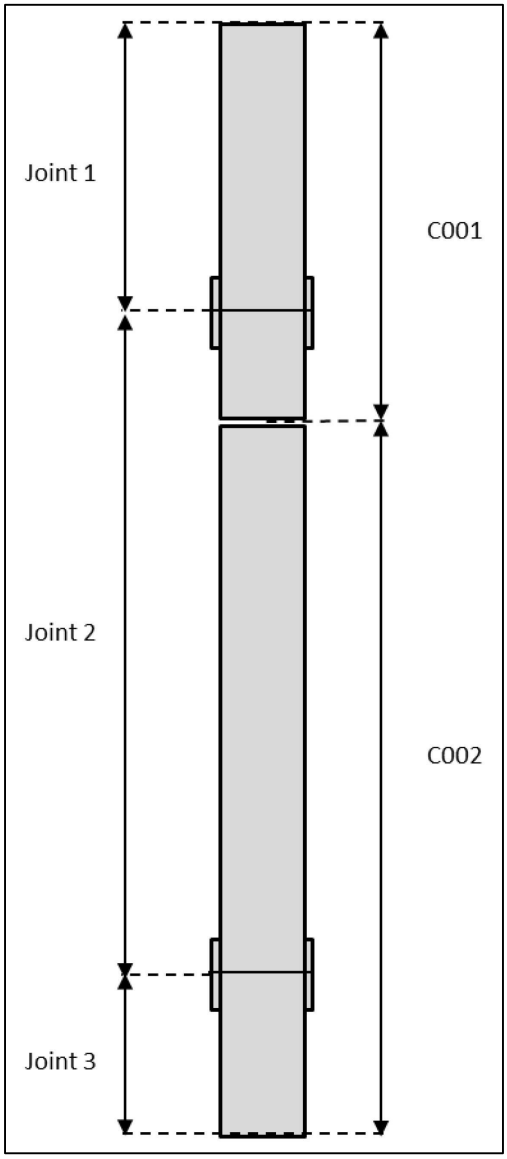


**Figure 25: Joint Sequence Number vs. Joint Number Example**

The parted casing separated the casing string into two sections. The upper section included C001 through C022. C001 was extracted on October 12, 2017, to remove the casing slips and install a temporary casing spool; this separated the parted sections downhole to prevent any accidental damage.

Casing was first inspected on the rig floor as it was being extracted. The visual inspection was followed by an NDE of the region below the connection. A cut was made with the cold cutter after the NDE (Figure 26). The casing was then placed on pipe racks at SS-25. Detailed visual examination and photo documentation of the casing were performed. Scale samples were taken at various OD locations for analysis. The detailed procedures are summarized in the Tubular Handling Protocol [13].

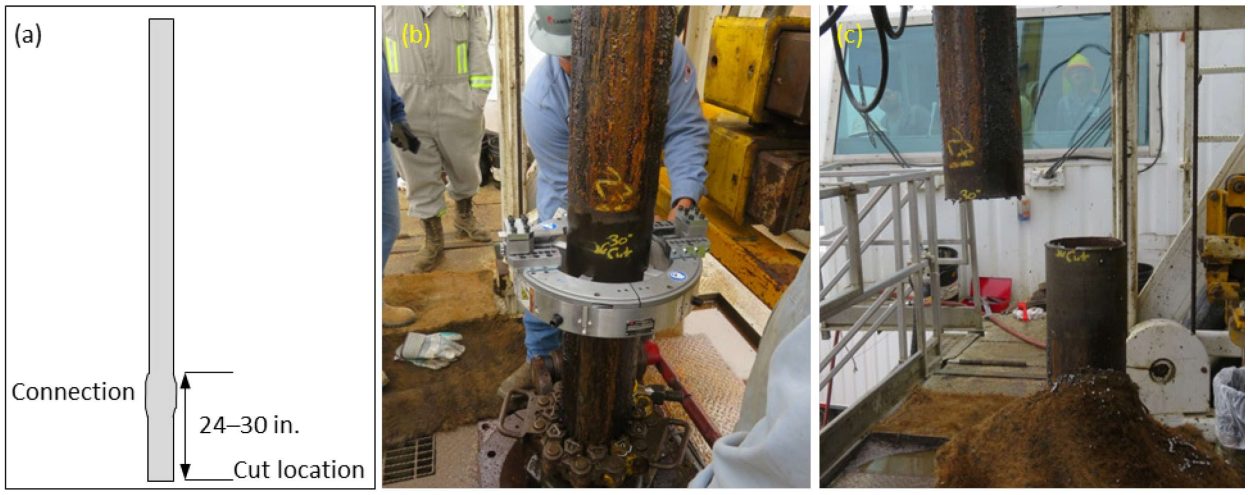


**Figure 26: 7 in. Casing Cutting Operation**

C022 was extracted on November 07, 2018. C022 contained the upper portion of the circumferential parting identified during logging and visually confirmed with the downhole camera. The circumferential fracture surface was thoroughly examined on the rig floor.

The upper circumferential fracture surface was examined on the SS-25 pipe rack. Figure 27 shows an (a) overall and (b) close-up image of the fracture surface. The images show that the fracture surface was obscured by the presence of oil and scale. The circumferential fracture surface appeared mostly flat with a pointed section that faced the south side of the rig floor. Figure 27 (c) shows corrosion features adjacent to the fracture surface.

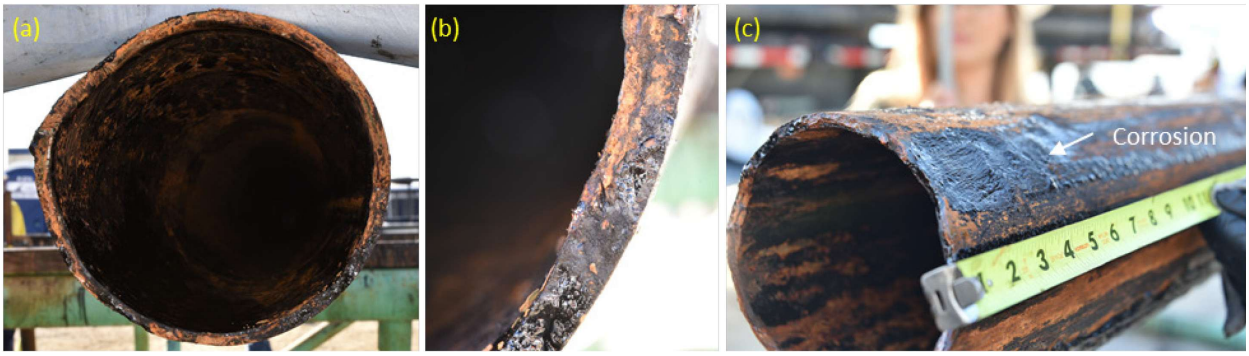


**Figure 27: Parted Casing (C022) on the SS-25 Pipe Rack**

At PS-20 the casing joints were cleaned by using Sentinel 909, brushes, and rags in accordance with the Tubulars Handling Protocol [13]. The cleaning procedures removed the oily deposits and revealed more of the corrosion features that were obscured during the rig and SS-25 inspections. Observations were photo-documented and recorded. The PS-20 inspection included magnetic particle inspection (MPI) and UT inspections in select regions. Connections were removed and given a new JSN after inspections. This was the second cut and was conducted at PS-20. The connections were removed for transportation and testing purposes.

Casing from the upper section (C001–C022) was examined first. C001 to C013 did not contain notable corrosion features; however, minor mechanical damage and linear indications were identified, which were later verified to be manufacturing anomalies. They had no role in the failure.

Shallow metal loss was first identified on the C014 connection and was present on the remainder of the extracted casing pipe bodies and connections. Corrosion was identified on many of the connections below C014 with increasing severity. Figure 28 shows the shallow corrosion on the C014 connection. Figure 29 shows corrosion on the connections for (a) C019 and (b) C020. The corrosion is similar to C014's but more severe.


**Figure 28: Shallow Metal Loss on Connection C014**

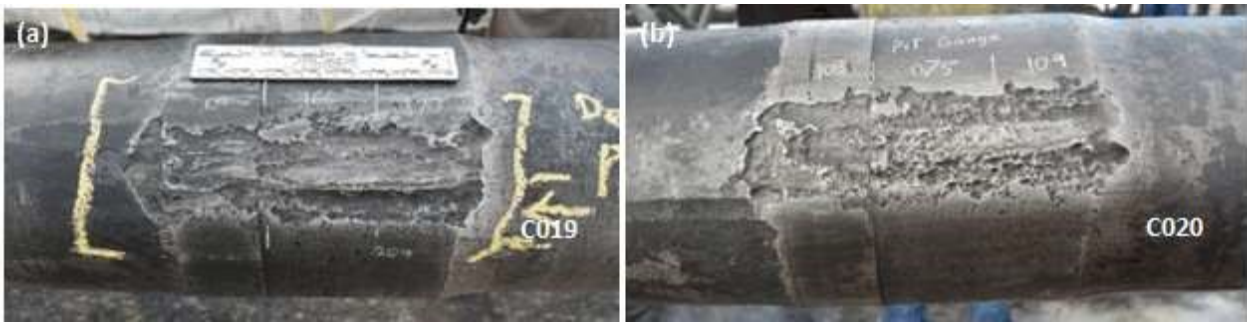


**Figure 29: Connection Corrosion on (a) C019 and (b) C020**

Corrosion was also identified on the pipe bodies, beginning with C014. Figure 30 shows examples of pipe body corrosion from (a) C016, (b) C017, and (c) C018. Figure 30 (c) shows corrosion with striated grooves slightly angled from the longitudinal axis of the pipe. This type of feature was identified at many locations along the casing below C014. Figure 31 shows examples of corrosion with striated grooves from (a) C018 and (b) C022. Figure 32 shows the largest corrosion feature identified during the PS-20 inspection. The shape and morphology appeared to be consistent with the features found on the connections (Figure 29).


**Figure 30: Pipe Body Corrosion on (a) C016, (b) C017, and (c) C018**

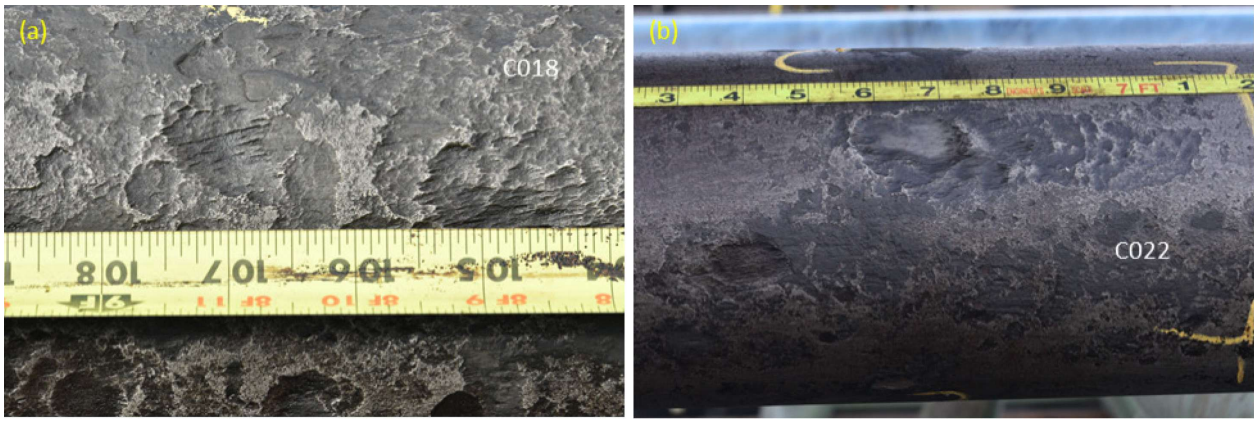


**Figure 31: Corrosion Examples with Striations from (a) C018 and (b) C022**


**Figure 32: Pipe Body Corrosion on C020**

The fracture surface was removed from C022 prior to cleaning and inspection. A cut location approximately 1 ft from the fracture surface was selected, cleaned, and inspected with MPI and UT. An additional cut was made on C022 to remove the connection. Figure 33 shows a diagram of the C022 cut locations. The diagram shows that the section containing the fracture surface was designated C022B after the cuts were executed. Cuts were made using the cold cutter as it had been done on the rig floor. Figure 34 (a) shows cutting joint C022. Figure 34 (b) shows the cutoff piece after cleaning with Sentinel 909. Figure 35 shows the C022B corrosion features adjacent to the fracture surface.

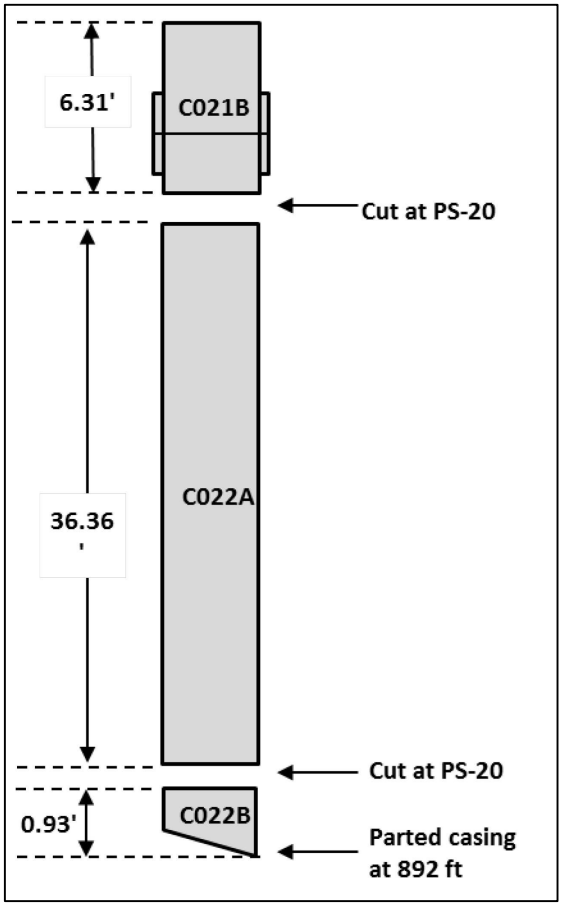


Figure 33: C022 Cut Locations


Figure 34: Parted Casing (a) Cutting from C022 and (b) After Cleaning with Sentinel 909

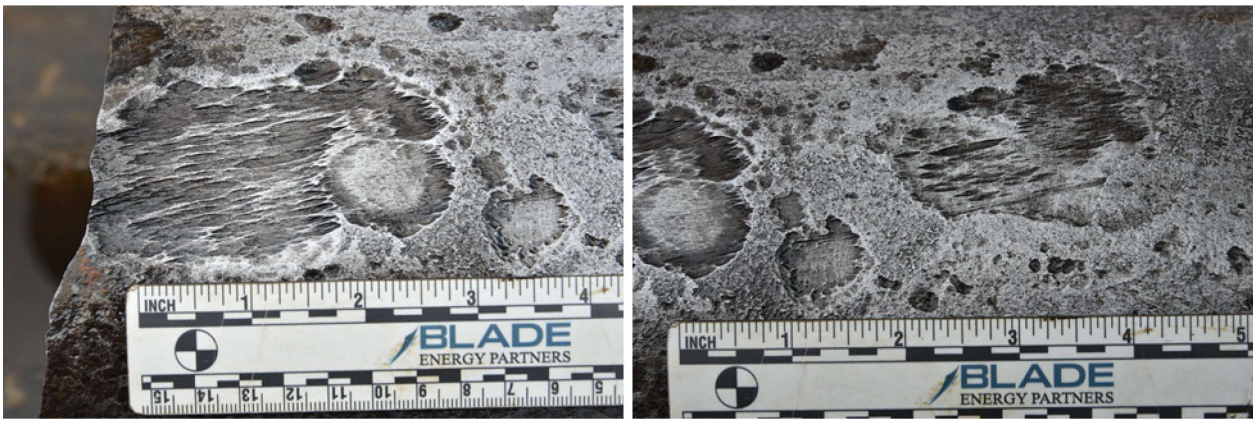


**Figure 35: Corrosion with Striated Grooves Adjacent to Fracture Surface**

The fracture surface was examined after being cleaned with Sentinel 909. Most of the fracture surface had been eroded, but chevron marks were visible in some areas. Figure 36 (a) shows the circumferential fracture surface after cleaning with Sentinel 909. Figure 36 (b) and (c) shows close-up images of the fracture surface taken in the field lab after undergoing ultrasonic cleaning.

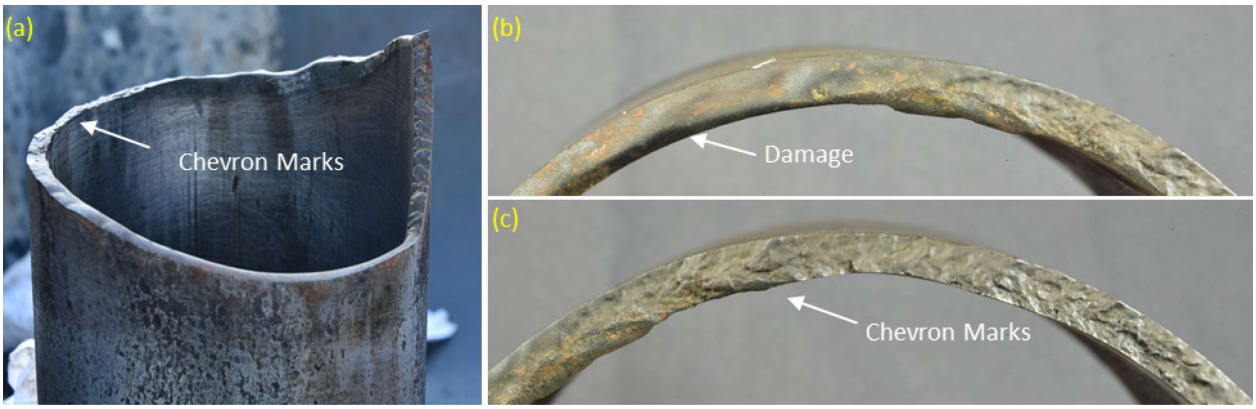


**Figure 36: (a) Circumferential Fracture Surface after Cleaning Showing (b) Erosion and (c) Chevron Marks**

The fish (lower section of the parted casing) was recovered using the specially designed pawl tool from National Oilwell Varco (NOV): the NOV Ratchet Pawl Casing Extraction tool. The tool was run on a new 7 in. workstring to latch onto the original 7 in. casing just below connection 22 between joint numbers 22 and 23. Figure 37 and Figure 38 show a layout drawing of the pawl tool and photographs of its use in SS-25, respectively. The ratchet pawls are spring-loaded fingers that fold inward as the tool descends over the 7 in. Speedtite connection and then spring back to perpendicular below the connection. Conventional fishing overshots and spears would have imparted substantial damage to the upward facing circumferential fracture surface. The NOV Ratchet Pawl Casing Extraction tool was specifically designed and manufactured for this application to prevent damage to the OD of the 7 in. casing, especially in the area where the casing parted. The EV camera was deployed through the pawl tool and assisted in locating and avoiding damage to the upward facing circumferential fracture surface. The 7 in. casing was successfully swallowed by the pawl tool. After three unsuccessful cut attempts using the Baker Hughes Mechanical Pipe Cutter, a chemical cutter was used to cut the casing at 939 ft. The 47 ft of 7 in. casing that was recovered included the lower section of the parted casing.

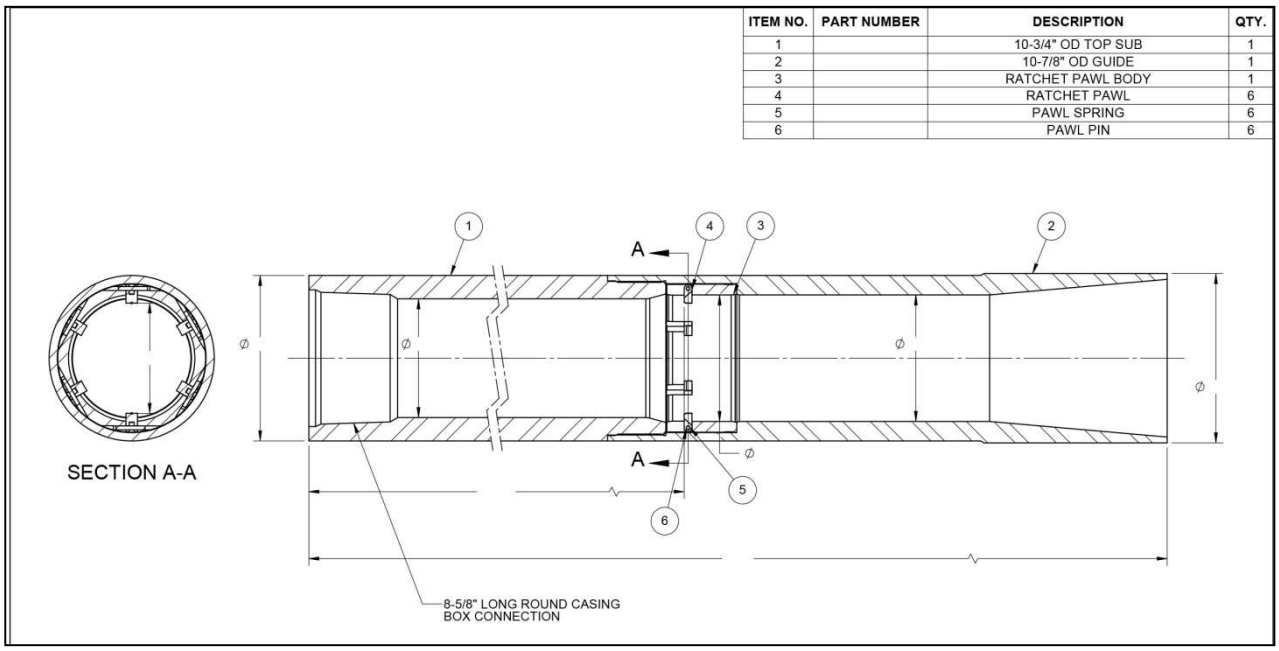


**Figure 37: Layout Drawing of NOV Ratchet Pawl Casing Extraction Tool**

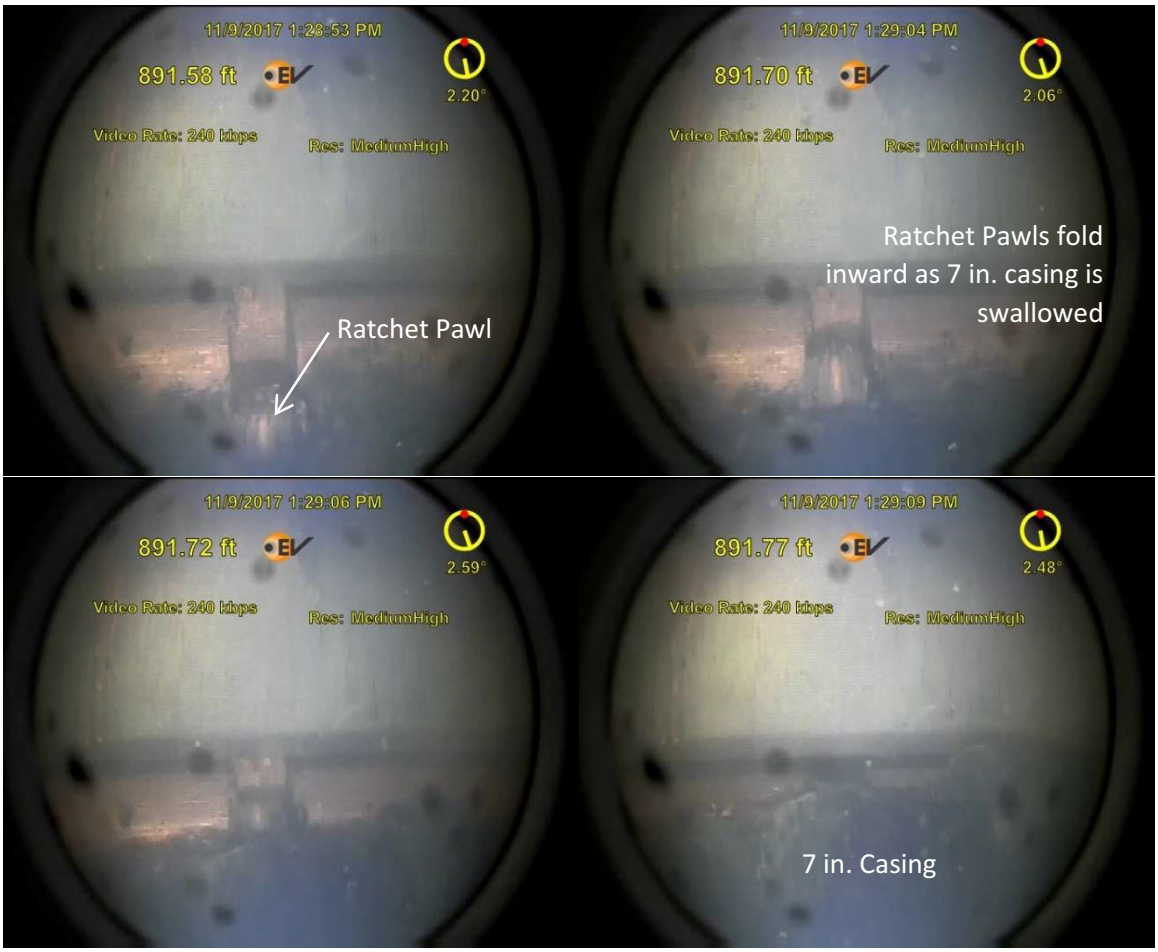


**Figure 38: Camera-Assisted Fishing of 7 in. Casing Using the Pawl Tool**

Figure 39 shows the fish on the rig floor with the tool (a) engaged and (b) removed. This was the first opportunity to visually examine the fish. The first major observation was that there was an axial rupture below the circumferential parting. C023 was moved from the rig floor to the pipe racks using the crane and a nylon sling. The pipe handler was not used to eliminate damage due to handling. The fracture surfaces were wrapped with VCI and covered for the night. C024 was extracted on November 15, 2017. A 13 ft section (C023A) of C023 was cut on the SS-25 pipe rack using the cold cutter to remove the axial rupture and circumferential parting. The pipe sections (C023A, C023B, and C024) were transported to PS-20 for further inspection. These pipe sections were inspected at PS-20 and preserved in the as-recovered condition for further analysis in Houston, TX. No onsite cleaning was done for these samples.

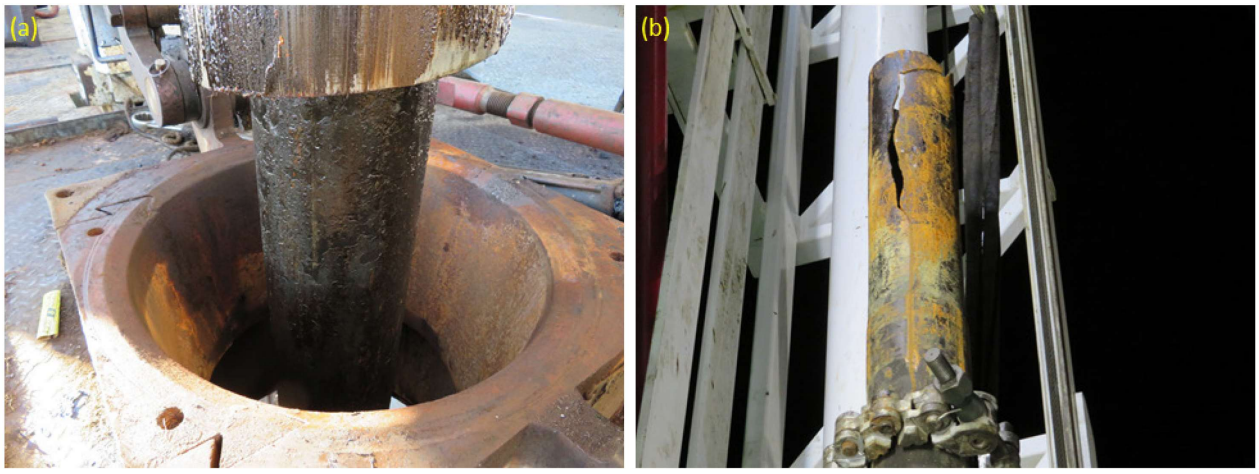


**Figure 39: Lower Section of the Parted 7 in. Casing (a) In and (b) Out of the Pawl Tool**

Figure 40 (a) and (b) show the axial rupture and circumferential parting on the 7 in. casing. The axial rupture was surrounded by a corrosion feature and was located below the circumferential parting. Wall thinning, along with bulging was observed near the middle of the axial rupture. The axial rupture had one lower arrest point away from the circumferential fracture, adjacent to the connection. The upper portion of the axial rupture turns similar to the lower arrest point, but was connected to the circumferential parting by an inclined fracture surface.

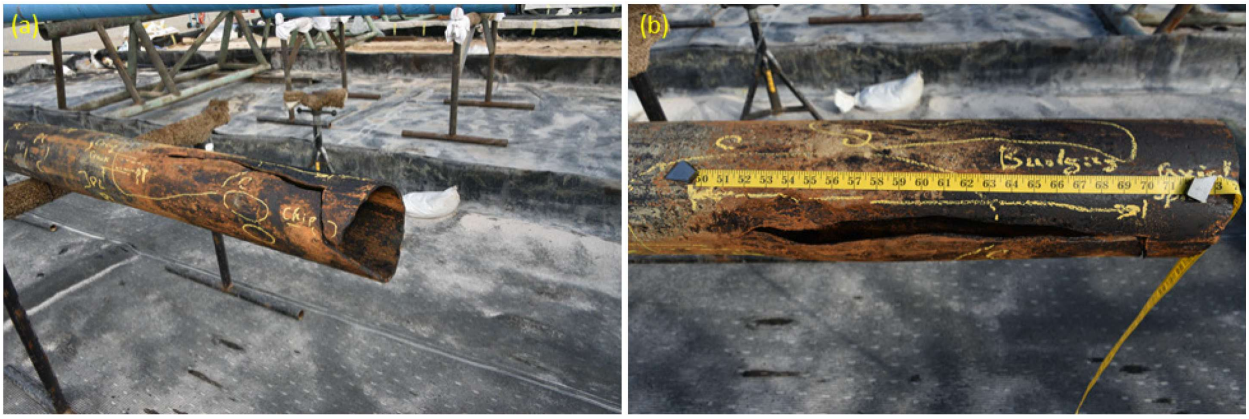


**Figure 40: Axial Rupture and Circumferential Parting (C023A)**

The fracture surface was covered with oil deposits and scale products but features were identifiable. Figure 41 (a), (b), and (c) show surface features, chevron marks, and other features, respectively.

C023A was preserved in the as-recovered condition and cut into smaller sections for transportation. A 5.8 ft section (C023A1) containing the axial rupture, circumferential parting, and connection was cut using the cold cutter. Figure 42 shows a diagram summarizing the cuts made to C023 and C024.


**Figure 41: Circumferential Parting Fracture Surface (a) Features, (b) Chevron Marks, and (c) Surface Erosion**

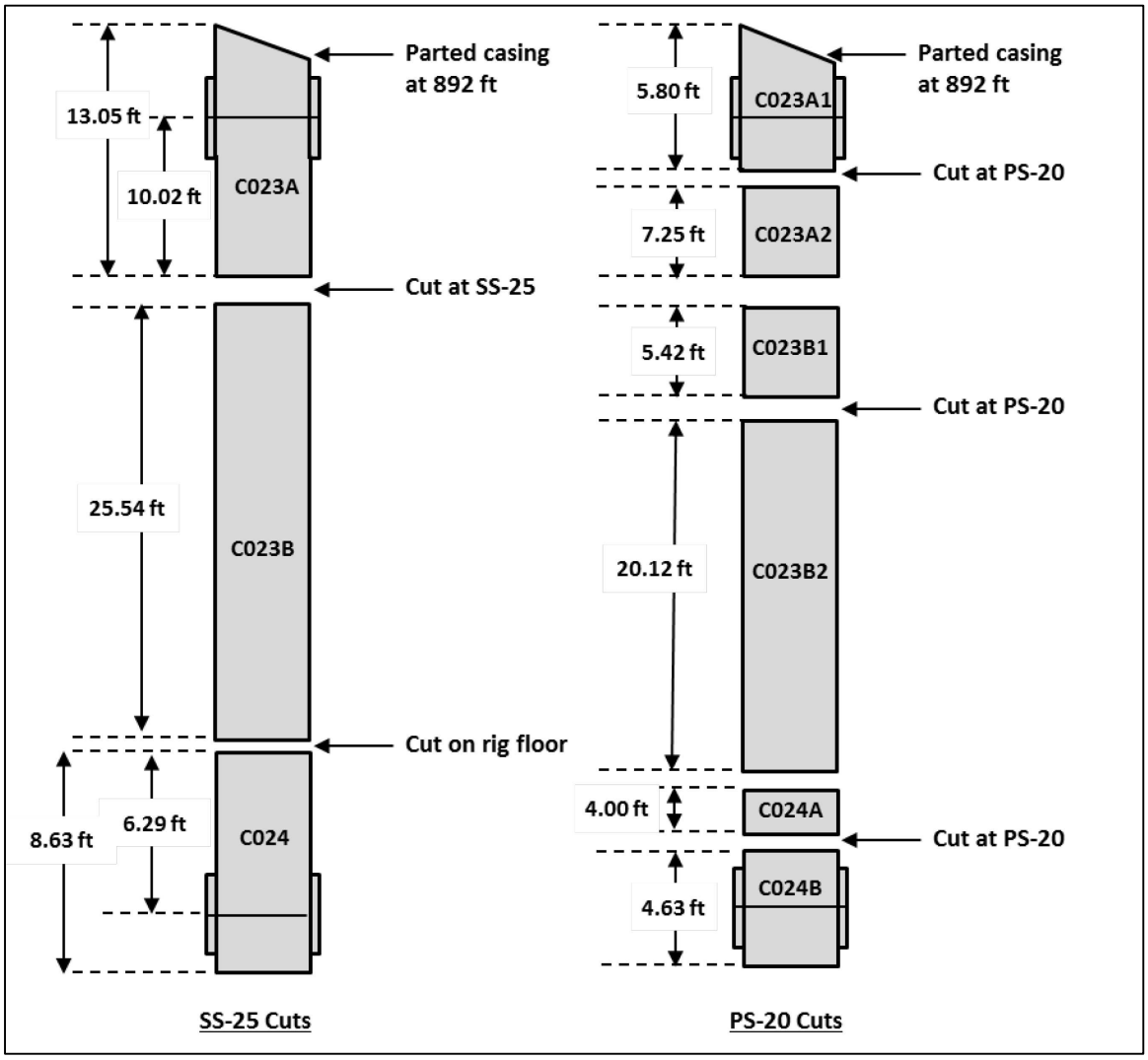


**Figure 42: C023 and C024 Cut Diagrams**

The top 23 joints (926 ft) of 7 in. casing were recovered in November 2017, leaving the top of the 7 in. stub 51 ft above the 11 3/4 in. shoe at 990 ft. The final two joints (C025 and C026) were extracted on August 08, 2018 after completing several other well operations.

## 2.4 Failure Events and Sequence

### 2.4.1 Overview and Summary

Figure 43 shows a schematic of the locations and depths for the 25 joints of 7 in. production casing extracted for the RCA. Depths are based on consolidation of data from downhole tools and physical measurements. The official depth for the circumferential parting is 892 ft, as the schematic shows. It is also apparent from Figure 43 that the 7 in. production casing was extracted from just below the shoe of the 11 3/4 in casing. Joint 24 and part of joint 25 were the last joint samples with OD corrosion as identified by the log data. Joint 22 exhibited the failure, which included the axial rupture and circumferential parting. Specimens taken from the axial rupture and circumferential parting were analyzed in detail to characterize the failure and define the failure sequence. Figure 44 shows the field photographs taken during extraction with a schematic of the axial rupture and circumferential parting. The image shows the failed casing oriented as it was in the well with the axial rupture below the circumferential parting.

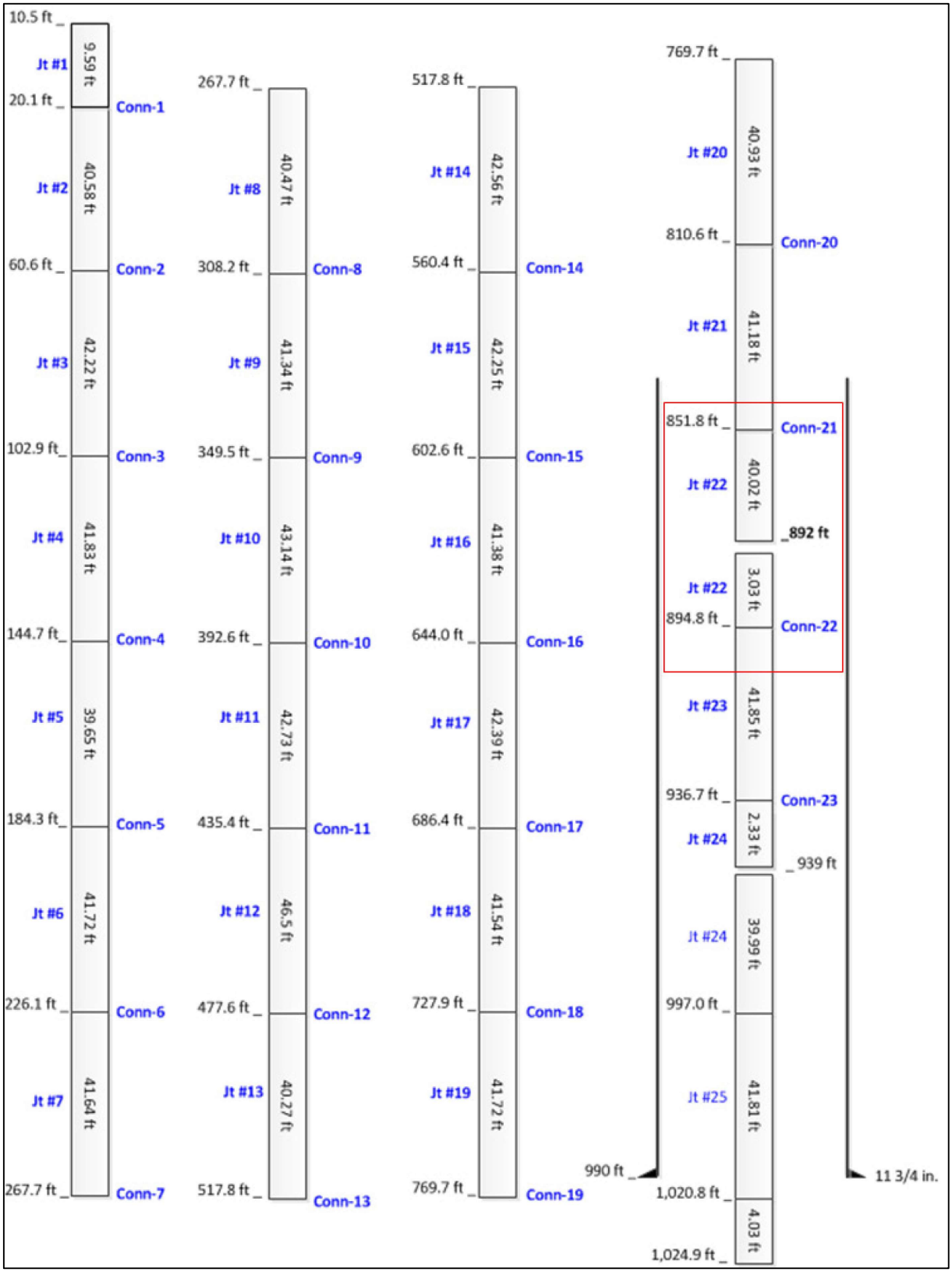


**Figure 43: SS-25 7 in. Casing String Schematic**

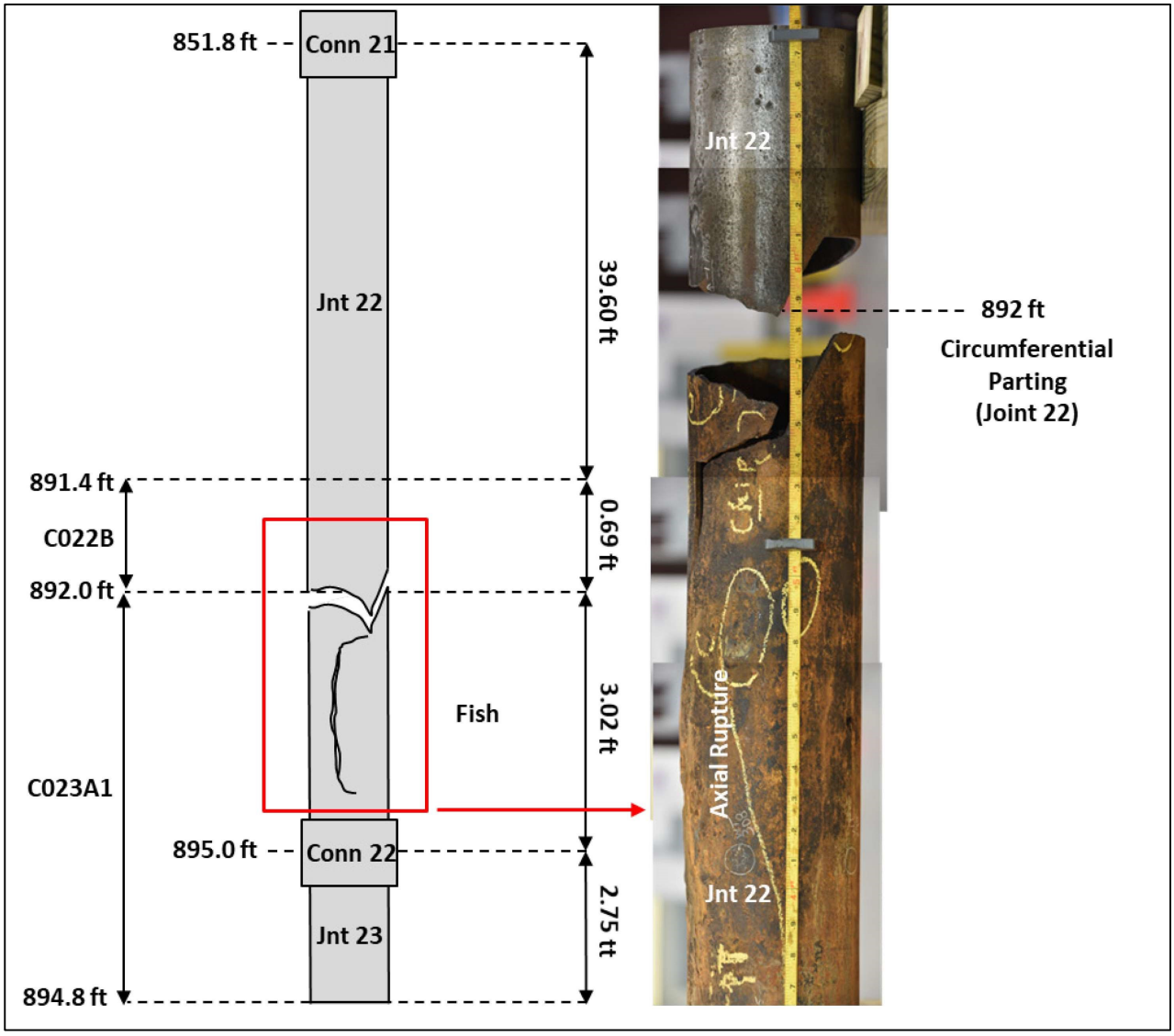


**Figure 44: Schematic and Photo of the Axial Rupture and Circumferential Parting (Joint 22)**

The laboratory examination showed that the 7 in. casing failure originated from an 85% wall loss area due to corrosion. The corroded casing failed, resulting in a 2 ft long axial rupture. Figure 45 (a) and (b) show the bulging and corrosion associated with the axial rupture.

The visual examination showed that during the axial rupture, plastic bulging occurred first, along with slow ductile tearing due to the internal pressure. Tearing instability occurred once the axial flaw reached the critical size, followed by rapid crack propagation in the axial direction. The crack changed direction (upper and lower turning points) and finally arrested due to dynamic energy consumption [14] [15] [16]. There were two turning points on both the upper and lower side of the rupture.

Figure 46 (a) and (b) show a close-up and laser scan image of the axial rupture. The failure origin is indicated by the white box. The direction of crack propagation is indicated on both sides of the origin by white arrows. The upper and lower crack arrest points are indicated by the green circles.

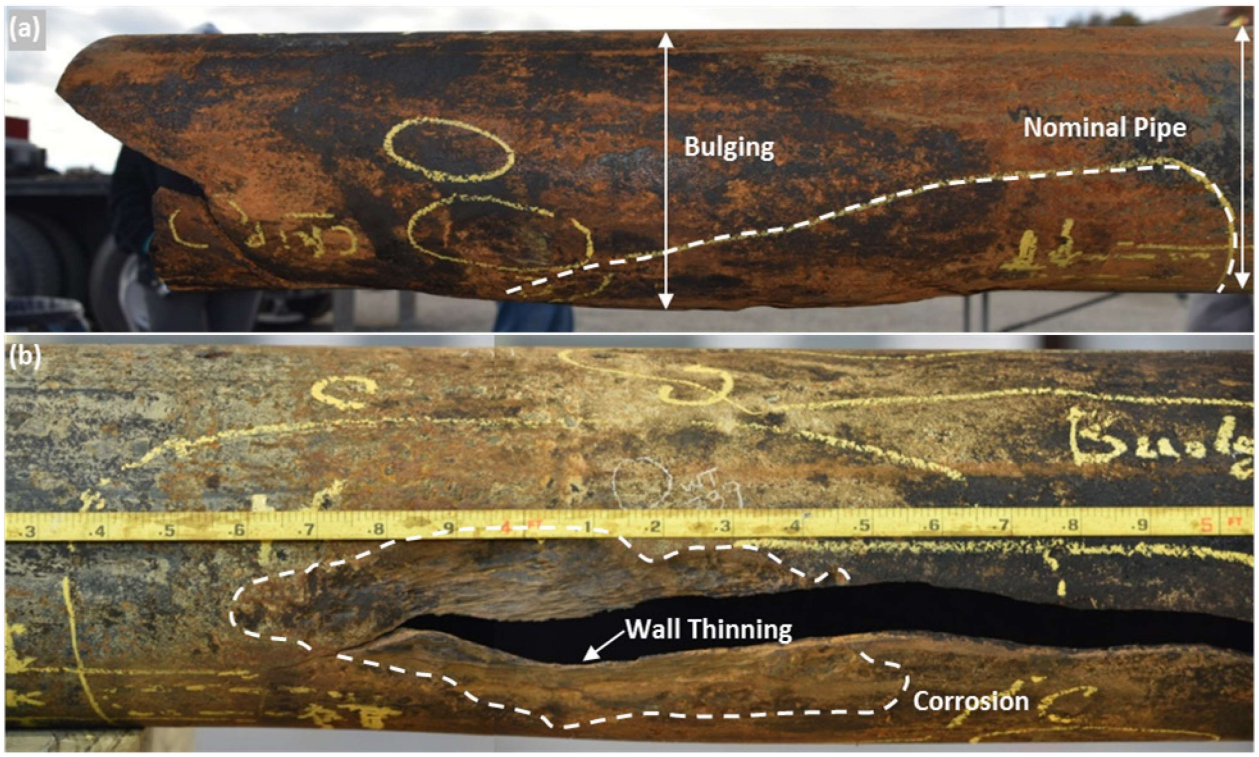


**Figure 45: Images of Axial Rupture Showing (a) Bulging and (b) Corrosion Associated with the Axial Rupture**

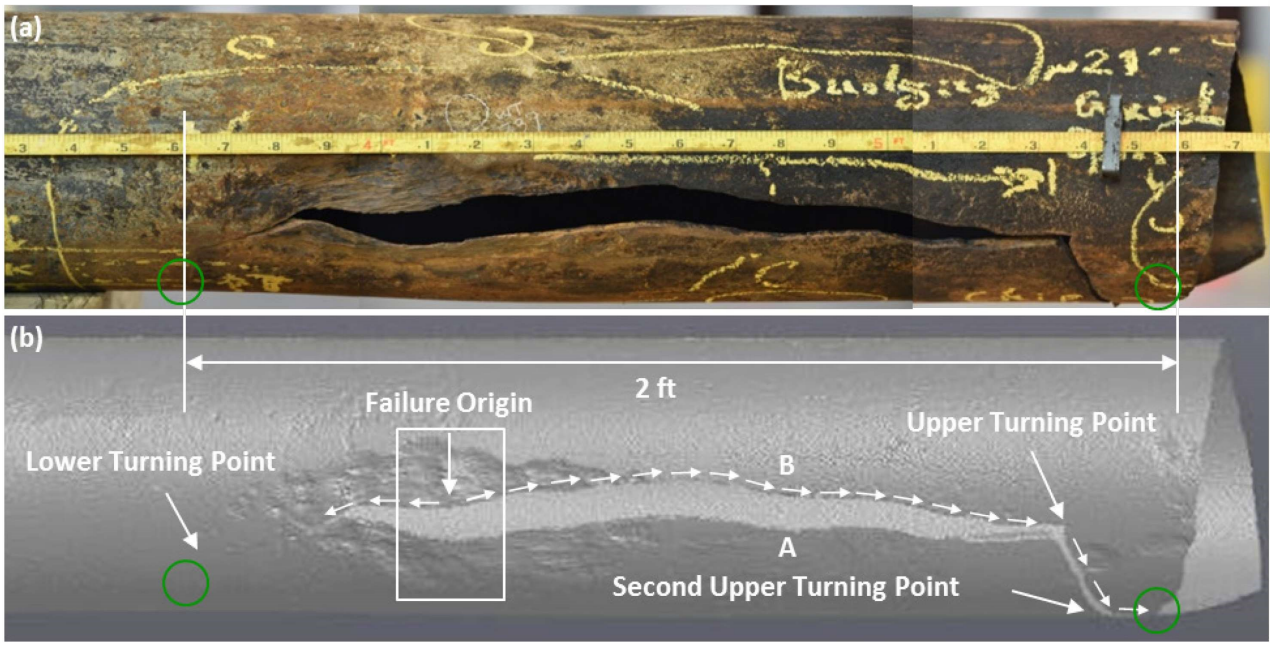


**Figure 46: (a) Field Photo and (b) Laser Scan Indicating the Origin, Lower and Upper Turning Points, and Lower and Upper Arrest Points**

The axial rupture occurred at an estimated temperature of 80°F. This estimate was based on the historical temperature profile data at the failure depth of 892 feet. This estimated temperature is consistent with the observed bulging and ductile tearing associated with the axial rupture failure.

Visual and stereoscopic examination of the circumferential parting showed that the failure was not a continuation of the axial rupture, but rather re-initiated near the corner on one side of the parted casing. The origin site was determined based on chevron marks identified on the fracture surface. Figure 47 is a (a) laser scan and (b) image which identifies the upper arrest point, circumferential parting initiation site, and the final overload failure. Figure 48 is stitched stereo images showing the chevron marks and propagation direction of the circumferential parting. These observations indicate that the axial rupture and circumferential parting were two separate events despite their close proximity, and that they are most likely related to each other. This is discussed in more detail later within this section.

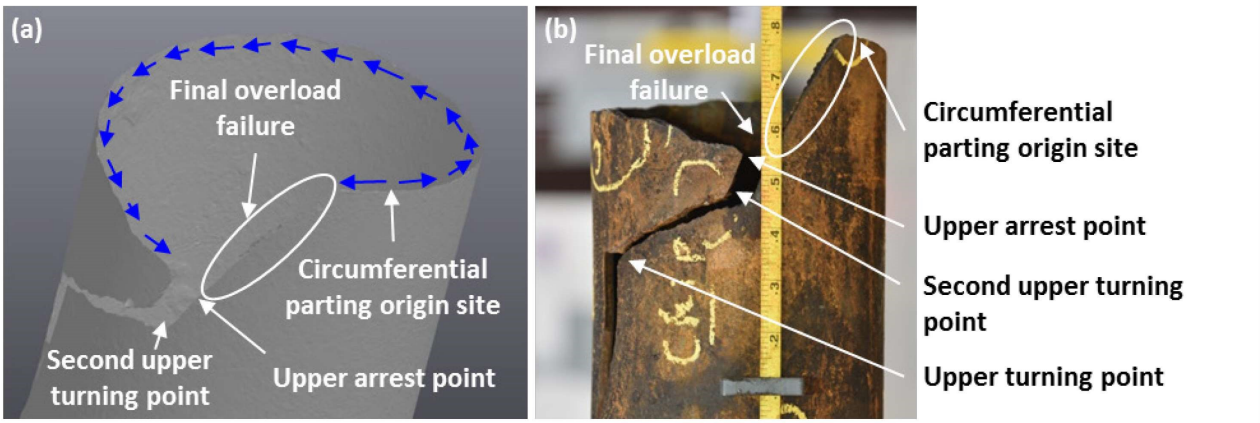


**Figure 47: (a) Laser Scan and (b) Photo Indicating Circumferential Parting Initiation Site and Final Failure**

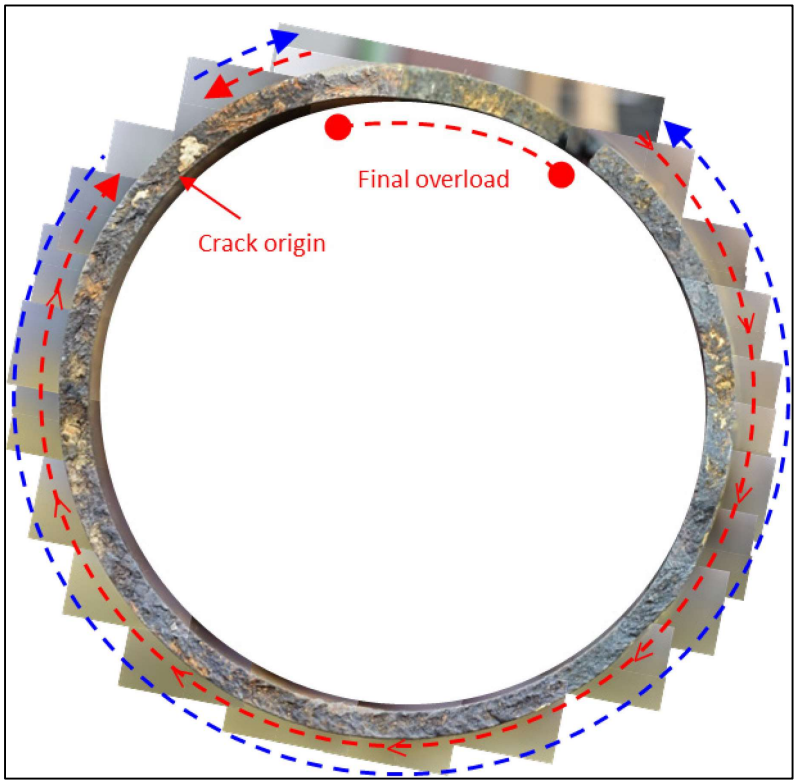


**Figure 48: Stitched Images of the Lower Circumferential Parting Fracture Surface**

The circumferential parting was brittle, which was different from the axial rupture. No evidence of local plastic deformation or overload necking was observed near the fracture surfaces on either side of the circumferential parting.

The previously discussed evidence and the detailed metallurgical investigation presented later in this section suggest that the circumferential parting of the 7 in. casing is a consequence of the axial rupture. The failure sequence for the axial rupture and circumferential parting is as follows:

1. An axial rupture occurred from an 85% metal loss due to corrosion.
2. Highly-compressed natural gas was released from the opening of the newly formed axial rupture.
3. Rapid cooling occurred due to the expansion of the gas from high to low pressure (Joule-Thomson effect).
4. The steel was brittle at the lower temperatures, and a crack initiated from a small flaw under the axial tensile loading, which resulted in circumferential parting.

Figure 49 is a schematic based on the laser scan data of C023A1, which illustrates the failure sequence for the axial rupture and circumferential parting. The full cleavage fracture mode was examined, and a temperature for the circumferential parting was estimated to be in the range of –76°F to –38°F (–60°C to –39°C).

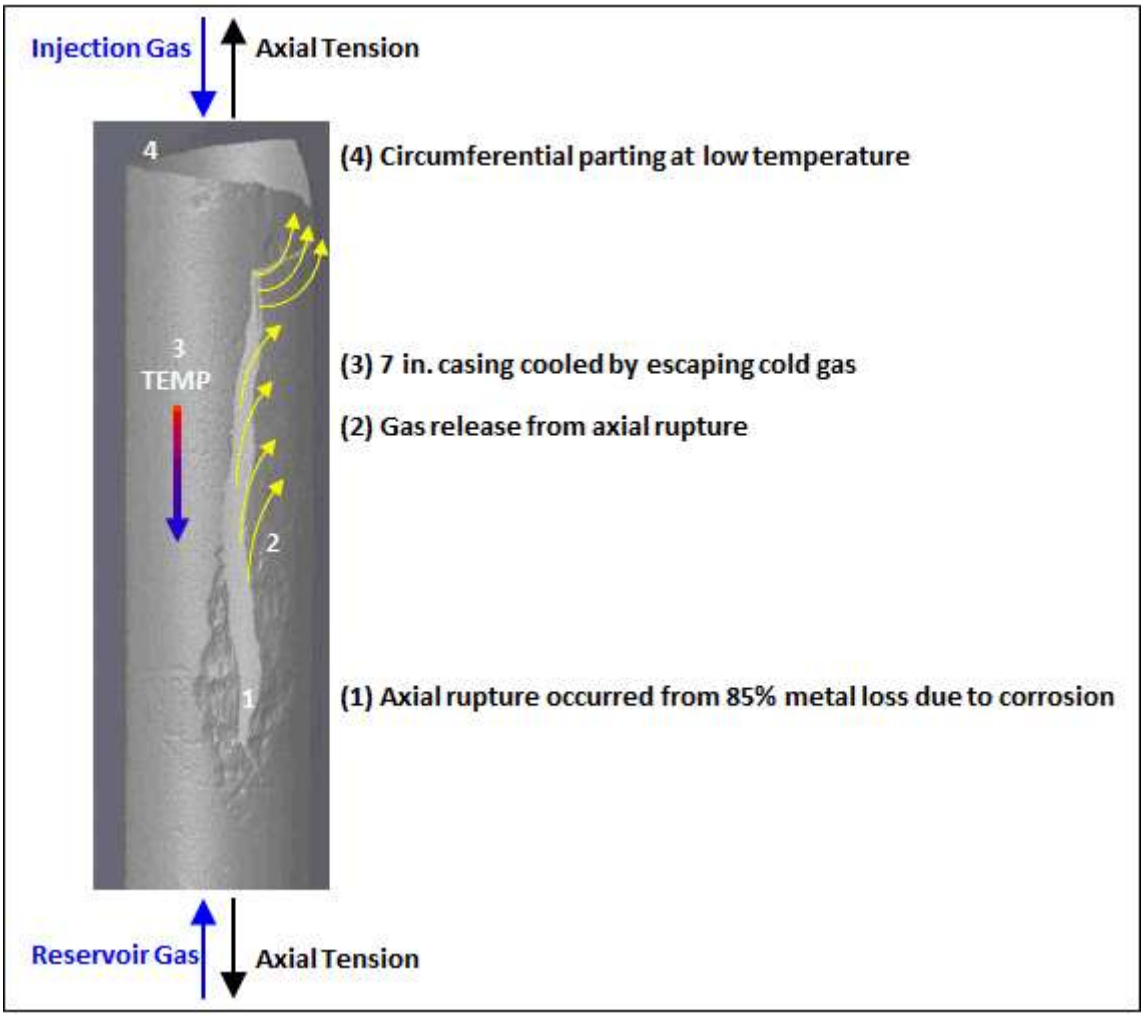


**Figure 49: 7 in. Casing Failure Sequence Schematic**

## 2.4.2 Axial Rupture Analysis

This section presents the investigation details for the axial rupture. Macroscopic (visual and stereo) and microscopic (optical and scanning electron microscope [SEM]) examinations were conducted. Results from the examinations were used to characterize the fracture surface and identify the cracking mechanism.

### Visual and Stereoscopic Examination

The axial rupture produced two mating fracture surfaces denoted as fracture surface A and B. Figure 46 (b) is a schematic based on laser scan data, which identifies key features of the axial rupture. Fracture surfaces A and B are identified in Figure 46 (b). Fracture surface A appeared to have experienced more plastic deformation (bulging) than fracture surface B. The following three fracture zones were identified based on the visual and stereoscopic examinations:

- Zone 1: Axial rupture origin
- Zone 2: Crack propagation

- Zone 3: Crack arrest

Figure 50 illustrates the three zones of the axial rupture. Zone 1 is a short section of the axial rupture, which was identified by severe wall thinning due to corrosion. Zone 2 extends from the lower and upper boundaries of Zone 1 to the boundary of the lower and upper arrest region. Lower and upper Zone 2 contained chevron marks. However, upper Zone 2 contained a featureless segment created by erosion. Zone 3 contained the lower and upper arrest region. The arrest points in Zone 3 cannot be seen in Figure 50 (a) or (b).

Zone 1 was determined based on the chevron marks in Zone 2. The apexes of the chevron marks generally point towards the origin of a failure. The chevron marks in Zone 2 pointed towards the area with the maximum metal loss. Both observations suggested that this area was the origin of the axial rupture, and it was denoted as Zone 1.

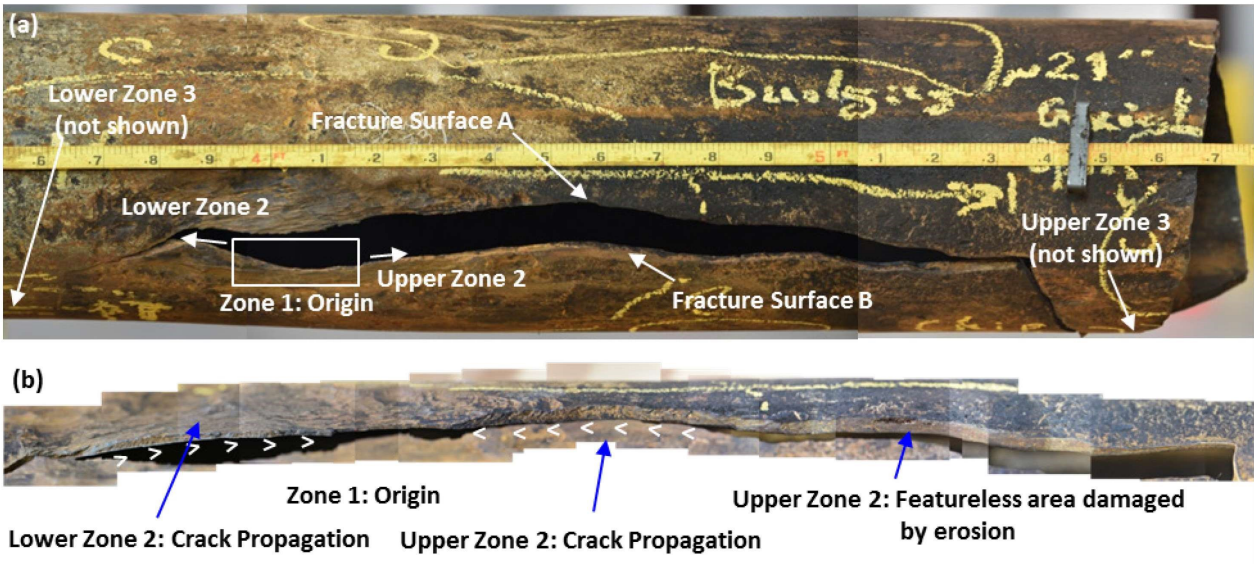


**Figure 50: (a) Front and (b) Top Views of Fracture Surface B Identifying the Three Zones**

To review the axial rupture region in some detail, a micro-fractographic assessment was undertaken with the following objectives:

- Characterization of the fracture mode for Zone 1
- Verification of the visual measurements for Zone 1
- Characterization of the fracture mode for Zone 2
- Characterization of the featureless segment of Zone 2
- Characterization of the fracture mode for Zone 3

## Micro-Fractographic Characterization of Zone 1 (Origin)

Zone 1 was the primary focus for the micro-fractographic characterization. The fracture surfaces were originally received as part of C023A1, which was a 5.5 ft section of 7 in. casing that contained the axial rupture, lower circumferential parting, connection 22, and part of Joint 23. The fracture surfaces were extracted from C023A1 using dry saw cuts. Four cuts were planned to extract the 14 in. section of the fracture surfaces. Figure 51 (a) shows a schematic of C023A1 with the four cut locations identified. Cut 1

was located through the featureless area in the upper portion of Zone 2 (above Zone 1). Cut 2 was a circumferential cut designed to remove the lower part of C023A1 from the pipe section that contained the target fracture surfaces. A 14 in. long pipe section remained after completion of Cuts 1 and 2. Cut 3 was longitudinal and extended from Cut 1 to Cut 2. Cut 3 was designed to go through the lower arrest point, which separated the two fracture surfaces and released the remaining residual stress. Cut 3 extracted fracture surface A. Cut 4 was longitudinal and extended from Cut 1 to Cut 2. Cut 4 extracted fracture surface B.

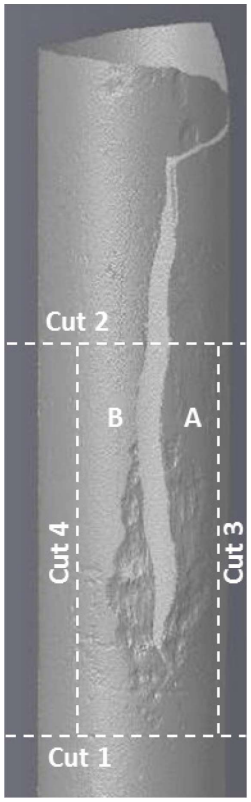


**Figure 51: Schematic of the Cut Locations Selected for Fracture Surface Extraction**

Fracture surface B was chosen for detailed examination and analysis. Fracture surface A was preserved for future study. Figure 52 shows how fracture surface B was cut into five smaller specimens. Cut locations were determined based on fracture surface features and size limitations imposed by the SEM. Fracture surface B was denoted as C023A1B2. Two specimens (C023A1B2B and C023A1B2D) were chosen for detailed examination to determine the fracture mode for Zone 1 (origin). These samples were chosen because they contained the entire origin, as well as a small portion of Zone 2 (crack propagation).

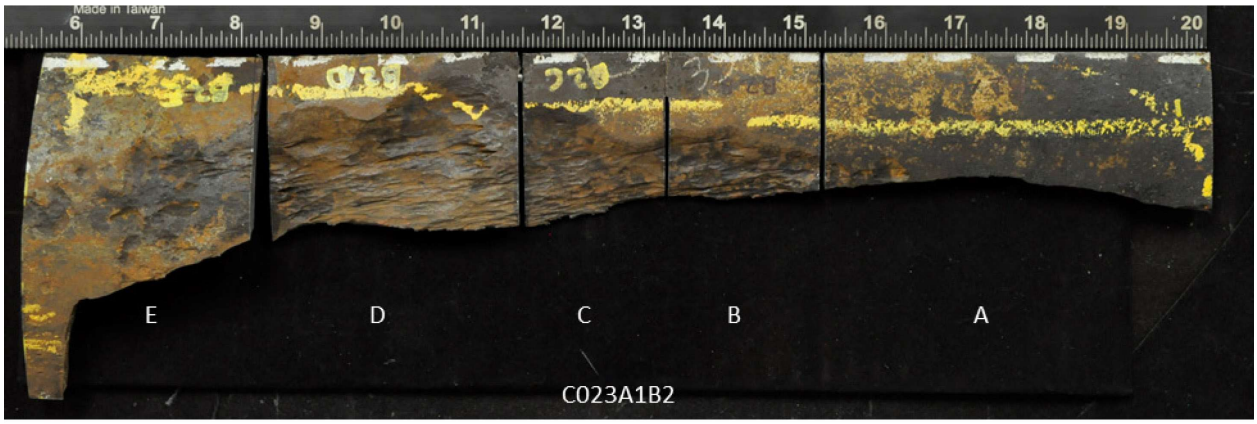


**Figure 52: Five Specimens Cut from C023A1B2 for Fractographic Study**

Following cutting, cleaning was necessary to observe the fracture surface using an SEM and make fractographic interpretations.

Cleaning requires the removal of contaminants and corrosion deposits while preventing corrosion damage to the fracture surfaces. A cleaning procedure was developed and tested to ensure both effectiveness and safety. The specimens were initially cleaned in an ultrasonic acetone bath for 3–5 minutes for degreasing and to remove loose contaminants and deposits. The specimens were then ultrasonically cleaned in a 1% Citranox bath for 3–9 minutes. Citranox was chosen based on Blade's experience and industry practice. Citranox is effective at removing metal oxides, corrosion deposits, and contaminants with minimal effect on the fracture surface [16].

Freshly produced fracture surfaces from Charpy V-notched (CVN'd) specimens were used to verify the cleaning procedure. The Charpy specimens were grade J55 steel from casing material extracted from the well. SEM examination of the fracture surface after cleaning found no resolvable attack at magnifications up to 1,000X. The Charpy and fracture surface tests showed that cleaning times up to 9 minutes could be used with minimal damage to the fracture surface.

The initial examination of the axial rupture suggested that the origin experienced ductile tearing based on the bulging and 85% wall loss caused by corrosion. Detailed fractographic investigation was undertaken to assess the nature of the surfaces.

C023A1B2C and C023A1B2D were examined with the SEM at several locations and magnifications to identify the fracture mode of the origin (Zone 1). Figure 53 shows the areas of interest (AOI) chosen during the SEM examination. C023A1B2C contained most of the origin and was selected for detailed examination. Figure 54 and Figure 55 are SEM images of two AOIs (A8 and A17) that represent the typical features identified in the origin during the examination. The images show woody-type morphology, deformation markings, possible dimples, and pearlite-like features. Cleavage and grain boundary facets were not observed in any of the AOIs in the origin.

A transition from ductile to a ductile–brittle mix was observed beginning at A19 (Figure 53). The transition showed a shift from a woody-type morphology to a mix of woody-type morphology and cleavage. The amount of cleavage facets appeared to increase from location A19 to A27. The observations implied that the speed of the axial rupture was increasing through the transition zone until the crack became fully unstable. Figure 56 is a SEM image from A19 showing the ductile–brittle mixed fracture mode. The images show areas of cleavage facets and deformation markings.

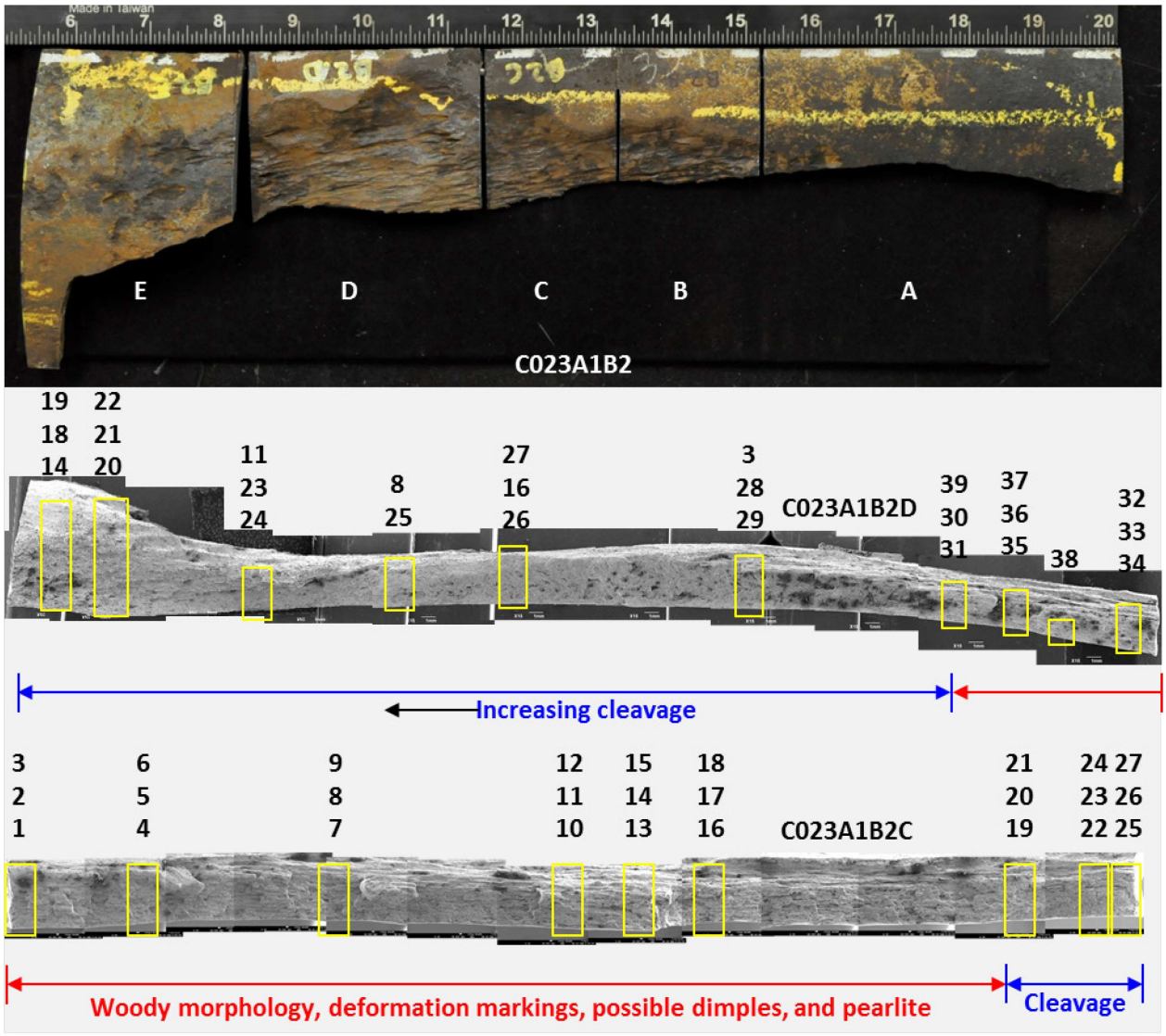


Figure 53: SEM Examination of the Cleaned Fracture Surfaces of C02A1B2C and B2D

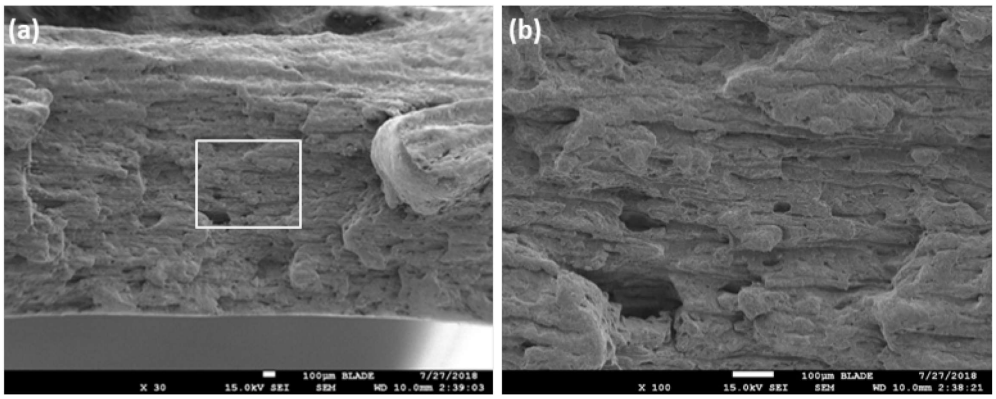


Figure 54: SEM Images of Area 8 Taken at (a) 30× and (b) 100×

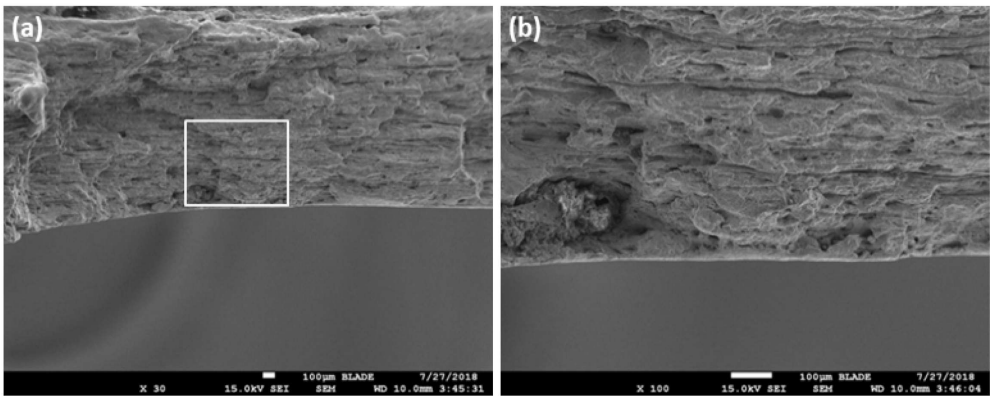


**Figure 55: SEM Images of Area 17 Taken at (a) 30× and (b) 100×**

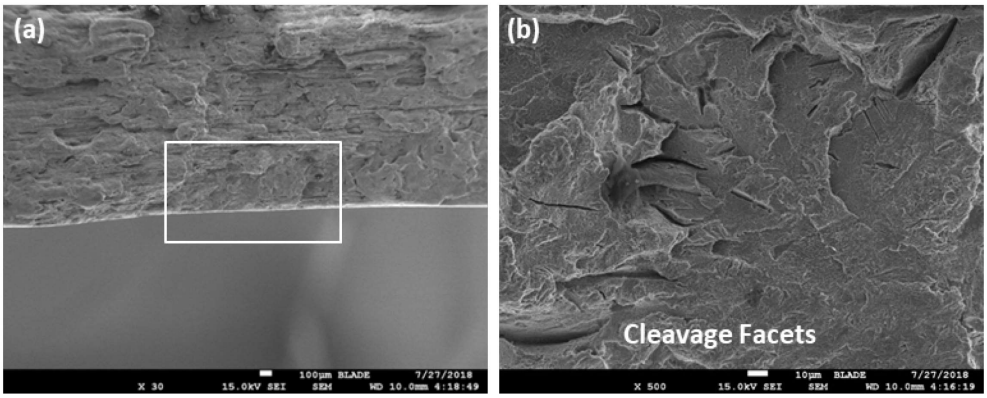


**Figure 56: SEM Images of Area 19 Taken at (a) 30× and (b) 500×**

The initial examination of the axial rupture suggested that the origin experienced ductile tearing based on the woody-type morphology and deformation markings. The fracture surface produced by J-R ductile tearing tests were used to confirm the ductile tearing observed in the origin. Specimen L4-000 was tested at room temperature, which was comparable to the downhole temperature at the time of the axial rupture. Figure 57 shows SEM images taken at 100× showing the woody-type morphology. Higher magnification images showed the dimpled nature of the surface.

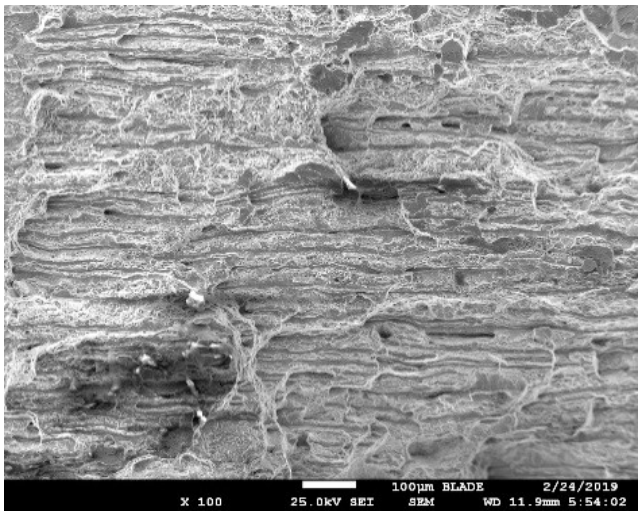

**Figure 57: SEM Images of J-R Specimen L4-000 Taken at 100×**

## Zone 1 Size Refinement

The origin was originally defined based on metal loss measurements and chevron marks identified on the fracture surface. The origin length based on this criterion was measured at 4.8 in. (123 mm). The origin was redefined based on micro-scale features identified on the fracture surface. The micro-scale-based measurement was defined as the length of fracture surface that exhibits fully ductile tearing with no cleavage facets. The origin length based on the new micro-scale definition was 2.13 in. (54 mm). Figure 58 shows the Zone 1 measurements for C023A1B2C and C023A1B2D based on the new origin definition. The origin was measured as 0.55 in. (13.9 mm) and 1.52 in. (38.7 mm) for C023A1B2C and C023A1B2D, respectively. The kerf from the saw cut was approximately 0.06 in. (1.4 mm). The measurements result in a total Zone 1 length of 2.13 in. (54.0 mm). The initial origin length was reduced by more than a factor of two.

The length difference of the origin based on the micro (SEM) and macro (visual) definitions reflects the difference in the role they played for the axial rupture. The micro definition measurement of 2.13 in. represents the initial size of the crack origin. The macro definition measurement of 4.8 in. represents the rapid propagation of the crack as indicated by chevron marks.

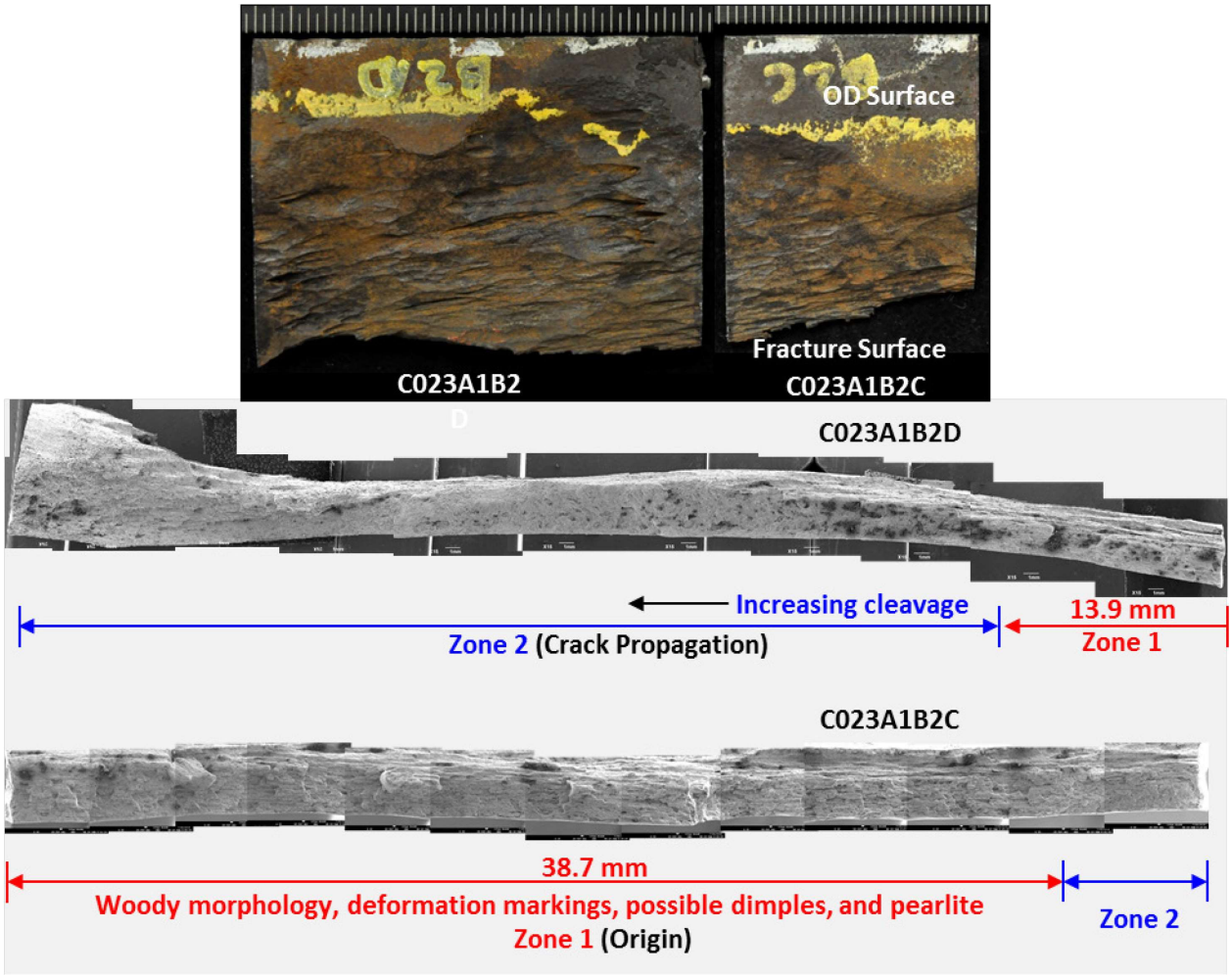


**Figure 58: Origin Measurements Based on Micro Definition for C023A1B2C and C023A1B2D**

A metallographic cross section was made to accurately measure the minimum remaining wall. The origin specimens (C023A1B2C and C023A1B2D) were visually examined to identify the thinnest area. The selected area was cross-sectioned, mounted, and polished for examination with a microscope. Figure 59 shows the location of the (a) metallographic section of C023A1B2C and the (b) measured remaining wall thickness on the polished specimen. The measured remaining wall was 0.0496 in. (1.26 mm), and the measured wall thickness of the unaffected area was 0.321 in (8.15 mm). The calculated maximum metal loss, or maximum corrosion depth, was 85% actual wall thickness. The refined measurement of 0.0496 in. was accurate and was used as an input parameter for failure pressure calculations.

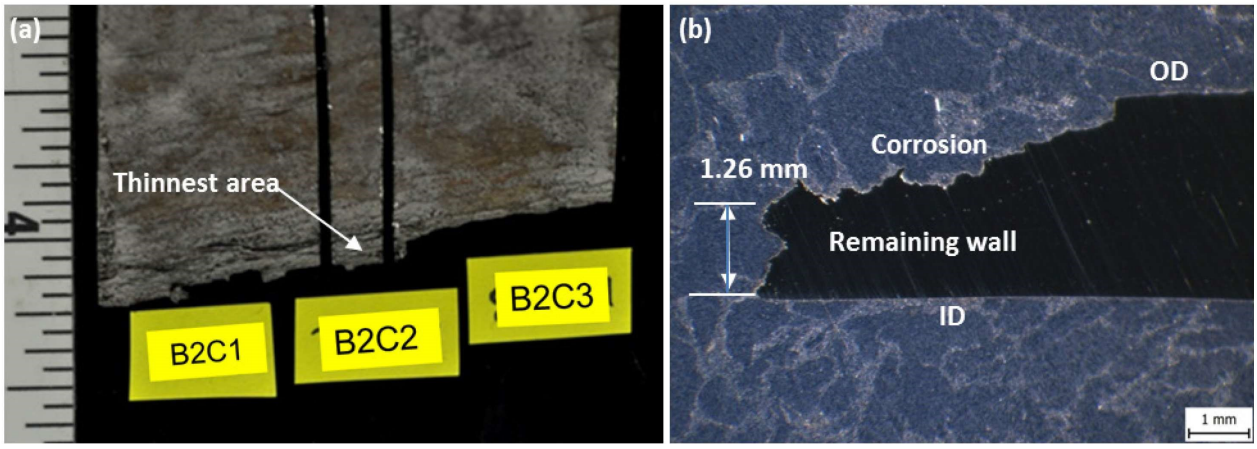


**Figure 59: (a) Macro and (b) Metallographic Image of C023A1B2C2 Showing the Remaining Wall**

Ductile tearing and bulging could have contributed to the remaining wall measurement by ductile deformation. The measured remaining wall would then have been a combination of the original metal loss due to corrosion and thinning caused by the axial rupture. Cross-sections adjacent to the fracture surface were examined to determine if bulging and ductile tearing contributed to the remaining wall thickness measurement. Detailed metallographic examination confirmed that the grains appeared equiaxed and not elongated. Therefore, the remaining wall loss of 85% was caused by metal loss due to corrosion.

## Micro-Fractographic Characterization of Zone 2 (Crack Propagation)

Zone 2 (crack propagation) was generally characterized by chevron marks on both sides of the origin. Chevron marks are evidence of rapid propagation of a mixed ductile–brittle fracture mode, at the micro-scale, during rapid crack propagation [17] [18]. The direction of the crack propagation is opposite to the apex of the chevron marks. This section describes the micro mechanism for crack propagation of Zone 2.

Zone 2 was separated into two sections by Zone 1. The two sections are referred to as Upper and Lower Zone 2 in reference to the zones' relative position in the SS-25 well (Figure 60). Lower Zone 2 was examined first with a detailed SEM examination of specimen C023A1B2D. Figure 60 also shows the C023A1B2D fracture surface before (middle) and after (lower) cleaning.

The SEM examination showed a mixed fracture mode that consisted of cleavage (brittle) and micro-void-coalescence and dimples (ductile). The amount of cleavage increased with distance from the origin, but decreased as the crack approached the lower turning point. Figure 61 shows typical SEM images taken from locations in Zone 2.

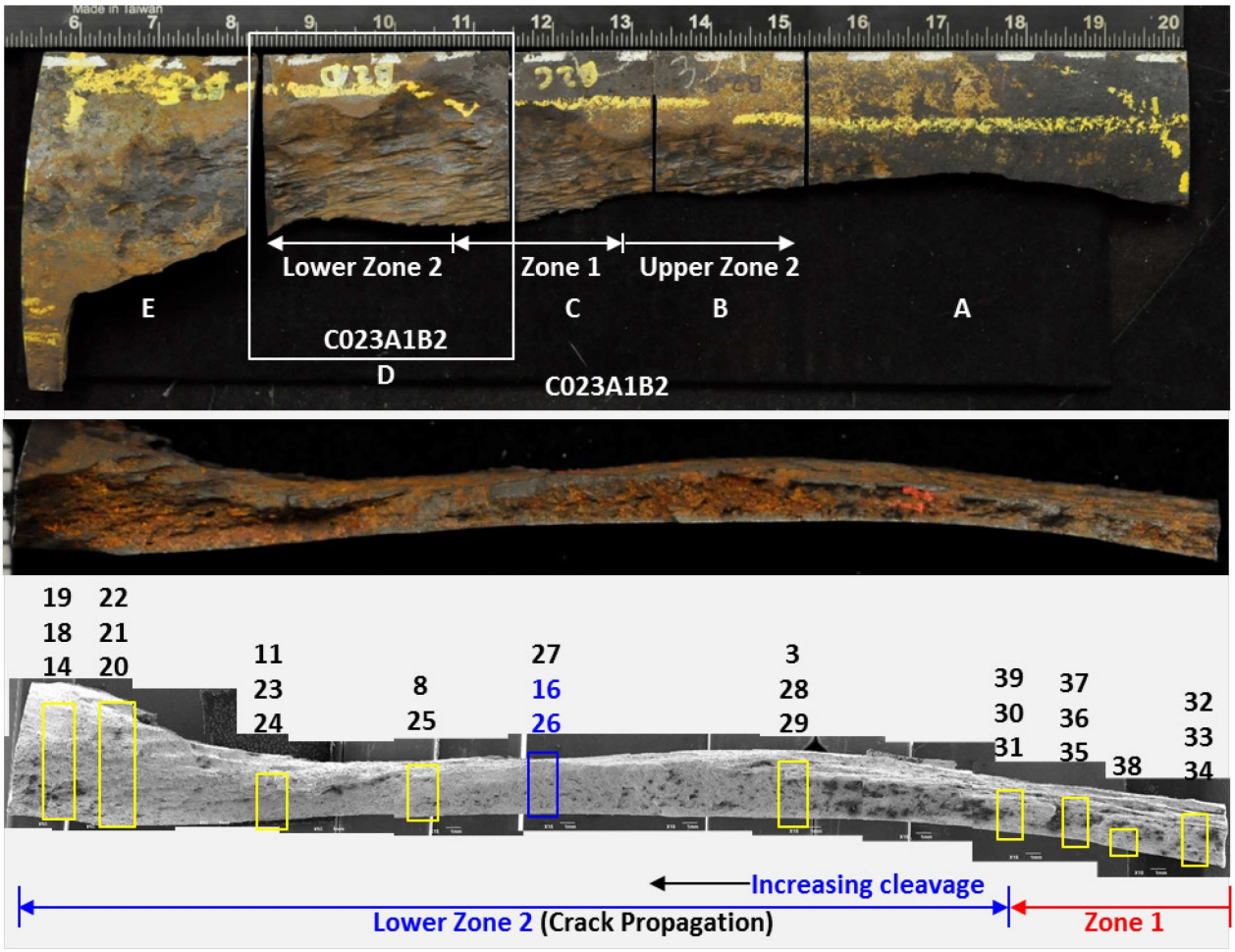


Figure 60: Images Showing Division Between Zone 1 and Lower and Upper Zone 2

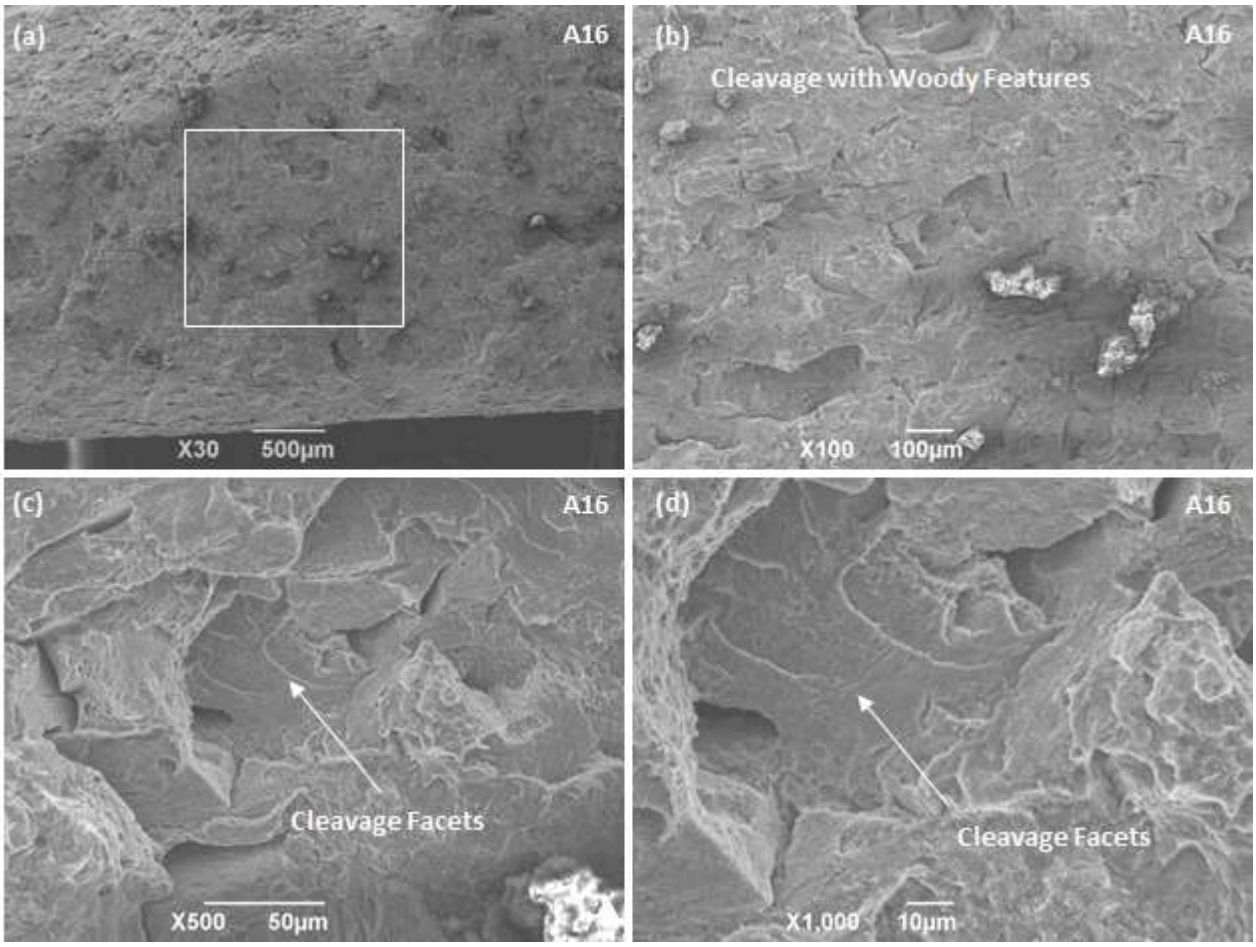


**Figure 61: SEM Images from Locations A16 and A26 Showing Mixed Fracture Mode**

The occurrence of cleavage in Zone 2 is understandable. In body-centered cubic metals, such as mild steels, cleavage is promoted by low service temperature, high strain rate, presence of stress concentrators (stress state), specimen size, material (composition and microstructure), and certain environments. The 7 in. casing axial rupture failure occurred at an approximate temperature of 80°F, which would not have caused cleavage during slow loading. Based on this observation, the main contributing factors for promoting cleavage were related to strain rate.

Half-size CVN tests were conducted at various temperatures for material extracted from the SS-25 7 in. casing joints. The measured average ductile-to-brittle transition temperature (DBTT) based on impact energy is 87°F (30.8°C), indicating that the material was susceptible to brittle failure. On the other hand, the strain rate in Zone 2 was high due to the high speed of crack propagation after the critical crack size was reached, and tearing instability occurred. The evidence suggests that the high strain rate and a DBTT value of 87°F contributed to the cleavage observed in Lower Zone 2.

Upper Zone 2 was also examined with the SEM, and the examination showed a mixed mode fracture containing cleavage and micro-void-coalescence (MVC, dimples), which was consistent with the Lower Zone 2 observations.

## Characterization of Featureless Segment of Upper Portion Zone 2

Upper Zone 2 contained a 9 in. long featureless region in addition to a region with chevron marks. The 9 in. featureless region appeared relatively smooth with no visible chevron marks. Visual examination of the featureless region suggested that the fracture surface had been eroded due to escaping gas caused by the axial rupture. Figure 62 shows an overview of Upper Zone 2. Fracture surfaces A and B are mating surfaces of the rupture, which show the Upper Zone 2 featureless segment. Fracture surface A was used to characterize the fracture surface, while B was preserved for future investigations.


**Figure 62: Overview of Upper Featureless Zone**

Two specimens were investigated to characterize the Upper Zone 2 featureless region. Figure 63 is a macro photograph of the featureless region. Specimen C023A1A1B5B contained a small section of the featureless zone and the upper turning point. Specimen C023A1A1B1C contained a portion of the featureless zone directly below specimen C023A1A1B5B. Both specimens were examined in detail with the SEM.

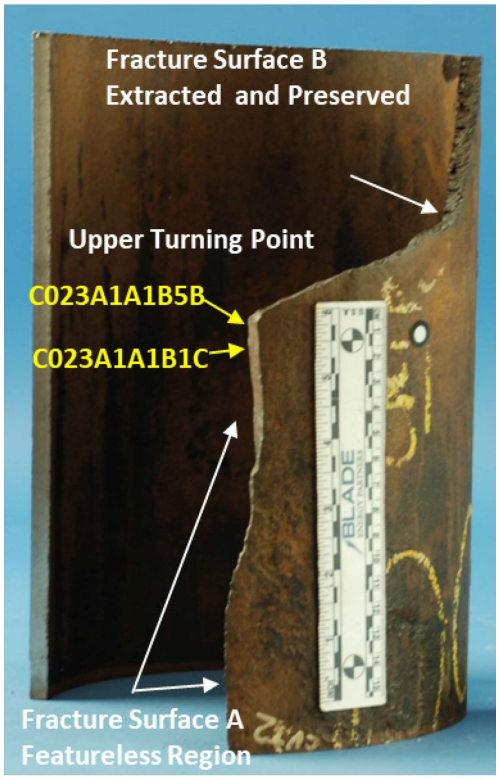


**Figure 63: Fracture Surface A Featureless Region of Upper Zone 2**

Specimen C023A1A1B5B was examined first. The specimen was extracted and cleaned ultrasonically in a 1% Citranox solution for six minutes at room temperature. SEM observations revealed an eroded fracture surface with fine erosion marks. Figure 64 shows the representative SEM images of the eroded fracture surface. Erosion marks left on the fracture surface were readily identified at magnifications above 500×. Figure 65 shows the measured width distribution of 30 randomly selected erosion marks, which were used to estimate the particle size of the solids in the released gas flow. The results showed that the erosion marks had a maximum measured width of 8 µm, and more than 60% of the erosion marks had measured widths within the range of 4–6 µm. Multiple factors contribute to the width of erosion marks, including solid particle size, hardness, brittleness, speed, and angle of impingement. The particles were assumed to be three times the size of the erosion marks. Based on this assumption, the maximum particle size was 24 µm, and more than 60% of the particle sizes were in the range of 12–18 µm. These observations confirm that the Upper Zone 2 featureless segment was produced by erosion. The observations of specimen C023A1A1B1C were consistent with C023A1A1B5B. Featureless regions were the result of erosion from high-pressure gas with sand particles.

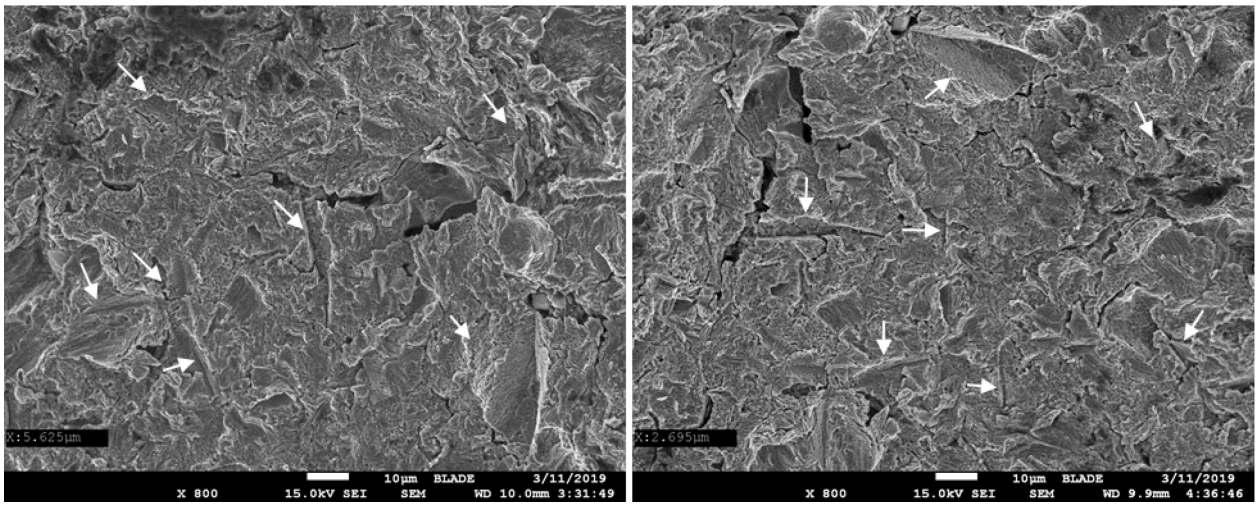


**Figure 64: Representative SEM Images of Erosion Marks (White Arrows) Taken at 800×**

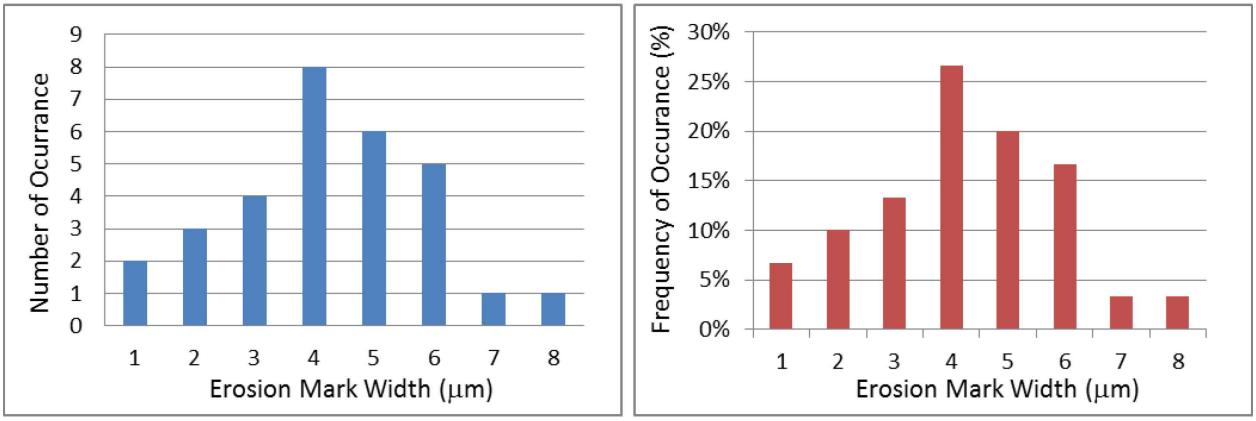


**Figure 65: Erosion Mark Width Distribution**

## Micro-Fractographic Characterization of Zone 3

Zone 3 contained the upper and lower crack arrest points. Zone 3 was divided into two areas, identified as Lower and Upper Zone 3. This is similar to what was done for Zone 2. Lower Zone 3 represents the arrest region below Zone 1 (origin), while Upper Zone 3 represents the arrest region above Zone 1. Figure 46 shows the locations of Upper and Lower Zone 3. The lower arrest point occurred after the crack underwent two directional changes (first and second lower turning points) due to energy dissipation and changes in stress state. The same sequence occurred with the upper arrest point. The lower arrest point was slightly past the second turning point, whereas the upper arrest point was approximately 2 in. beyond the upper second turning point. The difference in extension can be explained by a difference in constraint between the two locations. The lower arrest point was adjacent to connection 22, which provides additional constraint. The upper arrest point was approximately 2 ft from the lower arrest point in the pipe body. The pipe body provides less constraint as compared to the area adjacent to the connection.

SEM analysis of the lower and upper arrest regions was conducted. The lower arrest fracture surface appeared relatively smooth and flat at low magnifications. The fracture surface appeared to be faceted with some deformation marks when viewed at higher magnifications. Typical cleavage facets were not observed. This observation could be due to the fact that the original cleavage structure has been corroded away.

The micro-fractographic morphology observed in the area between the second upper turning point and upper arrest point consisted of cleavage facets and deformation marks. The OD fracture surface appears rougher than the ID side, which is consistent with more ductile deformation. Details for Zones 1, 2, and 3 of the axial rupture are discussed in the supplementary report *SS-25 Casing Failure Analysis* [19].

### 2.4.3 Initiation and Propagation of the Circumferential Parting

The results for the circumferential parting analysis are discussed in this section. The approach for the circumferential parting investigation was the same as for the axial rupture.

The circumferential parting produced two mated fracture surfaces identified as the lower and upper fracture surfaces. The upper fracture portion was designated as C022B. The lower portion of the circumferential parting was designated as C023A1.

The upper fracture surface was facing down after the parting and was severely eroded by the high-pressure gas escaping from the reservoir. The lower fracture surface was facing up during the blowout and appeared well preserved. Figure 66 (a) shows the lower and upper fracture surfaces during the visual examination. The specimens are oriented in the same position as they were in the well. The pointed section of C022B was identified as the south-facing side of the pipe on the rig floor. Figure 66 (b) shows the erosion to the upper fracture surface. Remnants of chevron marks were visible in some areas of the fracture surface. However, most of the surface appeared smooth and featureless. Figure 66 (c) shows the condition of the lower fracture surface during the examination. Chevron marks were visible and were well defined as compared to the upper fracture surface. The lower fracture surface had no indications of erosion and was later confirmed by stereo and SEM examinations.

The following three fracture zones were identified during the visual and stereoscopic examination of the circumferential parting:

- Zone 1: Circumferential Parting Origin
- Zone 2: Crack propagation
- Zone 3: Final overload failure of the remaining ligament

Figure 67 illustrates the three zones of the circumferential parting. Figure 67 (a) is a stereo image showing the three zones, origin, and the direction of the crack propagation. Figure 67 (b) is a 3D schematic showing the overall circumferential parting steps. Figure 67 (c) is a close-up of the Zone 3 fracture surface.

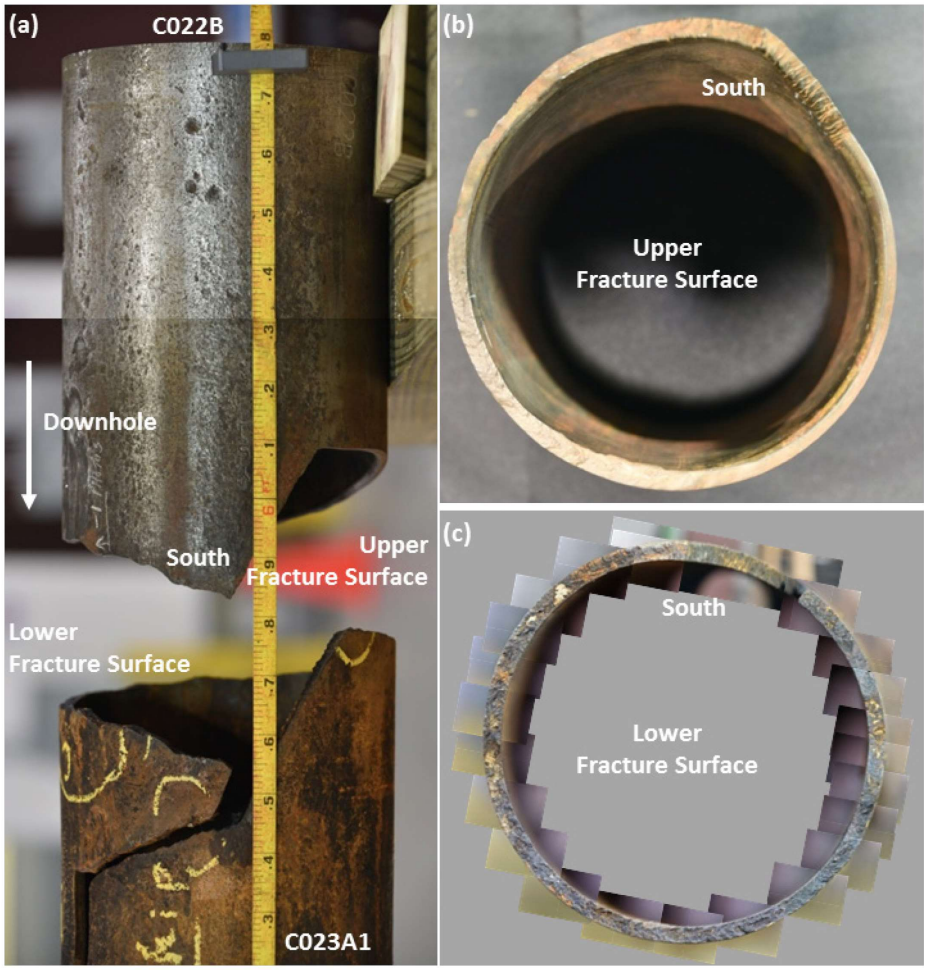


**Figure 66: (a) Circumferential Parting Showing the (b) Upper and (c) Lower Fracture Surfaces**

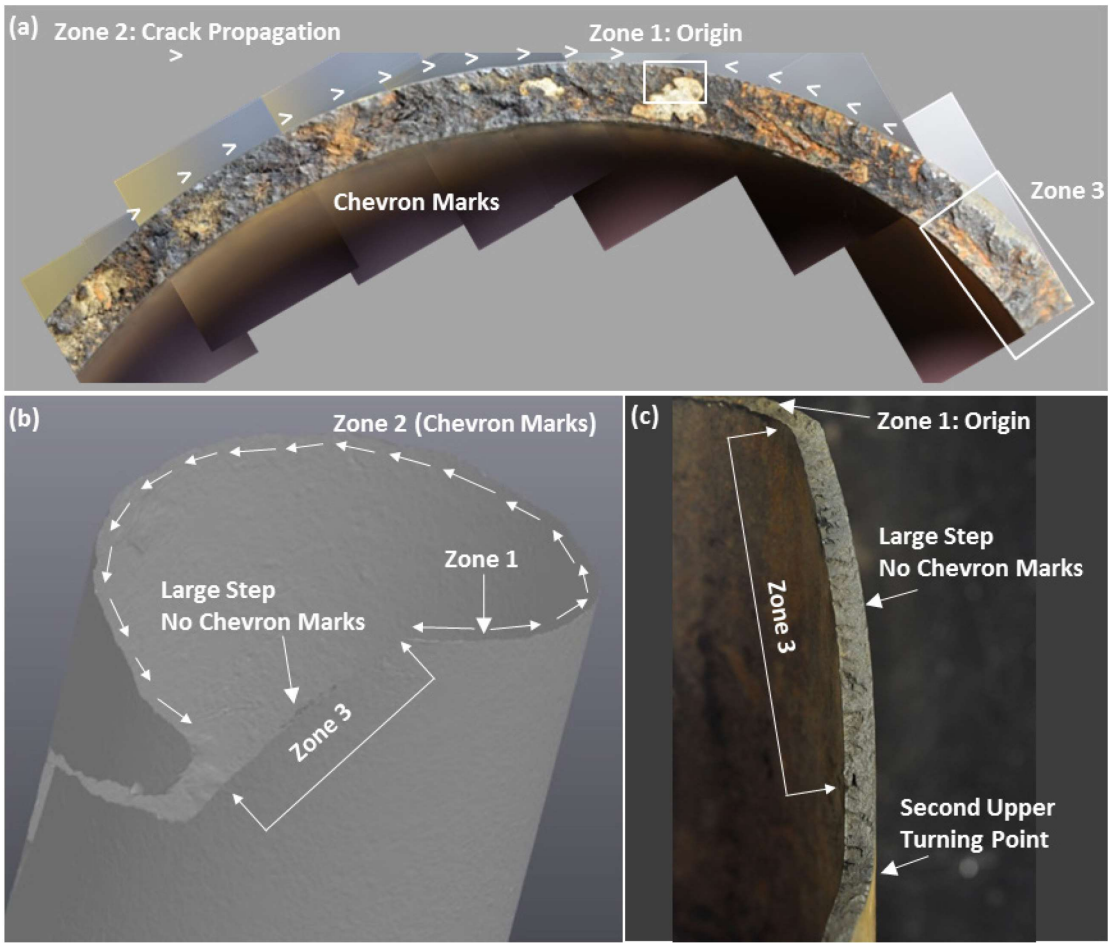


**Figure 67: (a) Stereo Image (b) 3D Schematic of Zones (c) Macro Image of Three Zones**

Zone 1 was identified based on the chevron marks observed on the fracture surface. An initial area was identified as a possible origin site based on visual and stereoscopic examinations. The proposed origin site was thoroughly examined with the stereo microscope and SEM to determine the origin size. Two semi-elliptical areas were identified as possible critical crack sizes (origin) for the circumferential parting. The first critical crack candidate was 14.55 mm long and 5.2 mm deep. There was uncertainty in identifying the fine chevron marks adjacent to the origin. A second critical crack candidate was identified, which extended just beyond the first critical crack candidate. The second critical crack candidate was 21.72 mm long and 5.22 mm deep. Figure 68 (a) shows the origin area for the circumferential parting. Figure 68 (b) and (c) show the location and sizes of the critical crack candidates.

Zone 2 was characterized by chevron marks with their apexes oriented towards Zone 1 (origin). Figure 69 shows the fracture surface in the non-cleaned condition. The chevron marks are clearly visible on a majority of the fracture surface in Zone 2. Zone 2 is identified by the dashed white circle in Figure 69. The dashed red and blue circles represent the chevron apexes and crack propagation, respectively. Zone 2 began at Zone 1 and arrested at the upper arrest point for the axial rupture. The beginning and end points for Zone 2 are indicated by the white dots at the end of the white circle.

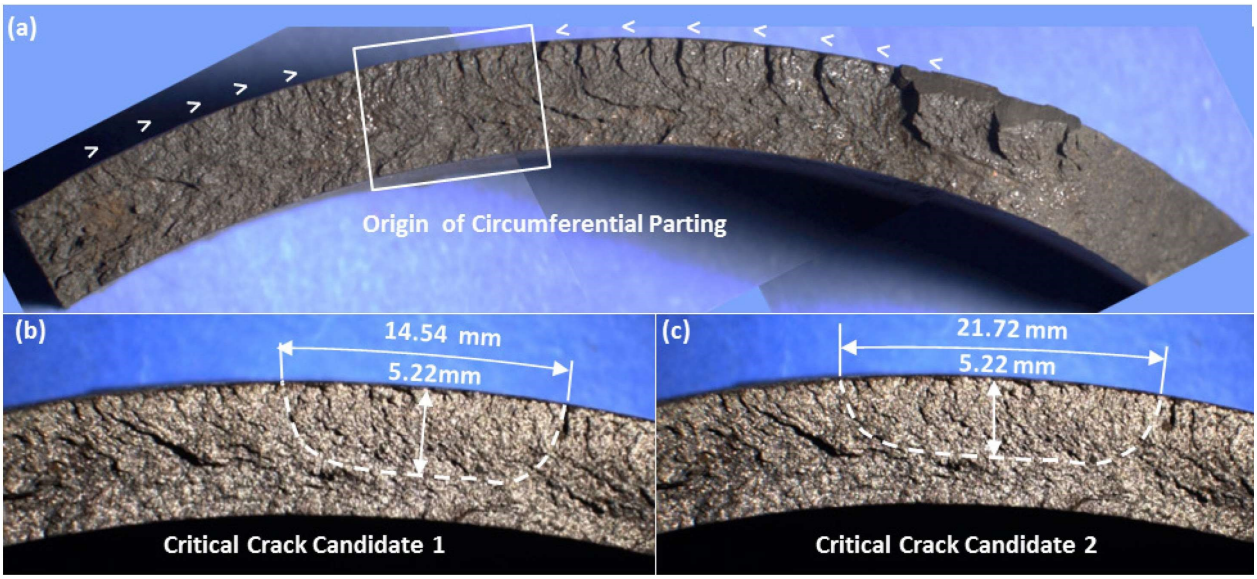


**Figure 68: Circumferential Parting (a) Origin, (b), and (c) Critical Crack Candidates**

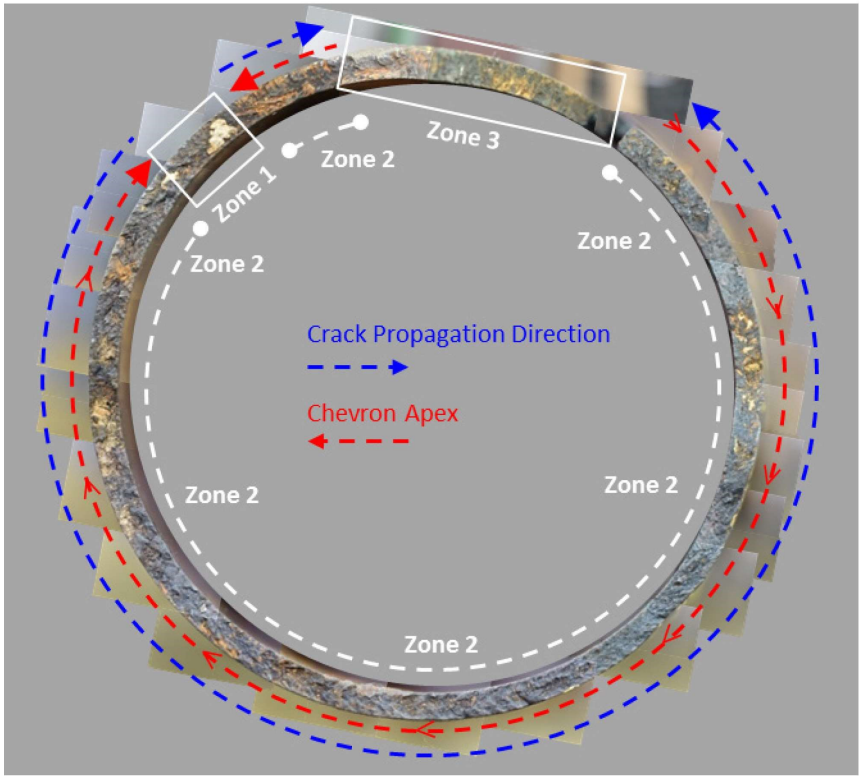


**Figure 69: Zone 2 Chevron Marks and Crack Propagation Direction**

Zone 3 was the large inclined step between the two circumferential crack tips produced by the spiral crack path. The fracture surface of Zone 3 was rough and did not contain chevron marks. The observations suggest that the fracture surface was not produced by a running crack but by an overload of the remaining ligament.

Additional detailed visual and stereoscopic examination showed that the circumferential parting was not an extension of the axial rupture. Chevron marks produced by the circumferential parting did not follow

the chevron marks produced by the axial rupture. The initiation site and chevron marks produced by the circumferential parting were located approximately 3.7 in. (94 mm) from the upper arrest point of the axial rupture. Figure 70 is a schematic of the crack path for the axial rupture and circumferential parting. The schematic shows how the circumferential parting initiated above the arrest point of the axial rupture. The crack propagated circumferentially until it reached the axial rupture arrest point. The final ligament failed due to the axial load generated by the weight and tension of the 7 in. casing string. The axial rupture and circumferential parting are thought to be two separate events because there was no evidence that the chevron marks from the axial rupture continued into the circumferential parting. The close proximity of the two failures suggests that they are related despite being two separate events.

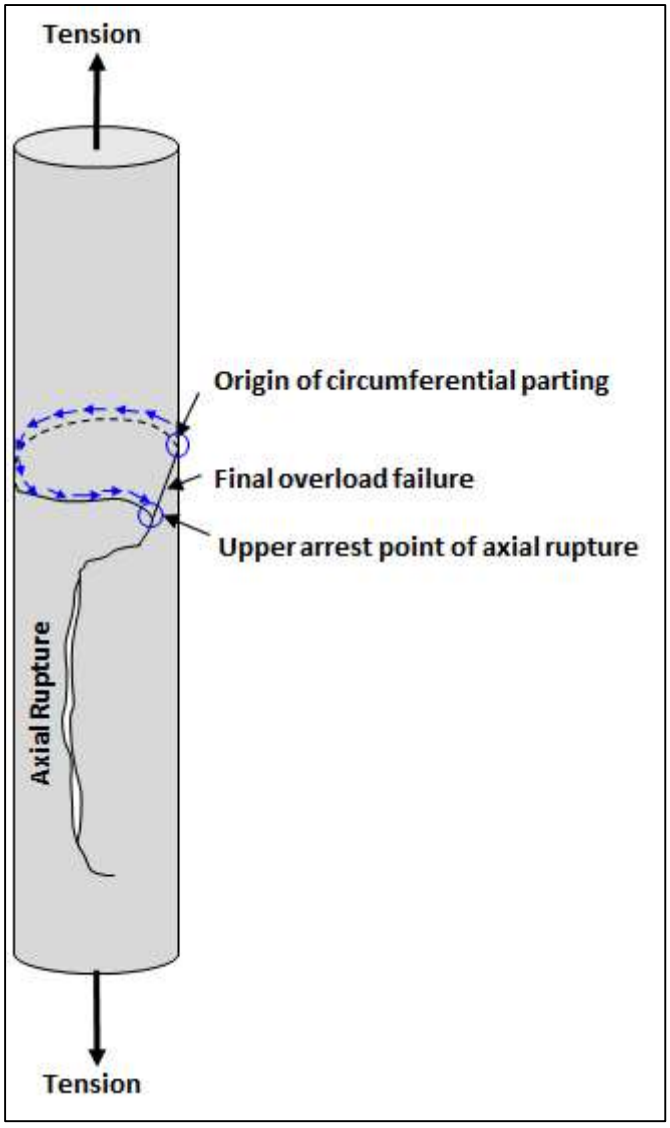


**Figure 70: Schematic of the Axial Rupture and Circumferential Parting**

Observations during the visual examination identified a significant difference between the axial rupture and circumferential parting. The circumferential parting was brittle, unlike the axial rupture, which was characterized by bulging and ductile tearing. The circumferential parting showed no evidence of plastic deformation or necking due to ductile overload. Measurements of the fracture surface were made to confirm this observation. Furthermore, Zone 1 of the circumferential parting was predominantly cleavage.

This is in contrast to Zone 1 of the axial rupture, which was characterized by micro-void-coalescence. These observations suggest that the axial rupture and circumferential parting occurred at different temperature regimes.

### 2.4.4 Quantitative Verification of the Failure Sequence

The metallurgical examination was complemented with quantitative assessment of the failure. This was necessary to verify the fractographic analysis and failure sequence.

The loads at 892 ft, at the location of the failure are summarized in Table 4. This was generated using a tubular mechanics and wellbore heat transfer analysis program StringNosis. The 12-hour loads are considered non-steady state and the 9 month are steady state. The intent was to identify any changes in load, and the axial loads are slightly higher in the steady state. Also, the effect of flow rates is reflected in the loads. The loads will be the basis of comparison for the modeling results discussed here.

**Table 4: Gas Injection Conditions and the Relevant Load Summary at a Depth of 892 ft**

| Surface Gas Inj. Temp. (°F) | Gas Inj. Rate (MMscf/D) | Inj. Period | Internal Pressure (psi) | External Pressure (psi) | Dog Leg Severity (Deg/100°) | Axial Force (lbf) | Temp. (°F) |
|---|---|---|---|---|---|---|---|
| 70 | 6 | 12 hr | 2,791 | 386 | 1.79 | 218,187 | 77 |
| 70 | 6 | 9 mo | 2,791 | 386 | 1.79 | 227,607 | 75 |
| 70 | 30 | 12 hr | 2,791 | 386 | 1.79 | 230,983 | 74 |
| 70 | 30 | 9 mo | 2,791 | 386 | 1.79 | 236,545 | 74 |

## Axial Rupture Assessment

Finite element (FE) models were used to model the corrosion features and estimate the failure pressure. In addition to 85% wall loss due to corrosion, there were striated grooves with V-shaped tips. The geometry was complex, and the FE models require substantial meshing for plastic strain estimation purposes. Consequently, three different models were analyzed to estimate the failure pressure.

Model 1 was a simplified model that focused only on the wall thinning effect (Figure 71). The wall loss of 85% (remaining wall of 0.047 in.) is depicted in the origin that was 2.13 in. The overall corrosion feature was 9.25 in. long.

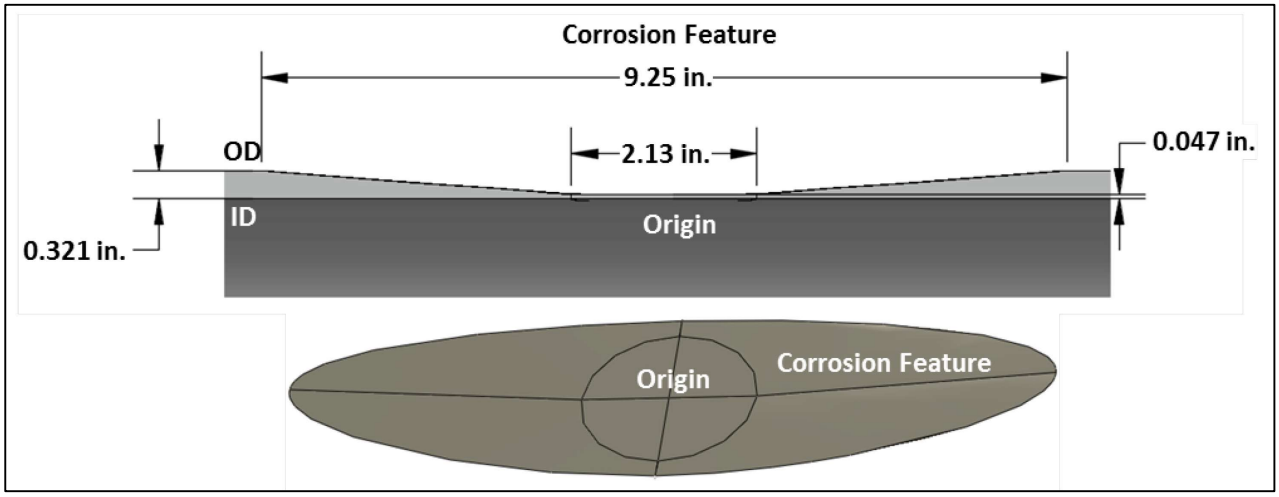


**Figure 71: Corrosion Feature Geometry Model 1**

Model 2 included a notch that depicted the striated grooves that were observed at the failure locations. The grooves' dimensions were measured, and the diameter of the notch was noted to be 0.2 mm. However, the small dimensions were beyond the capability of the FE modeling tools; a notch radius of 1.0 mm was used to capture the notch effect of the corrosion grooves. The bottom of the notch was placed at a depth such that the remaining wall was equal to 1.26 mm, which is the same remaining wall as Model 1.

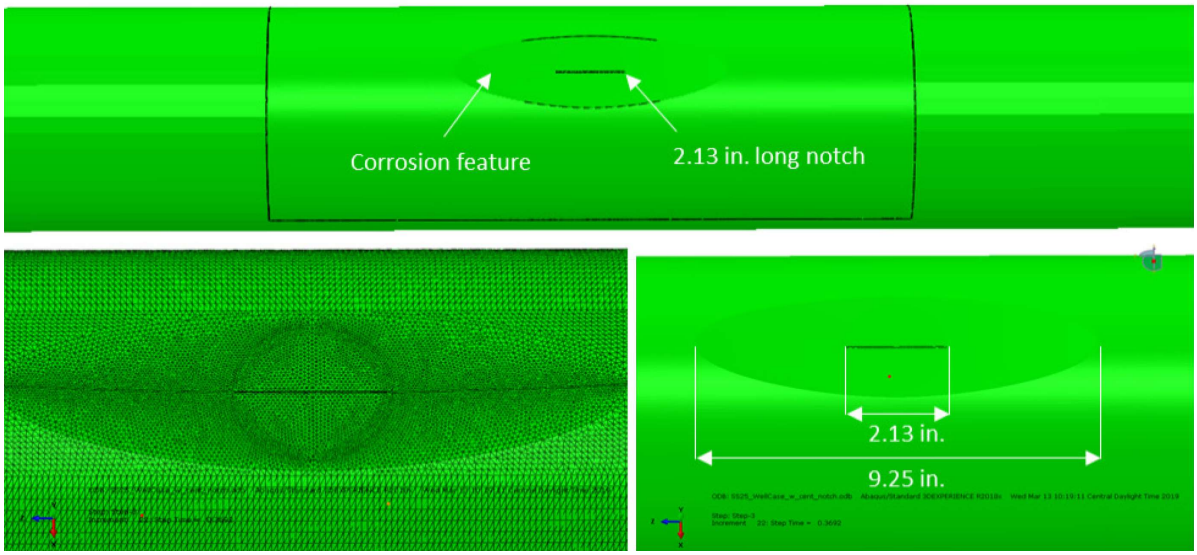


**Figure 72: Model 2 Schematic and Mesh for Corrosion Feature and 2.13 in. Notch**

Model 3 was designed to introduce the notch effect while maintaining the wall thinning within the ductile tearing region (2.13 in. circular region). The semi-elliptical bowl was modeled in the same way as Model 1. Unlike Model 2, the minimum wall thickness of 1.26 mm was maintained within the ductile tearing zone. A notch was introduced with a length increased to the macro definition of the origin (4.8 in.).

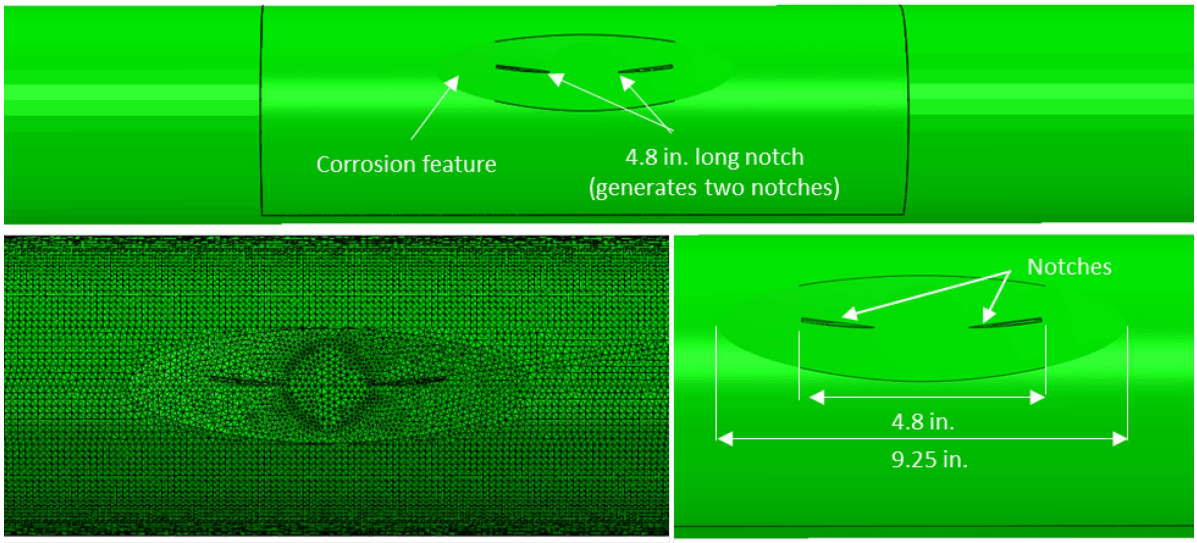


**Figure 73: Model 3 Schematic and Mesh for Corrosion Feature and 4.8 in. Notch**

The three models were developed to capture the complex effects of the corrosion feature geometry on the failure pressure. The material properties were obtained from true stress-true strain tests that were conducted for both longitudinal and transverse directions.

A strain-based damage model was used to predict the onset of cracking due to local plasticity. Failure strain limit is a function of the cumulative plastic strain, stress triaxiality, von Mises's stress, and the material critical strain. The ductile failure damage indicator (DFDI) shown in the following equation is a ratio of the applied strain corrected for the local stress state by the failure strain. Consequently, when the DFDI equals or is greater than 1, the local region will develop a crack.

$$D_i = DFDI = \frac{1}{1.65\epsilon_0}\int_0^{\epsilon_{eq}} exp\left(\frac{3}{2}\frac{\sigma_m}{\sigma_{eq}}\right) d\epsilon_{eq}$$

where,

$\epsilon_{eq} = equivalent\ strain$

$\epsilon_f = reference\ strain$

$\epsilon_0 = critical\ strain$

$\sigma_m = mean\ stress$

$\sigma_{eq} = equivalent\ stress$

$\sigma_1, \sigma_2, and\ \sigma_3 = principle\ stresses$

A DFDI value of 1.0 was used to determine the differential pressure at which a crack would initiate within the corrosion feature. The DFDI is predicted for the three models as a function of pressure, and Figure 74 shows the results. The DFDI evolution is exponential, which implies the DFDI increases from 1.0 to 1.4 with a small increase in pressure. This implies that the crack initiates and grows by ductile tearing.

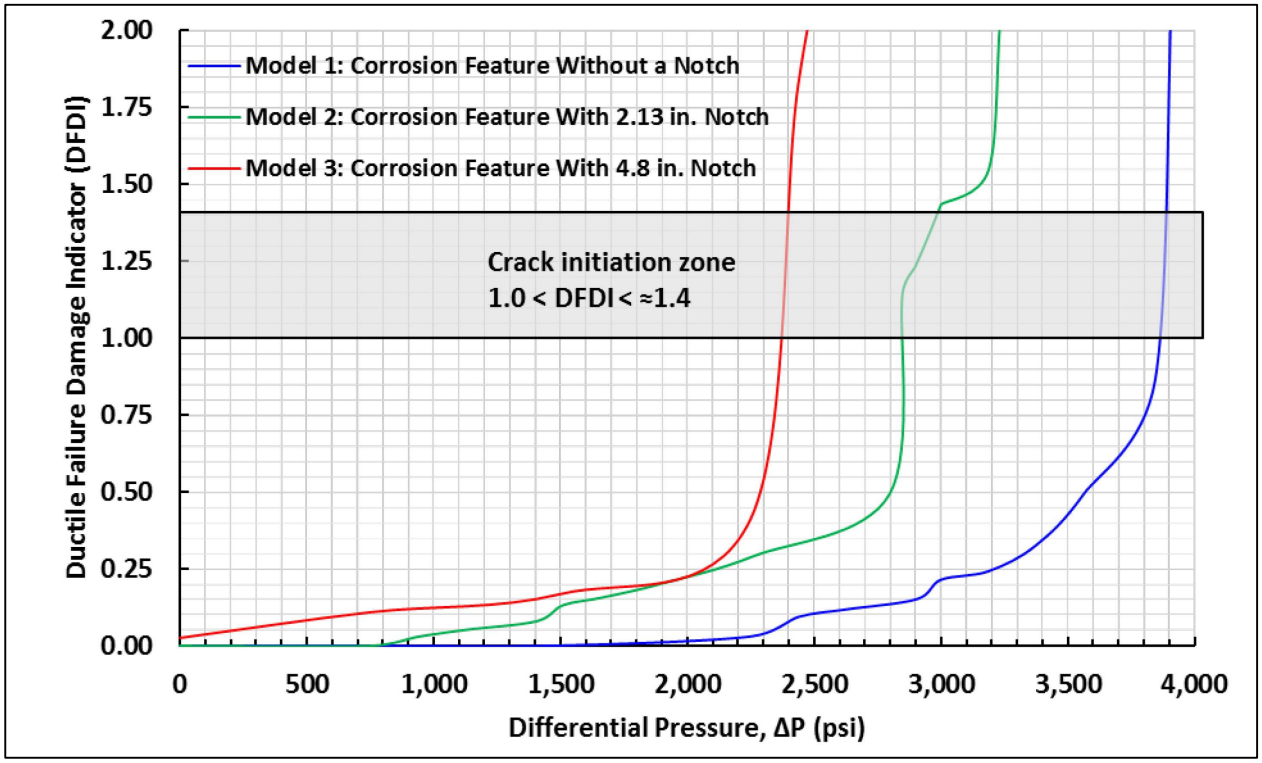


**Figure 74: DFDI Evolution with Differential Pressure for Models 1, 2, and 3**

Table 5 shows the point of crack initiation in the plastic region when DFDI equals 1. The pure corrosion wall loss model predicts a pressure of 3,850 psi for a crack to initiate in this region. As shown previously in Table 4, the internal pressure on October 23, 2015, reached around 2,700 psi on surface and 2,791 psi at 892 ft. Model 1 schematic of the corrosion is not reflective of the failure scenario. Models 2 and 3 have differential pressures ranging from 2,327 to 2,836 psi, which is in the range of the pressures that existed at 892 ft. Since neither model completely captures the complexity of the failure region due to limitations of the FE modeling, the predicted range of failure pressures is from 2,327 to 2,836 psi. The key finding from the modeling is that the presence of the grooves was an essential element of the failure occurring at 2,791 psi internal pressure.

**Table 5: Differential Pressure (ΔP) Summary**

| Model | Differential Pressure (psi) |
|---|---|
| **Model 1**: Corrosion feature without a notch | 3,850 |
| **Model 2**: Corrosion feature with a 2.13 in. notch | 2,836 |
| **Model 3**: Corrosion feature with a 4.8 in. notch | 2,327 |

FEA (finite element analysis) and DFDI showed that in a 2.13 in. long and 85% grooved corrosion, a deep crack will form at a differential pressure of 2,327−2,836 psi. To verify the instability that was observed during fractographic examination, an FE crack model was used to determine if a 2.13 in. long and 85% deep crack would be unstable. A fracture toughness-based failure criterion was used to assess the instability of the crack.

Charpy data were used to establish the fracture toughness of this material. The 7 in. casing J55 material exhibited lower shelf toughness properties at temperatures of 75°F (24°C ). At room temperature, the average full size Charpy is around 14 J. This Charpy was converted to lower shelf fracture toughness ($K_{IC}$) based on equations from BS7910 and equals 48.3 ksi-in$^{1/2}$ shown with a dashed line in Figure 75.

In the FE model of the crack, the crack tip stress intensity factor reaches a value of 48.3 ksi-in$^{1/2}$ equaling the fracture toughness when the internal pressure was approximately 1,950 psi. Figure 75 shows the results of the fracture mechanics analysis. The crack is unstable beyond 1,950 psi at room temperature. The results show that a 2.13 in. long and 85% deep crack would propagate at differential pressures ≥ 1,950 psi. The estimated strain-based failure pressure (2,327—2,836 psi) is above the fracture toughness-based instability pressure (1,950 psi). This shows that once the 2.13 in. crack formed by ductile tearing was unstable.

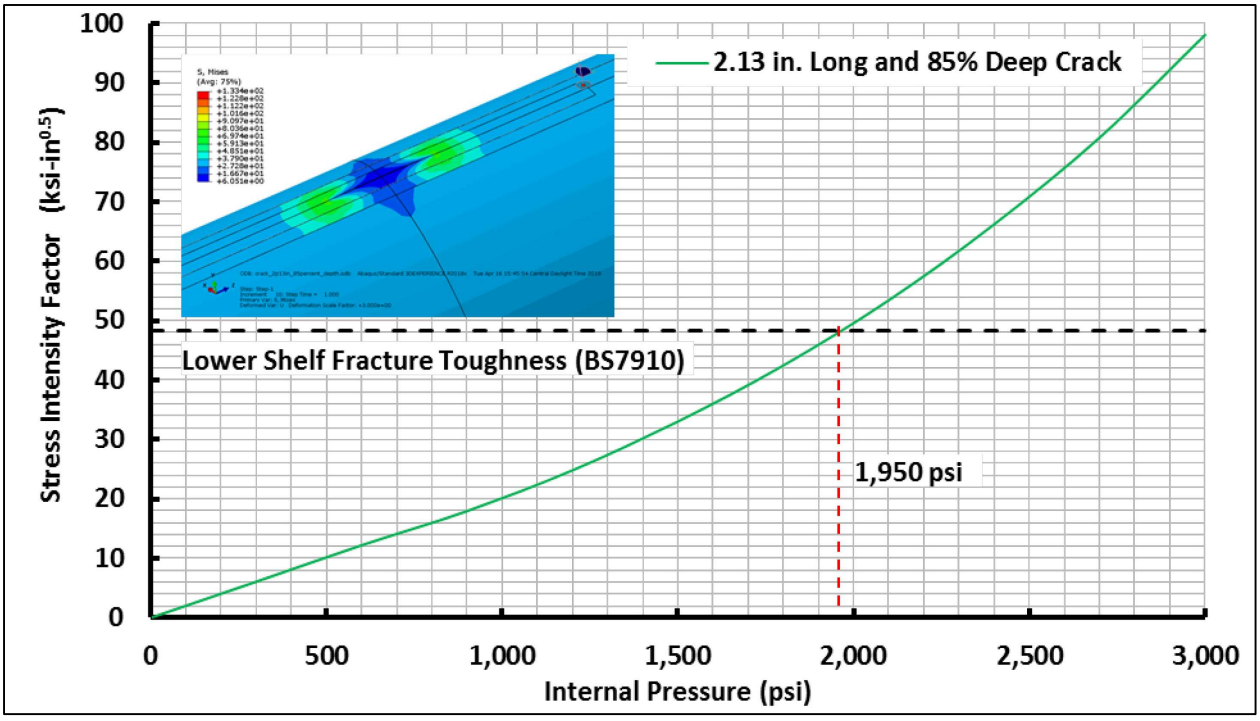


**Figure 75: Stress Intensity Factor Evolution with Applied Internal Pressure**

## Circumferential Parting Assessment

Based on the fractographic work, it was determined that following the axial rupture and gas expansion through the rupture region, the adjacent area cooled substantially. This should have resulted in a substantial reduction of toughness (Charpy and Fracture toughness).

In Section 2.4.3, the possible dimensions of the origin for the circumferential parting were identified. The axial stress of 35,541 psi based on Table 4 at 892 ft was used in the applied stress intensity (K) estimation. Using these two possible dimensions, the applied K at the defect was calculated using API 570 and BS7910. The K that is calculated for these two dimensions equals the toughness of the material at that temperature. The results are shown in Table 6. In order to estimate the temperature at failure, the Charpy data were used.

The average Charpy impact toughness data measured in the L-C (longitudinal-circumferential) direction as a function of temperature is shown in Figure 76.

$$C_v = 12.05 + 10.82 \cdot tanh\left(\frac{T - 42.49}{59.54}\right)$$

The region of interest is the lower shelf that is marked by the box in Figure 76. Fracture toughness has been correlated to Charpy data for the lower shelf based on BS7910, which is shown by the equation below.

$$K_{mat} = \left[\left(12\sqrt{C_v} - 20\right)\left(\frac{25}{B}\right)^{0.25}\right] + 20$$

where,

$K_{mat} = fracture\ toughness\ estimate\ \left(MPa\sqrt{m}\right)$
$B = thickness\ of\ the\ material\ for\ which\ an\ estimate\ of\ K_{mat}\ is\ required\ (mm)$
$C_v = lower\ bound\ Charpy - V\ Notch\ impact\ energy\ at\ the\ service\ temperature\ (J)$

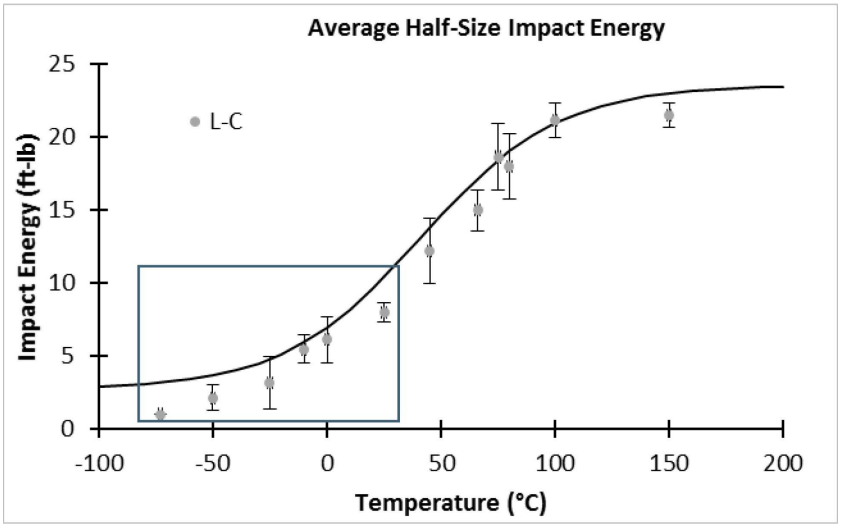


**Figure 76: Average Half-Size Charpy Impact Energy vs Temperature for L-C Orientation**

The fracture toughness that is estimated for the circumferential parting (Table 6) is correlated to Charpy. Then, from the Charpy data, the temperature is estimated and shown in the last column. The circumferential parting occurred at a temperature that would have ranged from –76°F to –38°F (–60°C to –39°C); the range is defined by the defect dimensions and the fracture mechanics model that is used.

**Table 6: Estimated Failure Temperature for Circumferential Parting for Two Critical Crack Candidates**

| Analysis | Crack Length (mm) | Crack Depth (mm) | Fracture Mechanics Model | Fracture Toughness $K_{IC}$ (ksi-in$^{1/2}$) | Estimated Failure Temperature (°C) |
|---|---|---|---|---|---|
| 1 | 14.54 | 5.22 | API 579 | 27.6 | –56.8 |
| 2 | 14.54 | 5.22 | BS 7910 | 26.9 | –60.4 |
| 3 | 21.72 | 5.22 | API 579 | 31.8 | –40.1 |
| 4 | 21.72 | 5.22 | BS 7910 | 32.1 | –39.1 |

### 2.4.5 Summary of Failure Sequence

The following conclusions can be made based on the visual (macro) and SEM (micro) investigations of the SS-25 7 in. casing failure:

- The 7 in. casing failure originated from an 85% metal loss due to corrosion, which resulted in a 2 ft long axial rupture under an internal pressure of 2,791 psi in the 7 in. × 2 7/8 in. annulus.
- Just prior to the axial rupture, the 7 in. casing bulged. This was followed by a slow ductile tearing within the thinnest corroded region. FEA suggested that once a 2.13 in. crack was initiated by ductile tearing, the crack propagated rapidly. Chevron marks were identified at a crack length of 4.8 in, which is the total length of the rapid crack propagation.
- The propagating cracks finally arrested after changing directions (upper and lower) due to changes in stress state and energy dissipation.
- The axial rupture occurred at an estimated temperature of 80°F; this estimate was based on the historical temperature profile data at the failure depth of 892 ft (joint 22) and is consistent with observed bulging and ductile tearing associated with the axial rupture.
- The circumferential parting was not a continuation of the axial rupture. The axial rupture and circumferential parting were two separate events even though they were in close proximity. The circumferential parting was brittle. There was no evidence of local plastic deformation or overload necking based on wall thickness measurements of the fracture surface.
- The circumferential parting was a consequence of the axial rupture. The release of highly-compressed natural gas from the opening formed by the axial rupture resulted in rapid cooling of the adjacent casing due to the expansion of the gas (Joule–Thomson effect).
- The circumferential parting occurred at a temperature range from –76°F to –38°F (–60°C to –39°C) based on fracture mechanics estimation.

Further details regarding the failure sequence and additional data can be obtained from the *SS-25 Casing Failure Analysis* supplementary report [19].

## 2.5 7 in. Casing Load Analysis

A detailed analysis of the 7 in. production casing was conducted to estimate the loads and the stresses caused by the loads applied to the casing leading up to the leak event. Load conditions were determined based on data collected during the RCA. The evaluation of the reduced casing burst strength caused by a reduction in casing wall thickness identified the remaining wall thickness (as a percent of nominal thickness) at which the casing would rupture when exposed to the well injection pressure.

Two methods of casing design were used in the analysis: Working Stress Design (WSD) and Reliability-Based Design (RBD). WSD is the conventional method of casing design used in the oil and gas industry. This method assumes maximum loads and minimum strength to calculate a safety factor (SF). A safety factor of one or greater is the design criterion to determine if the design is acceptable. However, WSD has limitations when attempting to predict failure. For example, a safety factor less than one does not indicate the casing will fail. Because of the limitations of WSD, RBD was used to estimate the probability of failure of the production casing for a range of remaining wall thickness. The RBD analysis showed that when the casing Remaining Body Wall (RBW) was below 30%, rupture of the casing could have been expected based on the load conditions.

The objective of the casing load analysis was to examine conditions under which casing failure could have occurred in the upper part of well SS-25. Specifically, the goal was to examine if the casing had been subjected to overload conditions that caused the leak incident on October 23, 2015. The reduction in wall thickness caused by metal loss from corrosion was a key parameter of the analysis.

A set of load cases was proposed to represent expected casing loads during the life of the well, particularly during the period immediately preceding the October 23, 2015 incident. Initial conditions (including applied overpull) were assumed to have created the casing stress state when the casing was run and cemented. Changes to the stress state caused by changes in pressure and temperature were calculated for each subsequent load case. For the injection load cases, an injection pressure of 2,700 psi was assumed based on reported conditions on and immediately before October 23, 2015. Because temperature of the casing decreased during injection, cool down temperature profiles were calculated for typical injection conditions. In addition, a cool down temperature profile recorded on November 8, 2015 [20] was considered because this represented measured temperature cool down of the casing and was the lowest temperature the casing likely experienced throughout its life.

The Top of Cement (TOC) was assumed to be the point of fixity for the 7 in. casing, and the TOC was confirmed by log data. The change in temperature of the uncemented casing above the TOC affected the axial force and stress state. Therefore, a TOC of 7,000 ft measured depth (MD) was assumed as the base case. However, over the long history of well usage, formation sloughing and cave-in at the 11 3/4 in. casing shoe (990 ft MD) may have led to bridging in the annulus. Bridging could have caused the 7 in. casing to behave as if it had been fixed at or just below the 11 3/4 in. shoe. This possibility was examined as a sensitivity case.

Finally, the RBW was a key sensitivity parameter reflecting wall reduction from corrosion. RBW was expressed as a percent of nominal wall with no wall loss as the base case.

For completeness, WSD checks were performed and the safety factors were reported. However, violation of WSD criteria does not imply failure—it merely implies inadequacy of design. Failure can only occur when the ultimate limit state of the tubular in the mode of interest is exceeded. Therefore, failure of casing was examined using the tension-burst limit state from API Technical Report 5C3 [21]. To account for uncertainties in the material properties and geometric parameters of the casing, a reliability-based

approach was used to calculate the Probability of Failure (POF) of the casing for any given load case. The commercial software tool StrinGnosis[i] V 3.1 was used in performing the probabilistic analyses. API Technical Report 5C3 [21]describes the basis of the statistical distributions for various strength-defining parameters, including wall thickness. A POF greater than $10^{-1}$ (greater than 90%) is interpreted as failure of the casing. Therefore, for any given load case, if the POF of the casing is lower than $10^{-1}$, it is not considered a failure, even if the corresponding WSD factor of safety is less than the minimum required. Details of the analysis are included in the supplemental report *SS-25 7 in. Casing Load Analysis* [22].

### 2.5.1 Conclusions

The following is a summary of the load analysis results:

- The results showed that for RBW less than 30% of nominal wall, ductile rupture of the casing would have been expected in a tension-burst failure mode. This was the case regardless of the extent of cool down during injection; therefore, wall loss was established as the key driver of failure. Thermally induced tension from cool down during injection increased the axial stress in which the highest stresses occur when the point of fixity was at the 11 3/4 in. casing shoe (990 ft).
- The results for predicting casing rupture were similar for a case where the casing was fixed at 7,000 ft, the original TOC, or if the casing was fixed at 990 ft. The point of fixity of the casing affected the axial stress when the casing was cooled or heated compared to the initial condition.

## 2.6 Connections

Threaded connections are used to assemble tubulars. When the 7 in. casing was extracted from SS-25, the casing was cold cut approximately 2.5 ft above and below each connection, leaving the connection made up with the intent of testing the connections.

### 2.6.1 7 in. Production Casing Connections

As discussed previously, 26 joints of production casing were extracted from SS-25. The production casing had a Speedtite connection. Very little information describing Speedtite connections is publicly available. The connection is no longer commercially available. The available information suggests that Speedtite connections are similar to Hydril's Super EU connections, and that Youngstown Steel (the manufacturer of the 7 in. casing run in SS-25) was licensed to cut Super EU connections and market them under the name ‘Speedtite’. Super EU connections are no longer commercially available either, but some information is publicly available regarding the connection features and design.

Super EU is a proprietary internally upset, two-step connection. The connection OD, at 7.444 in. is slightly larger than the 7 in. pipe OD. During manufacturing, pin threads are cut on the bottom end of each approximately 42 ft long joint, and the box threads are cut on the upper end of each joint. In the field, the pin from one joint is made-up into the box from another joint when the casing string is run in the well. Internal pressure leak resistance is provided by the post-makeup contact pressure from radial interference in the metal-to-metal seal labeled ‘A’ in Figure 77. When the casing is exposed to internal

[i] StrinGnosis is a tubular mechanics and wellbore heat transfer program developed and marketed by Blade Technology Corporation, LLC.

pressure, the seal contact pressure increases as the pin expands radially into the box, thereby increasing the internal leak resistance of the connection. The connection is also designed to provide external pressure resistance via another metal-to-metal seal labeled 'B' in Figure 77, and functions in a manner similar to that of seal 'A'. The torque shoulder, where the pin and box meet after the connection is made up, is located between the 'B' seal and the OD of the pin. This torque shoulder is the only source of torque during makeup because the threads are free running and therefore do not provide resistance to internal or external pressure.

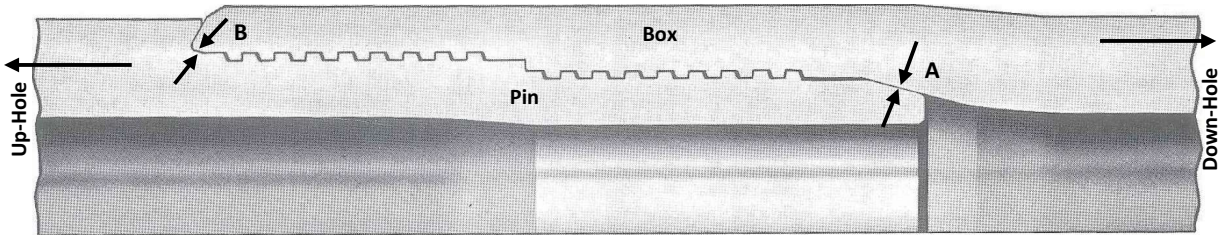


**Figure 77: Super EU (Speedtite) Connection Configuration**

Twenty-five connections were tested with nitrogen gas in pressure level increments of 500 psi up to a maximum of 3,300 psi. Due to the internal pressure, there were axial loads on the test piece that were lower than in the production casing downhole. The intent of the test was not to just identify whether it leaked or not, but also to quantify the flow rate if the connection leaked. The detailed test procedure is described in the *SS-25 7 in. Speedtite Connection Testing and 11 3/4 in. STC Assessment* supplementary report [23].

Most of the connections did not leak, however nine out of 25 did exhibit measurable leak rates as shown in Table 7. The tests began using a 4 SCCM flow meter. If during the test the flow meter range was not sufficient to measure the flow rate, then the test was stopped. A higher capacity flow meter was installed, and the test was re-started. In several cases a 50,000 SCCM meter had to be used. Therefore, some connections required multiple individual tests to complete the test program.

**Table 7: Connection Test Results Detail**

| Connection | Leak? | Flow Meter (SCCM) | Pressure (psi) | Max Leak Rate | Volume Leaked (cc) |
|---|---|---|---|---|---|
| C001B | 1. No | 1. 4 | 1. 3,300 | 1. 0 SCCM | 1. 0.24 |
| C002B | 1. Yes<br>2. Yes<br>3. Yes | 1. 4<br>2. 50<br>3. 500 | 1. 1,500<br>2. 2,500<br>3. 3,300 | 1. > 4 SCCM<br>2. > 50 SCCM<br>3. 101 SCCM | 1. > 112<br>2. > 550<br>3. > 11,200 |
| | | | Rate after 2.5 hours at 3,300 psi was ~78 SCCM | | |
| C003B | 1. No | 1. 4 | 1. 3,300 | 1. 0 SCCM | 1. 0 |
| C004B | 1. Yes<br>2. Yes<br>3. Yes | 1. 4<br>2. 4<br>3. 500 | 1. 2,000<br>2. 2,000<br>3. 3,300 | 1. > 4 SCCM<br>2. > 4 SCCM<br>3. 200 SCCM | 1. 124<br>2. 630<br>3. > 17,100 |
| | | | Rate after 1 hour at 3,330 psi was 140 SCCM | | |
| C005B | 1. No | 1. 4 | 1. 3,300 | 1. 3.4 SCCM | 1. 70 |

| Connection | Leak? | Flow Meter (SCCM) | Pressure (psi) | Max Leak Rate | Volume Leaked (cc) |
|---|---|---|---|---|---|
| | 2. No | 2. 50 | 2. 3,300 | 2. 0 SCCM | 2. 0 |
| C006B | 1. No | 1. 4 | 1. 3,300 | 1. 0 SCCM | 1. 0 |
| C007B | 1. No | 1. 4 | 1. 3,300 | 1. 0.4 SCCM | 1. 9.6 |
| C008B | 1. No | 1. 500 | 1. 3,300 | 1. 0 SCCM | 1. 0 |
| | 2. No | 2. 4 | 2. 3,300 | 2. 0 SCCM | 2. 0.078 |
| C009B | 1. No | 1. 4 | 1. 3,300 | 1. 0 SCCM | 1. 0.08 |
| C010B | 1. No | 1. 4 | 1. 3,300 | 1. 0 SCCM | 1. 0 |
| C011B | 1. Yes | 1. 4 | 1. 1,200 | 1. > 4 SCCM | 1. > 18 |
| | 2. Yes | 2. 500 | 2. 3,300 | 2. 90 SCCM | 2. > 6,500 |
| C012B | 1. Yes | 1. 4 | 1. 3,300 | 1. 1.7 SCCM | 1. 183 |
| | | | Rate after 2 hours at 3,300 psi was 1.1 SCCM | | |
| C013B | 1. No | 1. 4 | 1. 3,300 | 1. 0.7 SCCM | 1. 6.1 |
| C014B | 1. No | 1. 4 | 1. 3,300 | 1. 0.84 SCCM | 1. 7.5 |
| C015B | 1. No | 1. 4 | 1. 3,300 | 1. 0.17 SCCM | 1. 0.48 |
| C016B | 1. Yes | 1. 4 | 1. 1,000 | 1. > 4 SCCM | 1. > 2 |
| | 2. Yes | 2. 500 | 2. 2,500 | 2. > 500 SCCM | 2. > 5,000 |
| | 3. Yes | 3. 50,000 | 3. 3,300 | 3. 1,120 SCCM | 3. 117,500 |
| | | | Rate after 2 hours at 3,300 psi was 945 SCCM | | |
| C017B | 1. No | 1. 4 | 1. 3,300 | 1. 4 SCCM | 1. 67.7 |
| C018B | 1. No | 1. 4 | 1. 3,300 | 1. 0.14 SCCM | 1. 0.74 |
| C019B | 1. Yes | 1. 4 | 1. 1,000 | 1. > 4 SCCM | 1. > 90 |
| | 2. Yes | 2. 500 | 2. 3,300 | 2. > 500 SCCM | 2. > 700 |
| | 3. No | 3. 50,000 | 3. 3,300 | 3. 0 SCCM | 3. 0 |
| | 4. Yes | 4. 500 | 4. 3,300 | 4. 137 SCCM | 4. > 4,900 |
| | | | Rate after 4 hours at 3,330 psi was 15 SCCM | | |
| C020B | 1. No | 1. 4 | 1. 3,300 | 1. 0.3 SCCM | 1. 6.9 |
| C021B | 1. Yes | 1. 4 | 1. 1,000 | 1. > 4 SCCM | 1. > 80 |
| | 2. Yes | 2. 500 | 2. 3,300 | 2. 128 SCCM | 2. > 5,200 |
| | | | Rate after 2 hours at 3,330 psi was 91 SCCM | | |
| C023A1C | 1. Yes | 1. 4 | 1. 500 | 1. > 4 SCCM | 1. > 7 |

| Connection | Leak? | Flow Meter (SCCM) | Pressure (psi) | Max Leak Rate | Volume Leaked (cc) |
|---|---|---|---|---|---|
| | 2. Yes<br>3. Yes | 2. 50,000<br>3. 1,000,000 | 2. 2,500<br>3. 2,800 | 2. > 50,000 SCCM<br>3. 195 SLM | 2. > 350,000<br>3. > 1,180,000 |
| C024B | 1. No | 1. 4 | 1. 3,300 | 1. 0.65 SCCM | 1. > 18 |
| C025B | 1. Yes<br>2. Yes | 1. 4<br>2. 500 | 1. 1,400<br>2. 3,300<br>Rate after 4 hours at 3,330 psi was 110 SCCM | 1. > 4 SCCM<br>2. 237 SCCM | 1. > 27<br>2. > 35,000 |
| C026B1 | 1. No | 1. 4 | 1. 3,300 | 1. 0.17 SCCM | 1. 0.48 |

The highest leak rates came from C016B and C023A1C, which leaked at 1,120 SCCM (57 scf/D) and 196 SLM (9,967 scf/D) respectively. Connection C023A1C was located in the well 2.3 ft below where the 7 in. casing parted. The remaining seven leaking connections had very low flow rates.

None of the rates were high: there were no indications of any thread erosion as shown in Figure 78. The threads appeared to be in as-machined condition; however, the testing showed that for C021B at 1,000 psi the connection was leaking at more than 4 SCCM, whereas at 3,300 psi the leak rate was 128 SCCM. The leak rates were low and it could be stated that the gas seeped through the connections. The connection testing results were reproducible, implying that the nine connections leaked, albeit at low flow rates. Consequently, the conclusion based on the examination of the threads and the connection testing results was that hydrocarbon gas seeped through some of the connections at low flow rates.

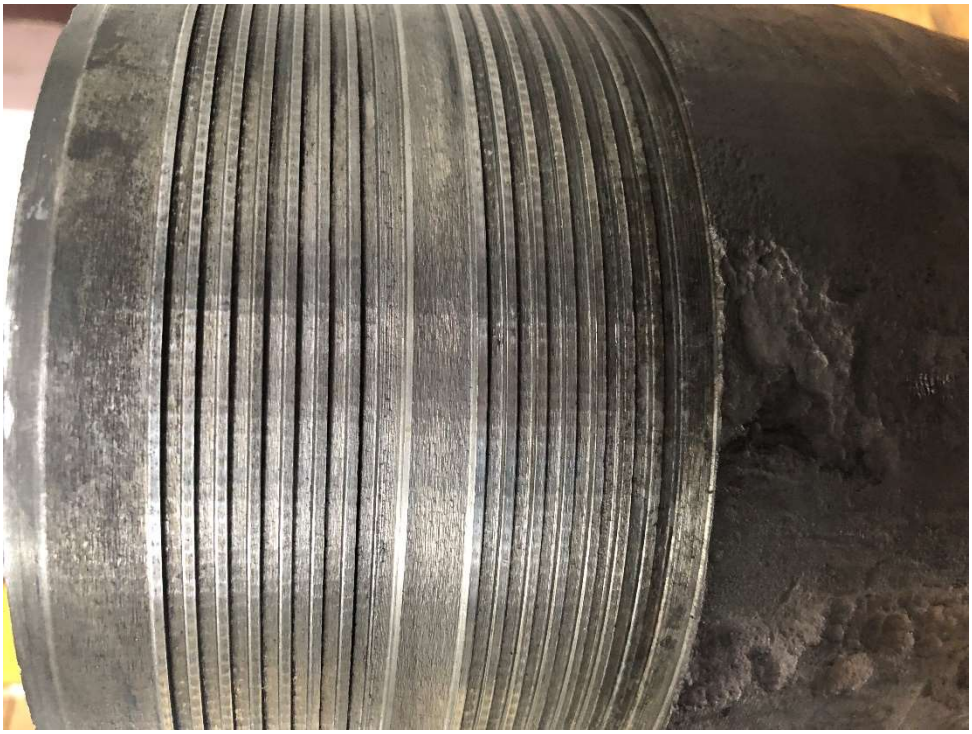

**Figure 78: Pin and Box from Leaking Connection C023A1C**

### 2.6.2 11 3/4 in. Surface Casing Connections

The surface casing string run on SS-25 was 11 3/4 in. 42 ppf H40 with STC connections set at 990 ft in October 1953. STC is a non-proprietary connection whose design and manufacturing requirements are specified in *API 5B - Specification for Threading, Gauging and Thread Inspection of Casing, Tubing, and Line Pipe Threads*. STC connections do not have metal-to-metal seals and instead rely on the interference bearing pressure created between the pin and box threads during make up. These threads also have a void at the thread root and crest areas that create a helical leak path through the connection, which must be plugged with thread compound to provide leak resistance.

The internal yield pressure of the 11 3/4 in. casing is 1,980 psi. The calculated, or design, leak resistance of the STC connections is also 1,980 psi. However, as recognized by the industry since the 1940s, the actual leak resistance for STC connections run in the field can be significantly lower. The original API tubular specifications were established with the intent to standardize pipe sizes and connections so that material from one mill could be used interchangeably with material from other sources. The specifications did not focus on leak resistance. The leak resistance equations provided by API also do not account for many threading variables, including dimensional tolerances and tension. The variables that affect STC leak resistance include the pipe OD and pipe yield strength, the thread attributes (lead, taper, pitch diameter), the thread compound (which degrades over time), the tension load (which reduces the thread bearing pressure), and the field make up practices (which impacts the thread bearing pressure).

Research on API threads conducted by T.H. Hill Associates in 1989 demonstrated that “the average pin screwed into the average coupling to the nominal power-tight position will have about 25–45% less leak resistance than supposed [24].” Due to pipe manufacturing practices and allowances, and practical limitations on machining, a bias towards small pins and large boxes is built into the API pitch diameter gaging method. This leads to most connections not achieving design leak resistance. The research showed that at least 2 1/2% of the STC connections in a string will have an actual leak resistance at least 67% lower than the design leak resistance [24].

Enertech Engineering conducted research for API that concluded that leak resistance is strongly influenced by: loading sequence, make up conditions, and dimensional tolerances (taper, thread lead and ovality). In the study it was found that lower yield strengths of both the pipe body and coupling result in lower connector leak pressures due to the material in the connector reaching yield stress at make-up. Tension causes a significant reduction in leak resistance due to reduced stab flank contact pressure [25].

The actual STC leak resistance is expected to be lower than the design value, and can be significantly lower with respect to gas leak resistance, which is much more challenging than leak resistance to a liquid (e.g., water, drilling fluids). This is why most proprietary connections used a metal-to-metal seal to provide gas leak resistance and do not rely on the threads and thread compound. STC connections are not gas tight. A great deal of industry work has been done since SS-25 was drilled to understand and improve the leak resistance and reliability of STC and similar API connections. This knowledge was unavailable in 1953.

STC connections are acceptable in the right application, such as for surface casing strings where the setting depths are relatively shallow, downhole pressures are low, and gas is rarely encountered. The main function of surface casing is to isolate fresh water and provide structural support for the rest of the well, and not to provide a gas tight barrier to a production string.

Considering the amount of time, the 11 3/4 in. casing had been in place, and the known limitations of STC regarding leak resistance which are exacerbated in the presence of gas, it is probable that the 11 3/4 in. casing and connection would leak gas at a very low pressure.

### 2.6.3 SS-25 Connection Testing Summary

Twenty-five SS-25 Speedtite connections were recovered and tested for leaks in a laboratory-instrumented test fixture. The following is a summary of the findings:

- 16 connections held the test pressure of 3,300 psi.
- 9 connections leaked; the two highest leak rates were 9,967 scf/D and 57 scf/D.
- 14 connections that were backed out had break-out torques ranging from 3,614 to 8,708 ft-lb, compared to the recommended makeup torque of 8,000 ft-lb.
- 4 connections threads were inspected for evidence of fatigue cracks or deformation caused by cyclic pressure loading. Neither fatigue cracks nor deformation was found, indicating that fatigue was not a contributing factor to the connection leaks. Fatigue would not be expected because of the relatively low well pressure changes.

The results of the testing confirm the lack of leak resistance of reduced OD connections in pre-1980s designs. Details of the connection testing procedure and results can be found in a separate report: *SS-25 7 in. Speedtite Connection Testing and 11 3/4 in. STC Assessment* [23].

### 2.6.4 Seeping Connections

The testing results demonstrated that the 7 in. casing connections probably seeped gas for a long period of time. The hydrocarbon gas that leaked through these connections entered the surface casing annulus and bubbled through the column of liquid. However, this gas then likely escaped through the 11 3/4 in. STC connections that have limited gas leak resistance. Hence, no pressure was detected during the surface casing pressure measurements. Further, it is also probable that the through wall OD corrosion (holes) on the surface casing would have provided an additional conduit for the seeping gas. The SS-25 gas contained around 0.8% $CO_2$. The $CO_2$ concentration was too low to have caused substantial corrosion of the carbon steel casing; however, it was likely to have been a nutrient source to the methanogens—a microbial organism that likely caused corrosion. This is discussed in further detail in Microbial Analysis (Section 2.8.3).

## 2.7 Groundwater

The 7 in. production casing exhibited external corrosion on the OD at depths higher than 700 ft. For corrosion to occur, an aqueous environment had to be present in this annulus. When this well was constructed, the cementing operations displaced cement to 7,000 ft, and leaving drilling fluid above top of cement. This drilling fluid would have been the environment that existed behind the 7 in. production casing following construction.

An assessment of the drilling records revealed the possible properties of the drilling fluid that were used in 1954. While drilling the 10 5/8 in. hole a Schlumberger electric logging tool was run. Prior to running the tool, the fluid properties, such as resistivity, density, and pH were characterized. This was done to appropriately correct the resistivity measurements for the fluid properties. The drilling fluid properties that were in the header of the SS-25 electric log [8] are summarized in Table 8. The fluid was water-based with some minor additions of oil. One of the main factors for corrosion is the pH of the drilling fluid; the higher the pH, the lower the corrosion rate. As shown in Table 8, the pH was elevated, ranging from 10 to 12.5, which is normal for drilling fluid. Such an environment would not corrode the carbon steel. The OD

of the 7 in. production casing would not have exhibited OD corrosion if the environment had remained the same as the drilling fluid.

**Table 8: SS-25 Schlumberger Electric Log Header Drilling Fluid Properties**

| Date | 1/12/1954 | 1/18/1954 | 1/20/1954 | 1/21/1954 | 2/8/1954 | 2/8/1954 | 2/14/1954 |
|---|---|---|---|---|---|---|---|
| Depth (ft) | 4,833 | 5,629 | 5,770 | 5,945 | 8,550 | 8,583 | 8,749 |
| Density (lb/ft$^3$) | 73 | 77 | 78 | 76 | 80 | 81 | 78 |
| Viscosity (sec) | 42 | 50 | 53 | 52 | 50 | 73 | 45 |
| Resistivity (ohm-m) | 3.0 | 2.8 | 3.0 | 2.0 | 1.8 | 1.9 | 1.9 |
| pH | 10 | 10 | 12 | 11 | 12 | 12.5 | 12 |
| Water Loss (cc) | 4 | 3.2 | 5.2 | 3.5 | 3.8 | 2.7 | 5.4 |

The fluid behind the 7 in. production casing had to be different than the original drilling fluid since there was corrosion on the production casing OD. There had to be an environment that was more dynamic, created by groundwater or another water source. Water injection from water disposal and other conventional oil production operations were considered; however the injection depths were significantly deeper and water injection wells were located farther away and closer to many other wells. Consequently, groundwater was the only feasible source of water that could have occupied the 7 × 11 3/4 in. annulus. Similarly, groundwater is the only water source that could have caused the 11 3/4 in. casing OD corrosion.

In order to confirm the presence of groundwater, Blade requested SoCalGas to drill a borehole to 1,100 ft to locate possible water sources. During the same period, the Los Angeles Regional Water Quality Board also requested a borehole for their purposes. It was agreed that one well would be drilled to meet both objectives. Blade's intent was to locate the water sources, log the open hole, and obtain relevant water samples for testing purposes.

The borehole was not located on SS-25. The SS-25 site was possibly compromised by the leak, numerous kill attempts and the persistent cold zone. All of this was demonstrated by the shallow geology investigation that was conducted on the SS-25 site during Phase I. Therefore, the borehole was located on SS-9 site, which was closest to SS-25, and was called TH-1. Geosyntec managed the drilling and associated operations. Blade prepared the basis of the design, water sampling locations, and logging program.

The drilling started with the Air Rotary Casing Hammer method (ARCH) to a depth of 80 ft and set the 11 3/4 in. casing. A Dual Tube Reverse Air Rotary and downhole hammer were used for the 6 in. hole section. Despite many drilling challenges the hole was completed to 555 ft. Fluid entered the hole at 380 ft and the water remained at the same level after four days of operational shut down. Grab water samples were obtained with a bailer for testing.

Many logging runs were completed. The intent of the logging program was to assess formations and identify any associated water source. The results are discussed here.

Once the hole reached 555 ft, the following Advisian logging runs were completed:

- Fluid temperature and conductivity.
- Acoustic Tele-viewer.

- Formation conductivity and natural gamma ray.
- Nuclear Magnetic Resonance (NMR).

Continued drilling problems necessitated a change to conventional fluid rotary drilling that allowed the drilling to reach 1,100 ft. At this depth, further logging runs were completed, and they included:

- Fluid temperature and conductivity (Advisian).
- Formation conductivity and natural gamma ray (Advisian).
- NMR (Advisian).
- Array Induction Imager Tool (AIT)-Platform Express (PEX) (Schlumberger).
- Dielectric scanner (Schlumberger).
- Spectral gamma ray (Schlumberger).
- Formation Micro Imager (FMI) (Schlumberger).
- Modular sonic imaging platform (Schlumberger).
- Combinable magnetic resonance and lithoscanner (Schlumberger).

The water chemistry for the grab samples from the shallower depths (Table 9) was typical of shallower groundwater samples:

- The concentration of calcium ranged from 106 to 266 mg/L.
- The concentration of sulfates ranged from 140 to 230 mg/L.
- The water was low in dissolved solids.
- The alkalinity ranged from 378 to 440 mg/L.

Geosyntec converted TH-1 at SS-9 into a monitoring well, and TH-1 became RMBW-1 (Deep). The shallow zones were all isolated, and the screens were set from 900 to 1,000 ft. From 1,000 to 1,100 ft, bentonite backfill occurred. RMBW-1 became a well that monitored the deep water samples. The deep water samples were collected, and the water chemistry was characterized.

**Table 9: Grab Water Samples from TH-1 (RBMW-1)**

| Sample ID | W-TH1-382 | W-TH1-382-DUP | W-TH1-555 | W-TH1-325 |
|---|---|---|---|---|
| Sampling Well | RBMW-1 | RBMW-1 | RBMW-1 | RBMW-1 |
| Depth (ft) | 382 | 382 | 555 | 325 |
| Sodium (mg/L) | 26.3 | 28.1 | 99.7 | 10.7 |
| Potassium (mg/L) | 4.51 | 3.89 | 5.30 | 0.978 |
| Magnesium (mg/L) | 36.0 B | 35.4 B | 43.2 B | 13.3 B |
| Calcium (mg/L) | 215 | 224 | 266 | 106 |
| Nitrate (as N) (mg/L) | ND<0.053 | ND<0.053 | ND<0.053 | 0.18 |
| Chloride (mg/L) | 17 | 15 | 15 | 28 |
| Sulfate (mg/L) | 190 | 190 | 230 | 140 |
| Alkalinity (mg/L) | 431 | 422 | 440 BU | 378 |
| Bromide (mg/L) | ND<0.058 | ND<0.058 | 0.063 J | 0.14 |
| Lithium (mg/L) | ND<0.0803 | ND<0.0803 | ND<0.00402 | ND<0.00402 |
| Strontium (mg/L) | 1.18 | 1.22 | 2.08 | 0.498 |
| Boron (mg/L) | 0.173 | 0.178 | 0.476 J | 0.0899 |
| Iron (mg/L) | 14.4 | 13.9 | 38.5 | 3.11 |
| Manganese (mg/L) | 0.443 | 0.457 | 0.619 | 0.0743 |
| pH by Field Method | 8.19 | - | 8.34 | 7.15 |

Geosyntec drilled an adjacent shallow monitoring well: RMBW-2 (shallow). The boring depth was only 450 ft, and the screen was set from 340 to 440 ft. Below 440 ft the well was backfilled with bentonite. The shallow water flow from this well was sampled, and the water chemistry was characterized.

The water chemistry from the monitoring wells RMBW-1 and RMBW-2 are shown in Table 10. Both samples were low in dissolved solids; however, the chemistry had distinct differences. The shallower sample had calcium of 171 mg/L consistent with the grab samples. The alkalinity was 385 mg/L with a pH of 6.75. The deeper samples were lower in calcium but had sodium concentrations of 469 to 475 mg/L. The alkalinity was much higher, around 866 to 881 mg/L and pH of 8.32. These monitoring samples are representative of the groundwater—still low in dissolved solids.

**Table 10: Water from Monitoring wells RBMW-1 and RBMW-2**

| Sample ID | GW-RBMW-1 | GW-RBMW-1-DUP | GW-RBMW-2 |
|---|---|---|---|
| Sampling Well | RBMW-1 | RBMW-1 | RBMW-2 |
| Depth (ft) | 900–1000 | 900–1000 | 340–440 |
| Sodium (mg/L) | 475 | 469 | 15.3 |
| Potassium (mg/L) | 5.05 | 5.20 | 1.26 |
| Magnesium (mg/L) | 3.97 | 3.98 | 18 |
| Calcium (mg/L) | 9.24 | 9.47 | 171 |
| Nitrate (as N) (mg/L) | ND<0.045 | ND<0.045 | ND<0.045 |
| Chloride (mg/L) | 44 | 44 | 27 |
| Sulfate (mg/L) | 10 | 10 | 140 |
| Alkalinity (mg/L) | 881 | 866 | 385 |
| Bromide (mg/L) | 0.11 | 0.12 | 0.12 |
| Lithium (mg/L) | 0.0521 | 0.0542 | ND<0.0402 |
| Strontium (mg/L) | 0.403 | 0.415 | 0.748 |
| Boron (mg/L) | 1.67 | 1.8 | 0.0887 |
| Iron (mg/L) | 4.46 | 3.83 | 0.0266 |
| Manganese (mg/L) | 0.0623 | 0.0587 | 0.0569 |
| pH by Field Method | 8.32 | 8.32 | 6.75 |

There is substantial literature regarding groundwater, and in order to understand the hydrochemical nature of the water, it is necessary to understand the relation between the chemical character of the water, mineralogy of the environment, and circulation of the water. During this project, the intent was not to understand the details of this process, but rather to confirm the source of the water that may have impacted SS-25.

The hydrochemical facies has been used to explain the distribution and genesis of different types of groundwater. Hydrochemical facies reflect the chemical process in the lithologic environment and the groundwater flow. Factors that control the chemical nature of the groundwater are mineralogy, transmissibility, and topography. Regions with major recharge of the water generally have water lower in dissolved solids.

Generally, natural waters contain few dissolved constituents, with cations and anions in chemical equilibrium. The common cations include two alkaline earths (calcium and magnesium) and also an alkali (sodium). The anions are bicarbonate, sulfate, and chloride. Consequently, in order to assess these waters, Alfred Piper developed a single point plotting of cations and anions on trilinear coordinates [26]. This is commonly referred to as a Piper Plot. It consists of three pieces: a ternary diagram representing cations, a ternary diagram representing anions, and a diamond plot representing a combination of the two. The diagram is depicted in Figure 79. All three fields have scales reading 0 to 100 parts. In the triangular field at the lower left, the three cation groups are plotted as a single point. Similarly, in the

triangular field at the lower right, the three anion groups are plotted as a single point. The central diamond shows the overall water chemistry, which is an intersection of the points projected from each of the triangular fields. The chemistry of the water is depicted as relative concentrations.

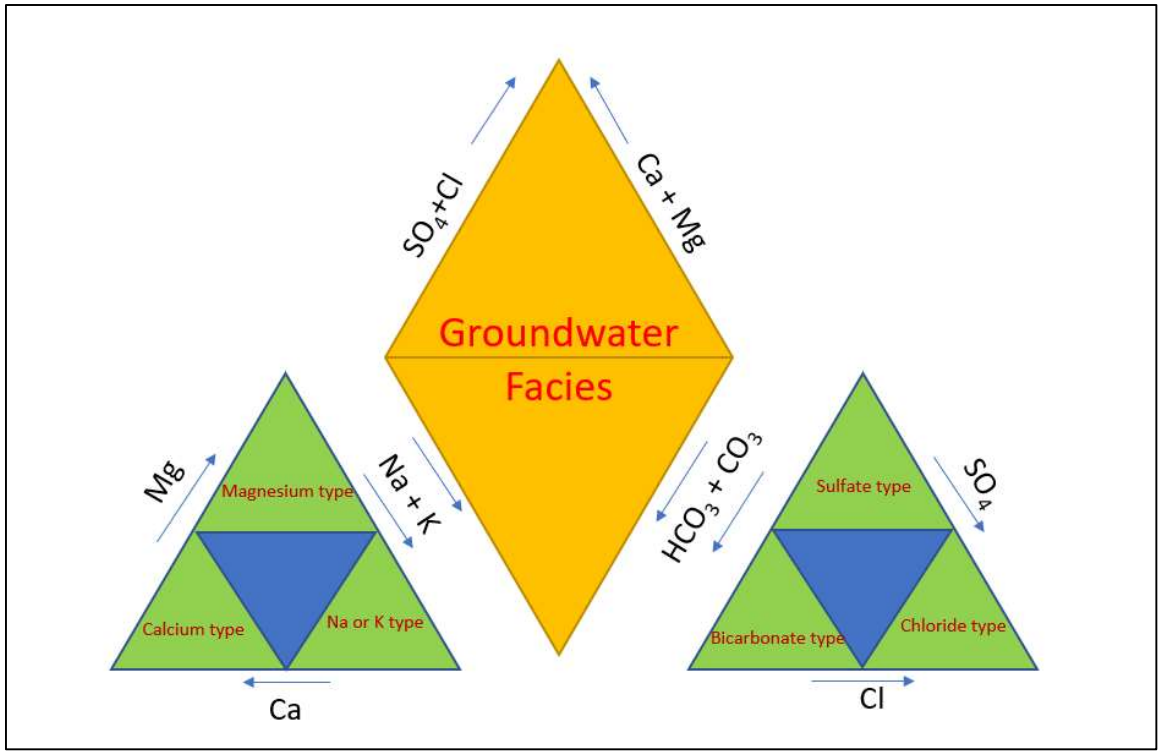


**Figure 79: Piper Plot Diagram**

To interpret the water samples, the grab samples that were collected while drilling and the samples collected from the two monitoring wells are depicted on a Piper Plot in Figure 80 [27]. The grab samples compared to the monitoring well samples from shallow depth were identical, which was expected. These waters had calcium cations with bicarbonate. However, the deeper sample was richer in sodium with bicarbonate anions. The cations were different for the shallow versus the deeper water samples.

The difference in the water samples may be due to a mechanism that is discussed in hydrochemical literature known as ion-exchange [28]. The interaction of the water with the clay minerals has been known to result in an exchange of the ion from the water with that adsorbed on a solid. Clays are known to have high ion-exchange capacities when compared to other minerals. As the water permeated deeper into the formation, it would have encountered other clay formations, and the calcium ion would have been replaced by the sodium ion. This mechanism explains the difference in water chemistry between the shallow and deeper samples.

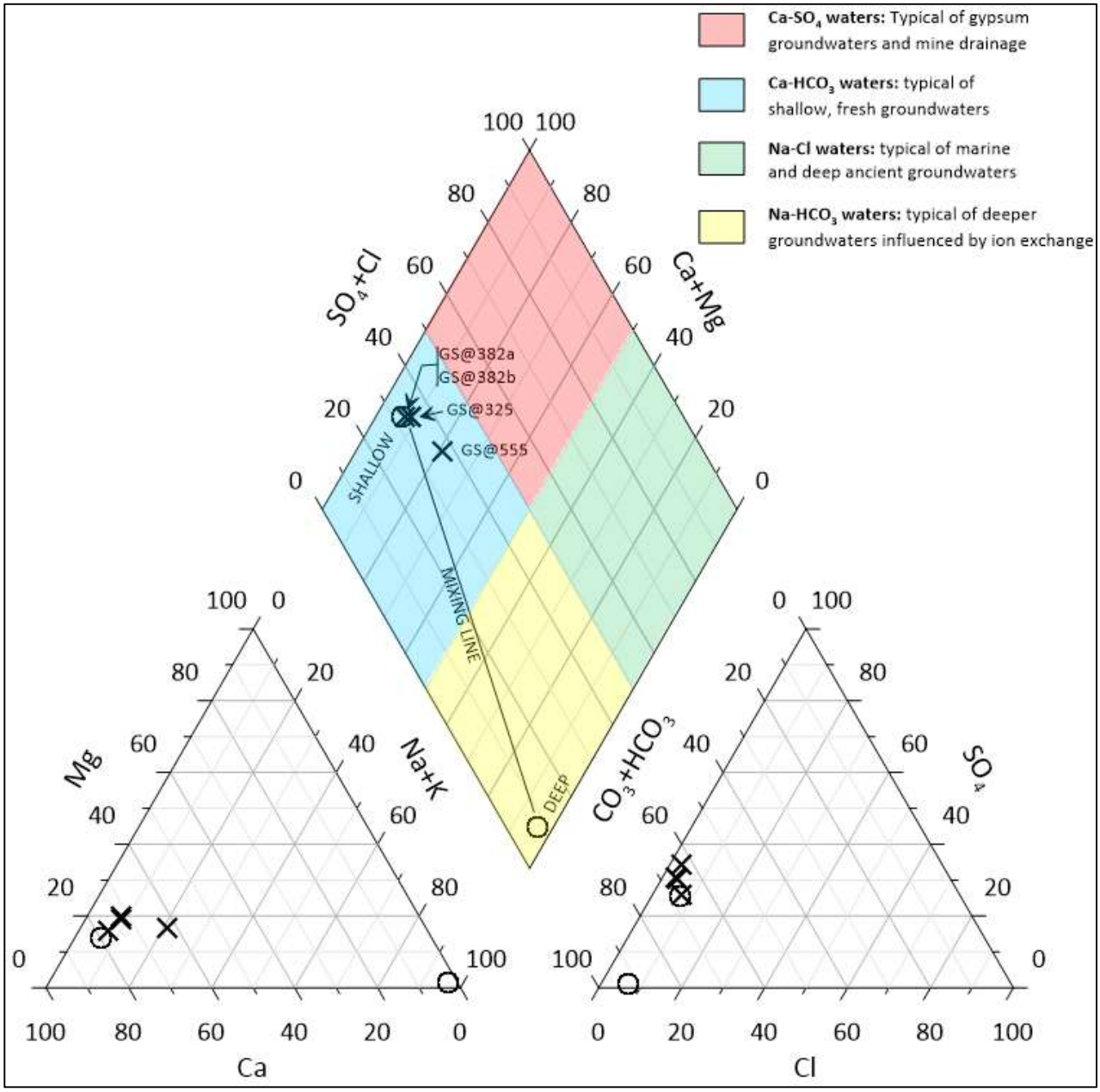


**Figure 80: Piper Plots Showing all the Water Analyses**

There were distinct shallow (340 to 440 ft) and deeper (900 to 1,000 ft) groundwater with slight differences in water chemistry. This water likely represented the environment in the production casing annulus and outside of the surface casing.

### 2.7.1 TH-1 Well Log Analysis

Several geophysical logs were run in both RBMW-1 (on SS-9 site) and the SS-25 well. The primary objective was to locate water zones, if any. Both these logs need to be considered in the interpretation, especially since the formations around the SS-25 wellbore may have been compromised because of the uncontrolled flow and numerous kill attempts. Therefore, RMBW-1 was used to understand the undisturbed subsurface hydrology and compare that to SS-25 (Figure 81).

First, let us discuss the Schlumberger log data from RMBW-1.

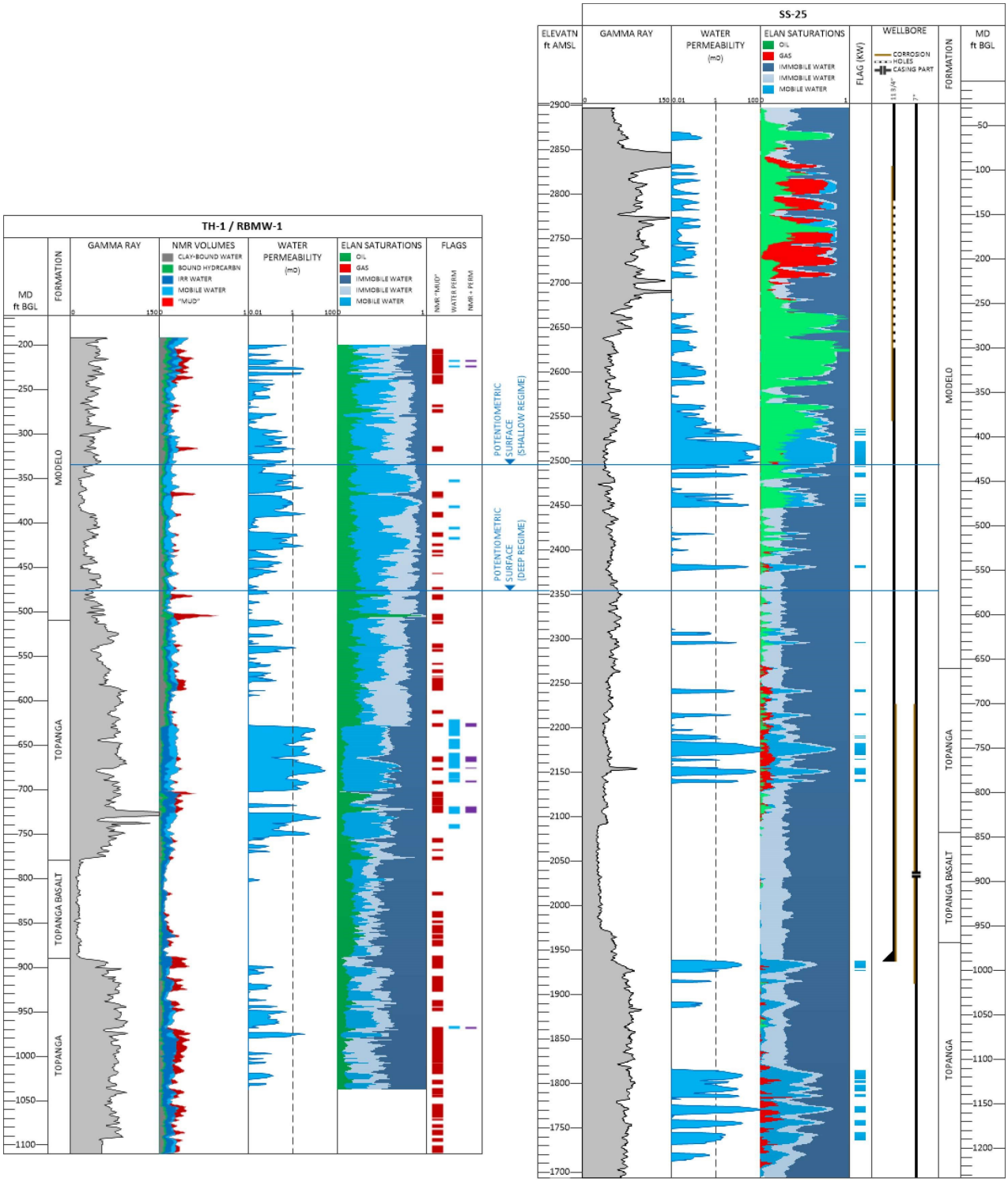


**Figure 81: Correlated Geophysical Logs for RBMW-1 and SS-25 Wells**

In the NMR track, the Mud column indicates high-permeability layers, which would be invaded by drilling fluids once the hole is filled to run the NMR logs. Since NMR logs can only be run in open holes, it was not possible to run an NMR log in the SS-25 well. The Modelo formation is above 510 ft in RMBW-1, whereas it is above 660 ft in the SS-25 well. Similarly, above the basalt, the Topanga formation ranges from 510 to 780 ft, whereas in the SS-25 well it ranges from 660 to 845 ft. After the basalt, the Topanga formation starts at 890 ft in RMBW-1 and starts at 970 ft in SS-25.

The water permeability track estimates the permeability based on correlations. The saturation track estimates the pore fluid type based on an assumed lithology model. The flag track indicates suspected water layers with high permeability based on both NMR measurements and water permeability estimates.

For RBMW-1, the following observations are made:

- Around six thin high-permeability water layers between approximately 310 and 420 ft are observed in the Modelo formation.
- One massive high-permeability water layer between approximately 620 and 690 ft is observed in the upper Topanga formation (above the basalt), and one thin and two thicker high-permeability layers are observed between approximately 710 and 740 ft.
- No high-permeability water layer is observed in the basalt.
- One moderately thick high-permeability water layer is observed just below the basalt at approximately 970 ft.

For SS-25, the following observations are made:

- One massive and several thinner high-permeability water layers are observed between approximately 400 and 450 ft in the Modelo formation.
- Several thin to moderately thick high-permeability water layers are observed between approximately 740 and 790 ft in the upper Topanga formation (above the basalt).
- Similarly to RMBW-1, no high-permeability water layer is observed in the basalt.
- A moderately thick high-permeability water layer between 990 and 1,000 ft is observed below the basalt, right at the 11 3/4 in. casing shoe, and several moderately thick high-permeability water layers between 1,110 and 1,190 ft are observed below the shoe.
- Hydrocarbons seem to have saturated the formation above 500 ft. Gas is apparent above 230 ft, and the massive water layer between 400 and 450 ft seems to have been (partially) displaced by oil (liquid hydrocarbons). These may be remnants of the escaped gas and/or kill fluids during the SS-25 incident and may provide clues to the path taken by fluids escaping from the wellbore.
- Gas saturation in the upper Topanga formation (between 610 and 800 ft) and below the basalt (1,110 ft and below) may indicate the path taken by fluids escaping from the wellbore during the SS-25 incident.

In summary, Figure 81 suggests that the mobile water is encountered in distinct higher-permeability layers in both Modelo and Topanga formations, but not in the basalt layer. From both logs, the basalt contains no water in SS-25 and RBMW-1. Below the basalt, there is a distinct water zone ranging from 990 to 1,010 ft in SS-25 right at and below the 11 3/4 in. shoe. There is a water permeability streak and mobile water between 990 and 1,010 ft in SS-25. This was likely the source of water that entered the production casing annulus. Further, several shallow high-permeability water layers are observed in both

SS-25 and RBMW-1 in the Modelo formation. These were likely sources of water for the corrosion observed in the 11 3/4 in casing.

### 2.7.2 Groundwater Source

The standing water level in RMBW-1 was 2,354 ft above mean sea level (AMSL) (483 ft) and in RMBW-2 was 2,496 AMSL (341 ft). Therefore, the source of groundwater must lie above these elevations. Figure 82 shows the elevation map around Aliso Canyon field. The 2,354 ft AMSL and 2,496 ft AMSL levels are marked. In Figure 82, the red-blue shaded (filled) region is the elevations between 2,354 ft AMSL and 2,496 ft AMSL. The red edge of the shaded area is the lower (2,354 ft AMSL) elevation; the blue edge of the shaded area is the higher (2,496 ft AMSL) contour. The source of groundwater must lie within these contours; however, there are no surface bodies of water (such as lakes and rivers) within these contours. Since there is no existing body of water that is a source of groundwater, precipitation that falls within these contours can be the only source of this water.

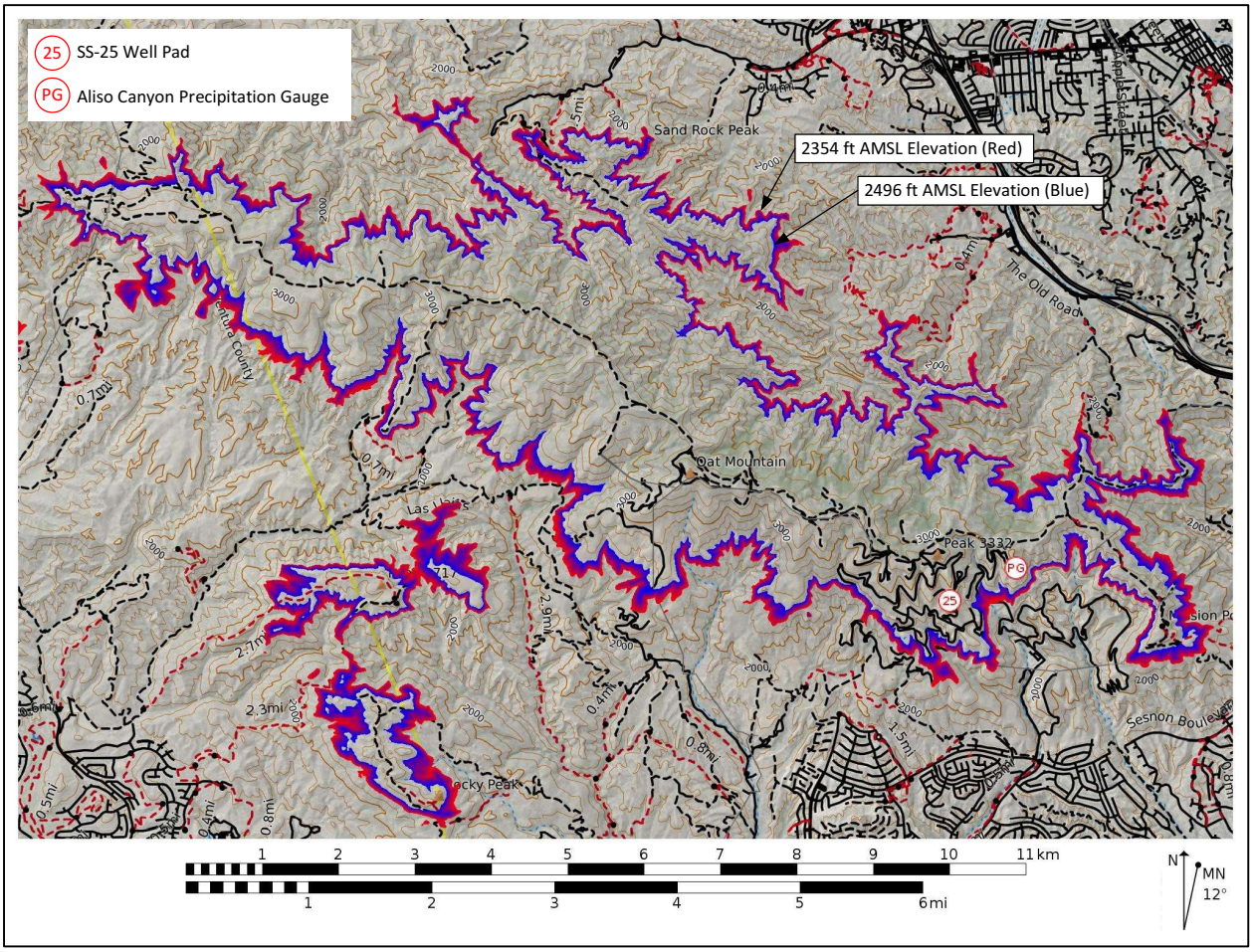


**Figure 82: Regional Elevation Contour Map [29]**

Figure 83 shows the Aliso Canyon's precipitation for rain years starting with 1996–1997. Data are taken from the Aliso Canyon's rain gauge for those years with complete records and estimated from San Fernando Valley's precipitation records for the remaining years. In addition, a cumulative precipitation surplus (positive) or deficit (negative) is also shown.

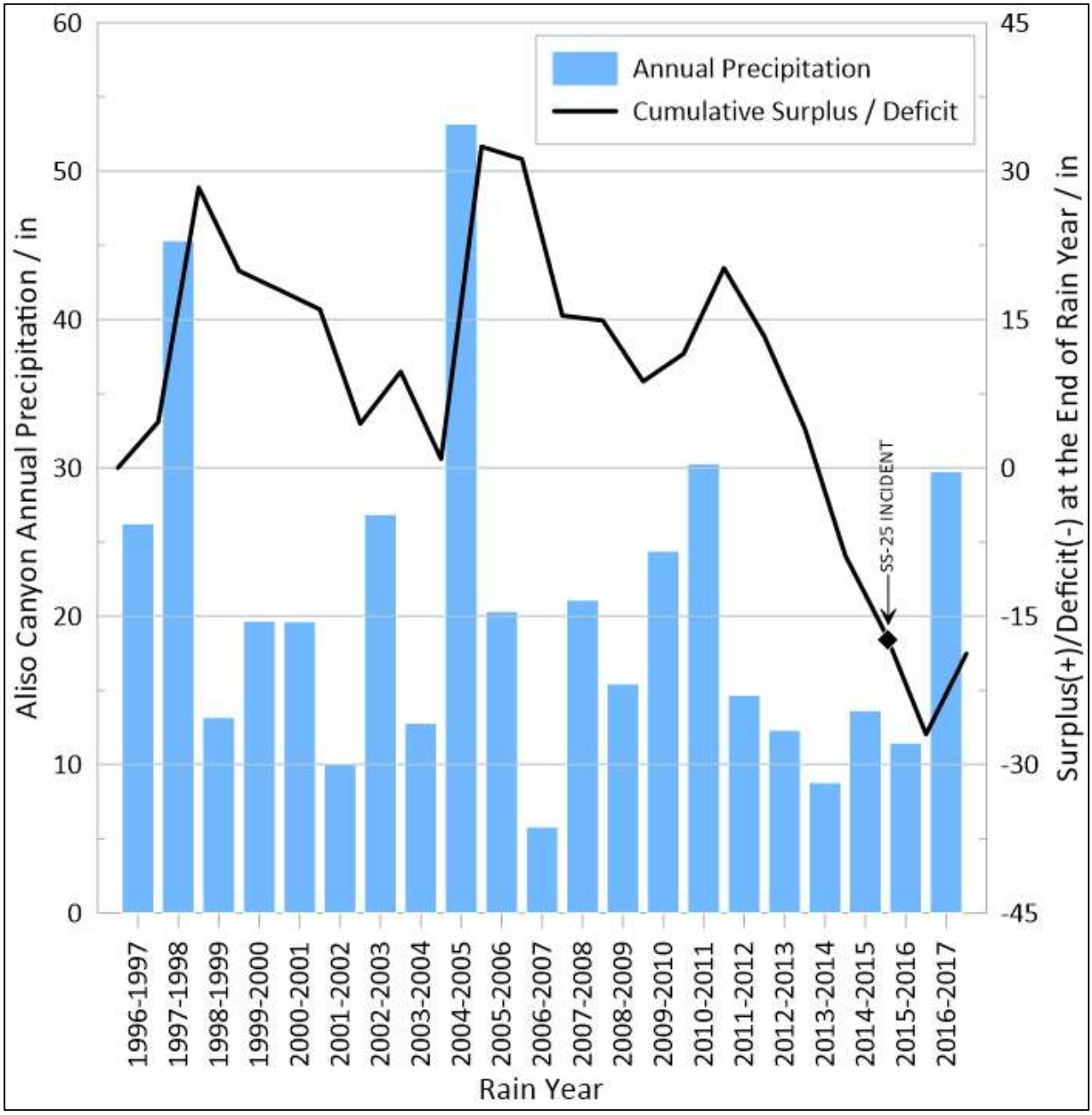


**Figure 83: Aliso Canyon Annual Precipitation (1996-2017)**

Cumulative surplus at the end of a rain year is calculated as follows: take the cumulative surplus at the end of the previous rain year, add the total precipitation during the current rain year, and subtract the normal annual precipitation of 21.58 in.

Cumulative surplus is set to zero at the end of the 1995–1996 rain year. Since precipitation is the source of groundwater, groundwater level should be related to precipitation level. First, groundwater level will vary within a given rain year. The groundwater level will rise during the rainy period from December to March, reaching its highest level at the end of the rainy period in March. The groundwater will then fall during the dry period from March to November, reaching its lowest level at the beginning of the subsequent rainy period. In addition, groundwater level will also vary from year to year: it will rise after

wetter-than-normal rain years, remain steady after normal rain years, and fall after drier-than-normal rain years. The groundwater level is proportional to the precipitation, so the groundwater level is expected to vary with the precipitation. In the rain year 2014–2015, there was a substantial deficit (–22 in.) in rain.

Consequently, the water level in the production casing annulus will rise and fall with the seasons and the extent of precipitation. Further, the water level in the annulus would have been at its lowest during the period of the incident.

### 2.7.3 Water Samples–Casing Hole Dynamics Tester

In mid-2018, Schlumberger, with Blade's supervision, performed several runs in the SS-25 and P-35 wells with the CHDT (Cased Hole Dynamic Tester) for the purpose of collecting fluid samples from behind the SS-25 11 3/4 in. surface casing and the P-35 7 in. production casing. The CHDT is a wireline operated tool which can stabilize itself at any given depth in the well and drill a hole laterally through the casing wall. A fluid sample can then be obtained through the hole.

The intent was to obtain multiple fluid samples from different depths (0 to 1,000 ft) for the purpose of identifying the nature of the fluids that might have existed in these locations prior to the SS-25 blowout. Samples from P-35 were obtained to verify the SS-25 observations.

Through interpretation of the chemical analyses of these samples, it was established that their mineral content varied in wide limits, from about 400 mg/L to over 60,000 mg/L. More importantly, it was also found that the sodium to potassium weight ratio in the many samples that were collected from both wells increased exponentially with a decrease in the chloride concentration, as shown in Figure 84.

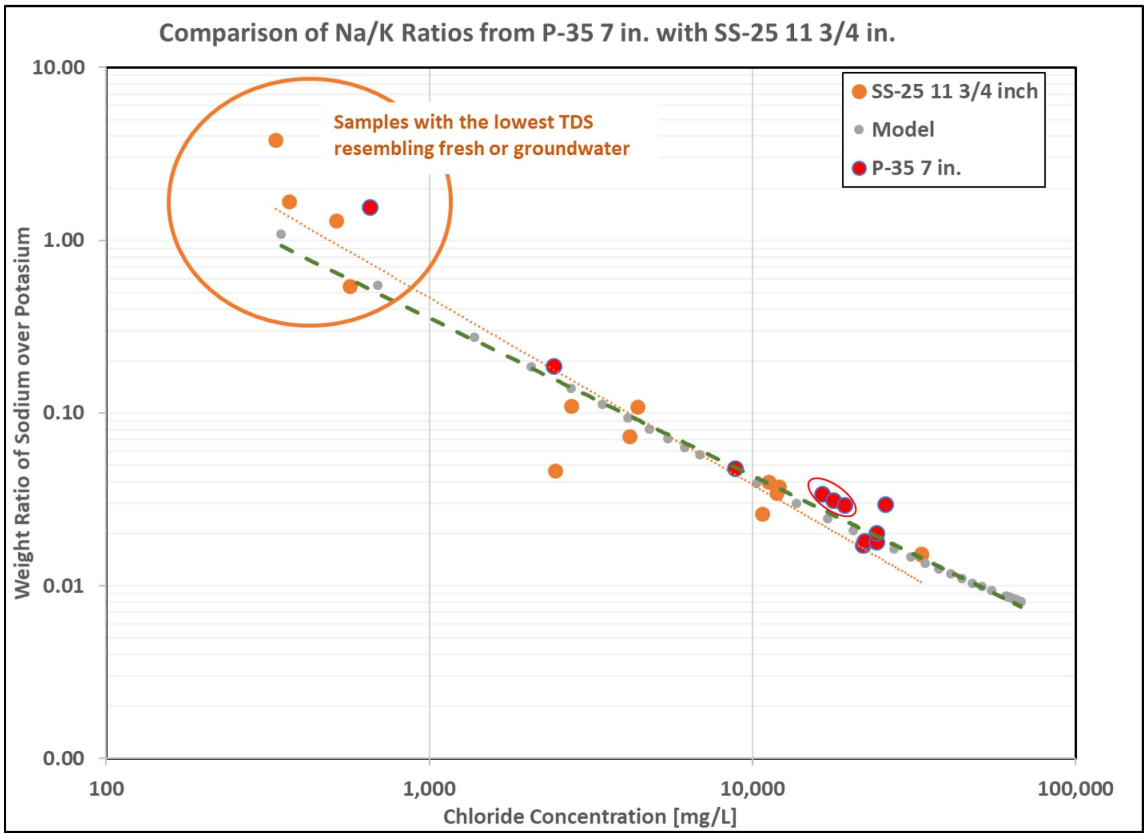


**Figure 84: CHDT Results-Ratio of Sodium over Potassium versus Chloride**

These results are interpreted by recognizing that during the drilling and completion of these wells, workover fluids, largely consisting of potassium chloride, got sequestered in areas of high permeability and porosity of the formations through which the wells were drilled. In certain locations around 900–1,000 ft (SS-25) and 400–500 ft (P-35), however, high Na/K ratios were found with very low chloride concentrations. This could only have occurred if low salinity groundwater rich in Na and low in K caused the residual, sequestered, workover fluid to be diluted. This dilution process was modeled and the model was found to result in identical relationships for both wells. These results conclusively establish the presence of low salinity groundwater at certain depths. Only if such low salinity groundwater were in fact flowing at these locations would the extreme dilution to less than 500 mg/L chloride in certain samples have been possible.

### 2.7.4 Mechanism

The groundwater resulting from run-off rain water likely entered the annulus and replaced the drilling fluid over time; or mixed with the drilling fluid and the composition of the annulus fluid changed over time. These are all possibilities, however, based on the evidence, the groundwater is ubiquitous and played a role in the external corrosion of the 7 in. casing.

The possible mechanism of the groundwater and drilling fluid interplay is depicted in Figure 85 that includes five steps. The first step, as shown in Figure 85, is the as is well completed condition with the drilling fluid in the 11 3/4 in. × 7 in. annulus. The second step is that over a period of time the drilling fluid would have leaked off into the formation. Over time in step 3, groundwater accesses the surface casing annulus and the OD of the 11 3/4 in. surface casing. The corrosion process would have initiated at this stage, especially as gas is seeping through connections. This finally results in external corrosion on the OD of the surface casing and the OD of the production casing. The fluid level in the surface casing annulus would have fluctuated with time and precipitation; however as discussed in the next section extensive 7 in. OD corrosion is observed from 700 feet and deeper.

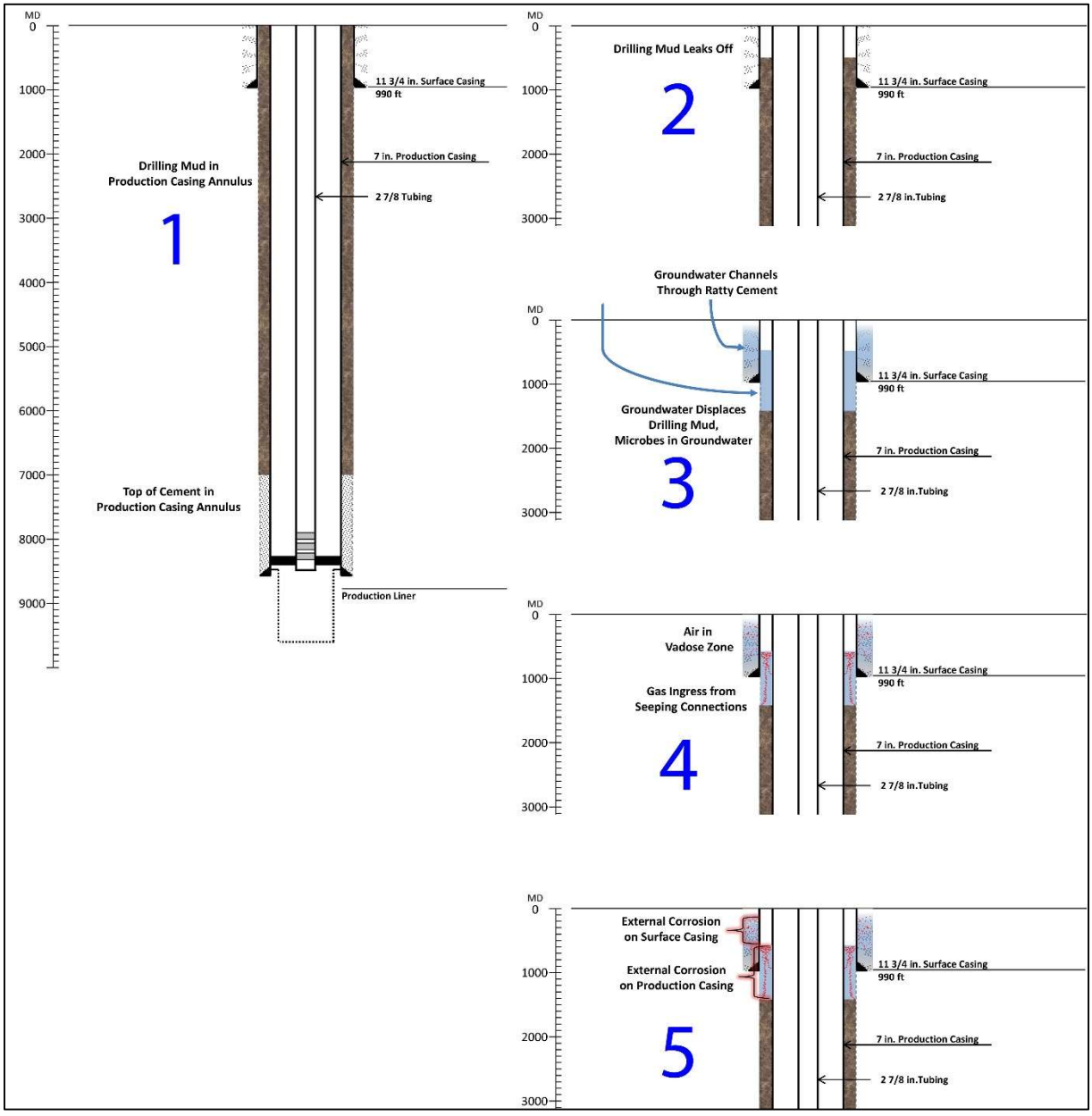


**Figure 85: Likely Mechanism of Groundwater Ingress into the Surface Casing and Production Casing Annuli**

In order to further assess the fluctuating levels of water in the annulus and ingress of groundwater at the SS-25, temperature logs are discussed and shown in Figure 86. The temperature logs are magnified to a depth of 1,200 ft and the data from years 2000 to 2014 including 1984 are also shown. The smaller deflections are evident and there are three distinct zones that are apparent. The shallow low temperature regions are related to surface cooling at the SS-25 site, which is a knoll and is generally cooled at surface. There is another consistent deflection at around 700 ft and was likely due to the presence of surface casing fluid level. There is mild variation to that depth and may be due to variations in groundwater level. Finally, there is a smaller deflection at around 1,000 to 1,100 ft and probably due to ingress of groundwater. These are likely interpretations of the temperature logs; the deflections/deviations are consistent over the years. The surface casing fluid level is consistent with the presence of OD corrosion.

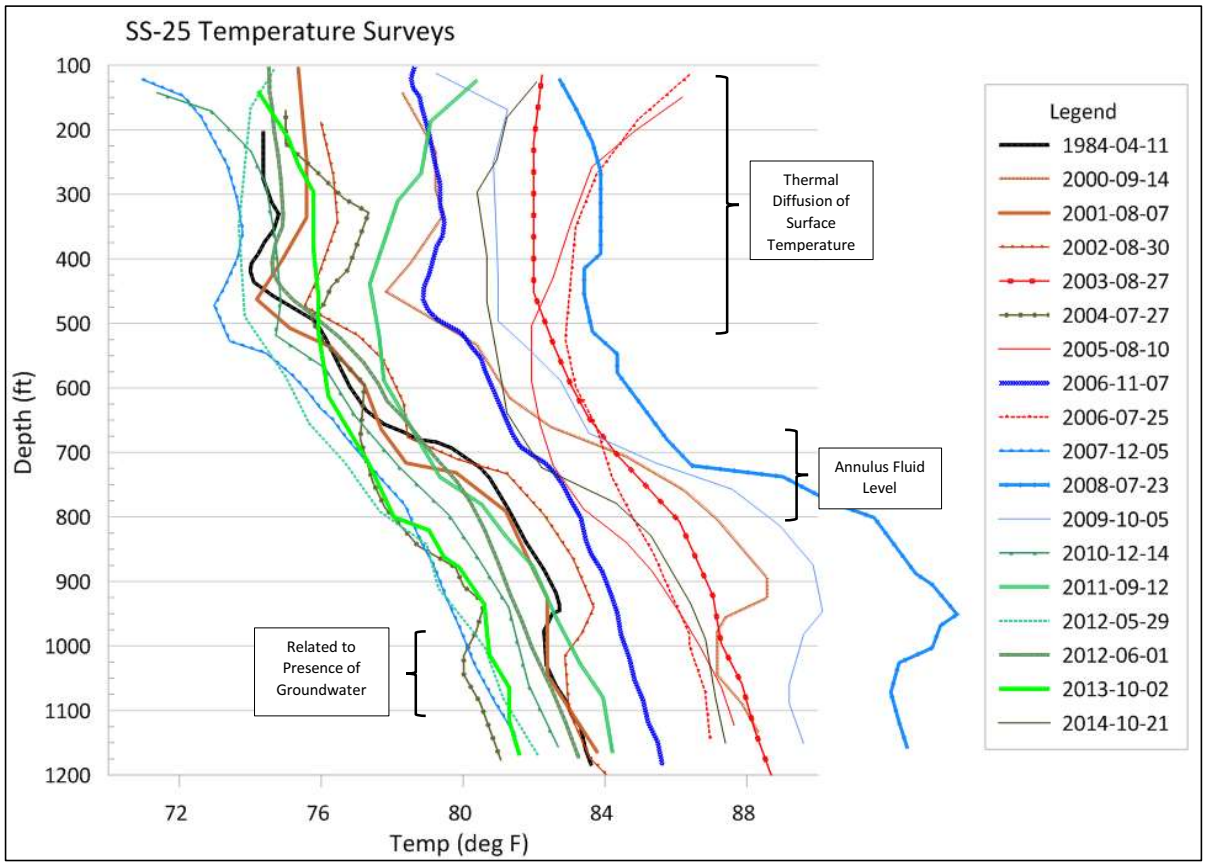


**Figure 86: Pre-Incident Temperature Surveys - Interpretation of Deflections, Depths 100–1,200 ft**

## 2.8 7 in. Casing Outside Diameter Corrosion

### 2.8.1 Corrosion Distribution

Visually, it was evident that there were OD corrosion features, with both their number and dimensions increasing with increasing casing depth. In order to quantify the corrosion features, all the extracted casings were examined using a laser scanner. The feature dimensions were recorded, and the feature types were characterized.

Prior to laser scanning, the joints were blasted with Black Beauty Extra Fine blast media, a coal slag media that is aggressive enough to provide a clean surface while simultaneously minimizing the amount of surface material that is removed. Extra Fine uses small particles designed for light duty brush-off blasting on surfaces that are generally clean. This is routinely used to clean surfaces of casing and pipelines to remove corrosion products and other debris. Following cleaning, the OD surfaces were laser scanned in 10 ft sections. The details of the scanning procedure are discussed in the *SS-25 Casing Failure Analysis* report [19].

The 3D map of the corrosion on joint 18 is shown in Figure 87; all indications greater than 5% of nominal wall thickness are identified in the image. The nominal dimensions used for all the scans were 7 in. for the OD and 0.317 in. for the wall thickness.

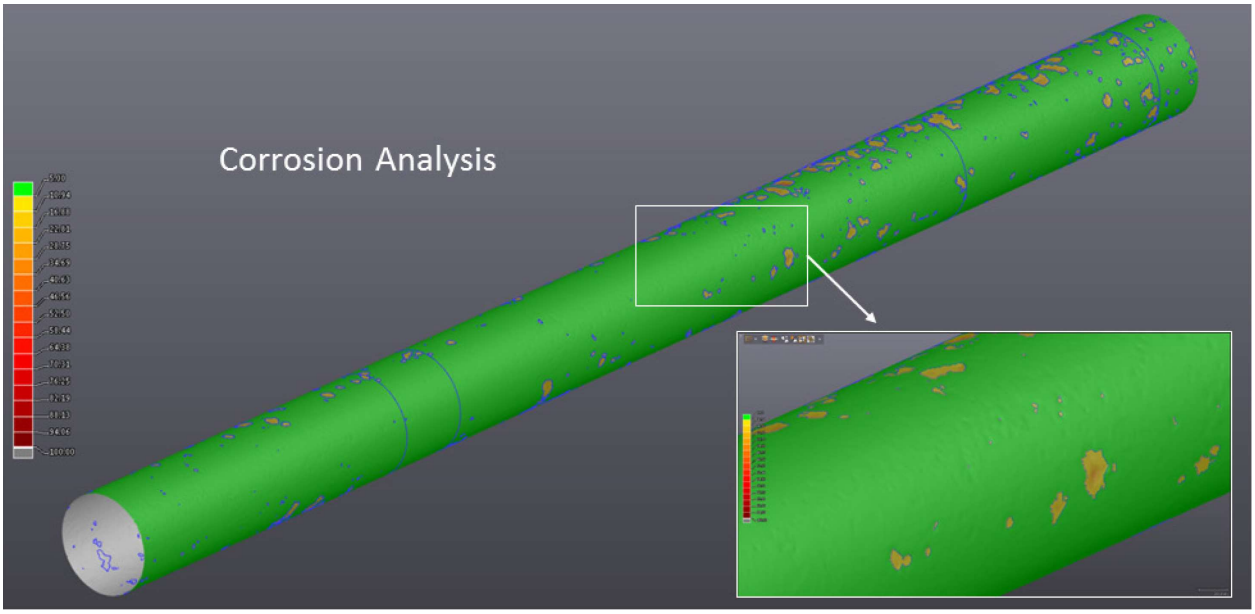


**Figure 87: 3D Color Map of Corrosion Analysis Results for C018A**

All the data collected from the casing joints are summarized in Figure 88. The corroded area, number of features per casing joint, max corrosion depth per each joint, corrosion depth for all features, and finally depth distribution versus orientation are shown, demonstrating the distribution of the corrosion for all twenty-five 7 in. production casings extracted including connections. There is very little to no corrosion from joints 1 through 17 to a depth around 700 ft. In terms of maximum corrosion depth, the failure joint 22 had corrosion penetration at the failure location that was 85% wall loss. The majority of the corrosion features were 40% and lower in penetration. Joints 21, 22, 23, and 24 had the largest concentration of deep corrosion features. The key observation for all the joints with OD corrosion is that

the distribution is oriented all around the circumference of the production casing. No preferential orientation was noted for the OD corrosion in the 7 in. production casing.

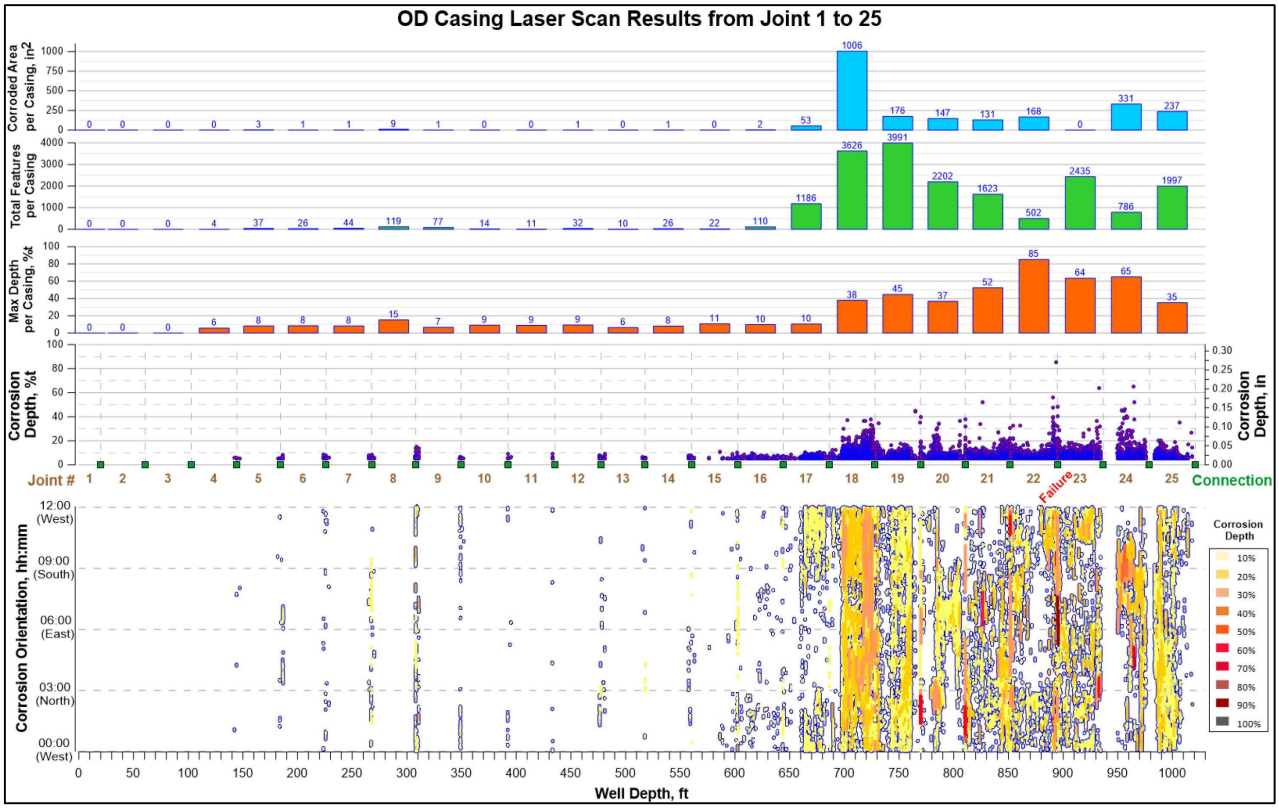


**Figure 88: 7 in. Casing Outside Diameter Corrosion Distribution for Joints 1 through 25**

Visual examination of the corrosion features revealed three different types of corrosion across the joints. The corrosion features were classified as Type I, II, and III.

Type I was typical of the failure location and was characterized by striations as shown in Figure 89. These striation features have a groove with a sharp 'V' on each end of the groove. Type I corrosion could be visually identified, and the size of these features varied by location. The striated grooves were noted in all the joints starting from joint 18 onwards; however, none of the connections exhibited this type of corrosion.

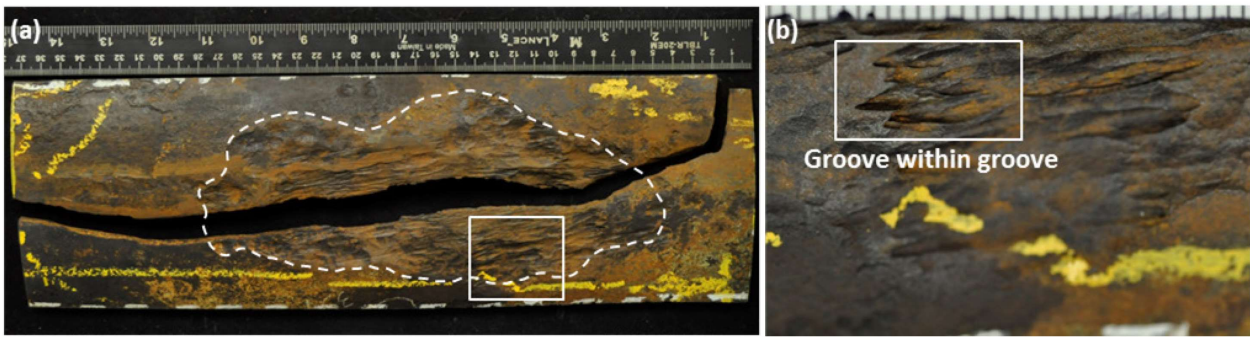


**Figure 89: (a) Joint 22 Axial Rupture and (b) Type I Feature Showing V-shaped Tips**

Another type of corrosion that was observed in the joints is classified as a Type II feature as shown in Figure 90. These features were isolated smaller pits, and quite often shallow. These were observed across all of the joints and some connections.

**Figure 90: Type II Corrosion—Isolated Small Pits**

Finally, Type III features appeared as very unusual elongated shapes. Several small scoop-shaped features adjacent to each other are seen within the elongated region as shown in Figure 91. The middle region of Type III feature is not severely attacked by corrosion. Nearly, every connection from connection 16 onwards exhibited Type III, and it was not noted on any of the joints, with one exception (joint 20).

**Figure 91: Type III Corrosion feature**

All the joints and connections were visually examined during laser scanning, and the types of corrosion were characterized. The shallower joints C015, C016, and C017 exhibited only the feature Type II. However, deeper in the well from C018 to C026, the joints had all three feature types, with Type I being predominant in many cases. In joint C020, Type III was observed in the casing body. None of the other joints had Type III on the body. The different types of features indicate various ongoing corrosion mechanisms.

### 2.8.2 Corrosion Features Related to the Failure–Type I

Type I corrosion at the failure location, as shown in Figure 89, is distinct in nature. The possible cause for such corrosion was assessed and investigated by using morphology, scale, and microbial data.

## Corrosion Characterization–Macro, Micro, EDS, and Raman

The axial rupture occurred at the location where the Type I corrosion feature was present (Figure 89). Type I features can be described as a patch of metal loss with striated grooves that are oriented 10 to 15 degrees off longitudinal axes. The grooves contained pointed tips as seen in Figure 89. Some groove tips were present within another groove. The Type I metal loss features were observed as isolated patches along the length of the SS-25 7 in. casing. The maximum wall loss within the patch was 85% of wall. Adjacent to the feature was unaffected metal surface (no metal loss).

The Type I feature was at the location of the axial rupture. As part of investigating the failure corrosion feature, many specimens with Type I corrosion features were extracted and analyzed by using the optical microscope, SEM, and energy dispersive spectroscopy (EDS). Three such specimens are discussed here in some detail. The specimens labelled C023A1B2 (A, B, and C) are all associated with the failure region. The other specimens are from corrosion locations that had not failed. Specimens were cross-sectioned, polished, and etched to investigate the profile of the grooves and groove tips. Selected specimens were analyzed using Raman spectroscopy to identify the corrosion products or groove deposits.

**Corrosion at the Axial Rupture Location (C023A1-B2A5, C023A1-B2C2, C023A1-B2D2B)**

The axial rupture specimen C023A1-B2 from joint 22 had a corrosion patch with striated grooves (Type I corrosion feature). The corrosion patch had a length of 9.5 in. along the longitudinal axis. The specimen was divided into smaller sections to facilitate the SEM investigation of the fracture surface and corrosion features. Specimen C023A1-B2A5 from the axial rupture had a visible tunnel in the groove that was visually identified (Figure 92). The tunnel orientation was parallel to the axial rupture fracture surface. The tunnel penetrated the base metal. Figure 93 shows the magnified image of the tunnel using the SEM image of the same tunnel in Figure 92. Within the tunnel there are scale deposits. Despite the samples being exposed to kill and other fluids since the leak event, the scales and other deposits within these tunnels should have been relatively unaffected.

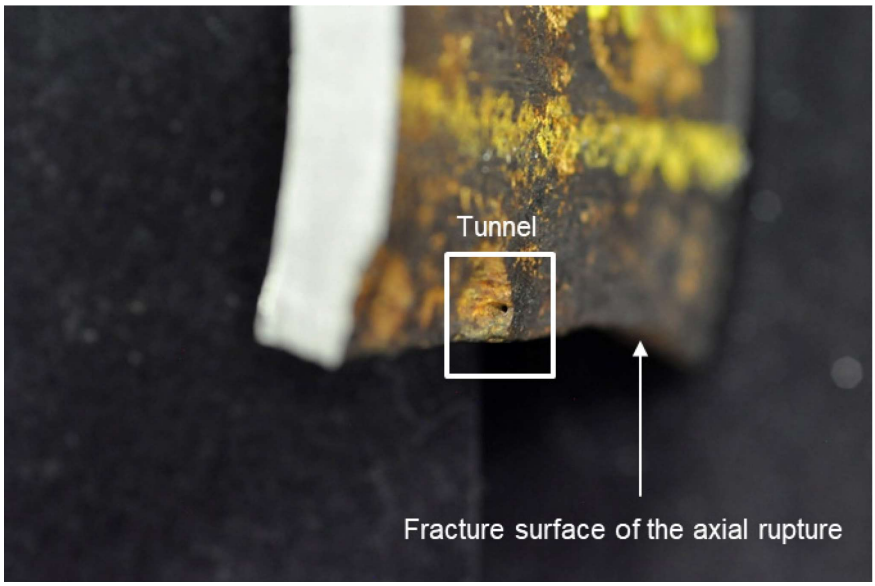


**Figure 92: C023A1-B2A5 Groove Tunnel Adjacent to Axial Rupture Fracture Surface**

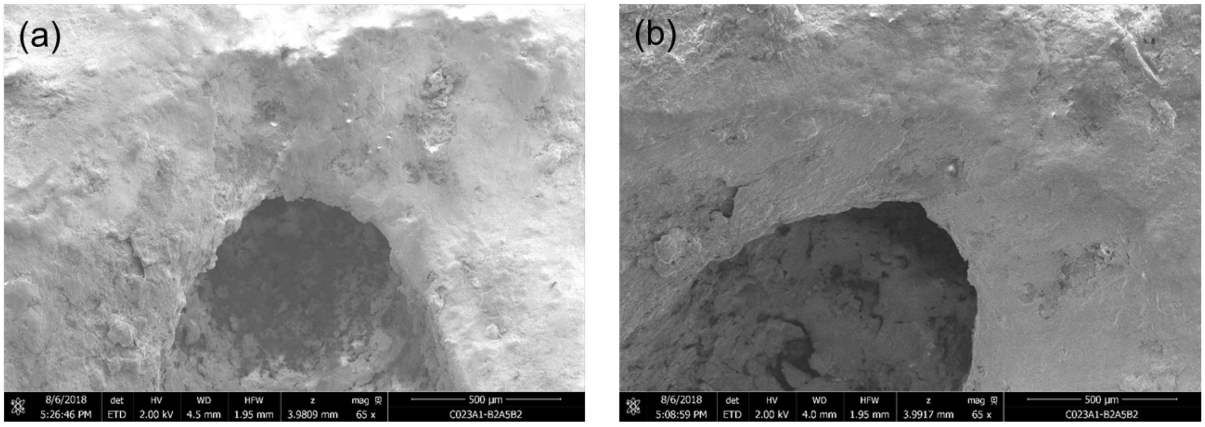


**Figure 93: Specimen C023A1-B2A5B2 Tunnel Seen at Different Angles**

Specimen C023A1-B2A5B2 was subjected to several focused ion beam (FIB) and metallographic cross sections. FIB is a tool that uses a gallium (Ga) ion source to cut the specimen at an angle while inside the SEM chamber and was used to assess the specimen or deposits to minimize any damage during sectioning. The intent of FIB sectioning was to avoid smearing and other modifications of the scale that might have occurred during traditional sectioning. The nature of the base metal and scale was investigated using the SEM after the FIB cross sectioning. The schematic of FIB sectioning and the corresponding SEM views are shown in Figure 94. FIB was used to remove a few microns following the local sectioning; the sectioned regions were pristine and revealed the nature of the deposit layers.

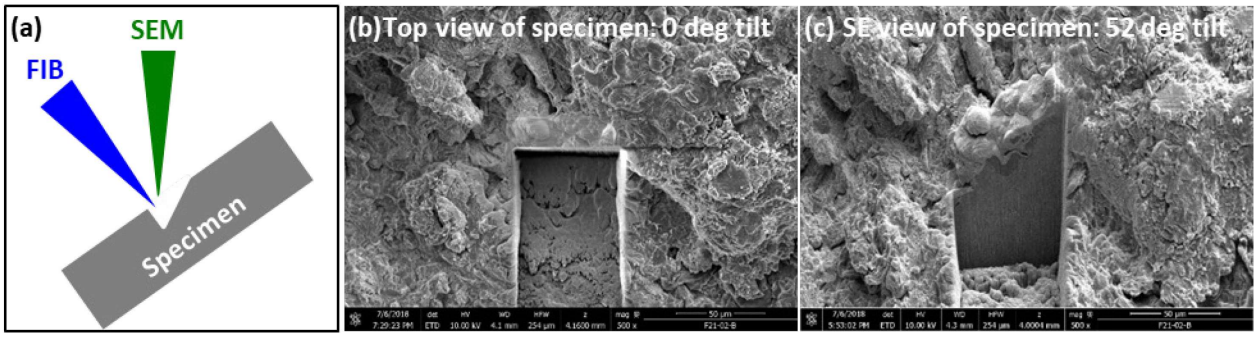


**Figure 94: (a) FIB Sectioning Schematic and SEM View of the Specimen (b) Without Tilt and (c) with a 52° Tilt**

FIB cross-sectioning was done on the wall of the tunnel to look at the deposit morphology on sample C023A1-B2A5B2. Figure 95 shows the corrosion deposit morphology, which looks like the bird's nest formation. This has been described by various authors who have studied atmospheric corrosion [30] [31] [32]. An EDS analysis revealed that the corrosion deposit contained ≈40 atomic percent (at%) Iron (Fe), 18 at% Carbon (C), 18 at% Oxygen (O), 9 at% Calcium (Ca), 0.2 at% Sulfur (S), and small amounts (<1 at%) of other elements. Another FIB cross section at the tip of the tunnel (Figure 96) reveals the corrosion products that form inside the tunnel. The main elements found with EDS were C (≈60 at%), Fe (≈19 at%), O (≈19 at%), and small amounts of S, K, Mn, Cl, Si, and Al. The corrosion product did not appear to be dense. Several layers of deposits were seen inside the tunnel.

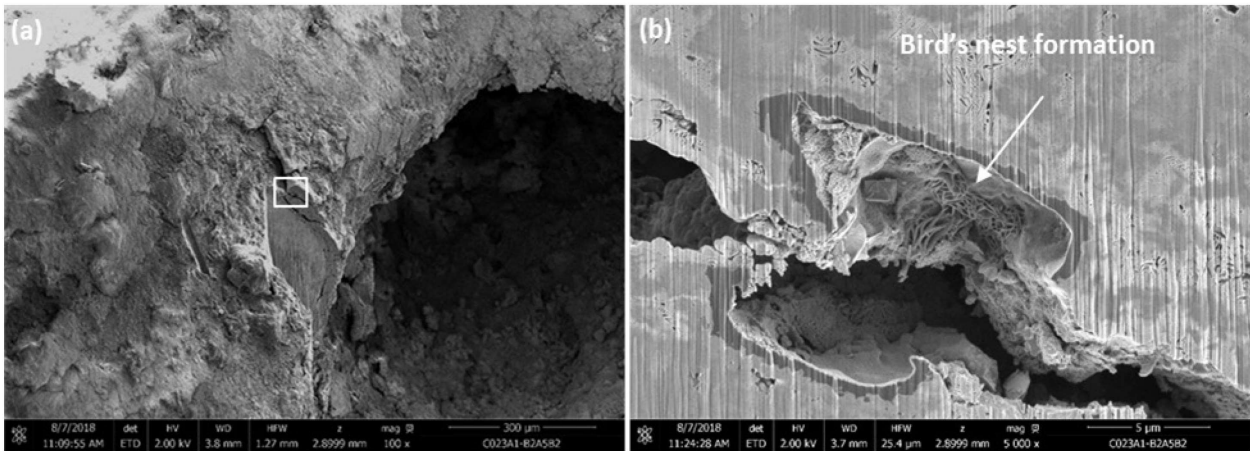


**Figure 95: FIB Cross Section of the Tunnel Wall in C023A1-B2A5B2 at (a) 100× and (b) 5,000×**

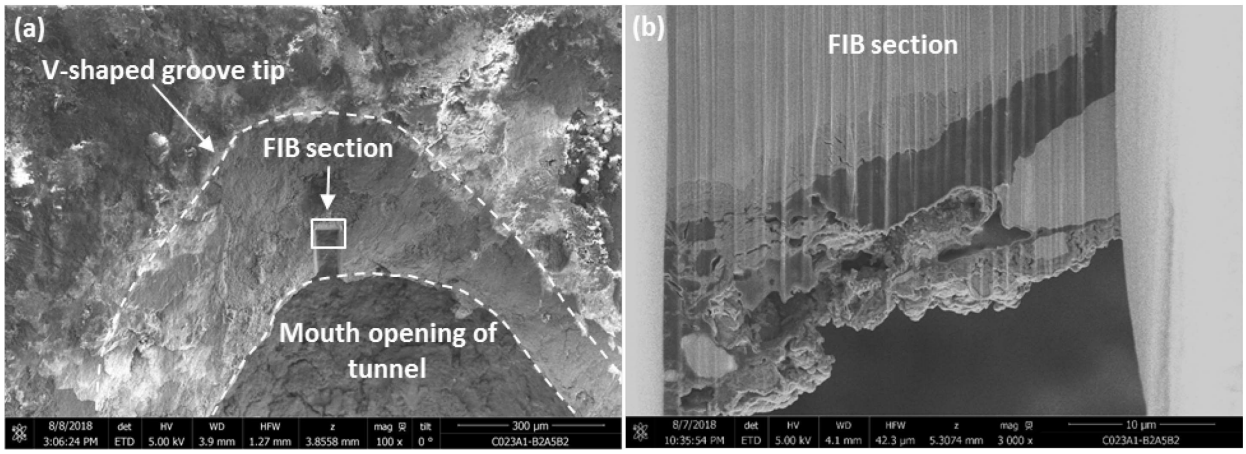


**Figure 96: FIB Cross Section of the Tunnel Tip in C023A1-B2A5B2 Viewed at (a) 100× and (b) 3,000×**

Further investigation of the area adjacent to the major tunnel identified a smaller tunnel at the initial formation stage. A closer look at the low magnification image in Figure 96 (a) shows a small, darker circular feature (white arrow) that appears to be another tunnel directly above the FIB cross section. Figure 97 shows a high magnification image of the circular feature. Material that appears to be extra-cellular was within the smaller tunnel. EDS analysis showed that the material surrounding the forming tunnel had a high amount of C (≈77 at%), with 10 at% Fe, 9 at% O, and 0.6 at% S. The high carbon on the extra-cellular looking material may indicate biological activity related to the formation of the tunnel.

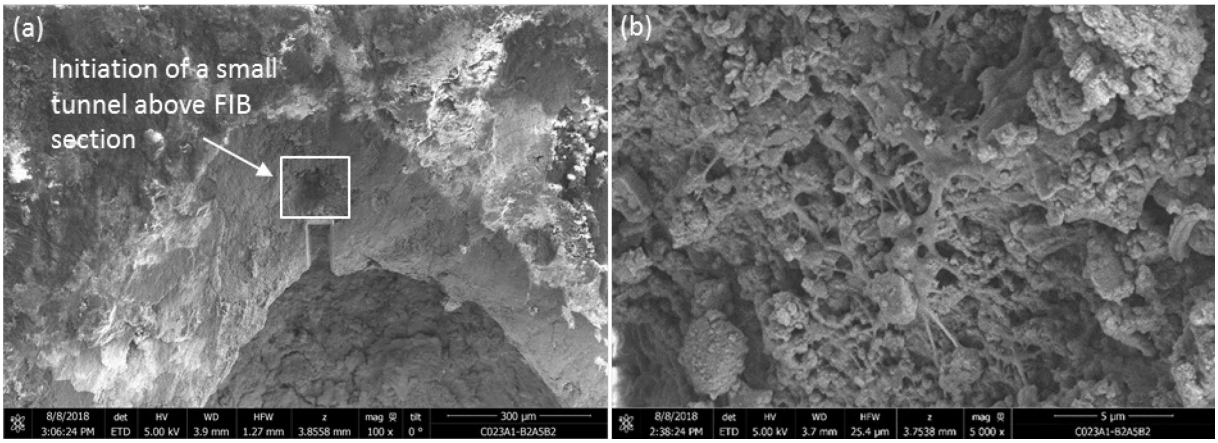


**Figure 97: C023A1-B2A5B2 (a) Small Tunnel and (b) Extra-Cellular Looking Material**

C023A1-B2A5B2A was subjected to a progressive-step wise metallographic sectioning across the major tunnel after the FIB investigation. The sample was mounted in epoxy. Figure 98 shows the groove profile of the depth of the tunnel along the longitudinal axis of the pipe after the second polish. The tunnel has a mouth opening of 0.0197 in. (0.5 mm) and extends 0.0393 in. (1 mm) into the metal. Figure 99 shows that the corrosion deposit at the tip of the tunnel is denser. Lamellar (plate-like) features are visible from SEM high magnification image in Figure 99. The presence of the lamellar cementite provides an anchor to the corrosion products [33]. EDS analysis showed that the corrosion product inside the tunnel was rich in O and C. The analysis also revealed that manganese sulfide (MnS) inclusion was present and surrounded by the corrosion product.

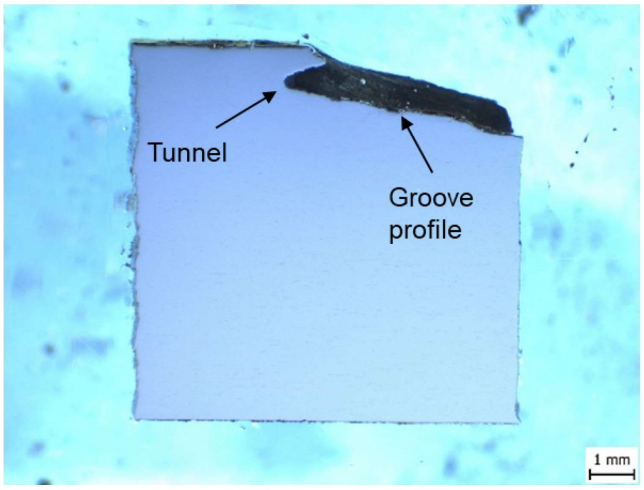


**Figure 98: Stereo Microscope Image of C023A1-B2A5B2A**

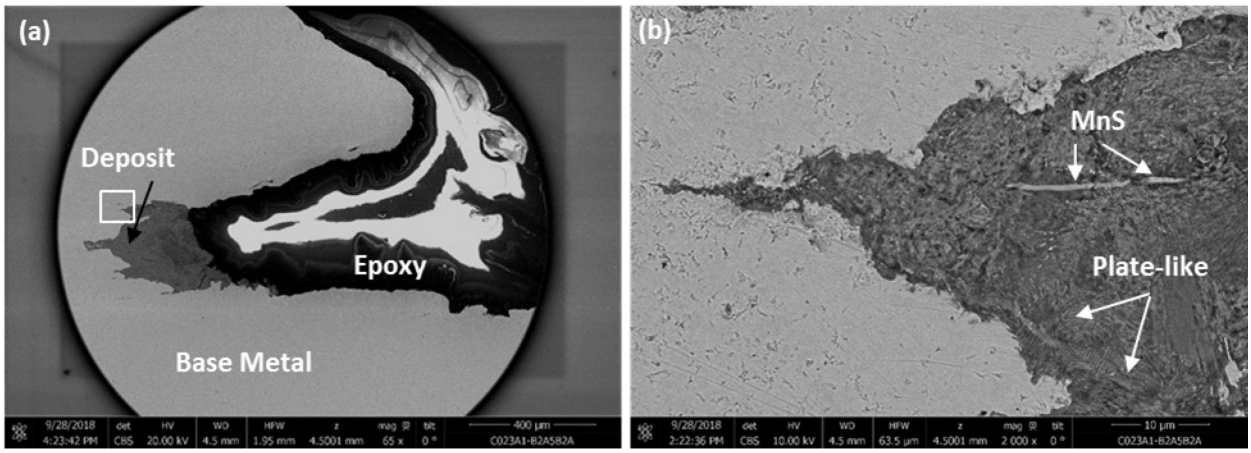


**Figure 99: (a) Second Metallographic Cross Section of C023A1-B2A5B2A and (b) High Magnification Image of Corrosion Deposit**

C023A1-B2C2 was extracted from the initiation site of the axial rupture fracture surface. The specimen was mounted in epoxy and polished. Figure 100 shows a cross section of C023A1-B2C2 indicating the presence of tunnels directly below the groove inside of the Type I corrosion feature. The cross section also shows that MnS inclusions are present in the tunnel along with the acicular corrosion deposit. Figure 101 shows the SEM image of the cross section and the sulfur and manganese mapping obtained with EDS. The corrosion products inside the tunnel were not very dense. They were identified as hematite, modified hematite, magnetite, and organic matter using Raman spectroscopy.

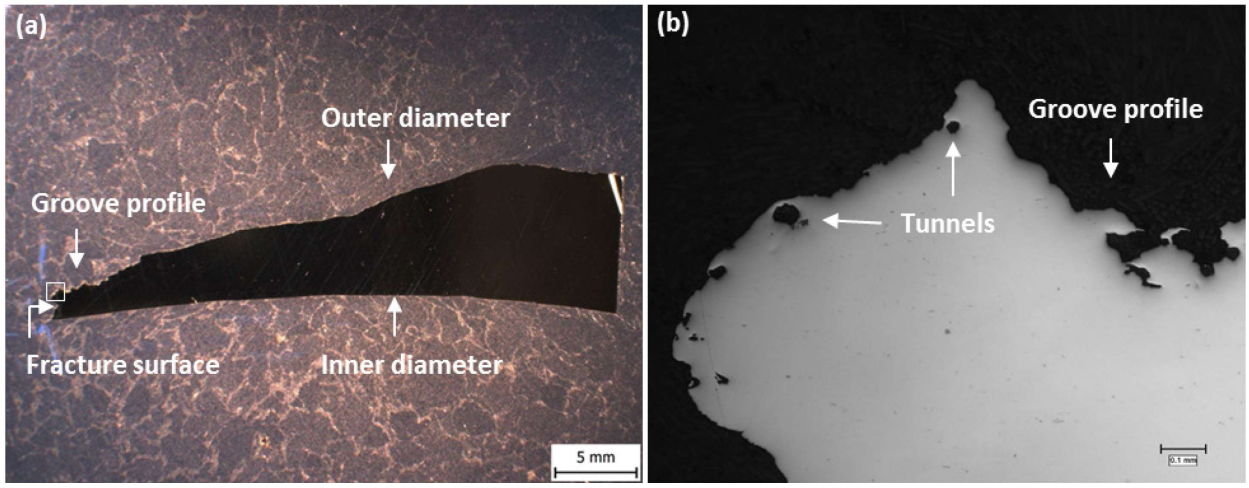


**Figure 100: (a) C023A1-B2C2 Mounted and Polished and a (b) High Magnification Image Near Fracture Surface**

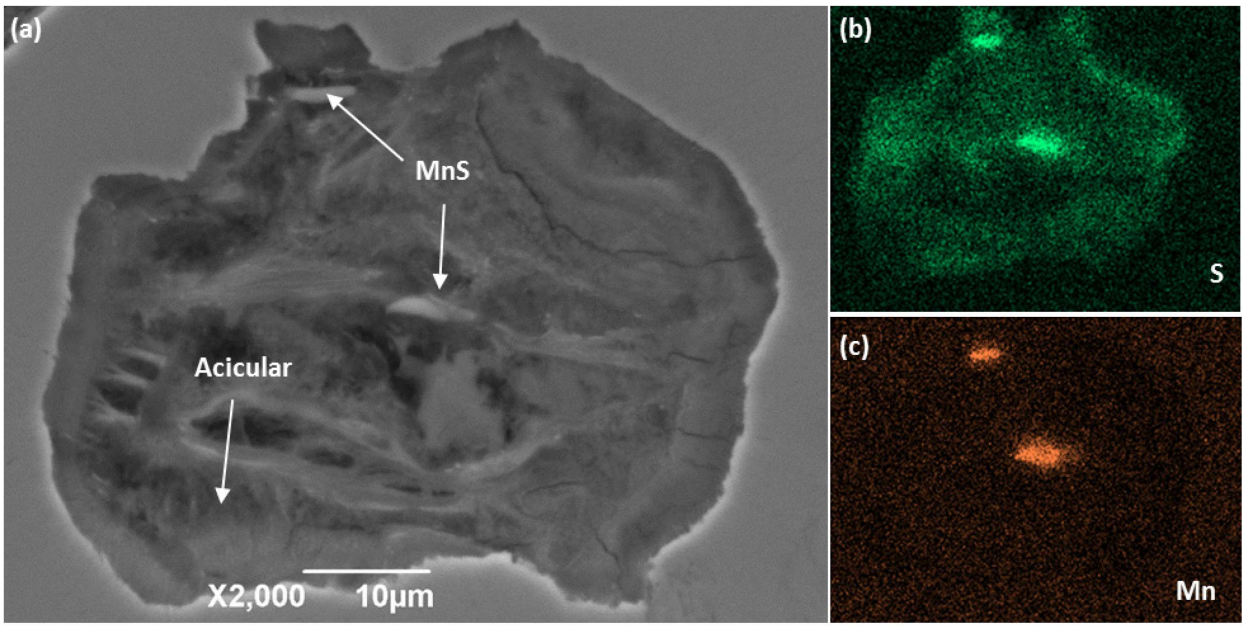


**Figure 101: (a) SEM image of Tunnel with Acicular Deposit and EDS Color Maps for (b) S and (c) Mn**

**Corrosion Adjacent to the Circumferential Parting (C022B1)**

Specimen C022B1 was extracted from the failed joint (joint 22). The specimen was located adjacent to the circumferential parting. The corrosion patch is approximately 3.5 in. long in the longitudinal direction and contained two regions. Region 1 of the corrosion patch has striated grooves that are visible within the entire region. Region 2 of the corrosion patch contains groove tips that are visible on the edge; however, striated grooves are not very visible on the mid region (Figure 102). The crystalline deposits were also observed on the striated grooves. Raman spectroscopy analysis of specimen C022B1 showed presence of carbonate, iron oxide combination, and organic matter. The number of grooves and groove density was quantified in a patch of corrosion, which was then compared to MnS density. There was no relationship between the two; the MnS density was much higher than the groove density. The

conclusion of this study was that there was no apparent correlation between MnS inclusions and the grooves.

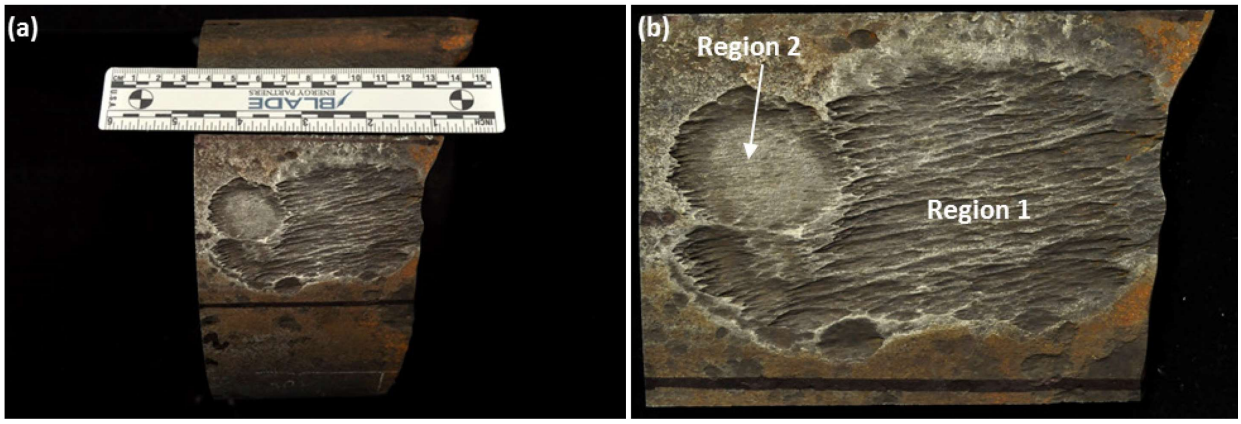


**Figure 102: (a) C022B1 Specimen Extracted from the 7 in. Casing Adjacent to the Circumferential Fracture; (b) Macroscopic View of C022B1 Specimen After Cutting**

**Corrosion (Type I) Extracted from Joint 21**

Specimen C021A3C was extracted from joint 21 of the SS-25 7 in. casing. This specimen exhibited a corrosion patch with striated grooves (Figure 103 [b]) approximately 3 in. long along the longitudinal axis. Groove tips were seen within larger groove tips and the striated grooves were visible over the entire corrosion patch. Raman analysis showed the presence of hematite ($Fe_2O_3$) and an iron oxide combination of hematite ($Fe_2O_3$), goethite (α-FeO(OH)), and ferrihydrite ($Fe(OH)_3$).

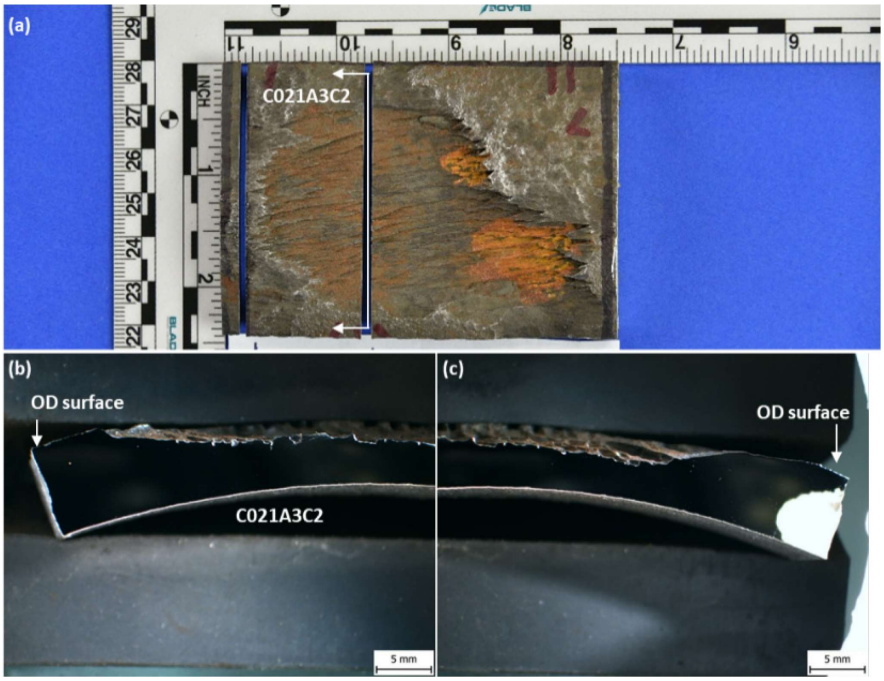


**Figure 103: (a) C021A3C Pipe Section from 7 in. Casing; (b) and (c) Cross section near center**

Specimen C021A3C was sectioned across the striated grooves to investigate the groove profile and tips. Figure 103 (b) and (c) shows the profile of the grooves within the corrosion patch and unaffected OD

surface indicated by arrows. This image shows severe metal loss towards the center of the corrosion patch. Each individual groove contributed to the metal loss profile.

The cross section of specimen C021A3C2 near the groove tips revealed several tunnels underneath the groove tip. C021A3C2 groove tips were cross sectioned 1 mm ahead of the V-shaped groove tips. The dark circles in Figure 105 reveal the presence of several tunnels underneath Tips 1 and 2. Figure 106 are metallographs taken after the polished surfaces were etched of tunnels under Tips 1 and 2. Figure 106 (a) shows that even small tunnels can occur at 850 µm below the OD surface, and in Figure 106 (b) under Tip 2, the tunnels appeared to coalesce into a larger tunnel. A closer look at the tunnel under Tip 1 in Figure 106 (a) shows tunnels of various diameters that are isolated within the ferrite-pearlite microstructure. None of these tunnels appeared to be connected. In contrast to these, under Tip 2, the tunnels appeared to have coalesced into a large tunnel, as shown in Figure 106 (b).

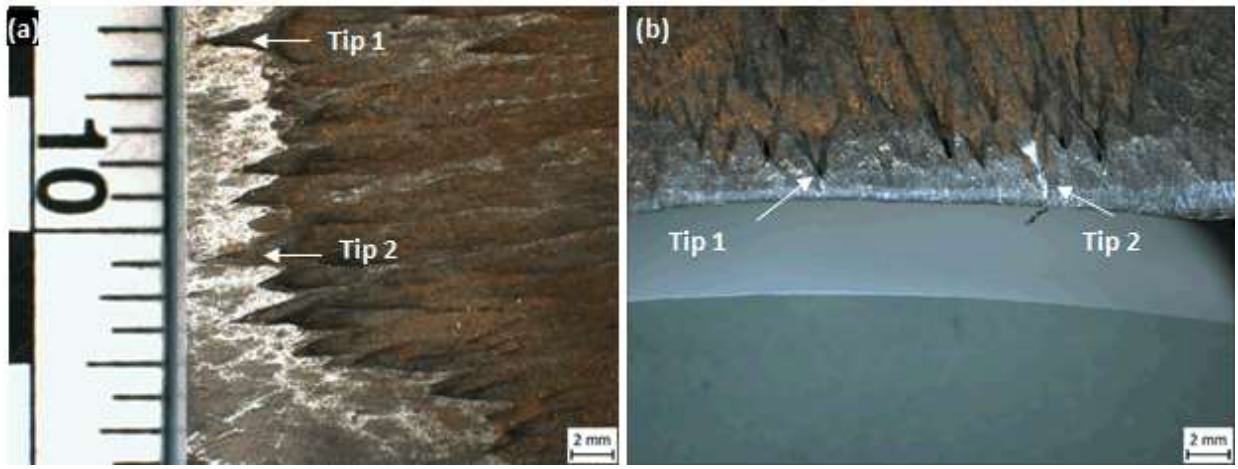


**Figure 104: (a) Top View of Specimen C021A3C2; (b) Tilted View of Specimen C21A3C2 Sectioned Near the Groove Tips**

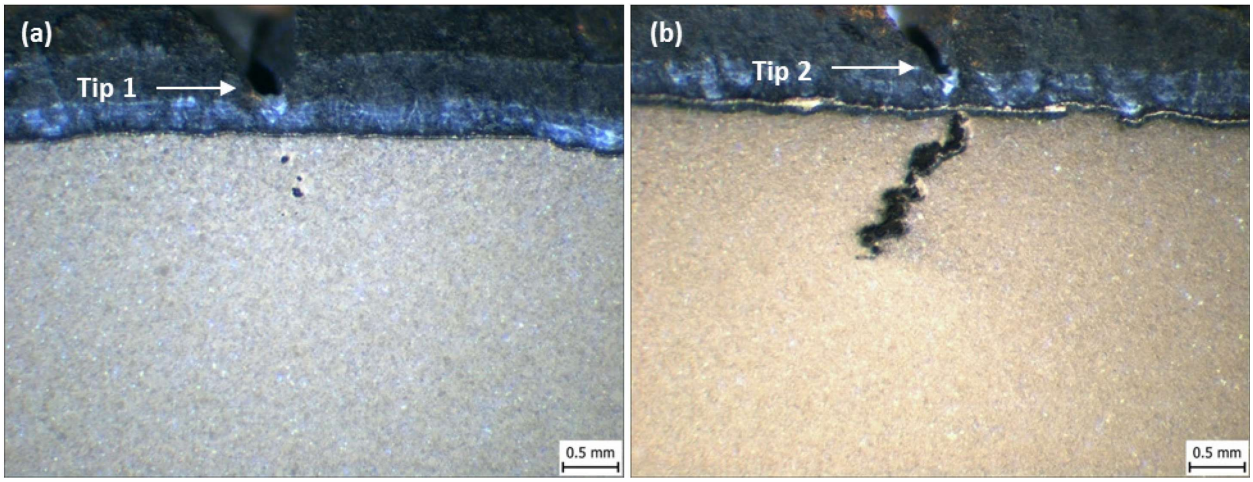


**Figure 105: Stereo Microscope Images of Tunnels beneath (a) Tip 1 and (b) Tip 2**

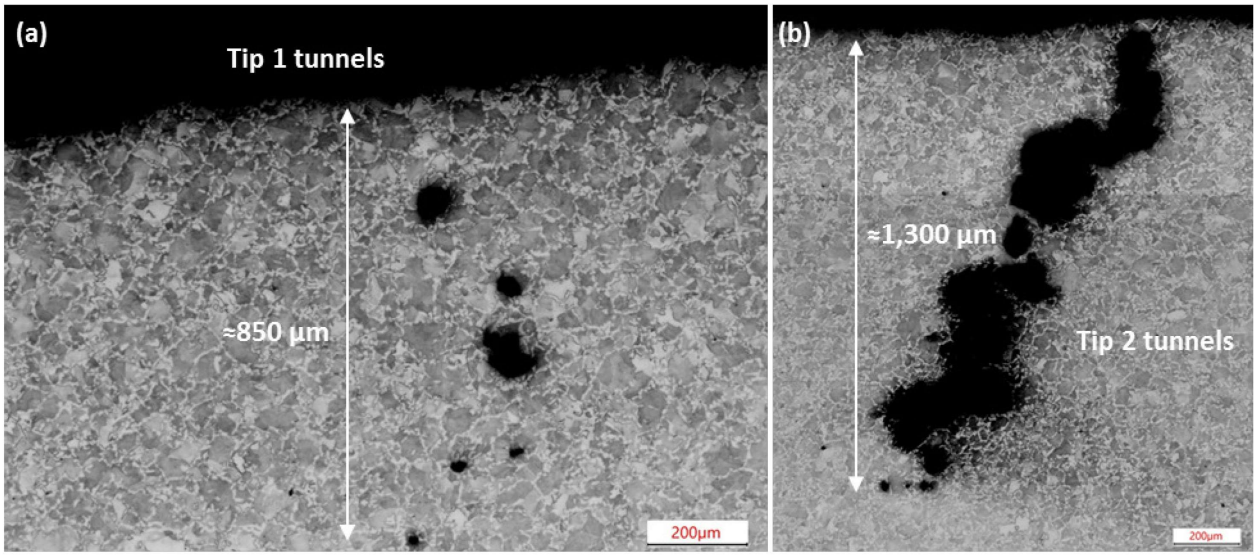


**Figure 106: Microstructure Adjacent to Tip 1 and Tip 2 Tunnels**

All the tunnels were filled with corrosion product. SEM images taken at higher magnification show the presence of the lamellar feature and MnS inclusion in the corrosion products. EDS confirmed the presence of MnS and showed that the corrosion product was rich in O. The lamella structure was seen both on the etched pearlite (alternating layers of ferrite and cementite) and on the corrosion products). There seemed to be a preferential anodic dissolution of ferrite, leaving the cementite behind.

Specimen C021A3-C2 was re-polished, which removed approximately 1 mm of material from the previously-polished surface (Figure 107). Tips 1 and 2 in Figure 107 clearly indicate that the tunnels under Tip 1 grew in size and the tunnels under Tip 2 merged into a larger tunnel. Raman spectroscopy identified organic matter, modified hematite, and magnetite in the corrosion products present in the tunnel.

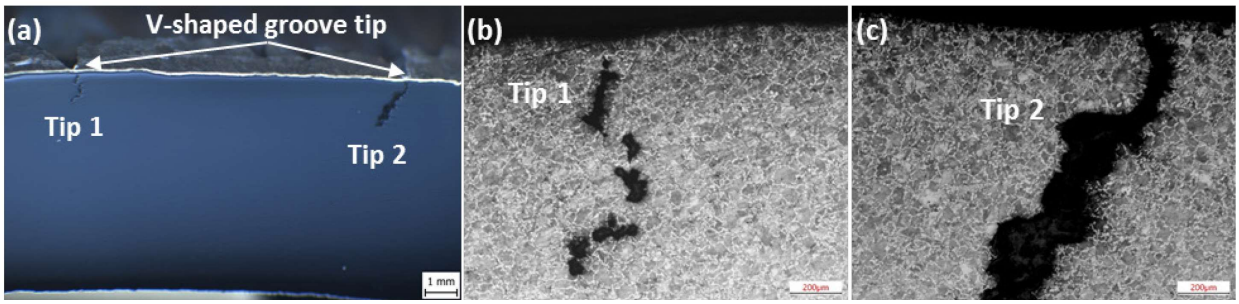


**Figure 107: Specimen C021A3-C2 after Second Polish**

The presence of tunnels was confirmed in multiple striated groove samples. Further SEM analysis of the products within the grooves and tunnels continued to exhibit high C in EDS and hematite and other iron oxides through Raman spectroscopy. The presence of organic matter was also confirmed through Raman Spectroscopy.

## X-Ray Diffraction Analyses of Corrosion Scale

Scale samples were collected from the OD surface of the 7 in. casing, during extraction in the field, for compositional analysis. The X-Ray diffraction (XRD) weight percentages of the compounds present in the

scales collected from Joints 1 to 24 were dominated by barite ($BaSO_4$) and sylvite (KCl). These products were used during the kill and extraction operations. The XRD data were recalculated by removing the sylvite and barite. The intent was to identify the predominant corrosion products.

The amount of magnetite ($Fe_3O_4$) in the scale samples was higher for joints in the lower portion of the well. In general, scale collected from joints at shallow depths contained higher percentages (>5%) of goethite (α-FeO(OH)) and lepidocrocite (γ-FeO(OH)), while scale samples collected from deeper locations contained more (>20%) magnetite ($Fe_3O_4$).

Magnetite is commonly formed in anaerobic conditions (with little to no oxygen). Joints 18 to 24 contained greater than 20% weight percent magnetite. These joint numbers also have deeper corrosion based on the laser scan data. The environment was different deeper in the well; more anaerobic in nature.

Mackinawite and pyrite, which are common products in sulfate-reducing bacteria influenced corrosion were not found. This observation is consistent with the absence of sulfur within the tunnels per the EDS that was conducted.

The change in the dominant corrosion products were a consequence of changing annulus environment. It appears to be predominantly anaerobic in nature. Carbon dioxide or hydrogen sulfide driven corrosion mechanisms appear unlikely.

## Summary

The key takeaways from the corrosion characterization are:

- Type I corrosion feature is a metal loss patch containing striated grooves that oriented approximately parallel to the longitudinal axis. Most of the grooves contained other groove tips. The shape of the grooves was not related to the microstructure of the 7 in. casing. The grooves were elongated along the longitudinal axis of the 7 in. casing, but the 7 in. casing had an equiaxed microstructure.
- Tunnels were present in the Type I corrosion feature. Several tunnels existed at the tip of striated grooves. Tunnels coalescence was noted in at least one sample. In addition to that in some cases the corrosion products within the tunnel demonstrated the presence of extra-cellular looking materials.
- Organic matter was commonly reported by Raman spectroscopic analyses on the OD of the SS-25 7 in. casing. The presence of organic matter on the SS-25 7 in. casing, especially those that are seen inside the tunnels, could only be due to microbiological activities.
- Location of the Type I corrosion features on the outer diameter surface of the 7 in. casing showed that corrosion patches were randomly located along the circumference of the casing. There was no specific orientation where Type I corrosion features were prevalent. The randomness in the orientation of the Type I corrosion feature indicated that the corrosion mechanism was unlikely due to crevice or galvanic corrosion where the 7 in. casing might have been in contact with the 11 3/4 in. casing. If Type I corrosion was mainly due to crevice or galvanic corrosion the location of Type I corrosion features should have been concentrated on one side of the OD circumferential surface. However, this was not the case for the Type I corrosion features.
- The nature of the corrosion surface, striated grooves with tunnels, precludes other forms of corrosion. It makes many of the traditional corrosion mechanisms unlikely. Microbial corrosion is the likely mechanism.

More detailed information regarding the corrosion assessment can be found in the *SS-25 Casing Failure Analysis* supplementary report [19].

### 2.8.3 Microbial Analysis

The most informative microbiological samples were collected from joints 24 and 25 from the 7 in. OD. These were collected at the rig floor as the joints were being extracted from the wellbore. Multiple samples were collected from each of the two joints. There were three types of samples summarized in Table 11:

- Casing OD scale was the dried, gray layer of fluid, pipe scale, and possibly microbial biofilms that coated the casing surface.
- Oily material consisted of occasional globules of greasy black material, presumably tar and crude oil from the well.
- Two background samples included a sample of the soil on the road and drilling fluids pooling on the rig floor drip pan.

**Table 11: Wells SS-25, Casing Joint and Background Samples Set Details**

| Sample Set | Number of Samples | Sample Details |
|---|---|---|
| SS-25 Oily Material | 11 | Crude oil accumulated on casing OD |
| SS-25 Casing JSN-CO25 | 16 | 7 in. Casing Joint 24 OD Material, Sampling Depth 978.9 ft |
| SS-25 Casing JSN-CO26 | 13 | 7 in. Casing Joint 25 OD Material, Sampling Depth 1,021.4 ft |
| SS-25 Background | 2 | Soil from rig area, fluids on rig floor drip pan |

Two DNA based analyses were used:

- Quantitative Polymerase Chain Reaction Method (qPCR)—it provides the total number of microorganisms per g or ml of sample. It detects live and dead cells. It quantifies based on number of copies of ribosomal RNA gene isolated from the sample. Primers are used to detect a wide range of microorganisms. However, it does not identify the individual organisms.
- Amplicon metagenomics—it identifies the type of organisms and relative abundance of each organism to other organisms. It does not provide absolute quantification. The DNA isolation efficiency is reduced by sample composition, leading to samples for which no data is obtained.

Casing joints C025 and C026 contained Archaeal (form of microbe) signatures at an average cell density of 9.5E+07 cells per gram of sample based on qPCR. However, the Archaeal signatures for the oily material and the background samples were below the detection limits. There were distinct markers for the casing OD scale samples versus the others.

Despite having 42 samples in total, due to sample drying during collection, DNA isolation efforts were only successful for 14 of the 42 samples. Amplicon metagenomic analysis was conducted on all 14 samples [34].

The sample types were distinctly different from each other in the relative abundance of the organisms as shown in Table 12. The scale samples are dominated by the methanogenic Archaea. This is in contrast to the oil samples that had the hydrocarbon biodegrading bacteria (*Halomonas*). The background sample had biodegrading bacteria but not hydrocarbon biodegrading bacteria. The traits that are normally associated with MIC, such as iron reducing bacteria and sulfidogens, were not found in abundance in the samples.

**Table 12: Marker Organisms for Each Sample Type**

| Organism | Oil, Average % | Scale, Average % | Soil, Average % |
|---|---|---|---|
| Methanobacterium sp. | 0.049 | 31.62 | 0.614 |
| Methanobacterium aarhusense | 0.008 | 8.649 | 0.685 |
| Methanocalculus sp. | 0.033 | 3.874 | 0.000 |
| Halomonas sp. | 58.04 | 1.892 | 0.115 |
| Pseudomonas sp. | 6.886 | 0.469 | 0.097 |
| Nocardioides sp. | 0.000 | 0.000 | 20.229 |
| Sphingomonas sp. | 0.007 | 0.001 | 9.177 |
| Dietzia sp. | 0.090 | 0.011 | 8.974 |
| Values are the % of the population averaged for each sample type. Yellow indicates values for marker organisms | | | |

The organisms present in each individual scale samples from casing joints C025 and C026 were further evaluated in some detail in Table 13. A review of these samples indicates that while there are sample-to-sample variations in microbial populations, all samples contained methanogenic Archaea at levels between 22% to 77%.

*Methanobacterium sp*. together with the related *Methanobacterium aarhusense* were the most abundant organisms overall in SS-25 joints C025 and C026 samples. *Methanobacterium* species are hydrogenotrophic methanogens from the Archaeal Class, Methanobacteria commonly found in anaerobic digestors and hot springs. *Methanobacterium* species have also been shown to dominate cathodic biofilms [35]. *Methanobacterium* related organisms have been demonstrated to be more active in the presence of iron, suggesting they can utilize iron directly, which contributes to a direct role in metal corrosion [36].

Additional methanogenic genera detected at levels greater than 1% of the population were *Methanocalculus* and *Methanocorpsculum*. *Methanocalculus* is a genus of hydrogenotrophic methanogens from the Archaeal class, Methanomicrobia. Members include alkaliphilic methanogens, such as *Methanocalculus natronophilus*. *Methanocalculus* species are associated with corrosion in oil and gas operations [37] [38].

*Methanocorpusculum sinense* are methanogens from the Archaeal class, Methanomicrobia. *Methanocorpusculum* species are commonly found in anaerobic digestors activated sludges. They are not currently known to be associated with corrosion.

*Alkalibacterium sp.* were particularly widespread and abundant across many samples originating from Aliso Canyon. As such, they are probably important components of the local microbiology. *Alkalibacterium* is a genus of alkaliphilic, anaerobes of the bacterial Phylum Firmicutes. *Alkalibacterium* are members of the Lactobacillaceae, a bacterial family that includes the well-known, common lactic acid bacteria (LAB) found in fermented dairy and plant materials, such as yogurts and sauerkraut. There

are eight species within the *Alkalibacterium*, and they are not typical components of oil and gas system's microbial populations, suggesting they are simply organisms native to the region around Aliso Canyon and reflective of the geological influence on the environment, rather than being promoted specifically by the natural gas activities in the area. A role of *Alkalibacterium* in MIC has not been reported or established.

**Table 13: Predominant Species Composition of Individual Casing Scale Samples**

| Predominant Species Composition of Individual Casing C025 and C026 Samples, % of Microbial Population | | | | | | | | | |
|---|---|---|---|---|---|---|---|---|---|
| Individual Species | CO25-S07 | CO25-S08 | CO25-S17 | CO25-S21 | CO26-S01 | CO26-S04 | CO26-S06 | CO26-S12 | CO26-S16 |
| *Methanobacterium aarhusense* | 0.4 | 0.004 | 0.06 | 1.0 | 0.1 | 7.6 | 0.9 | 42.5 | 24.9 |
| *Methanobacterium sp.* | 23.7 | 22.4 | 37.9 | 26.5 | 26.6 | 48.0 | 42.3 | 34.1 | 22.6 |
| *Methanocalculus sp.* | 0 | 0 | 1.3 | 4.4 | 25.5 | 2.9 | 0.5 | 0.02 | 0.04 |
| *Methanocorpusculum sinense* | 0 | 0 | 2.9 | 0 | 0.01 | 0.6 | 0 | 0.01 | 0 |
| *Alkalibacter sp.* | 5.8 | 20.4 | 0.1 | 0 | 0.04 | 0.1 | 0.5 | 0.5 | 0.09 |
| *Alkalibacterium sp.* | 24.0 | 31.8 | 24.1 | 17.2 | 19.7 | 6.4 | 2.8 | 8.3 | 0.2 |
| *Alkaliflexus sp.* | 12.6 | 0.6 | 0.2 | 0.4 | 0.01 | 0.1 | 0.3 | 0.02 | 0.013 |
| *Halolactibacillus halophilus* | 1.1 | 0.2 | 3.0 | 2.6 | 7.6 | 11.08 | 2.4 | 1.1 | 1.3 |
| *Ercella succinigenes* | 6.8 | 0.8 | 0.02 | 0.1 | 0.01 | 0.02 | 0.05 | 0 | 0 |
| Select traits and list of organisms found to be present in greater than 1% of the total population of well SS-25 casing joints C025 and C026. Values are the percent abundance, color-coded as such: Yellow are >10%, Blue are 1% - 10%, Gray are 0%. | | | | | | | | | |

SS-25 was considered an anaerobic system that had varying water level depending on the season in Aliso Canyon. The change in the water level could have also affected the local environment in which the microbes lived and attached to the OD of the 7 in. casing. The nutrients present in the groundwater could have also been altered by changes in season. Presence of $CO_2$ in the environment from seeping connections could have provided a catalyst for the reactions.

## Summary

- SS-25 casing samples were shown to have average microbial levels of 9.5E+07 cells per gram dried casing fluid.
- Between 22% to 77% of all microorganisms were determined to be methanogenic Archaea. This indicates a casing surface population of methanogenic Archaea of over 1E+07 per g sample.
- Two genera, *Methanobacterium* and *Methanocalculus*, were the predominant Archaea identified in the samples. *Methanocalculus* and *Methanobacterium* species have been shown to be directly associated with metal corrosion in oil and gas systems.

- The combination of high cell density on the casing surface along with the identity of methanogens related to those known to cause metal corrosion suggest that the population has the potential to cause corrosion.
- The microbial population on the surface of the SS-25 casing is consistent with a microbial population able to cause metal corrosion.

The genus and species identification are consistent with the physical evidence regarding the nature of the corrosion and the corrosion scale chemistry assessment previously discussed.

Additional details regarding the microbiological analysis can be found in the *SS-25 Analyses of Microbial Organisms on 7 in. Production Casing* supplementary report [34]

## 2.9 11 3/4 in. Surface Casing

The 11 3/4 in. casing was partially cemented, and there were no easy means of extraction. There was no way to extract the 11 3/4 in. casing without damaging the casing itself, and compromising the P&A as required by DOGGR.

Therefore, logging was the primary means of interpretation of the condition of the surface casing and its annulus. Running logging tools was conducted through the tubing, production casing, and finally through the surface casing. The technologies could be categorized as follows:

- Integrity Logs (condition of the surface casing)
  - MID tools were used to provide a qualitative estimate of metal loss on surface casing through tubing or casing. It was used for planning purposes.
  - Caliper tools were used to quantify metal loss and other features on the casing ID.
  - UCI/HRVRT (High Resolution Vertilog) tools were used to quantify and locate the metal loss features.
  - A camera was used to visually assess the features on the ID of the surface casing.
- Reservoir/Annulus Logs
  - INTeX was used to assess the condition of the cement.
  - An Isolation Scanner was used to assess the condition of the cement and solid/liquid/gas in the annulus.
  - A Sonic Scanner was used to assess the formation outside of the surface casing.

The various technologies complement each other and were necessary because the fluid level inside the 11 3/4 in. was around 300 ft. The dry region required the magnetic tools, and the liquid regions allowed the use of ultrasonic tools. Further, the ID cleanliness impacted the quality of data obtained from the various logging technologies: ultrasonic is more sensitive as compared to magnetic. The ultrasonic technology provided more accurate dimensional data when compared to magnetic data.

The combined technologies clearly identified the following integrity issues with the surface casing:

- Joints with external metal loss
- Joints with holes

- Joints with internal metal loss
- Joints with ovality
- Joints with casing wear

The results are summarized by depth and joint number in Table 14. Here are some key observations regarding the surface casing:

- At shallow depths in the casing, ranging from 90 to 385 ft, there were holes or metal loss indications. The various technologies, including caliper, UCI and HRVRT identified these through wall metal losses. The camera data were consistent with the logging data, and a typical photograph of the hole is shown in Figure 108. A total of 58 holes were identified, with 50 of them in joint 5 at depths ranging from 152.1 to 195.4 ft.
- External corrosion or corrosion on the OD of the 11 3/4 in. casing were evident; these were adjacent to the holes. Consequently, the holes were at least partially caused by external corrosion on the surface casing. The dimensions of these holes were obtained from EV camera that inspected the ID of the 11 3/4 in casing.
- Failure pressure was estimated using RSTRENG, assuming three different hole diameters and variable wall loss. The results are summarized in Figure 109, which shows that the external corrosion would have resulted in a hole at penetrations ranging from 80 to 90% of wall loss. The holes may have been a consequence of an internal pressure of 800 psi or higher. The pressure in the surface casing annulus surged to 800 psi at one point right after the axial rupture. The holes are likely a consequence of the axial rupture.
- Some of these approximately 58 holes could have existed prior to the 7 in. casing axial rupture. Many of the holes exhibited sharp corners that may have been more typical of a burst failure, implying that they occurred due to a pressure surge in the surface casing. These holes provided a pathway for the gas to the surface that further complicated the well-control operations. These holes provided a less resistant pathway to the surface, resulting in a higher gas leak rate.


**Figure 108: Picture of Hole in 11 3/4 in. Casing with Dimensions from Video Imaging at 145 ft**

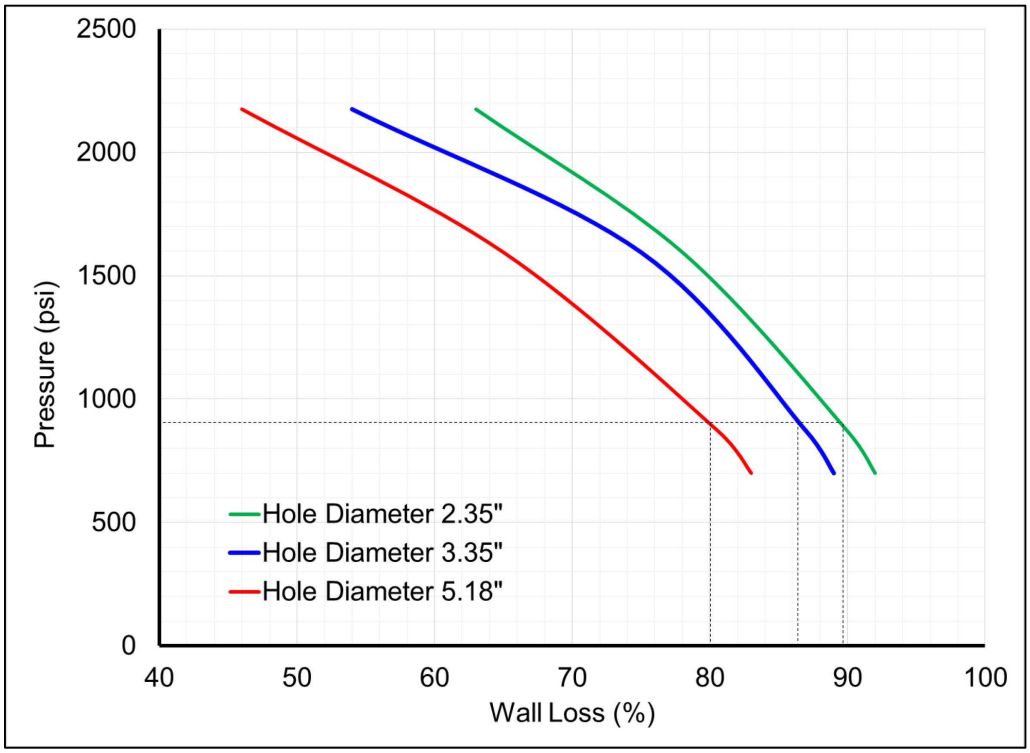


**Figure 109: RSTRENG Safe Pressure Limit as a Function of Wall Loss**

**Table 14: 11 3/4 in. Casing Defect Summary**

| Joint Number | Heavier than 42 lb/ft | External Metal Loss | Holes | Internal Metal Loss | Ovality | Casing Wear | Top Body (ft) | Body Length (ft) |
|---|---|---|---|---|---|---|---|---|
| 1 | Y | | | | | | 12.6 | 13.7 |
| 2 | | | | | Y | | 26.5 | 42.5 |
| 3 | | Y | | | Y | | 69.1 | 42.4 |
| 4 | | Y | Y | | | | 111.6 | 40.2 |
| 5 | | Y | Y | | | | 152.1 | 43.1 |
| 6 | | Y | Y | | | Y | 195.4 | 41.3 |
| 7 | | Y | Y | | | Y | 237.0 | 42.5 |
| 8 | | Y | Y | | | Y | 279.7 | 40.4 |
| 9 | | Y | | | | Y | 320.3 | 41.2 |
| 10 | | Y | | | Y | Y | 361.7 | 34.7 |
| 11 | | | | | | Y | 396.6 | 27.5 |

| Joint Number | Heavier than 42 lb/ft | External Metal Loss | Holes | Internal Metal Loss | Ovality | Casing Wear | Top Body (ft) | Body Length (ft) |
|---|---|---|---|---|---|---|---|---|
| 12 | | | | | Y | y | 424.3 | 41.7 |
| 13 | Y | | | | | y | 466.2 | 36.4 |
| 14 | | | | | Y | y | 502.8 | 41.3 |
| 15 | | | | | | | 544.3 | 43.6 |
| 16 | | | | | Y | | 588.1 | 36.8 |
| 17 | | | | | | | 625.1 | 36.8 |
| 18 | | | | | | | 662.1 | 40.0 |
| 19 | | | | y | | | 702.3 | 41.6 |
| 20 | | | | y | | | 744.1 | 37.8 |
| 21 | | | | y | | | 782.1 | 42.0 |
| 22 | | | | | | | 824.3 | 41.8 |
| 23 | | | | y | | y | 866.4 | 40.5 |
| 24 | | | | y | | y | 907.1 | 41.9 |
| 25 | y | | | y | y | y | 949.2 | 38.3 |

The other key observation from Table 14 is the presence of internal corrosion on the 11 3/4 in. casing at depths below 700 ft. Ignoring the casing wear, which is uniform, there is metal loss or internal corrosion from 700 to 900 ft. At many of these locations, the 7 in. casing had OD corrosion corresponding to the locations on the 11 3/4 in. casing. This is consistent with a water level of approximately 700 ft in the surface casing annulus.

## 2.10 Overall Interpretation of the Failure

### 2.10.1 Key Facts

The following is a summary of key facts that were identified from the field, laboratory, logging, testing, and analyses of the SS-25 failure:

- The SS-25 well had a cement top of around 7,000 ft in the 7 in. × 11 3/4 in. annulus. There was no cement above 7,000 ft: drilling fluid was left above the top of cement during well construction.
- The SS-25 well had lost circulation while cementing the 11 3/4 in. surface casing. There were no indications of cement above 600 ft.
- The 7 in. casing failure was an axial rupture and a circumferential parting above the 11 3/4 in. surface casing shoe at a depth of 892 ft.

- The axial rupture exhibited bulging (indication of ductility) and the failure origin is along the region of maximum wall loss. The length of the origin is 2.13 in. (53.9 mm). SEM examination confirmed the ductile nature of the origin. Chevron marks were consistent. The origin was identified as Zone 1. The failure at a differential pressure of 2,389 psi was predicted by the finite element model, thus verifying the origin dimensions.
- Zone 2 was a mixed brittle-ductile fracture mode that was representative of a high strain rate cracking in the chevron-marked regions. Zone 3 was the featureless zones with erosion due to gas flow.
- The running cracks were arrested at the upper and lower turning points due to energy dissipation.
- The axial rupture was the first failure of the 7 in. production casing at 892 ft. The temperature of the casing was around 80°F.
- The circumferential parting occurred after the axial rupture. The fracture surfaces are cleavage in nature and happened at lower temperatures ranging from –76°F to –38°F (–60°C to –39°C).
- The gas escaping through the axial temperature through various mechanisms, including transpiration cooling, is at temperatures as low as –30°F. This is broadly consistent, within the limitations of CVN measurements and modeling, with the temperatures estimated through the fracture mechanics analyses of the circumferential parting.
- The external corrosion was significant on the 7 in. production casing beyond depths of 700 ft with corrosion depths greater than 15 to 20% of wall thickness. Joint 22 (the failure joint) had many corrosion features great than 50% of wall thickness. With the exception of two features, none of the other joints exhibited corrosion significantly greater than 30% of wall thickness.
- The failure location had corrosion that was striated groove in nature, characterized as a Type I feature. Such features were noted in many of the lower joints. There were grooves within grooves.
- The Type I feature (the failure corrosion feature with striated grooves) had tunnels extending into the unaffected metal at the ends of these grooves. Numerous tunnels were identified in the Type I corrosion samples analyzed.
- The biological nature of the deposits was observed within the tunnels and at the bottom of the grooves. This was repeatedly characterized using the FIB and SEM. The organic nature of these deposits was also characterized using the Raman spectroscopy.
- The XRD analyses demonstrated the presence of hematite and magnetite as the primary scales in joint 15 and beyond. Absence of mackinawite and other iron sulfide scales eliminate the possibility of sulfate-reducing bacteria.
- Siderite was noted in lower concentrations, and the predominant presence of hematite and magnetite indicated that a $CO_2$ corrosion mechanism was not active. This was further verified through the Pourbaix diagram.
- Amplicon metagenomics (DNA analyses of live and dead cells) characterized the scale samples collected from Joints 24 and 25 in detail. Predominant DNA analyses indicated that methanogens were in abundance in both joints.
- Nine out of 25 connections leaked during the connection tests. The leak rates were very small. Gas seeped out of some of these connections. Sixteen connections did not exhibit any gas leakage.

- Two boreholes were drilled on SS-9: one to 1,100 ft and the second one to 500 ft. The two monitoring boreholes sampled groundwater from 900 to 1,000 ft and from 340 to 440 ft. There were low concentrations of ions. Shallow water was richer in calcium and deeper water was richer in sodium.
- A review of the logs in SS-25 showed mobile water right at the shoe of the 7 in. casing at 990 ft.
- Analyses of CHDT water from outside the 11 3/4 in. casing from SS-25 and 7 in. casing from P-35 indicate dilution of annulus fluids with likely low salinity groundwater.
- The J55 material (from the shallow 7 in. production casing) had a ductile-brittle transition temperature of 40°C. It was high in carbon content (0.47 to 0.5%) as compared to modern steels.

### 2.10.2 Interpretation

The failure occurred through a patch of corrosion. This patch of corrosion was characterized by striated grooves, and the ends of the groove had a sharp 'V' shape. Further, these grooves consisted of grooves within, almost fractal in nature. Examination of the ends of the grooves revealed tunnels that began at the ends of the groove and that penetrated parallel to the groove into the metal. One sample revealed the formation of multiple parallel tunnels that aligned and developed into grooves.

Direct examination of the corrosion deposits within the tunnel revealed their nature, which included lamella, acicular, flower petal formation, bird's nest formation, and also extra-cellular looking fibers rich in carbon. Many of these descriptions of corrosion deposits have been identified in literature as caused by MIC. The literature data were generated from controlled experiments with deliberate exposure to microbes.

Scale samples were extensively sampled from Joint 25, and the results from amplicon metagenomics (DNA-based) repeatedly revealed methanogens in multiple samples. Methanogens are a form of Archaea. There is some literature demonstrating the ability of methanogens to cause pitting corrosion with $CO_2$ in a laboratory experiment. MIC was the most likely cause of the Type I corrosion with striated grooves, and based on the limited data, methanogens were most likely cause of the MIC.

The SS-25 well was originally constructed as an oil well with the 7 in. production casing. The top of cement on the 7 in. casing was around 7,000 ft and above the cement was drilling fluid. Based on available data, this fluid would have had a pH ranging from 10.5 to 12.5 at the time of well construction. The shoe of the 11 3/4 in. surface casing was at 990 ft. The runoff water permeated the ground through faults and accessed the shoe at around 990 ft as groundwater. The drilling fluid either leaked off or was displaced with groundwater over time. Depending on the precipitation, the water level would have varied over time. Based on the OD corrosion on the 7 in. production casing, it is likely that from 700 ft and below there was constantly an aqueous environment over time. The groundwater would have carried microbiological organisms. The environment in the 7 in. × 11 3/4 in. annulus changed based on precipitation levels, but was otherwise stagnant.

In 1977, when SS-25 started operating as a storage well, the casing and tubing were used for gas injection and withdrawal. Some of connections seeped gas and small amounts of $CO_2$ entered the production casing annulus. The microbiological organisms grew in population and caused physio-chemical reactions that likely caused the corrosion process to occur. The corrosion rates would have been quite low, on an average of 5 to 10 mpy. This is expected because, as corrosion occurs, a scale is formed on the steel surface and there is no mechanism of removal of this scale. Any further corrosion

requires mass transfer through the scale. The corrosion rates are anticipated to be low in a relatively stagnant environment. There would be some seeping $CO_2$ recharge, but otherwise there was no movement of fluid or removal of scale.

The nature of this corrosion was indicated by the presence of striated grooves. These grooves behaved as a notch with a small radius. The corrosion continued to grow. As the gas continued to be injected in SS-25, the pressure over the year 2015 increased. As the injection pressure was around 2,700 psi (differential pressure of around 2,400 psi), as shown in the FEA modeling, the material at the bottom of the corrosion sheared and failed. Instantaneously, after the casing fractured over 2.13 in., the unstable crack continued to grow upwards and downwards, then turned and stopped. A large gas leak resulted from the 2 ft long casing rupture. The gas contained 70 MMscf/D of injection gas and 90 MMscf/D of reservoir gas. This gas expanded through the axial rupture.

This gas entered the 7 in. × 11 3/4 in. annulus and the pressure in the annulus increased. The surface casing had extensive OD corrosion at depths ranging from 80 to 300 ft. This was because of the shallow groundwater generated due to the precipitation. When the corrosion depths reached 50 to 70% of wall thickness of the H40 surface casing, the casing would rupture. Numerous through-wall defects were formed in the surface casing and provided a pathway for gas to escape. As gas continued to escape from the axial rupture location, the gas expansion caused the local temperature to drop. The thermal modeling predicted temperatures in the vicinity of –34°C.

The J55 7 in. casing material had a high ductile-to-brittle transition temperature of around 40°C. The upper shelf Charpy toughness was around 10 to 21 ft-lb. However, as the temperatures dropped, the toughness dropped to 1 to 7 ft-lb at the –10°C and lower temperatures. At these low temperatures, another crack initiated and grew circumferentially to separate the 7 in. production casing at 892 ft. The circumferential parting occurred within 1 to 2 hours of the axial rupture.

# 3 SS-25 Post-Leak Events

This section describes Blade's analysis of the events between October 23, 2015, when the SS-25 leak was first discovered, and February 11, 2016, when the SS-25 leak was stopped.

Blade conducted the following studies in analyzing the post-leak events:

- Estimation of the gas storage reservoir deliverability at SS-25
- Nodal modeling of the wellbore to estimate the uncontrolled leak rates
- Analysis of injection network deliverability prior to the uncontrolled leak
- Analysis of post-failure gas pathway and temperature anomalies
- Modeling of the seven kill attempts performed on SS-25

Blade's objectives in analyzing these events were to answer the following questions:

- When did the failure occur?
- What was the initial leak rate? How did this leak rate change over time?
- What phenomenon caused the low temperatures that facilitated the brittle circumferential parting identified by the metallurgical analysis?
- What was the leak path? How did the leak path change over time?
- How did the injection network respond to the failure? Could the failure have been detected in real time by a surveillance system?
- Why did each of the kill attempts fail? What could have been done differently to make each kill attempt successful?
- How much gas leaked from the reservoir during the incident?

## 3.1 Chronology

The SS-25 well leak was discovered on the afternoon of October 23, 2015, as follows:

1. Smell of gas was reported to SoCalGas at 3:15 PM by personnel from another operator driving by the SS-25 well site.
2. SoCalGas personnel were deployed to the well site at 3:20 PM.
3. SoCalGas personnel also smelled gas. They found and fixed a leak in a small pipe between the SS-25 wellhead and a pressure gauge monitoring the 11 3/4 in. × 7 in. annulus. The pressure gauge recorded 140 psi.
4. SoCalGas personnel closed the injection header valve. The surface safety valve (SSV) on the 7 in. casing immediately closed, indicating that the 7 in. × 2 7/8 in. annulus pressure at the wellhead was less than its set point of 300 psi.
5. SoCalGas personnel could still hear gas "moving in the wellhead" and "moving down the well [39]".
6. SoCalGas personnel swept the well site with a handheld device, but no natural gas was detected.

7. Around 7 PM, gas was detected on the main road at the SS-25 site (Figure 110). Personnel were evacuated from the well site, and the road was closed. SoCalGas began mobilizing for well kill operations and started recording wellhead pressures every 30–60 min.
8. A contractor checked and repaired the wellhead seals the next morning (because SoCalGas had initially suspected a wellhead seal leak), but the gas leak continued.
9. SoCalGas proceeded with the first attempt to kill the well (Section 3.4).


**Figure 110: Location Where Gas was First Detected on October 23, 2015 [39]**

Table 15 summarizes the key events during the subsequent period until the SS-25 leak was brought under control on February 11, 2016.

**Table 15: Chronology of Key Events During the SS-25 Incident**

| Date | Day | Event(s) |
|---|---|---|
| October 23, 2015 | 1 | SS-25 leak was discovered at 3:15 PM and injection header valve was closed at 3:30 PM. |
| October 24, 2015 | 2 | Wellhead seals were tested and repaired without any effect on the SS-25 leak.<br>Kill attempt #1. Failed. Tubing plugged. |
| October 25, 2016 | 3 | Field injection was stopped. |
| November 6, 2015 | 15 | Tubing ice plug was cleaned out using coiled tubing. |
| November 8, 2015 | 17 | Production logs (temperature, noise, spinner, pressure) were run in SS-25. |
| November 12, 2015 | 21 | Field depressurization was started. |

| Date | Day | Event(s) |
|---|---|---|
| November 13, 2015 | 22 | Kill attempt #2. Failed.<br>Blowout vent opened 20 ft from the wellhead and shot "debris 75 [ft] into the air." SS-25 "blew out in the conventional sense [6]."<br>Relief well was planning started. |
| November 15, 2015 | 24 | Kill attempt #3. Failed. |
| November 17, 2015 | 26 | Notice of Intention to Drill New Well for P-39A relief well was filed with Division of Oil, Gas and Geothermal Resources (DOGGR). |
| November 18, 2015 | 27 | Kill attempt #4. Failed. |
| November 20, 2015 | 29 | SoCalGas decided to drill P-39A relief well. |
| November 23, 2015 | 32 | Permit to drill P-39A relief well was issued by DOGGR. |
| November 24, 2015 | 33 | Kill attempt #5. Failed.<br>30 ft × 10 ft crater was created at well site by fluids from kill job. |
| November 25, 2015 | 34 | Kill attempt #6. Failed. |
| December 4, 2015 | 43 | P-39A relief well was spudded (started drilling). |
| December 22, 2015 | 61 | Kill attempt #7. Failed. |
| February 11, 2016 | 112 | Relief well intersected with SS-25 and brought it under control. Leak was stopped. |
| February 14–17, 2016 | 115–118 | SS-25 was permanently isolated from the gas storage reservoir with cement. |

## 3.2 Well Deliverability and Injection Network Response

The existing field and SS-25 well measurements were used by Blade after the event to analyze the leak. Such measurements could have been analyzed before and during the leak event with models built from data available before the leak. The measurements included the following:

- Prior to the leak:
  - Continuous measurements of injection pressures and temperatures at the injection network compressor station
  - Daily field-wide injection volumes at the injection network compressor station
  - Weekly pressure measurements at the SS-25 well site
- Once the leak started and during the leak event:
  - Continuing pressure measurements at the compressor station
  - Regular pressure measurements at the SS-25 well site

Blade built models using Petroleum Experts IPM Suite—a suite of industry-standard applications, vetted and used extensively by large and small oil and gas companies. The tools used in this study are:

- PROSPER (PROduction, and Systems PERformance)—for SS-25 well modeling to understand the well flow prior to the leak, at the time the leak occurred, and after the leak occurred.
- GAP (General Allocation Program)—for Aliso Canyon surface network modeling to understand the injection gas deliverability to SS-25 at the time the leak occurred.

Blade built the GAP and PROSPER models by using the data that were available pre-leak. The models were used for leak analysis. These types of models are often used in the industry to continuously diagnose issues potentially before and after they occur. If models had been in place at the time of the leak, a maximum leak rate could have been calculated and used to design appropriate kill attempts.

### 3.2.1 SS-25 Well Injection and Withdrawal PROSPER Model

Building the PROSPER SS-25 well model required:

- Characterization of the fluid for the determination of fluid properties.
- Characterization of the reservoir near the wellbore for the inflow deliverability.
- Description of the well, including geothermal gradient, deviation survey, tubing, and casing.

The data required for building the well injection and withdrawal model were provided by SoCalGas. Some of the data were deduced from available information, but the following data were unknown:

- Inflow deliverability. It was determined by SS-25 production well tests for the last 37 years.
- Tubing and casing surface roughness. A best estimate was determined through analogies.
- Heat transfer coefficients. Lack of these data impacted the certainty in temperature estimates but caused minimal uncertainty in rate measurements.

PROSPER was accurate in predicting the behavior of a sales gas that was 95 mole percent methane.

Figure 111 shows the well tests for the previous 20 years on a performance chart. Wellhead pressures (WHP) were converted to bottomhole pressures by using the well model. In the figure, the well test itself is marked as a circle with a line connecting back to the reservoir pressure that was estimated from the provided static shut-in pressure. (As expected, the reservoir pressure varied by month of test according to the yearly cycle of demand.) The colors and symbols are as follows:

- Green dashed lines with green circles indicate well tests that follow a consistent trend and are considered valid.
- Red dotted lines with red squares indicate well tests that have flowing bottomhole pressures greater than reservoir pressure and are thus questionable.
- Orange dotted lines with orange diamonds indicate well tests with excessive drawdowns and are thus questionable.

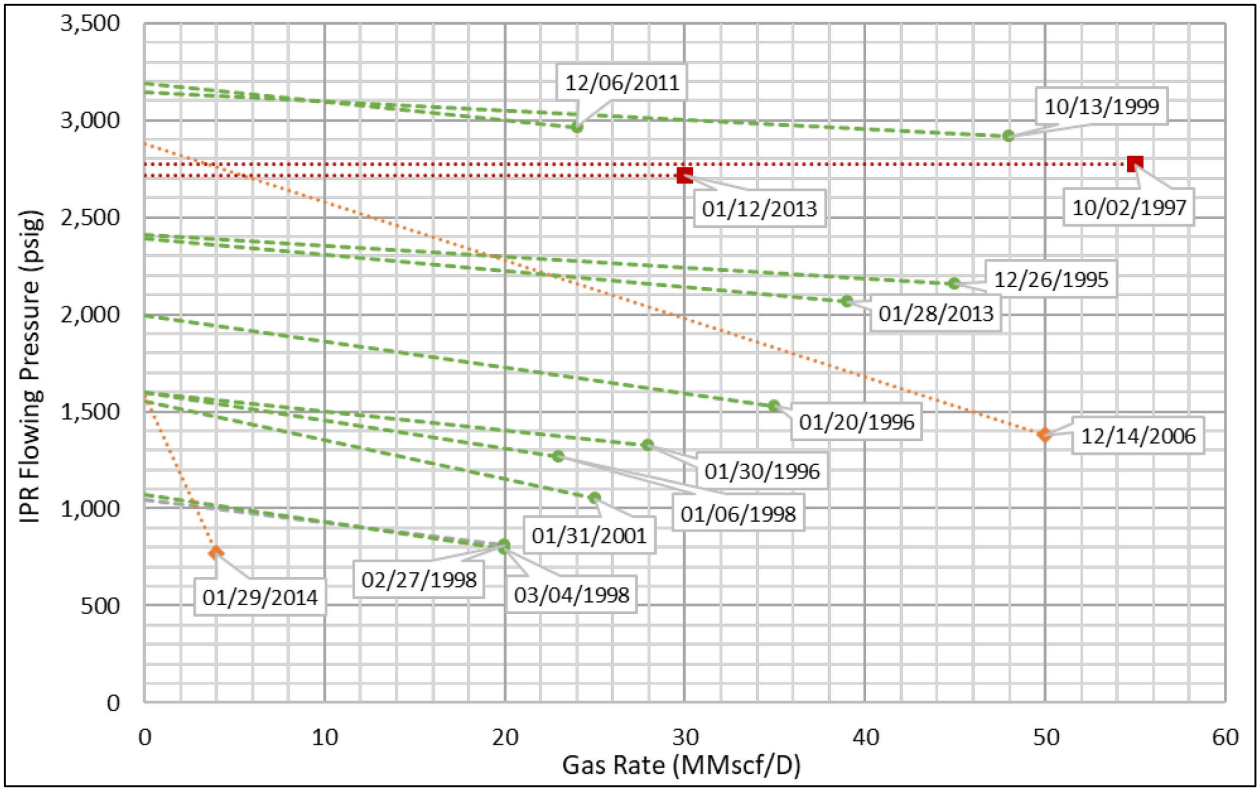


**Figure 111: SS-25 Validation of Well Tests 1995–2015**

The questionable test of January 12, 2013 (in red), was re-run on January 28, 2013. The questionable test of January 29, 2014 (in orange), was not re-run; it was the test that was the most recent prior to the leak. Any adjustments based on the January 29 test that were made to any model would have under-predicted deliverability. This most recent test was inconsistent with the tests of the last 20 years.

Separating upflow from inflow was not possible because the matching of the withdrawal well tests was from surface measurements with no downhole measurements. Inaccuracies in the upflow model would have yielded inaccuracies in matched properties for the inflow model. Without both surface and downhole measurements, there were too many degrees of freedom; therefore, a best-fit, averaged model was derived from the tests. Uncertainty in the tubing-casing state would have yielded an uncertainty in the estimation of the leak flow rate when the injection to SS-25 was shut in. Certainty came when the model matched measured data (production casing pressure) over the entire leak period.

The conversion from surface to downhole at the mid-point of perforations (necessary to estimate inflow properties) was affected by the uncertainty in the pipe roughness. The flowing conditions for the withdrawal well tests were such that the frictional pressure loss resulting from the pipe roughness was significant when compared to the gravity pressure loss due to the gas density gradient. Blade analyzed the valid well tests from the 37-year period prior to the leak to determine if the tests could be used to ascertain the pipe roughness.

Figure 112 shows the best-estimate pipe roughness for well tests from the last 37 years. The roughness differed from test to test, and friction was significant (it averaged 45 to 60% of pressure loss in the outflow model).

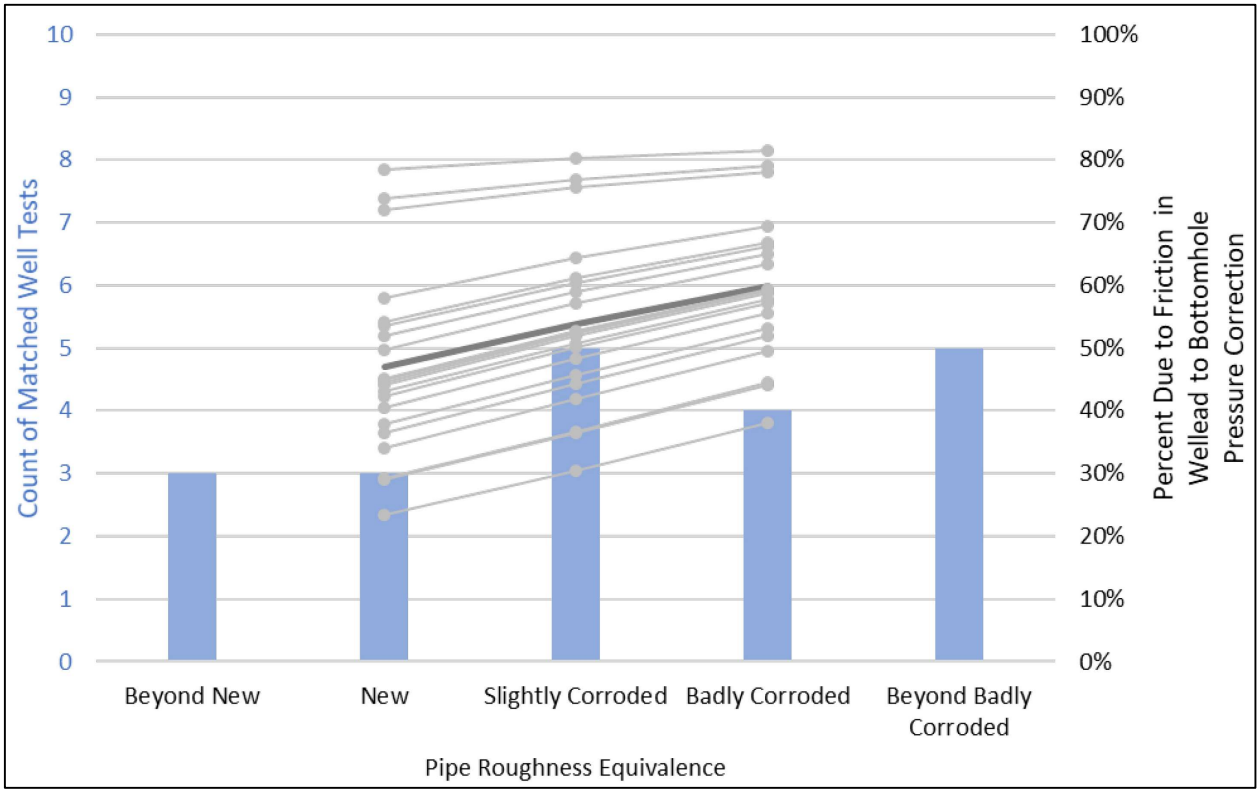


**Figure 112: SS-25 Pipe Roughness Study for Well Tests 1980–2015**

Because there was sufficient random scatter in the well tests, a best-estimate approach was to assume the presence of pipe roughness in the slightly corroded category. (This was also supported by metal loss logs, which were run after the well was killed.) The scatter in the well tests resulted in uncertainty in the downhole flowing conditions and, consequently, uncertainty in the inflow properties. The best estimates would be statistically averaged estimates. A maximum leak rate could have been calculated by assuming new pipe roughness, for example, to engineer kill attempts.

Figure 113 shows the best estimated match of the analyzable flow tests for the last 20 years using the best-estimate properties shown in Table 16. Blade's inflow performance relationship (IPR) estimates for each well test are plotted as solid, thin blue lines. The model's drainage area reservoir pressure varied, at the most, 100 psi from the static measured pressure at the time of the test.

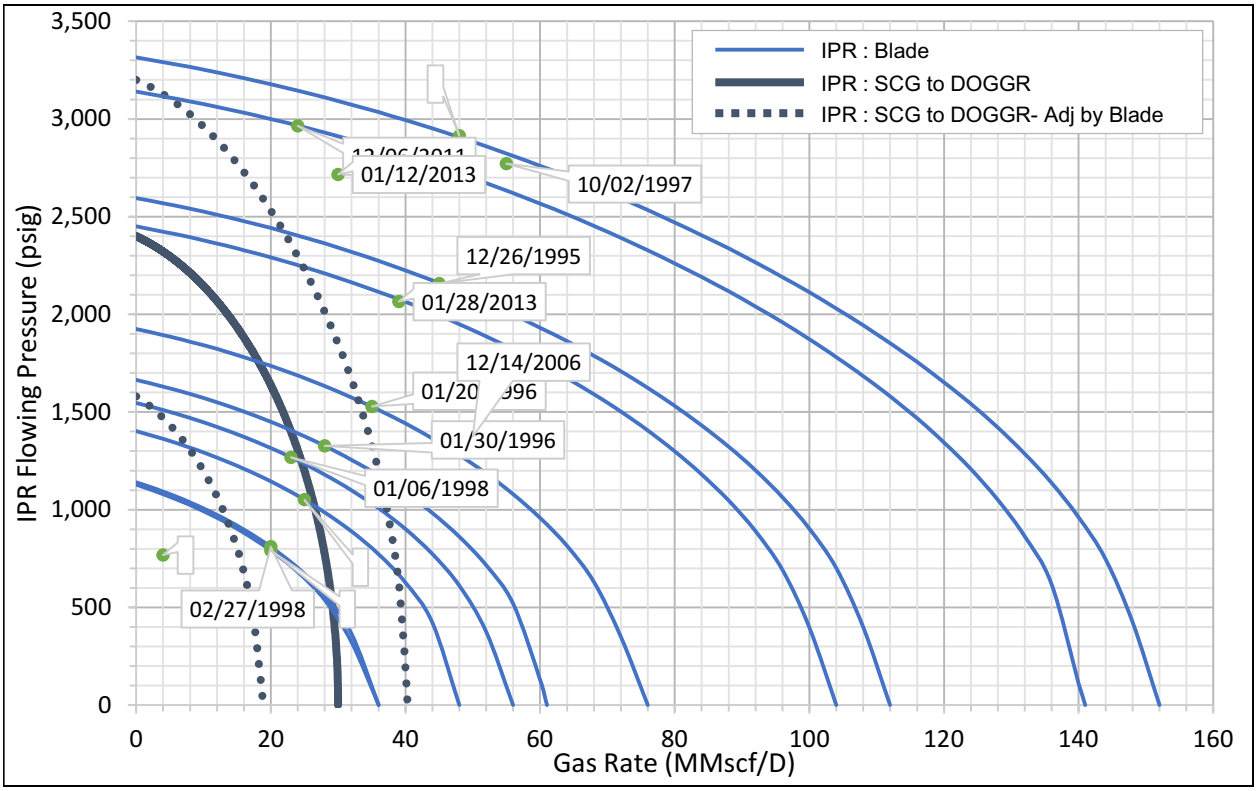


**Figure 113: SS-25 Match of Well Tests 1995–2015**

**Table 16: Reservoir Properties at SS-25 Calculated from Well Tests**

| | |
|---|---|
| **Reservoir Pressure** | 3,200 psi |
| **Permeability** | 80 md |
| **Reservoir Thickness** | 45 ft |
| **Reservoir Porosity (net)** | 0.20 |
| **Connate Water Saturation** | 0.20 |
| **Perforation Interval (net)** | 45 ft |
| **Wellbore Radius** | 5 in. |
| **Wellbore Skin** | 0 |
| **Non-Darcy Flow Factor** | 0.0844 $(MMscf/D)^{-1}$ |
| **Tubing / Casing Roughness** | 0.0072 in. |

Blade identified an IPR curve that first appeared in a SoCalGas response to a DOGGR request [40]. This request implied that a national laboratory was modeling the kill attempts on behalf of DOGGR, and DOGGR wanted the laboratory to use the same data that the well-control company was using. This SoCalGas-provided IPR curve is plotted in Figure 113 as a solid, thick navy line.

The SoCalGas IPR did not match Blade's best-estimate IPR, which was derived from valid well tests. The Blade model could be used to match the SoCalGas IPR by changing the permeability from 80 to 30 md and increasing the gas turbulence to 0.5 $(MMscf/D)^{-1}$. Blade adjusted the reservoir pressure of the SoCalGas IPR, and this was still not representative of any well test. A more representative IPR obtained from proper modeling of the production well tests would have been a better basis for designing kill attempts.

Figure 114 shows Blade's IPR model as of October 23, 2015, after injection was shut down. It also shows the SoCalGas IPR adjusted to the initial reservoir pressure. That IPR model was not representative of the actual flow; it underestimated the actual leak rate by a factor of 3.4–3.6.

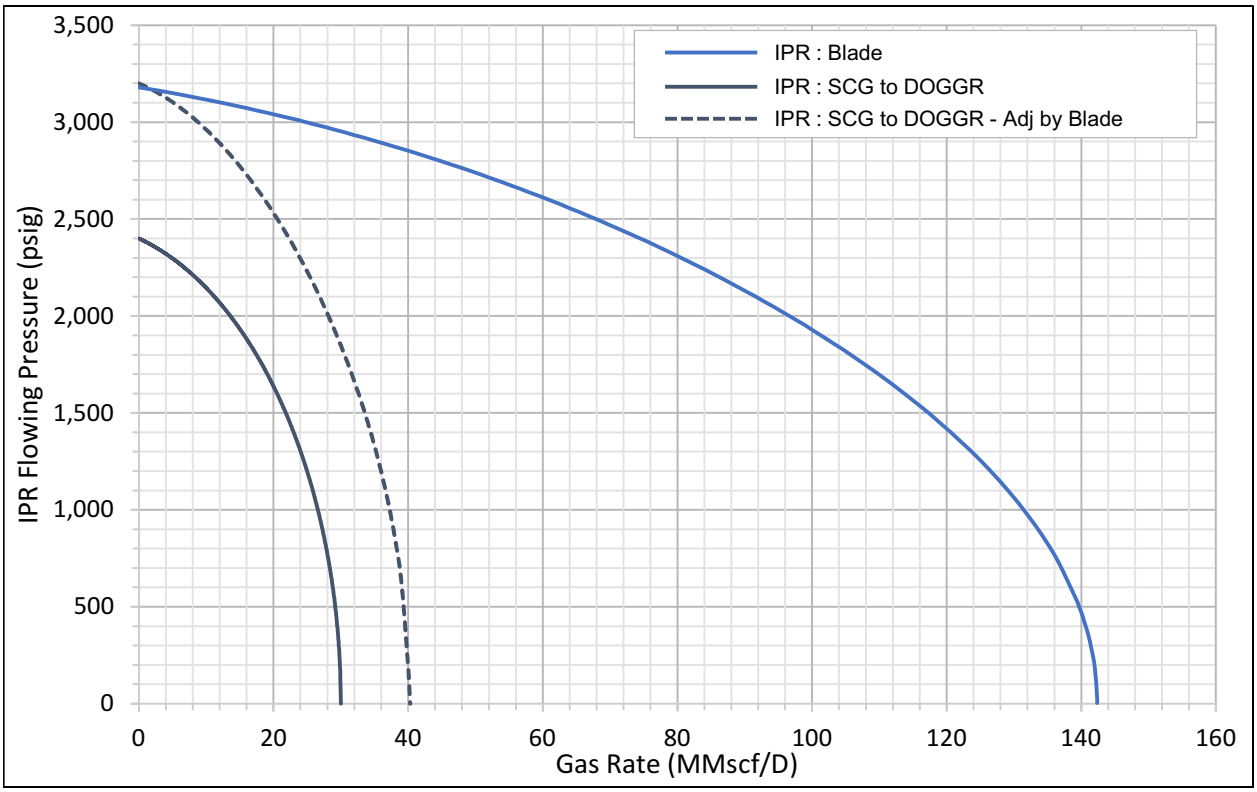


**Figure 114: SS-25 IPR Model for October 23, 2015**

The configuration of SS-25 at the time of the incident provided SoCalGas with a different method, independent of IPR models, to estimate the flow rate. In SS-25, the injection was down the 7 in. × 2 7/8 in. production casing annulus. The tubing was static (i.e., not flowing). Therefore, the wellhead tubing pressure measurements, when corrected for the hydrostatic gradient, provided a direct measurement of the flowing bottomhole pressure. The flowing WHP was also available. The geometry of the 7 in. × 2 7/8 in. production casing annulus was known. Therefore, the difference between the tubing and annulus pressures in a model of the annulus could have been used to estimate the leaking gas flow rate.

Blade performed such *tubing-upflow only* calculations. Figure 115 compares the results of these calculations (in red) with the more accurate *upflow-inflow* (or IPR) models (in green). The tubing-upflow estimates prior to and after the kill attempts matched the upflow-inflow model for new pipe. This further validated Blade's IPR model, which was used in reviewing the kill attempt designs. During the kill

attempts, the well flow was more unstable, and the estimates were more scattered. Both methodologies for rate estimates suggested that the first kill should have been designed for at least 93 MMscf/D.

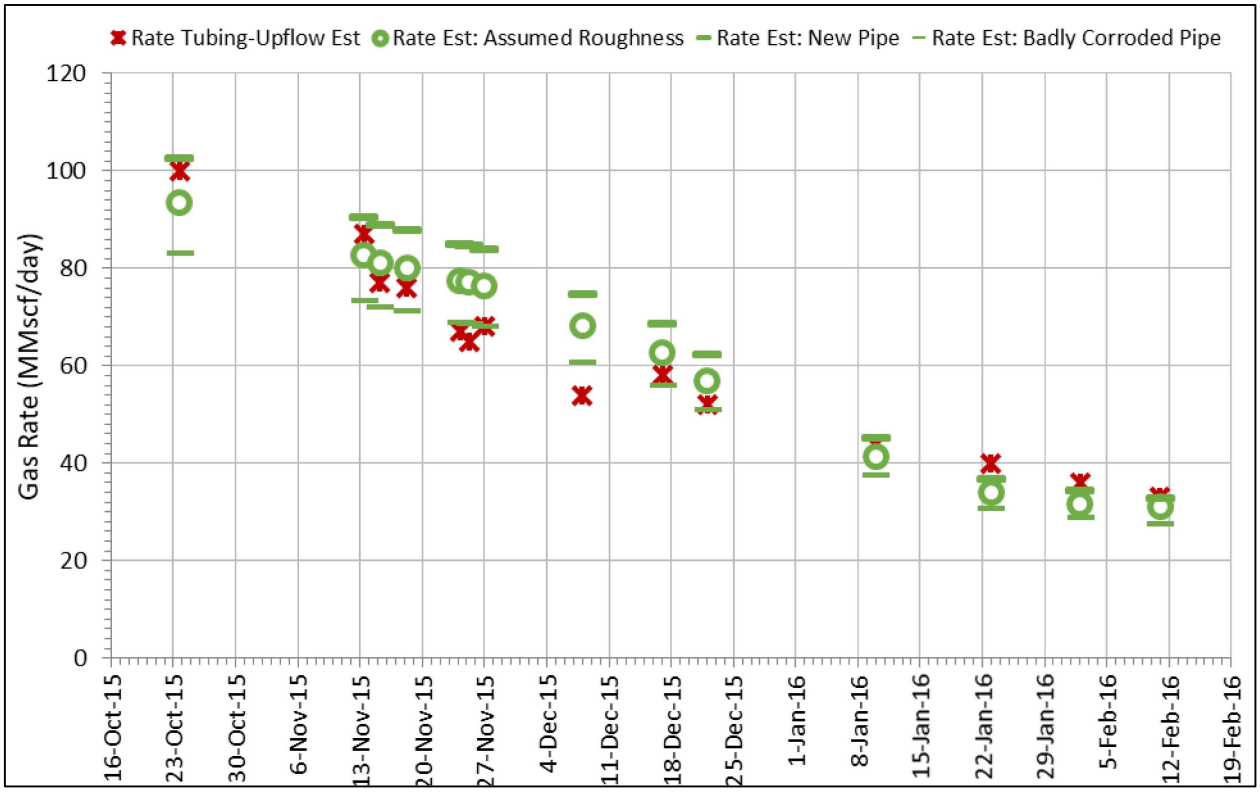


**Figure 115: SS-25 Key Rate Estimates using Upflow-Only and Upflow-Inflow Models**

There was a third method available to estimate the leak rate. This is shown in Figure 116, where Pws is the static WHP (i.e., well shut-in or not flowing) and Pwf is the flowing WHP upstream of the choke. This process allows the calibration of the well deliverability and the estimation of the well flow rates at various pressure differences. The results are shown in Figure 114; the initial leak rate on October 23 matched the 91 MMscf/D estimated through the more accurate model. SoCalGas did use this method to estimate the leak rate; however, the leak rates were estimated to be ranging from 56 MMscf/D to 62 MMscf/D because the downstream choke pressure was used instead of upstream choke pressure.

The key observation from the PROSPER analysis discussed above is that the gas rates were significantly higher than those estimated during the incident. The higher gas rate could have been correctly estimated using industry-standard flow simulations or other methods using data available at the time of the incident. Additional details regarding the well deliverability modeling and analyses please refer to the supplementary report on SS-25 Nodal Analysis with Uncontrolled Leak Estimation [41].

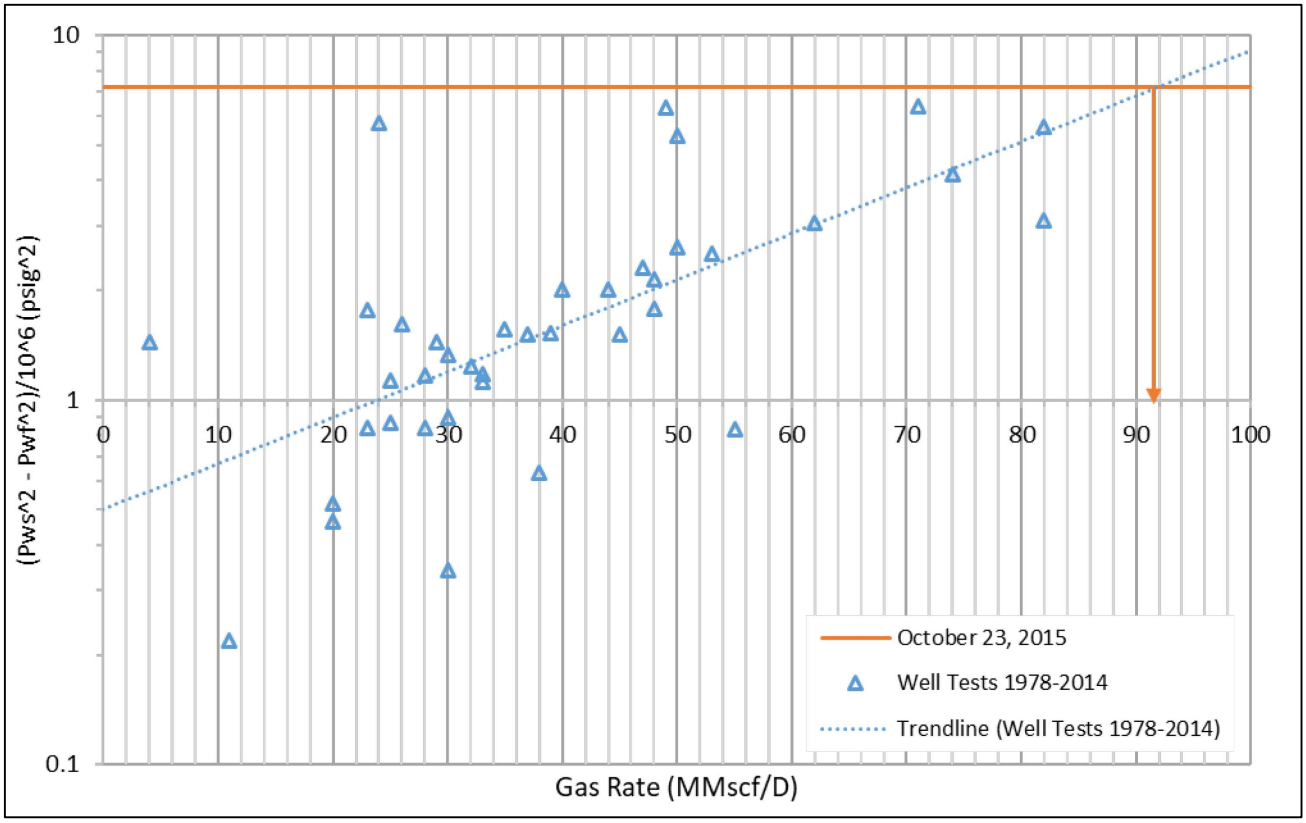


**Figure 116: P-Squared Rate Estimate for October 23, 2015**

### 3.2.2 Aliso Canyon Network Injection GAP Model

Blade used the following data (provided by SoCalGas) to build the GAP Aliso Canyon network model:

- Characterization of the fluid for the determination of fluid properties
- Measured pressure at the western injection manifold near the compressor station
- Discharge temperature at the compressor station
- Adjusted-allocated daily gas injection rate at each well
- Weekly SS-25 WHP measurements
- Pipe description and choke and check valves settings

Blade calibrated the gas injection network model to capture the performance of the network in the absence of a leak (base case) by using the measured discharge pressure at the western injection manifold near the compressor station and the monthly volume equivalent daily injected gas rates for the wells. In the absence of a leak, the equivalent daily gas injection rate for SS-25 was allocated as 3–5 MMscf/D. The corresponding measured discharge pressures at the western injection manifold ranged between 2,800 and 2,860 psi. The network model calculated the WHP as 2,725–2,775 psi for the seven days analyzed.

The calibrated network model was then used to simulate various leak scenarios in SS-25 by varying the WHP and re-calculating the network gas injection rates. The study simulated the leak by reducing the SS-25 WHP without changing the choke settings. The model showed that with the possible changes in WHP, gas was being injected into SS-25 at a significantly higher rate than the base case injection rate.

On the day of the leak, October 23, 2015, the field was injecting at 303 MMscf/D. There were also hourly pressure and temperature measurements at the injection manifold near the compression station. The SS-25 injection line choke was 1 in., and the critical flow rate across the choke was 70 MMscf/D. This 70 MMscf/D rate was the rate being siphoned off the injection network by the leaking SS-25 (before the injection was shut off at 3:30 PM).

Table 17 shows the estimated pressure at three points in the flow path in the injection system to SS-25. Only PIT_WFI_DY1, the pressure at the inlet to the trunk line to the western area of the field (including SS-25), was monitored continuously. The change in the pressure was only 1 psi, so the leak siphoning off 70 MMscf/D would have gone (and most likely did go) unnoticed. If there had been a better field surveillance of, for example, pressures at the wellheads, the leak could have been detected immediately.

The model showed that in the event of a leak in SS-25, the pressure variations at the compressor station would have been minimal and not significant enough to be detected. Therefore, if the pressure were being monitored only at the western injection manifold near the compressor station, then the increased gas volume injected into SS-25 in the event of a leak could have remained undetected. Additional details can be found in the supplementary report on Network Deliverability Analysis [42].

**Table 17: Change in the Pressure before and after the Production Casing Failure**

| Location | Before Failure (psi) | After Failure (psi) | Pressure Change (psi) |
|---|---|---|---|
| Western Leg Inlet (PIT_WFI_DY1) | 2,819 | 2,818 | –1 |
| SS-25 Well Site Injection Manifold* | 2,741 | 2,727 | –14 |
| SS-25 Wellhead | 2,738 | 756** | –1,982 |
| * SS-25 Well Site Injection Manifold feeds both SS-25 and SS-25B wells. (SS-25A is not available for injection.)<br>** All wells modeled as sinks in GAP; well flow was not modeled. Post-choke pressure once the well is at critical flow depends on the well model. | | | |

## 3.3 Evolution of the Leak

Physical examination of the extracted 7 in. casing found an axial rupture of approximately 2 ft of length. The 7 in. casing parted at 892 ft. Video camera imaging found multiple holes in the 11 3/4 in. surface casing between 134 and 300 ft. The gas from SS-25 therefore exited the 7 in. casing at 892 ft, flowed through the holes in the surface casing between 134 and 300 ft into the rock formation, and eventually found its way to the surface and into the atmosphere. The shallow geology which influenced the flow in the rock formation is discussed next, followed by what occurred inside the well itself.

### 3.3.1 Shallow Geology

After the gas leaked from the well, depending on the shallow geology, it might not have flowed immediately to the surface. It might have remained underground for a period of time before escaping into the atmosphere. This might have impacted the results of the direct measurement of the gas volume leaked because the measurements would have been terminated before all the gas had been accounted for. Gas might have also escaped at the surface away from the SS-25 well site, and this might have impacted the tracer flux ratio measurements because not all the methane would have been tagged.

The shallow geology in the Aliso Canyon area is complex, and it can change dramatically from site to site. For this reason, there can be and are inconsistencies in the large amount of geological data at the SS-25 site and the nearby SS-9 and P-39 sites. In the modeling, Blade gave the greatest weight to data from the SS-25 site and to data that were consistent across the three sites.

This section develops a qualitative picture of the shallow geology to identify pathways and barriers for the leaking gas to flow away from SS-25. Also of interest are the lithology, porosity, permeability and water saturations. This information was used to develop a thermal reservoir simulation model to test the understanding of the leak and to explain the temperature anomalies observed at the SS-25 site.

The SS-25 site has three wells: SS-25, SS-25A, and SS-25B. Blade reviewed the drilling reports for the depths where total lost circulation occurred. (Total lost circulation occurs when all drilling fluid leaks off into the formation with none returning to surface.) These thief zones had high permeabilities and pore volumes and were candidates for channels along which leaking gas could flow away from SS-25. There were potentially two channels for the leaked gas to flow away from SS-25: a shallower one at approximately 169 ft and a deeper one at 741 ft. Because loss of circulation depths were similar in all three wells, it was likely that the two channels observed at SS-25 extended across the entire SS-25 site.

Advisian cored and logged several shallow boreholes at the SS-25 site, with the deepest hole being 150 ft. The rock was found to be heavily weathered with abundant near-vertical fractures, which suggested high permeability and porosity in the matrix. Lost circulation was prevalent. NMR logs were also run in the four shallow boreholes and found that the water content typically ranged from 10 to 20%. Furthermore, the water was mainly capillary water. This indicated that the matrix porosity was of the same range, i.e., 10 to 20%. (The porosity of the fracture and vugs was additional.)

Mud logs were available from the TH-1 borehole, which was drilled at the SS-9 site (about 600 ft south of SS-25) and the relief well P-39A (1,475 ft southeast of SS-25). Mud logs provided a map of lithology versus depth, giving a picture of the layers of barriers (soft moist clay rich layers) interbedded with channels where gas could flow. A sufficient number of thick barriers exist to restrict gas flow in the vertical direction, unless faults or fractures cut across them. Due to abundant clay layers, clay smear might have sealed these faults and made them appear conductive locally but sealed over longer distances. With the exception of the top 200–300 ft, where the formation was heavily weathered, the rest of the formation was expected to have low ratio of vertical to horizontal permeability. Deeper than 200–300 ft, gas would have flowed more laterally than vertically.

The Isolation Scanner Log for the SS-25 surface casing showed poor cement bonding behind the casing above 400 ft. The report of the cement job of the surface casing indicated little, if any, cement made it up that high. Gas leaking from the holes in the surface casing between 134 and 300 ft would have readily flowed through the regions without cement and the heavily weathered near-vertical fractures.

The surface casing shoe was at 990 ft. The Isolation Scanner Log showed better quality cement at this depth than above 400 ft, but it also showed that a micro-annulus existed. The Isolation Scanner Log also

showed that between 700 ft and 900 ft the cement quality was poor. When the 11 3/4 in. × 7 in. annulus pressure built to as high as 800 psi, the gas might have fractured the rock around the surface casing shoe (estimated fracturing pressure is 400 to 815 psi) and further damaged the cement behind the surface casing. The gas leaking from the shoe could have then flowed up behind the surface casing and away from SS-25 through the channels.

In summary, the lost circulation records of the wells in the SS-25 site showed two channels for gas to flow away from SS-25. The mud logs showed that there were flow barriers that restricted gas from flowing vertically in the formation. The Isolation Scanner Log showed cement behind the surface casing was poor and thus provided a path for the gas leak to flow up behind the surface casing to the two identified channels.

### 3.3.2 Flow within the Well

On October 23, 2015, when the leak was first discovered, the well was shut in. The shut-in pressure of the tubing was 1,700 psi, the 7 in. × 2 7/8 in. annulus was 270 psi, and the 11 3/4 in × 7 in. annulus was 140 psi. The SSV also immediately closed because the pressure in the 7 in. × 2 7/8 in. annulus had fallen below the SSV's set point, which was between 270 and 300 psi.

To determine when the 7 in. casing failure occurred, Blade first modeled the flow in SS-25 prior to the shut-in. The problem was solved by using PROSPER. Figure 117 shows the SS-25 well flow problem posed to PROSPER and the pressure, rates, and temperatures that PROSPER calculated. First, focusing on the flow from the wellhead down the 7 in. × 2 7/8 in. production casing annulus to the leak point at 892 ft, the WHP required to drive 70 MMscf/D to 892 ft was 620 psi, and the arrival pressure at this depth was 465 psi. The WHP of 620 psi was too high to cause the SSV to close. In fact, even if the pressure at 892 ft were 260 psi (and it could not have been this low because 260 psi was the pressure at the holes in the surface casing as shown in Figure 117-B), the WHP would still have been about 500 psi. This means that when SS-25 was on injection, even if the 7 in. casing had already failed, the SSV would not have closed. The only time the SSV would have closed would have been when the well was shut in and the 7 in. casing had already failed. This is confirmed by the fact that the SSV closed immediately when SS-25 was shut in on the afternoon of October 23, 2015.

Figure 118 shows the hourly pressure and temperature reading at the compressor station. The pressure gauge, PIT-WFI_DY1, measured the pressure in the trunk line to the western area of Aliso Canyon, which included SS-25. The pressure varied between about 2,815 psi and 2,790 psi. When the pressure was 2,815 psi, SS-25 was injecting. The system was shut in around 3 PM on October 22, 2015; injection was restarted between 3 and 4 AM on October 23, 2015.

Had the 7 in. casing failed during the shut-in period, the pressure reading of PIT-WFI_DY1 would have fallen to as low as 300 psi, the low pressure set point of the SSV. This is because the leak at SS-25 would have drained the gas in the trunk line leading to SS-25 until the SSV closed. Figure 118 shows that PIT-WFI_DY1 during the shut-in period prior to the final shut-in. No anomalously low-pressure reading was observed. The 7 in. casing did not fail during this shut-in period. The 7 in. casing, therefore, must have failed during the final injection period, which started after 3 AM on October 23, 2015.

Figure 117 shows that prior to the shut-in of SS-25, the total estimated leak rate at 892 ft. through the production casing was 160 MMscf/D, of which 70 MMscf/D was from the injection system and 90 MMscf/D from the reservoir. This period, however, lasted less than half a day before the leak was detected and the well was shut in.

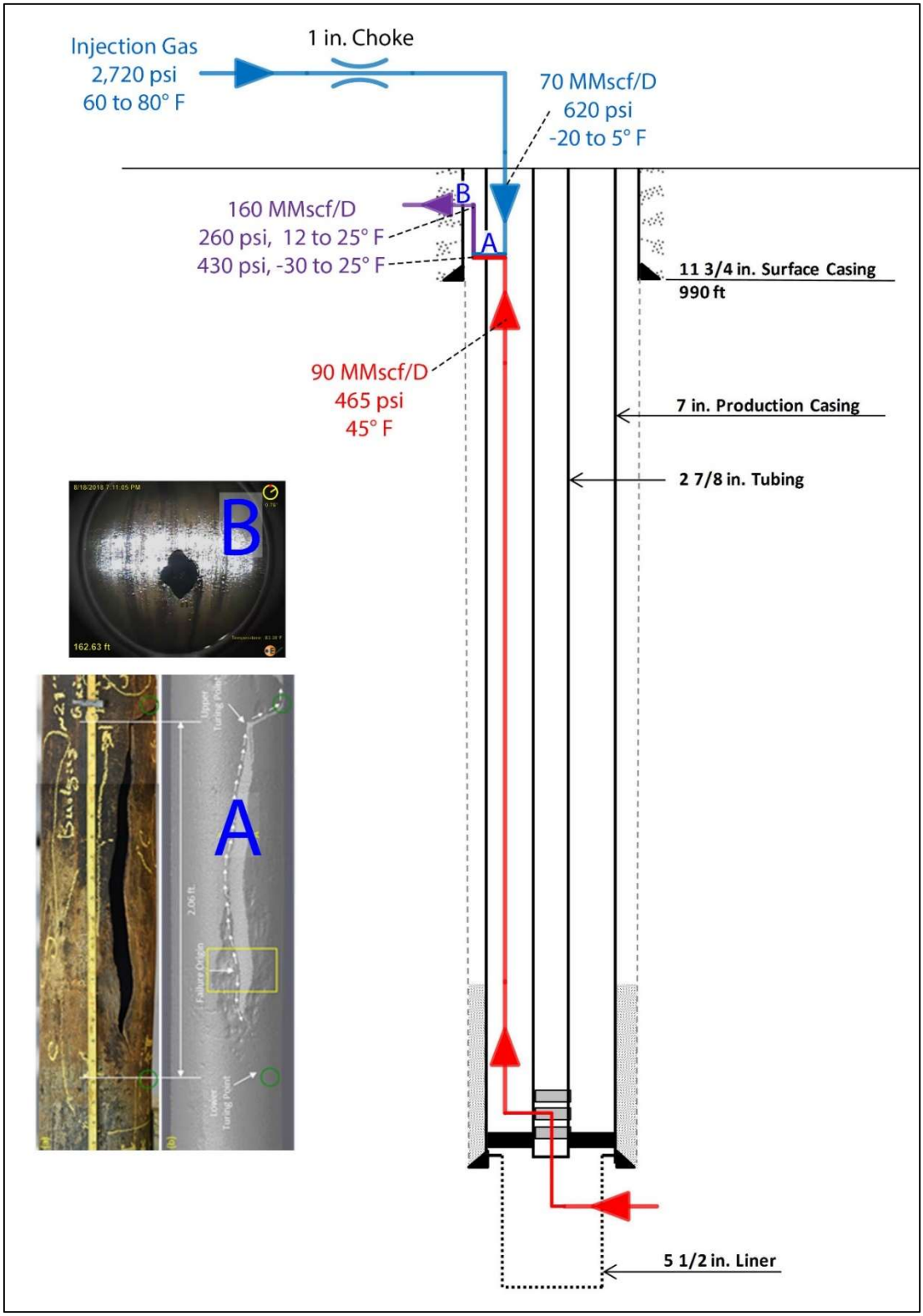


**Figure 117: Summary of the PROSPER Results Prior to Shut-In of SS-25, A-Ruptured 7 in. Casing and B-Hole in the 11 3/4 in. Casing**

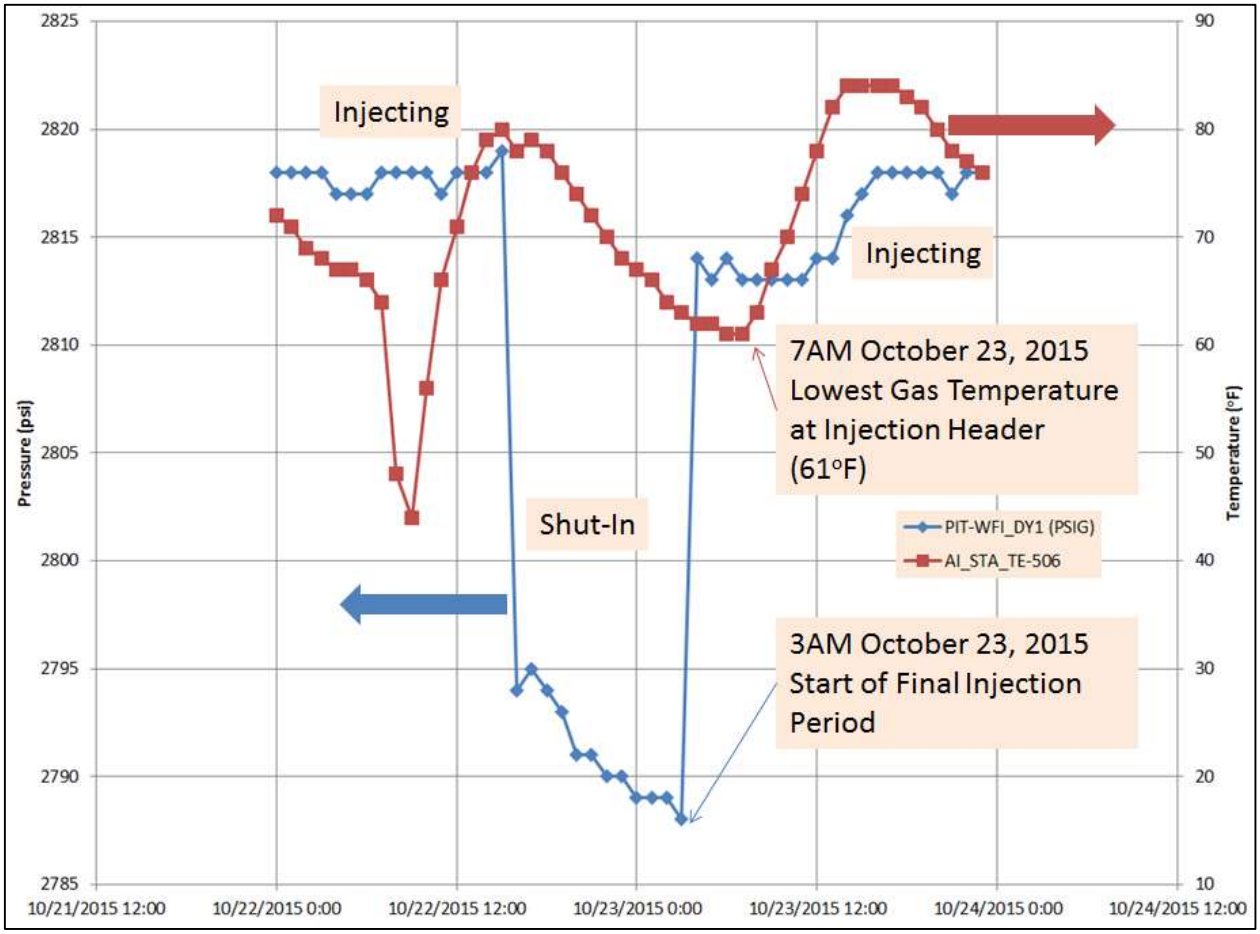


**Figure 118: PIT-WFI_DY1 Hourly Pressure and AI_STA_TE-506 Hourly Temperature Measurements**

Metallurgical analysis showed that the 7 in. casing failed in two steps. The first was the instantaneous 2 ft long axial rupture that occurred at ambient temperature. The axial rupture (Figure 117-A) was followed by a low temperature brittle circumferential parting of the 7 in. casing. The parting was brittle and required extremely low temperature (–78°F to –38°F).

PROSPER estimated that the temperature of the reservoir gas was 10 to 20°F and this was the lowest temperature seen at 892 ft after the shut-in of SS-25. This would not be cold enough to explain the low temperatures indicated by the metallurgical study. The brittle failure therefore could not have occurred any time after the shut-in. Both the ductile and the brittle failure occurred prior to the shut-in of SS-25. This confirms that none of the kill attempts or other events after discovery of the leak (and after the shut-in of SS-25) affected the 7 in. casing failure.

Such low temperatures however could have occurred prior to final shut-in of SS-25. Figure 118 shows that the temperature at the compressor station was between 60°F and 85°F. SS-25 is about 1,000 ft higher in elevation relative to the compressor station. Therefore, the inlet gas temperatures to the SS-25 1 in. choke were likely several degrees lower. The pressure drop across the 1 in. choke was estimated to be 2,100 psi. Using the 0.56°F/14.7 psi J-T coefficient, this pressure drop corresponded to a decrease in temperature of about 80°F. The outlet temperature of this 1 in. choke therefore ranged from –20 to 5°F. PROSPER estimated that the flow down the 7 in.× 2 7/8 in. annulus led to an additional 8°F temperature

drop (assuming minimal heat gain or loss through the 7 in. casing). The estimated temperature of the 70 MMscf/D gas at 892 ft was between –30 and 0°F.

Part of the cold injection gas stream exited the 7 in. x 2 7/8 in. annulus at the upper portion of the axial rupture. Similarly, part of the warm reservoir gas stream exited the 7 in. x 2 7/8 in. annulus at the bottom portion of the axial rupture. The remnants of both streams mixed and exited the axial rupture. As the cold injection gas exited the 7 in. casing at the upper section of the axial rupture, it likely blew the warm reservoir gas away from the 7 in. casing surface, thus keeping the 7 in. casing cold; this is transpiration cooling. Depending on how effective this transpiration cooling effect was, the 7 in. casing could have reached the injection gas temperature, as low as –30°F.

References [43] and [44] studied the transpiration cooling effect experimentally and numerically. The magnitude of this effect depends on the ratio of the blowing stream rate (injection gas in this case) and the bulk stream rate (reservoir gas in this case). In these references, this ratio was less than 1%. In the SS-25 case, this ratio was 70–80%. Therefore, the effectiveness of transpiration cooling in keeping the 7 in. casing cold would have been greater than what is shown in these references. The –30°F estimated through thermal modeling was reasonably close to the temperature range indicated by the metallurgical study.

Figure 118 shows that during the final injection period, the lowest temperature measured at the compressor station occurred between 7 and 8 AM on October 23, 2015. Consequently, the gas temperature at the failure location would have been the coldest during this period. This suggests that the circumferential parting likely occurred between 7 and 8 AM. Therefore, the initial axial rupture must have happened sometime prior to the parting but after the start of injection on October 23, 2015.

On October 28, 2015, the fluid level was measured as 43 ft in the 11 3/4 in. × 7 in. annulus and at 164 ft in the 7 in. × 2 7/8 in. annulus. These fluid levels were likely the top of the ice plugs that had formed in the well. The source of the ice was the 89 bbl of 8.6 ppg KCl that had been pumped down the 7 in. × 2 7/8 in. annulus on October 24, 2015, as part of kill attempt #1. Part of this water was entrained by the gas flowing up the 11 3/4 in. × 7 in. annulus; it coated the walls of the surface casing and froze. The coating of ice was thick enough to resemble a fluid level. The pressure in the 11 3/4 in. × 7 in. annulus also rose from 140 psi to 450 psi by October 25, 2015, and 800 psi by October 30, 2015. The holes in the 11 3/4 in. × 7 in. annulus were likely obstructed by ice.

The estimated fracturing pressure at the shoe was 400–815 psi. During the period from October 25, 2015, to when the ice in the well was finally removed on November 6, 2015, the pressure in the 11 3/4 in. × 7 in. annulus ranged from 400–800 psi. The surface casing shoe was fractured during this period because the flowing pressure likely exceeded the formation strength. This provided the path for the gas out of the well during this period. Gas would have been flowing below the surface casing shoe at 990 ft, diminishing the gas leak rate at the surface. In fact, the on-site DOGGR representative reported that the gas leak rate did diminish significantly, and the gas leak from the side of the hill did stop during this period [6].

This redirection was important because the surface casing annulus pressure was as high as 800 psi between October 25 and November 6, 2015 (Figure 119). PROSPER estimated that, at these pressures, the temperature of the leaking gas could have reached 60°F. If the bulk of this warm gas had flowed up the 11 3/4 in. × 7 in. annulus, the upper section inside the well would have thawed out significantly, increasing the gas flow to the surface. However, because this did not occur, the upper section stayed cold.

On November 6, 2015, a solution of glycol and 10.8 ppg $CaCl_2$ was pumped down the tubing and unblocked the pathways, allowing the gas to flow out of the 11 3/4 in. holes again. The pressure in the 11 3/4 in. × 7 in. annulus fell to 60 psi, which was lower than the initial 140 psi pressure. The kill attempt #1 might have opened up additional pathways for the gas, and the deicing operation might have unplugged them. The DOGGR representative reported that after the deicing operation, the gas leak rate increased substantially [6]. Figure 120 summarizes how the flow paths changed from prior to the shut-in to after the deicing operation.

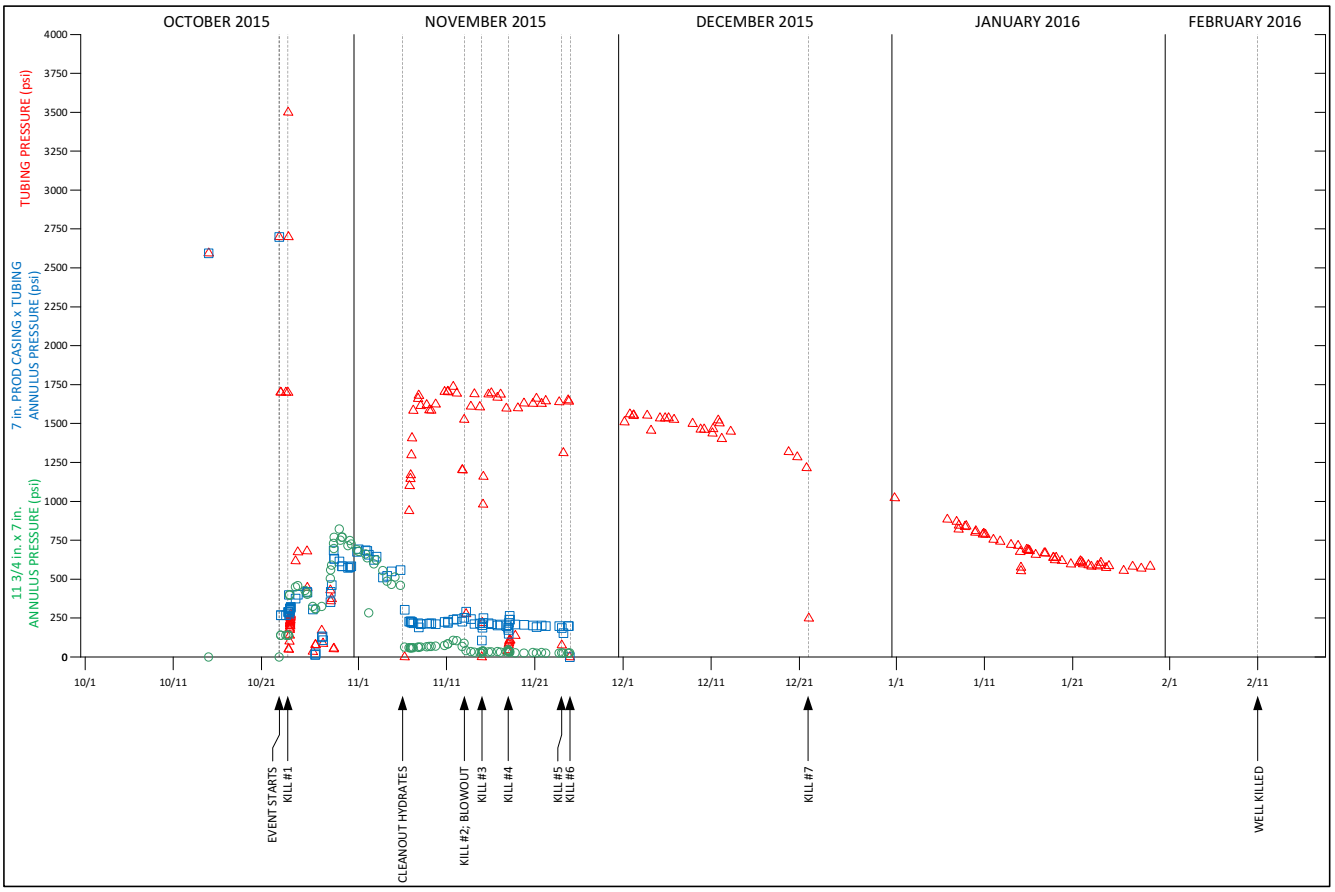


**Figure 119: SS-25 Wellhead Pressure Measurements During the Incident**

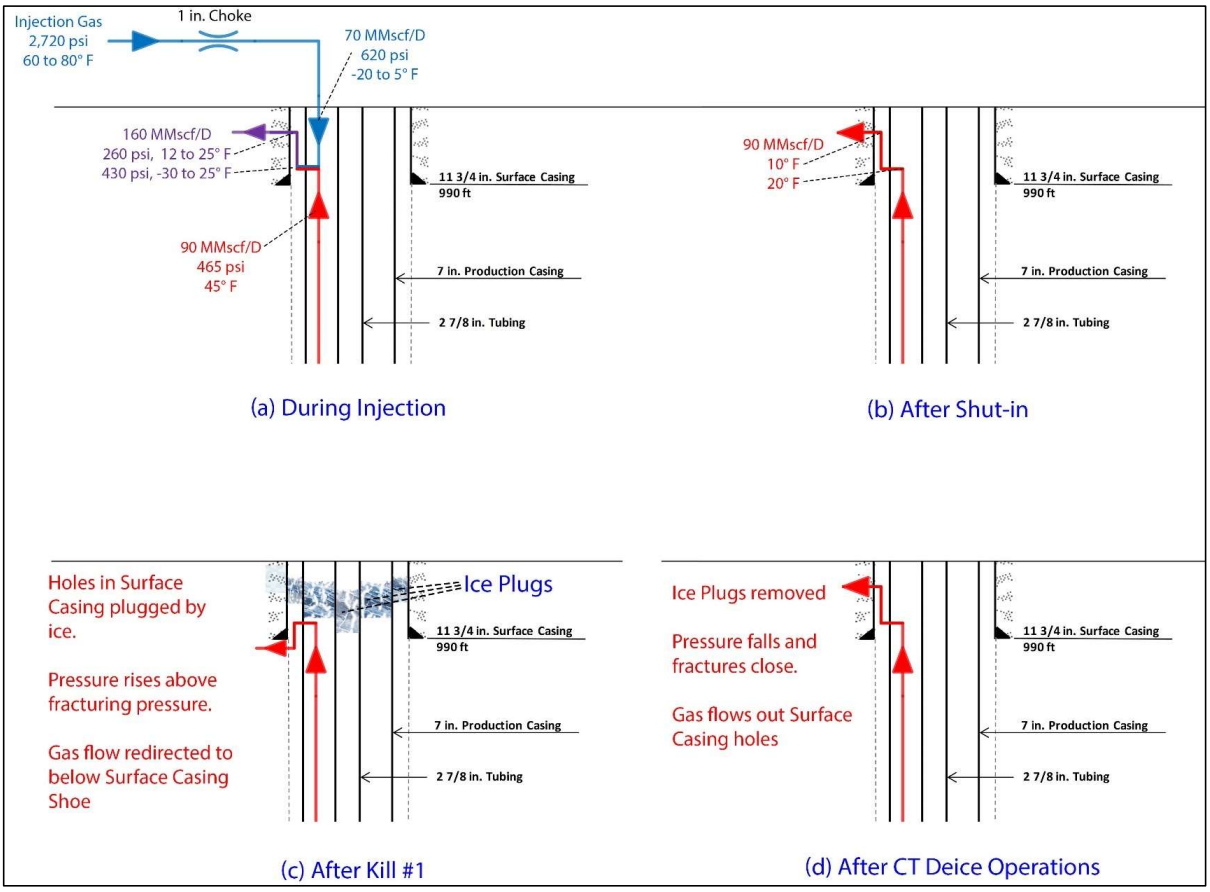


**Figure 120: Summary of the Leak Paths Prior to SS-25 Shut-In to after Deicing Operation on November 6, 2015**

As the reservoir pressure declined, the gas temperature increased (because the lower pressure drop led to less cooling of the gas). This in turn warmed the formation around SS-25. During kill attempt #2 on November 13, a crater began to form around SS-25, and the warm gas vented into the atmosphere, thus preserving the cold temperatures in the formation farther away from SS-25. When SS-25 was finally killed by the relief well, the cold gas that was away from SS-25 flowed back toward the crater and cooled down the area around SS-25.

This scenario of how the leak evolved led to unusual temperature readings at SS-25 and the surrounding area. Unusual low temperature readings were recorded at SS-25, SS-25A, and SS-25B. These temperature measurements allowed us to test the scenario.

To test this scenario, a thermal reservoir simulation model was built using CMG's thermal reservoir simulator, STARS. The model was kept simple and the grid was kept coarse to avoid going beyond the limited available data. Where data were missing, reasonable values were assumed. These parameters were not tuned to achieve a better match, but sensitivity studies were performed to test how robust the results were to the choices made. The simulated temperatures compared reasonably well with the observed data, which confirmed the scenario. This is discussed in the *Analysis of the Post-Failure Gas Pathways and Temperature Anomalies at the SS-25 Site* supplementary report [45].

## 3.4 Kill Attempt Analysis

Between October 24 and December 22, 2015, seven kill operations were attempted to bring the well under control and to stop the leak (Table 18). The first was managed by SoCalGas and the remaining six were managed by a well-control company contracted by SoCalGas. None of the attempts were successful, and each attempt made the surface conditions worse.

In designing a kill operation, the objective is to place a fluid of sufficient density into the wellbore such that the hydrostatic pressure exerted by this fluid is higher than the pressure of the flowing gas. The two primary design variables are the fluid density and pump rate. The primary constraint is that the pressure rating of the surface wellhead equipment must not be exceeded. (In this case, the surface equipment was rated to 5,000 psi.) In general, the lower fluid densities require higher pump rates and result in higher pressures at the wellhead.

**Table 18: Descriptions and Results for Kill Attempts #1–7 (October 23–December 22, 2015)**

| Kill Attempt & Date | Description | Results | Successful |
|---|---|---|---|
| #1 (October 24) | 10 ppg polymer pill (down tubing) | Tubing plugged after 11.8 bbl pumped. | No |
| | 8.6 ppg lease water (down casing in pump-and-bleed operation) | Additional gas flow noted at surface<br>Gas broke through at surface after 89 bbl of fluid pumped. | |

| Kill Attempt & Date | Description | Results | Successful |
|---|---|---|---|
| #2 (November 13) | 10 bbl of 9.4 ppg polymer pill<br>683 bbl of 9.4 ppg $CaCl_2$<br>10 bbl of 9.4 ppg polymer pill<br>3 bbl of 8.6 ppg brine water<br>Maximum pump rate 8 bpm<br>Maximum pump pressure 1,526 psi | Observed increased gas flow and liquid from fissures.<br>Pony motor went down. Shut down pumping.<br>Brine, oil, and gas flowing from fissures on pad.<br>Well blew out in the conventional sense. Blowout vent opened 20 ft from wellbore, shooting debris 75 ft into the air. | No |
| #3 (November 15) | 170 bbl of 9.4 ppg $CaCl_2$<br>19 bbl of 18 ppg barite pill<br>50 bbl of 9.4 ppg $CaCl_2$<br>Maximum pump rate 8 bpm<br>Maximum pump pressure 1,645 psi | Gas rate from fissures increased, followed by oil and brine.<br>Flow from fissures stopped briefly and then began to flow gas. | No |
| #4 (November 18) | 230 bbl of 9.4 ppg $CaCl_2$<br>35 bbl of 18 ppg barite pill<br>50 bbl of 9.4 ppg $CaCl_2$<br>Maximum pump rate 9 bpm<br>Maximum pump pressure 1,975 psi | Gas rate from fissures increased. Observed oil and brine from fissure.<br>Barite to surface was reported. | No |
| #5 (November 24) | 50 bbl of 9.4 ppg GEO Zan pill<br>950 bbl of fresh water<br>35 bbl of 18 ppg barite pill<br>56 bbl of 9.4 ppg $CaCl_2$<br>Maximum pump rate 13 bpm<br>Maximum pump pressure 4,167 psi (Reported value. Telemetry system shows maximum tubing pressure of approximately 3,600 psi) | 30 ft × 10 ft crater developed and gas rate increased.<br>Recovered 700 bbl of fluid from location. | No |
| #6 (November 25) | 50 bbl of 9.4 ppg GEO Zan LCM pill<br>910 bbl of fresh water<br>100 bbl of 9.4 ppg GEO Zan LCM pill<br>56 bbl of 9.4 ppg $CaCl_2$<br>Maximum pump rate 13 bpm<br>Maximum pump pressure 4,164 psi | Gas activity increased in crater.<br>Water flow from crater increased.<br>Flow line from 7 in. and tubing head broke. Nipple on wellhead broke. Pump line to 7 in. casing head broke.<br>Cratering around the wellhead increased and damaged several casing valves.<br>Tubing pressure went to zero, and then started increasing. | No |

| Kill Attempt & Date | Description | Results | Successful |
|---|---|---|---|
| #7<br>(December 22) | 107 bbl of 15 ppg WBM<br>100 bbl of 15 ppg WBM with LCM<br>125 bbl of 15 ppg WBM<br>Maximum pump rate 5.8 bpm<br>Maximum pump pressure 1,157 psi (at start conditions) | Mud, oil mist in crater.<br>Liquid began to come out of the casing at surface.<br>Shut down due to rocking of wellhead and unloading mud from crater.<br>Pump line to top tee broke off due to movement of wellhead.<br>Tubing pressure went to zero, and then started increasing. | No |

This subsection analyzes why each one of the kill attempts failed and if any of them could have been successful. Blade set-up the SS-25 physical system within the Drillbench Blowout Control software (Figure 121). After shut-in and prior to kill attempt #1 on October 24, 2015, gas had flowed from the reservoir into the bottom of the tubing, entered the 7 in. × 2 7/8 in. annulus via ports near the packer, flowed up the 7 in. × 2 7/8 in. annulus, exited the 7 in. casing through a leak at 892 ft, and finally flowed to the surface through the formation. When the pumping of the kill fluid down the tubing of this physical system was initiated, the influx gas and kill fluid met in the tubing, and the combined flow entered the annulus through the ports.

Prior to kill attempt #2 on November 13, 2015, a plug had been set in the tubing at 8,393 ft, and the tubing had been perforated a few feet above the plug. Within the software, the plug and perforations were represented as a bit with nozzles, forming the equivalent flow area of the perforations. When the pumping of kill fluid down the tubing of this physical system was initiated, the kill fluid entered the annulus via the bit nozzles (perforations) while influx gas flowed up from below. The modeling details and approach are in the *SS-25 Transient Well Kill Analysis* supplementary report [46].

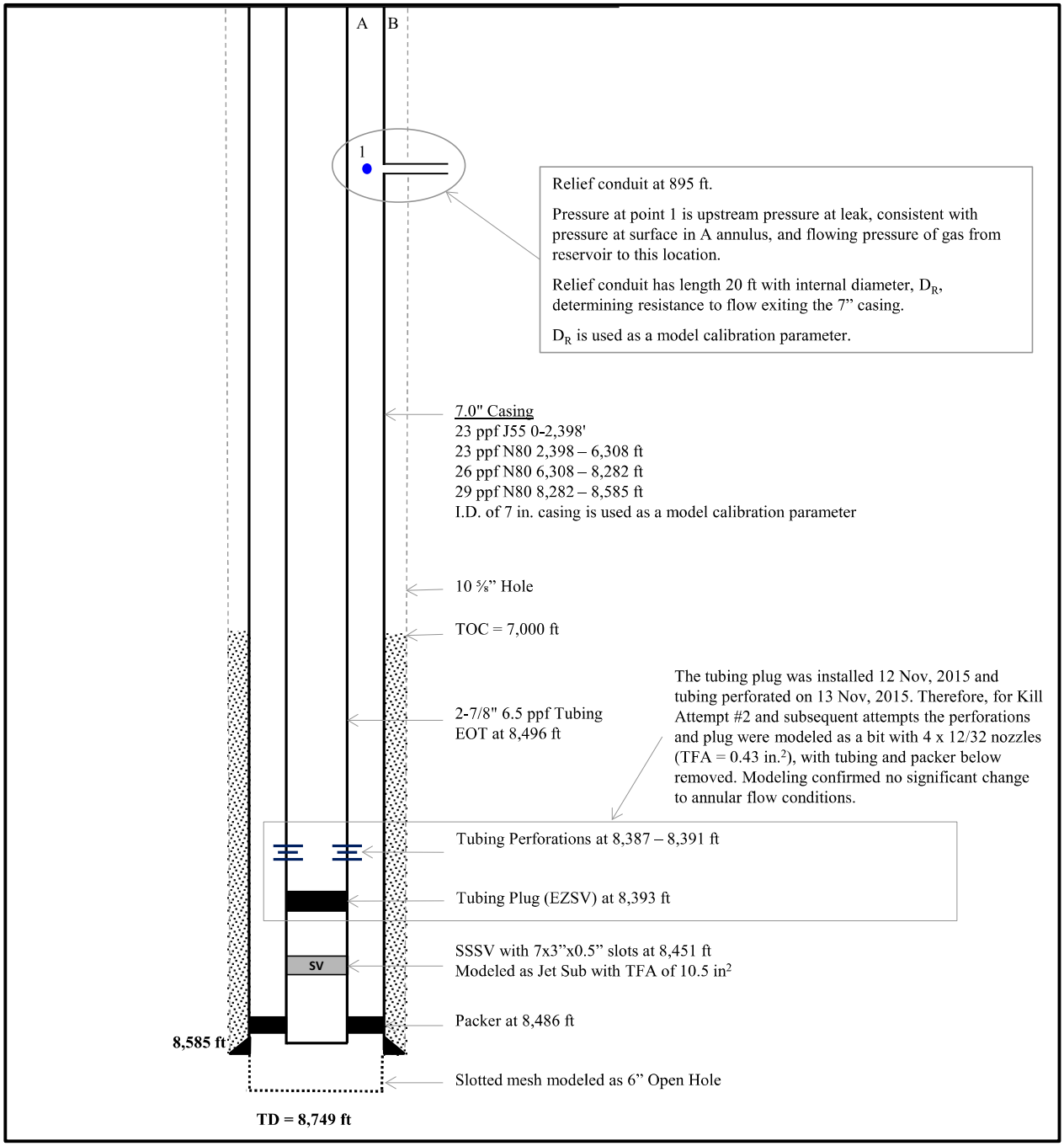


**Figure 121: Physical Model as Set up in the Drillbench Blowout Control Model**

### 3.4.1 Kill Attempt #1 (October 24)

On October 24, 2015, SoCalGas executed the first kill attempt to bring the SS-25 leak under control (Table 18). First, a polymer pill was attempted to be pumped down the tubing, but the tubing plugged, most likely due to the formation of an ice or hydrate plug. Next, a pump-and-bleed kill procedure was attempted down the 7 in. production casing. After 89 bbl of kill fluid was pumped, gas flow appeared in cracks on the ground, and the kill procedure was terminated early.

The plugging of the tubing during kill attempt #1 was most likely due to flash freezing of the water in the kill fluid. Section 3.3 indicates that temperatures between 10°F and 20°F were likely present—water will flash freeze at these temperatures. Blade also considered that hydrates acted as a plugging agent. However, kinetics of hydrate formation are not well understood, and there has been no documented occurrence of flash formation of hydrates. Therefore, it was more likely that the tubing plugged due to flash freezing of water in the kill fluid, indicating that the true crystallization temperature (TCT) of the kill fluid was not low enough. Hydrates might have formed after, and in addition to, the initial formation of ice.

At the end of kill attempt #1, the 11 3/4 in. × 7 in. casing annulus pressure increased from 140 psi to 400 psi. This increase indicated a change in subsurface conditions, most likely plugging of the initial leak path by ice and shifting of the leak to deeper formations.

At the time of kill attempt #1, the estimated leak rate was 93 MMscf/D. Blade's analysis indicates that the 10 ppg fluid was not dense enough to kill the well at realistic pumping rates. The well could have been killed by pumping a 12 ppg fluid at 10 bpm or a 15 ppg fluid at 7 bpm (Table 19).

**Table 19: Kill Attempt #1 Alternatives**

| Gas Rate (MMscf/D) | Kill Fluid | Kill Rate (bpm) | Gas Flow Stopped? Yes/No | Time to Stop Gas Flow (min.) | Time for One Circulation (min.) | Time Less than One Circulation Yes/No | Surface Pressure when Influx Ceased (psia) | Maximum Pump Pressure (psi) | Successful Kill? Yes/No |
|---|---|---|---|---|---|---|---|---|---|
| 93 | 12 ppg | 10 | Yes | 27 | 28 | Yes | 4,327 | 4,342 | Yes |
| | 15 ppg | 7 | Yes | 38 | 39 | Yes | 628 | 1,733 | Yes |

This kill attempt was a reasonable response because the extent of the failure in SS-25 was unknown. Similar well kill operations had been carried out in the past on wells with casing leaks, namely Frew 3 in 1984 and Fernando Fee (FF) 34A in 1990. The two wells were killed successfully by pumping fluid down the tubing. Later analysis of the SS-25 casing failure and gas flow rates showed that there were significant differences in the SS-25's conditions when compared to Frew 3 and FF-34A's conditions. Additional details are available in *Analysis of Aliso Canyon Wells with Casing Failures* supplementary report [47].

Gas broaching to surface from cracks in the ground following kill attempt #1 indicated that SS-25 had serious problems and that a shallow casing leak likely existed.

The subsequent kill attempts were designed and implemented by a well-control company contracted by SoCalGas.

### 3.4.2 Kill Attempt #2 (November 13)

On November 13, 2015, the well-control company executed kill attempt #2, which was also unsuccessful. Increased gas, liquid, and brine flow were observed from fissures in the surface. A "blowout vent opened 20 [ft] from the wellbore and began shooting debris 75 [ft] into the air [6]"(Table 18).

Blade simulated kill attempt #2 in detail (Figure 122). When the FBHP[ii] (flowing bottomhole pressure) (solid red line) is less than the reservoir pressure (dashed red line), the gas will flow from the reservoir into the wellbore as shown by the influx rate (solid navy line). The well is killed if the FBHP is higher than the reservoir pressure so that the influx rate is zero.

Figure 122 shows the results of the kill attempt as it was executed. As kill fluid was pumped into the well, the FBHP (solid red line) increased, and the influx rate (navy line) decreased (between 11:30 AM and 11:55 AM and between 12:05 PM and 1 PM). However, the FBHP did not rise above the reservoir pressure (dashed red line), and the influx rate did not go to zero; therefore, the well was not killed. When the pump was turned off (between 11:55 AM and 12:05 PM) or pump rate (orange line) was reduced (after 1 PM), the FBHP decreased, and the influx rate increased. In fact, between 12:05 PM and 1 PM, both the FBHP and the influx rate stabilized at 2,500 psi and 28–29 MMscf/D; this indicates that the kill attempt was not sufficient to kill the well even if the pumping had continued indefinitely.

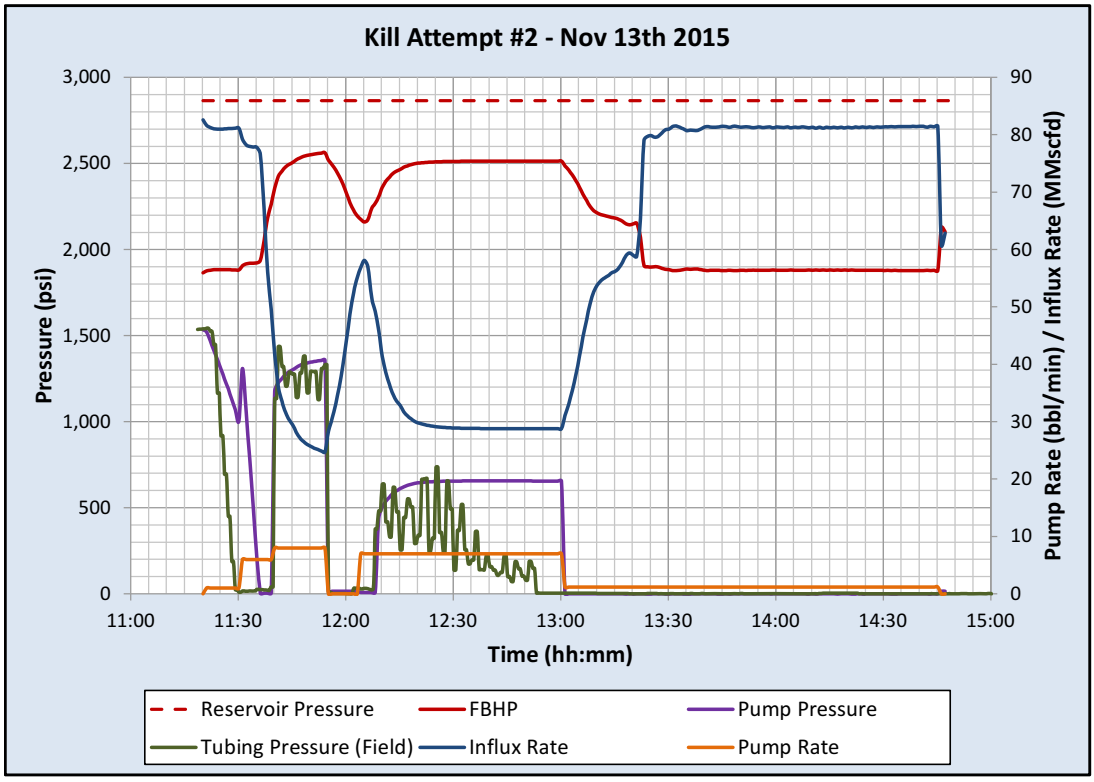


**Figure 122: Simulation of Kill Attempt #2**

At the time of kill attempt #2, the estimated leak rate was 83 MMscf/D. Blade's analysis indicates that the 9.4 ppg fluid was not dense enough to kill the well at a realistic pumping rate. The well could have been killed by pumping a 12 ppg fluid at 9 bpm or a 15 ppg fluid at 6 bpm (Table 20). (Blade's analyses assume that kill fluids would have been pumped down the tubing; it would have been impossible to kill SS-25 by pumping down the 7 in. casing.)

[ii] FBHP in this section refers to the kill fluid hydrostatic pressure plus the kill fluid friction pressure at the perforations.

**Table 20: Kill Attempt #2 Alternatives**

| Gas Rate (MMscf/D) | Kill Fluid | Kill Rate (bpm) | Gas Flow Stopped? Yes/No | Time to Stop Gas Flow (min.) | Time for One Circulation (min.) | Time Less than One Circulation Yes/No | Surface Pressure when Influx Ceased (psia) | Maximum Pump Pressure (psi) | Successful Kill? Yes/No |
|---|---|---|---|---|---|---|---|---|---|
| 83 | 12 ppg | 9 | Yes | 27 | 31 | Yes | 3,629 | 3,644 | Yes |
| | 15 ppg | 6 | Yes | 45 | 46 | Yes | 0 | 1,550 | Yes |

Sufficient pumping capacity of 1,600 HHP (hydraulic horsepower) was available on site, and 295 HHP (18%) were used for the pumping operations. As Table 20 shows, a 12 ppg fluid at a pump rate of 9 bpm should have killed the well. The maximum pump pressure would have been 3,644 psi.

### 3.4.3 Kill Attempts #3–6 (November 14–25)

Between November 14 and November 25, 2015, the well-control company executed four other kill attempts (kill attempts #3–6). All four kill attempts failed, and the SS-25 surface conditions worsened. All four kill attempts were similar in design. The main components of the kill fluids were 9.4 ppg $CaCl_2$ fluid for kill attempt #3–4 and fresh water (estimated 8.34 ppg density) for kill attempts #5–6. The estimated gas leak rates were 81 MMscf/D for kill attempts #3–4 and 78 MMscf/D for kill attempts #5–6. Blade analyses indicate that the fluid densities were not high enough to kill the well at realistic pump rates for any of the four kill attempts. The well could have been killed with either 12 ppg or 15 ppg kill fluid at realistic pump rates (6–8 bpm) (Table 21–Table 24).

**Table 21: Kill Attempt #3 Alternatives**

| Gas Rate (MMscf/D) | Kill Fluid | Kill Rate (bpm) | Gas Flow Stopped? Yes/No | Time to Stop Gas Flow (min.) | Time for One Circulation (min.) | Time Less than One Circulation Yes/No | Surface Pressure when Influx Ceased (psia) | Maximum Pump Pressure (psi) | Successful Kill? Yes/No |
|---|---|---|---|---|---|---|---|---|---|
| 81 | 12 ppg | 8 | Yes | 35 | 35 | Yes | 2,416 | 2,431 | Yes |
| | 15 ppg | 6 | Yes | 43 | 46 | Yes | 0 | 1,521 | Yes |

**Table 22: Kill Attempt #4 Alternatives**

| Gas Rate (MMscf/D) | Kill Fluid | Kill Rate (bpm) | Gas Flow Stopped? Yes/No | Time to Stop Gas Flow (min.) | Time for One Circulation (min.) | Time Less than One Circulation Yes/No | Surface Pressure when Influx Ceased (psia) | Maximum Pump Pressure (psi) | Successful Kill? Yes/No |
|---|---|---|---|---|---|---|---|---|---|
| 81 | 12 ppg | 8 | Yes | 35 | 35 | Yes | 2,395 | 2,410 | Yes |
| | 15 ppg | 6 | Yes | 42 | 46 | Yes | 0 | 1,502 | Yes |

**Table 23: Kill Attempt #5 Alternatives**

| Gas Rate (MMscf/D) | Kill Fluid | Kill Rate (bpm) | Gas Flow Stopped? Yes/No | Time to Stop Gas Flow (min.) | Time for One Circulation (min.) | Time Less than One Circulation Yes/No | Surface Pressure when Influx Ceased (psia) | Maximum Pump Pressure (psi) | Successful Kill? Yes/No |
|---|---|---|---|---|---|---|---|---|---|
| 78 | 12 ppg | 8 | Yes | 32 | 35 | Yes | 2,314 | 2,329 | Yes |
| | 15 ppg | 6 | Yes | 38 | 46 | Yes | 0 | 1,464 | Yes |

**Table 24: Kill Attempt #6 Alternatives**

| Gas Rate (MMscf/D) | Kill Fluid | Kill Rate (bpm) | Gas Flow Stopped? Yes/No | Time to Stop Gas Flow (min.) | Time for One Circulation (min.) | Time Less than One Circulation Yes/No | Surface Pressure when Influx Ceased (psia) | Maximum Pump Pressure (psi) | Successful Kill? Yes/No |
|---|---|---|---|---|---|---|---|---|---|
| 78 | 12 ppg | 8 | Yes | 32 | 35 | Yes | 2,303 | 2,318 | Yes |
| | 15 ppg | 6 | Yes | 38 | 46 | Yes | 0 | 1,459 | Yes |

Blade analysis indicates that at the time of kill attempt #5, the well was flowing at 78 MMscf/D. Table 23 shows that 12.0 ppg fluid pumped at 8 bpm or 15.0 ppg fluid at 6 bpm would have also stopped the gas flow. The fluid would have tended to maintain a stable fluid column because of the damage to the reservoir permeability, while clear water or clear brine would not have remained stable because of fluid loss into the permeable reservoir.

Kill attempt #6 was a near repeat of kill attempt #5, except that the 35 bbl barite pill was replaced with a 100 bbl 9.4 ppg LCM pill, and a higher pump rate was applied to the kill. It appeared to have killed the well, but fluid loss into the formation kept the annular fluid column from stabilizing. It is probable that continued pumping from the surface might have kept up with the fluid loss, but surface plumbing failures prevented the well from being kept filled. The use of fresh water and clear brine contributed to the attempt's failure because of fluid loss into the formation and loss of hydrostatic pressure, which allowed the well to flow after the kill attempt.

At this point, the wellhead and surface casing were structurally unstable. Gas and fluid flow around the surface location removed enough soil and formation to allow considerable oscillation of the wellhead.

### 3.4.4 Kill Attempt #7 (December 22)

The final well kill attempt was executed by the well-control company on December 22, 2015. After installing guy wires to reduce wellhead oscillations, the pump job for this kill attempt consisted of pumping 15.1 ppg water based mud (WBM), with LCM, at a rate of 5 bpm. (Reports are inconsistent—the actual rate may have been 5.8 bpm.) After pumping 300 bbl, the injection rate was reduced to 0.5 bpm for 15 minutes. Pumping was terminated due to rocking of the wellhead and a subsequent failure of the injection connection. The reports are vague regarding the reported pressure, but it seems that the flow from the crater slowed considerably for a while.

The estimated leak rate was 60 MMscf/D. Results of Blade's simulations are shown in Figure 123. As pumping continued, the FBHP (solid red line) approached the reservoir pressure (dashed red line), and both influx rate (solid navy line) and pump pressure (solid purple line, also WHP) went to zero. This behavior was consistent with what was observed in the field during the kill attempt. At 10:30 AM, the well was just about to be killed, although premature shutdown of the pumps resulted in the FBHP decreasing and the influx rate increasing. Pumping needed to continue for some time after the well had seemed to have been killed to ensure that the well had been effectively killed. This did not happen in the field because the pumps were shut down early. Blade's analysis (Table 25) confirms that the well should have been killed with either 12 ppg fluid pumped at 6 bpm or 15 ppg fluid pumped at 5 bpm.

This was the first attempt to utilize an engineered approach—some documents indicate that well kill modeling had been attempted prior to the job. It appears that the well was almost dead when the surface equipment failed, but because of the inability to continuously fill the well, the production zone resumed flowing after some (undetermined) time.

The 11 3/4 in. × 7 in. annulus valve on the wellhead backed out during this kill attempt, which created an unrestricted gas flow path to the surface. The gas flow out of the 2 in. threaded outlet contributed to the enlargement of the crater on the south side. It is likely that the crater, unsupported lines and valves, wellhead movement, and vibration contributed to the valve backing out, which made the overall surface situation worse.

In conclusion, kill attempt #7 was a "near kill" that failed because the pumping was terminated early due to concern for potential wellhead damage. A contributing factor was the cumulative damage done by previous, unsuccessful kill attempts to the well site and wellhead, which caused this kill attempt to be terminated early.

By December 22, 2015, after more than 4,000 bbl of various fluids had been pumped into the well, most fluids returned to the surface under high velocity. Additionally, a large volume of gas had escaped through the surface fissures and crater. The surface conditions had deteriorated to a point that it became unsafe for personnel to work near the wellhead. The relief well P-39A started being drilled on December 4, 2015, and it was successful in killing SS-25 on February 11, 2016.

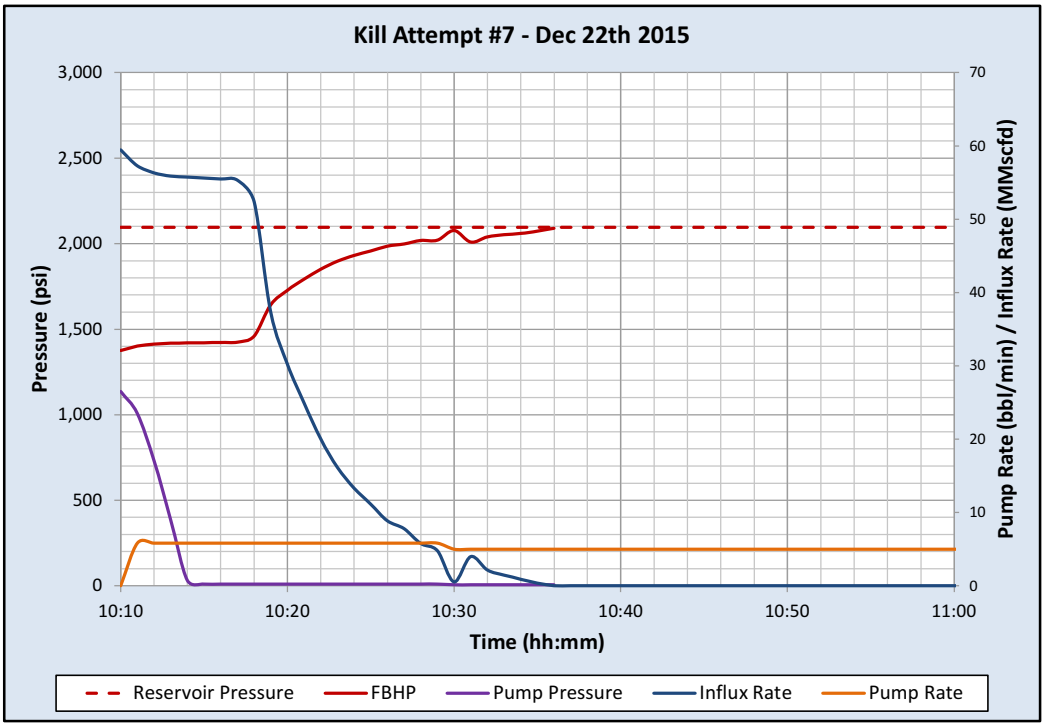


**Figure 123: Simulation of Kill Attempt #7**

**Table 25: Kill Attempt #7 Alternatives**

| Gas Rate (MMscf/D) | Kill Fluid Density | Kill Rate (bpm) | Gas Flow Stopped? Yes/No | Time to Stop Gas Flow (min.) | Time for One Circulation (min.) | Time Less than One Circulation Yes/No | Surface Pressure when Influx Ceased (psia) | Maximum Pump Pressure (psi) | Successful Kill? Yes/No |
|---|---|---|---|---|---|---|---|---|---|
| 60 | 12 ppg | 6 | Yes | 34 | 46 | Yes | 0 | 1,151 | Yes |
| | 15 ppg | 5 | Yes | 33 | 55 | Yes | 0 | 1,151 | Yes |

## 3.5 Total Gas Leak Volume

The cumulative gas release volume was estimated using the modeling results. Figure 124 presents Blade's SS-25 withdrawal rate estimate for the duration of the uncontrolled leak using the PROSPER model described in Section 3.2.1 The kill attempts are shown to highlight the rates that the kill attempts should have been designed to kill. Kill attempt #1 had a discharge rate of 93 MMscf/D, kill attempts #2 to #6 had discharge rates from 83 to 78 MMscf/d, and kill #7 had a discharge rate of 60 MMscf/D. Blade derived the best-estimate rate from data available after the well was killed.

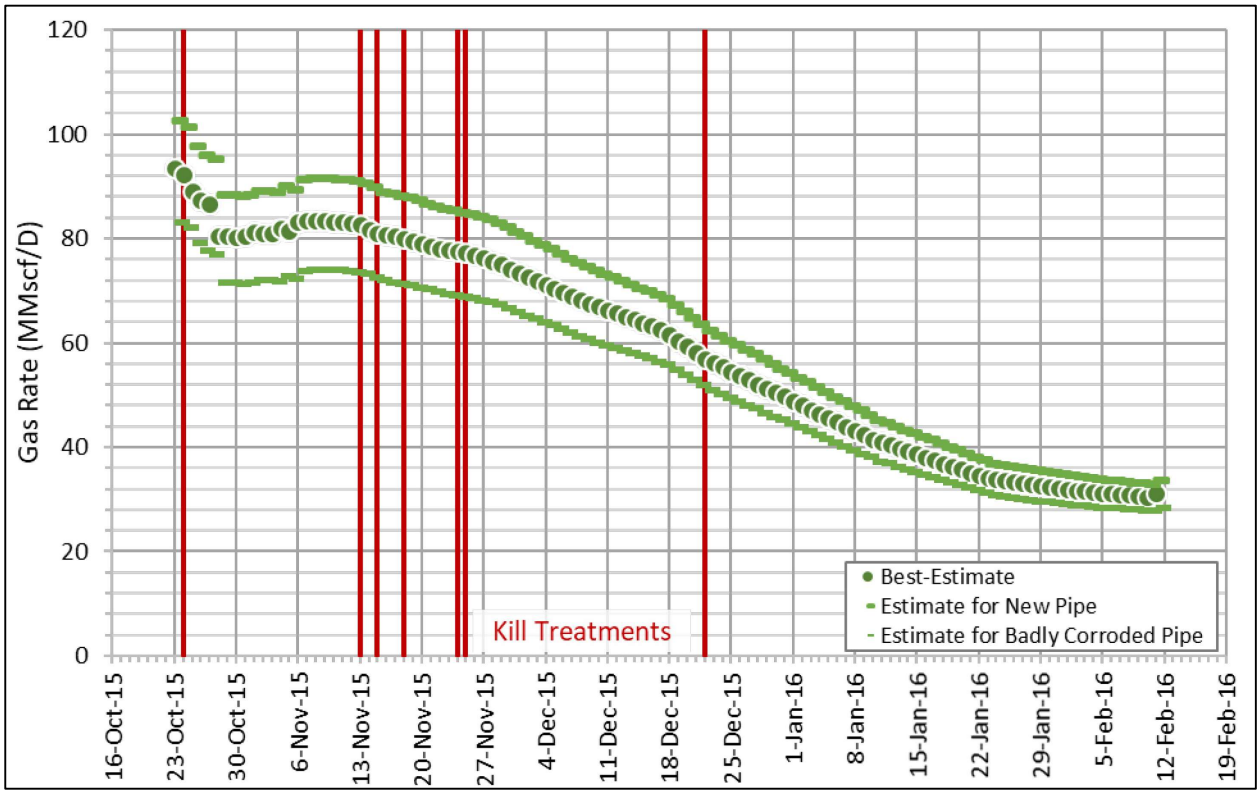


**Figure 124: SS-25 Leak Rate Estimate (October 23, 2015–February 11, 2016)**

Figure 125 presents Blade's SS-25 cumulative leak estimate for the duration of the incident. If the uncontrolled leak had ended by kill attempt #2, the methane discharge would have been less than one-third of the final amount.

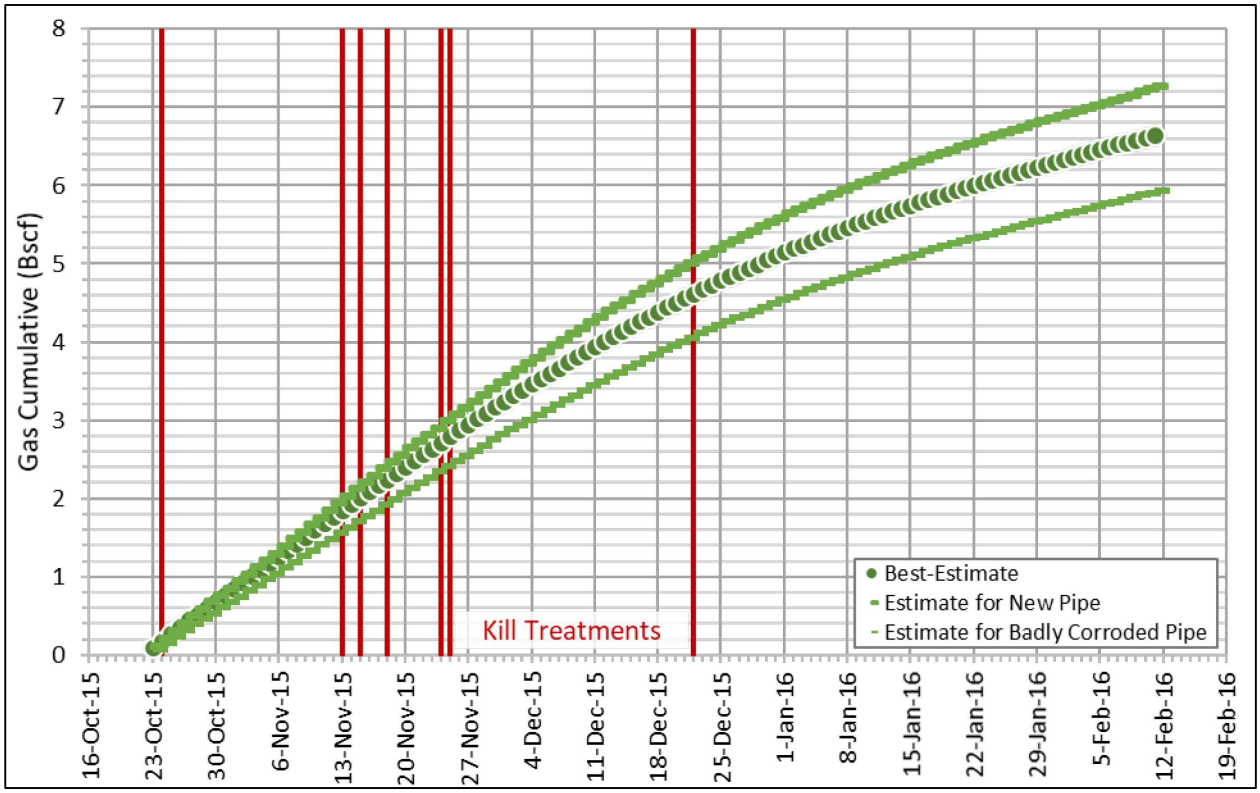


**Figure 125: SS-25 Leak Cumulative Estimate (October 23 to February 11)**

Table 26 compares Blade's estimate to other estimates of the cumulative amount of gas leaked by SS-25.

**Table 26: Aliso Canyon Hydrocarbon Leak Estimates**

| Source | Cumulative Gas (BSCF) | Methane Equivalent ($10^6$ kg) |
|---|---|---|
| Scientific Aviation Estimate [48] | 5.3 | 97 |
| California Air Resources Board (CARB) Estimate [49] | 6.0 | 109 |
| Tracer Flux Ratio | 4.7 | 86 |
| SoCalGas Inventory Variance | 4.6 | 84 |
| Blade Best Estimate | 6.6 | 120 |
| Blade Estimate if Badly Corroded Pipe* | 5.9 | 107 |
| Blade Estimate if New Pipe* | 7.2 | 131 |

*The new and badly corroded pipe estimates give upper and lower bounds, respectively, and Blade's well work showed that the piping was not at these limits.

CARB derived their estimate following a review of the Scientific Aviation estimate. Scientific Aviation estimated the airborne emissions of the leak by analyzing data gathered by flying a specially equipped aircraft over the leak site [48]. Figure 126 shows the estimated airborne rates (converted from metric tons of methane to standard gas rates using the equation of state model from Blade's SS-25 PROSPER well model).

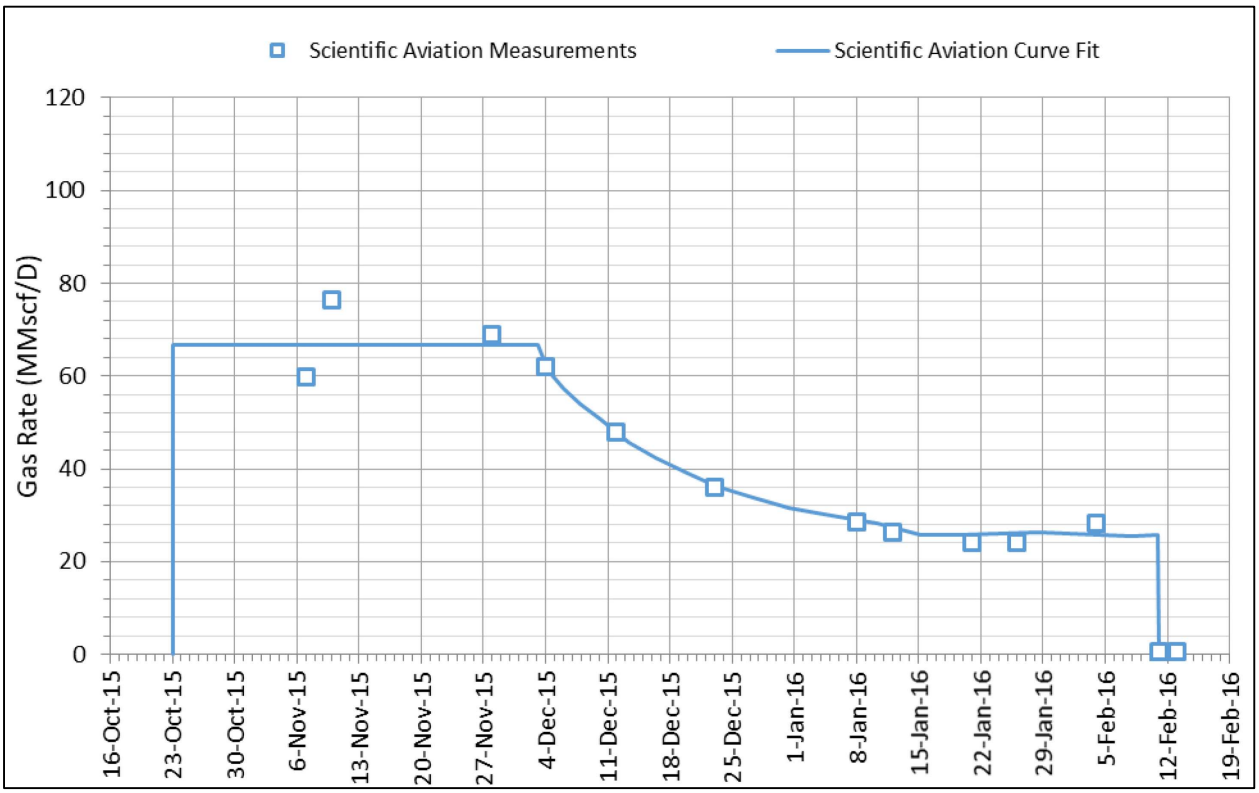


**Figure 126: SS-25 Measured Leak-Rate History–Scientific Aviation**

Although Scientific Aviation's plane was nearby for other measurements when the SS-25 leak occurred and mobilized quickly to measure the leak, the initial leak rates were not measured. Also, only airborne hydrocarbons were measured, and this did not necessarily represent the total leak. Hydrocarbons could have dispersed through the fracture matrix and taken an unknown path that delayed emissions to the air. This dispersion and delay were likely to affect the Scientific Aviation measurements.

Figure 127 compares the rates of Scientific Aviation with those of this report. The lower estimated rates, which assumed badly corroded tubing and casing, were the lower limit, and the higher estimated rates, which assumed new tubing, were the upper limit. Pulled production casing and logging after the leak showed evidence of metal loss, corrosion, and scaling. The best rates were from the assumed pipe roughness based on corrosion and scaling and were always just at or above the Scientific Aviation rates. Note that the plateau rate assumed by Scientific Aviation for the six weeks was a result of limited measurements.

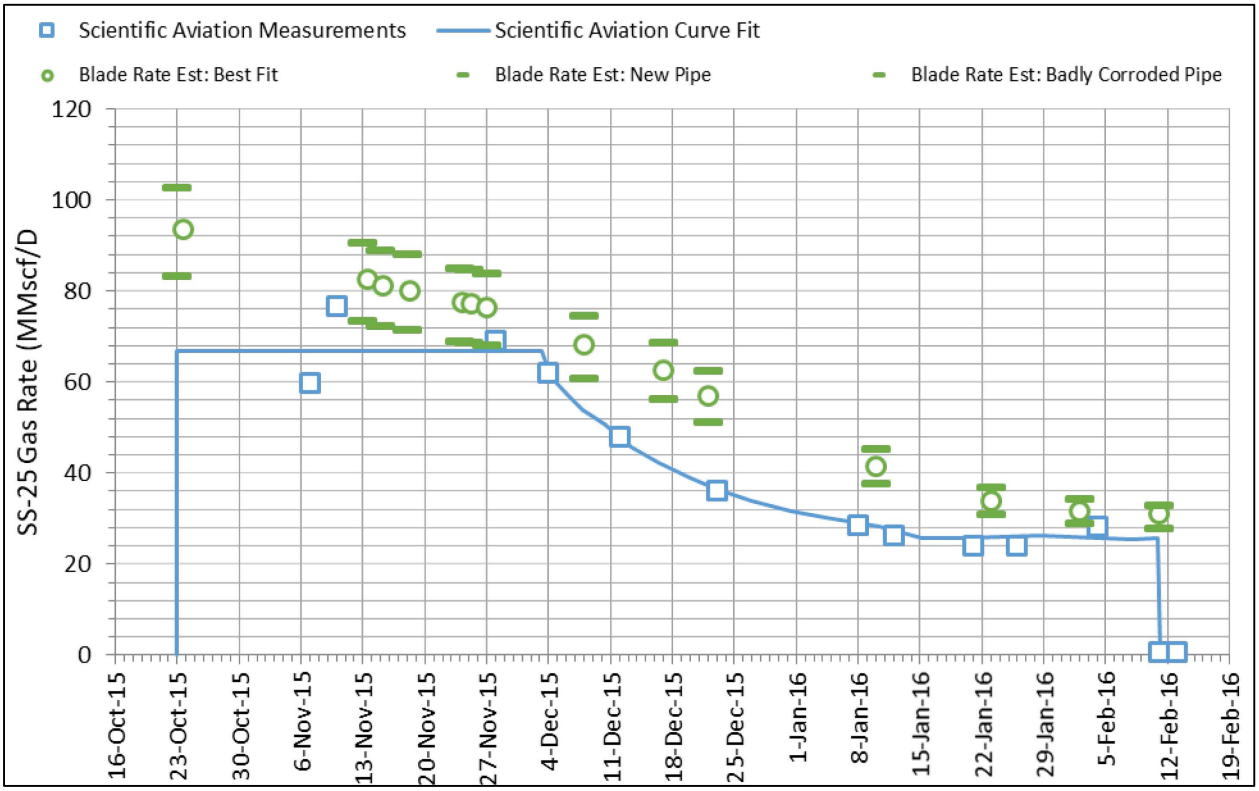


**Figure 127: SS-25 Leak-Rate History Comparison–Blade and Scientific Aviation**

The tracer flux ratio method was similar to the Scientific Aviation method in that both attempted to measure gas leaking into the atmosphere instead of gas leaving the gas storage reservoir. Both methods would have missed any gas that leaked into and remained in the subsurface formations.

SoCalGas's inventory variance method is similar to Blade's in that it attempts to quantify the gas leaving the reservoir. Using the storage capacity of the reservoir, the method first determined the total gas lost from the reservoir. Volumes that had been withdrawn using other wells during depressurization were then subtracted from this amount to calculate the amount of gas that leaked through SS-25 (Table 27).

**Table 27: Gas Leak Volumetric Estimate through Inventory Verification Method**

| | |
|---|---|
| **Inventory before incident (October 23, 2015)** | 77 Bscf |
| **Inventory after incident (February 29, 2016)** | –0.9 Bscf |
| **Total Gas Leaving Reservoir** | 77.9 Bscf |
| **Gas Withdrawn Using Other Wells** | 73.3 Bscf |
| **Gas Leaked through SS-25** | 4.7 Bscf |

The gas storage capacity of the reservoir is given by the following relationship:

$$P/Z = 34.24468V + 1639.24520$$

Where $V$ is the inventory in Bscf, $P$ is the average reservoir pressure in psi, and $Z$ is the gas compressibility factor (dimensionless). Based on this relationship, each 1 Bscf increase in inventory will increase the average reservoir pressure by 31–32 psi ($Z$=0.91–0.92). The discrepancy between the Blade's total

volumetric estimate of 6.6 Bscf and SoCalGas's estimate of 4.7 Bscf is 1.9 Bscf. This corresponds to about a difference of about 60 psi in reservoir pressure. It is conceivable that there is this much error in the estimation of the average pressure measurements.

Also, the inventory verification method estimated the gas leaked through SS-25 at only 6% of the total gas removed from the reservoir (the remaining 94% were removed by controlled withdrawal through other wells.) Therefore, any uncertainty in the inventory before the incident, inventory after the incident, or gas withdrawn using other wells would result in a larger uncertainty in the SS-25 gas leak amount. For example, a 1% error in each of these quantities may vary the calculated SS-25 gas leak amount by up to 30%.

Therefore, the best estimate for the total gas volume that leaked through the failed SS-25 is 6.6 Bscf with a possible range of 5.9–7.2 Bscf. Lower volumes yield lower rates that are inconsistent with the well model calculations. The gas was approximately 95% methane with no liquids and for this PROSPER is quite accurate—PROSPER has been vetted by the oil industry and used reliably for decades.

## 3.6 Conclusions

Blade studies of the October 23, 2015–February 11, 2016, post-leak period concluded the following:

- The SS-25 well went back on injection between 3 AM and 4 AM on October 23, 2015. The SS-25 axial rupture likely occurred after injection had started. The subsequent circumferential parting occurred between 7 and 8 AM the same day.
- At the time of failure, SS-25 was injecting gas into the reservoir.
- Upon failure, the initial leak rate was 160 MMscf/D. 90 MMscf/D from this rate originated from the gas storage reservoir, and the remaining 70 MMscf/D originated from the injection network.
- The injection network was capable of supplying this additional gas rate to SS-25. The pressure changes as the injection network readjusted to supply this additional gas rate to SS-25 were too small to be detected in real time with the surveillance system in operation at the time. To detect the failure in real time, a surveillance system would have had to be monitoring wellhead injection pressures between the chokes and wellheads.
- The low temperatures, which caused the brittle circumferential parting, originated from the gas being siphoned from the injection network. The gas leaking from the reservoir was not sufficiently cold to cause the temperatures needed for brittle failure. Therefore, the brittle failure occurred during the period of injection.
- When the SS-25 injection was shut in at 3:30 PM on October 23, the leak rate decreased from 160 MMscf/D to 93 MMscf/D.
- After exiting the 7 in. casing at 892 ft, the gas initially flowed through holes in the 11 3/4 in. casing at 134–300 ft. Most of this gas would have flowed to the surface through the heavily weathered and vertically fractured top 200–300 ft of formation; however, some would have flowed horizontally through permeable or fractured layers away from the SS-25 well site, and some would have remained in the subsurface.
- Seven kill attempts were undertaken between October 24, 2015, and December 22, 2015. All failed.

- Kill attempt #1 on October 24 failed due to plugging of tubing and 7 in. casing because of flash formation of ice resulting from low temperatures and the use of a kill fluid with a too high crystallization temperature. However, the kill fluid was not dense enough to kill the well in any case. The formation of ice, and possibly hydrates, also blocked the shallow leak paths. The leaking gas most likely fractured the 11 3/4 in. casing shoe at 990 ft and leaked to deeper formations.
- Deicing of the tubing on November 6 likely unblocked the original shallower leak paths.
- Kill attempt #2 caused the SS-25 well to "blow out in the conventional sense" by opening a blowout vent and shooting debris into the air [6].
- Kill attempts #2–6 failed because the kill fluids used were not dense enough to kill the well. There were no data that indicated transient modeling was conducted to design these kill attempts. Some calculations may have been done; however, gas flow rates were not incorporated into any kill design. Each kill attempt caused additional damage to the wellhead and well site.
- Data show that kill attempt #7 was modeled and the pressures went to zero briefly during the kill attempt. The kill attempt was terminated early because of wellhead movement, failed pump lines, and concern about cumulative damage to the well structure and site.
- The SS-25 leak was stopped on February 11, 2016, with the P-39A relief well.
- The total volume of gas that leaked from the reservoir between October 23, 2015, and February 11, 2016, is estimated at 5.9–7.2 Bscf, with a best estimate of 6.6 Bscf. Some of this gas might have remained in the subsurface but most escaped into the atmosphere.

# 4 Aliso Canyon Casing Integrity

The intent of this section is to discuss casing integrity issues on a field wide basis. Many casing leaks occurred in Aliso Canyon; similarities between these leaks and SS-25's leak and the approach to well integrity were examined. In 1988, SoCalGas made a concerted effort to conduct casing inspection. These results are discussed. Casing inspection logging runs were performed on other Aliso Canyon wells before and after the SS-25 incident; the results of these logs were analyzed to ascertain the extent of the shallow production casing corrosion at Aliso Canyon. Finally, the gas storage well integrity regulations were also analyzed.

## 4.1 Aliso Canyon Historical Summary

The Aliso Canyon oil field was discovered in 1938 by J. Paul Getty's Tidewater Associated Oil Company. The major lease names are Fernando Fee, Mission Adrian, Porter, Standard Sesnon, Sesnon Fee, and Frew. Peak oil production was in 1955. The original owners of the Aliso Canyon wells were Getty Oil Company, Standard Oil Company of California, and other individual interests—collectively called *Sesnons*.

A need for additional gas supply was identified by SoCalGas's affiliates Pacific Lighting Service Company and Pacific Lighting Exploration (collectively Pacific[iii]) and was explained to the California Public Utilities Commission (CPUC) in the application for a Certificate of Public Convenience and Necessity on January 17, 1972: due to the insufficient existing gas sources, a supply deficiency was expected for the 1973–1974 and 1974–1975 winter seasons, and the gas storage wells in the Sesnon and Frew zones in the Aliso Canyon Field would enable SoCalGas to supply natural gas during peak demand conditions.

The field started being converted from oil and gas production to gas storage in 1973.

Well SS-25 leaked gas to surface from October 23, 2015, to February 11, 2016, when the leak was stopped by a relief well P-39A. Blade started the RCA in January 2016.

On January 31, 2016, Blade requested SoCalGas to provide a list of all Aliso Canyon wells. On February 11, 2016, Blade requested additional data, such as drilling date, total depth, well status, and well construction. The information was provided to Blade on March 15, 2016 [50]. Figure 128 shows the following data as of January 1, 2015, related to operators and wells:

- The top pie chart shows the breakdown of operators. SoCalGas operated 194 wells of the 243 wells in Aliso Canyon.
- The middle pie chart shows the operators of the 187 non-plugged wells at Aliso Canyon: SoCalGas, Termo, and Crimson Resource Management Group.
- The bottom pie chart shows the breakdown of the statuses of 134 gas storage wells: 94 active, 17 idle, 16 plugged, 6 new, and 1 canceled. There were 117 non-plugged gas storage wells initially, but a few of them were in the process of abandonment or re-abandonment. The remaining 114 non-plugged gas storage wells became the basis of the DOGGR Comprehensive Safety Review, which is discussed later.

[iii] Pacific purchased, transmitted, and stored natural gas for sale exclusively to SoCalGas. Pacific and SoCalGas merged in 1985.

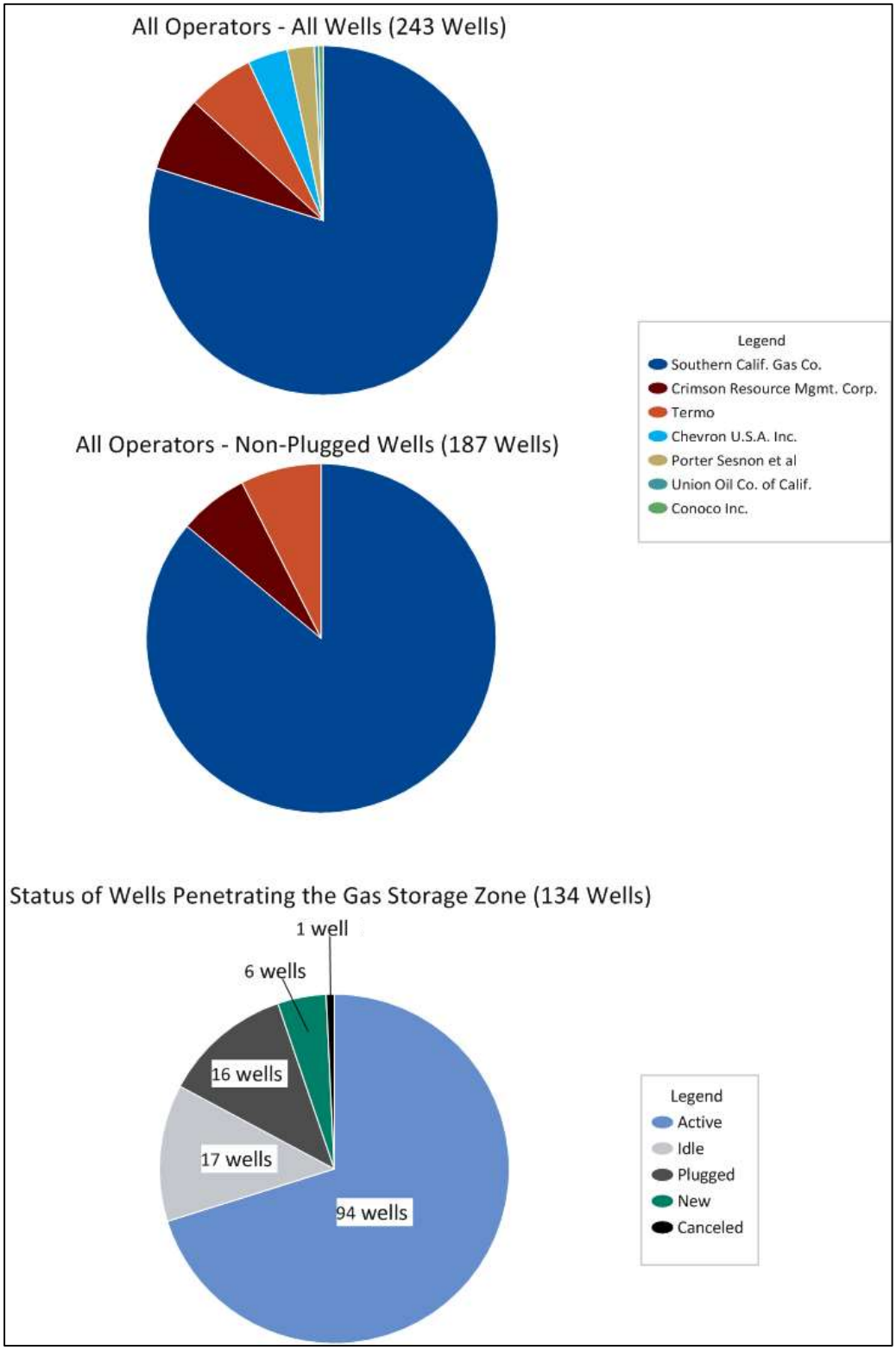


**Figure 128: Aliso Canyon Operators and Wells [50]**

## 4.2 Historical Casing Failures

Blade analyzed 124 Aliso Canyon wells from a list downloaded from the DOGGR website on May 9, 2018, designated by DOGGR as gas storage or gas storage/oil and gas. The history of the wells in this list is assumed to be representative of the mechanical condition of the gas storage wells in the Aliso Canyon Field. Failed production casings[iv] and/or liners[v], the main focus of this analysis, are conditions or defects, such as casing and connection leaks, parted casing, and tight spots, where the casing fails to perform in the manner it was designed for.

A well that had a casing failure as part of its history is considered a failed well. A well can have one or multiple casing failures in the same casing or in more than one casing or liner in the same well. The number of failed wells, casing failures, and types of failures are discussed here. Additional details of the casing failure analysis can be found in the report *Analysis of Aliso Canyon Gas Storage Wells with Casing Failures* [47]. The full report lists the wells reviewed and details of each casing failure by well.

### 4.2.1 Aliso Canyon Casing Failure Overview

Table 28 shows the number of wells and production casing sizes for the 124 Aliso Canyon gas storage wells.

**Table 28: Breakdown of the Production Casing Size for the Gas storage Wells Reviewed**

| Casing OD | 9.625 in. | 8.625 in. | 7 in. | 6.625 in. | Total |
|---|---|---|---|---|---|
| Well Count of Wells Reviewed | 26 | 35 | 61 | 2 | 124 |

Table 29 shows the overall numbers of wells reviewed, number of well failures, and the number of casing failures for the Aliso Canyon gas storage wells. Forty-nine of the 124 gas storage wells (40%) had at least one casing failure—99 failures in the 49 wells with an average of 2 failures per well.

**Table 29: Count of Wells with Casing Failures**

| No. Wells Reviewed | No. Wells with Casing Failures | No. Casing Failures |
|---|---|---|
| 124 | 49 | 99 |

Casing leaks and tight spots make up the majority of the casing failures (Table 30). While tight spots can lead to casing leaks, the greater concern is the number of casing leaks and parted casing that cause loss of casing integrity. Casing leaks and parted casing make up 68% of the casing failures.

[iv] Production casing is the term used to define the casing outside of the production tubing.
[v] A liner is a casing that is set below a previously set casing where the top of the liner is below the wellhead.

**Table 30: Breakdown of the Types of Casing Failures**

| Well Type | No. Wells with Failed Casing | Failure Type and Count | | | | |
|---|---|---|---|---|---|---|
| | | No. Casing Leaks | No. Tight Spots | No. Parted Casing | Other[a] | Total Failures |
| Well and Failure Count | 49 | 63 | 29 | 4 | 3 | 99 |

[a] Other types of failures include split casing in wellhead, earthquake damage, and deformed casing.

Figure 129 shows a breakdown of the number of wells reviewed, wells with casing problems, and casing failures by spud date (the start date of the well drilling process) at ten-year intervals. As the plot shows, most of the drilling activity happened in two groups: from 1939 to 1959, when the field was developed for oil and gas production, and from 1970 to 1979, when many of the gas storage wells were drilled.

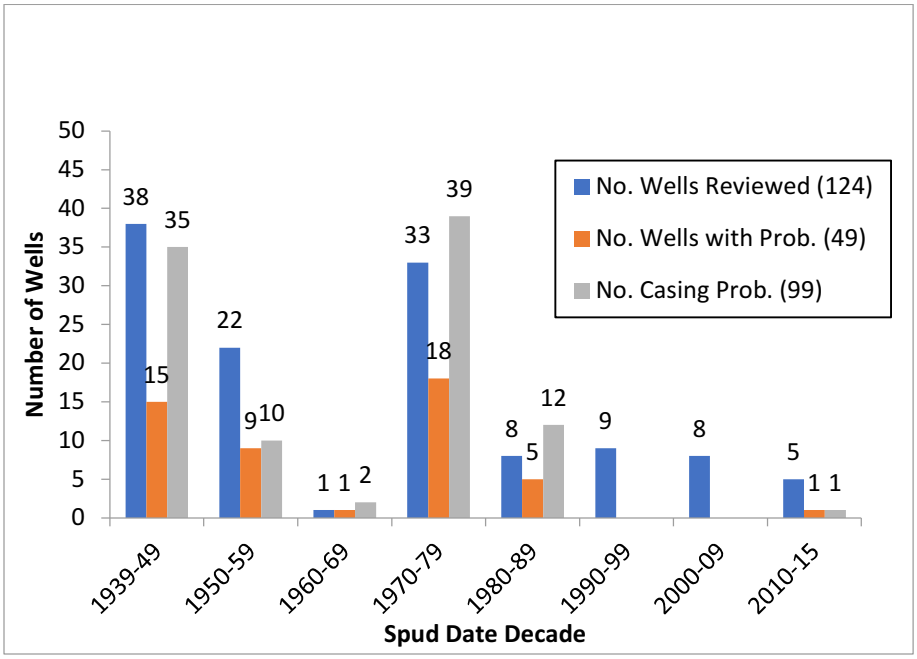


**Figure 129: Number of Wells Reviewed, Wells with Failures, and Casing Failures**

Table 31 shows the number and types of casing failures for the 99 failures by spud date decade. As the data show, many failures occurred in the oil and gas wells drilled in the 1930s and 1940s—which were converted to gas storage wells—and gas storage wells drilled in the 1970s after the field had been converted to gas storage. One tight spot was reported in the 22 wells drilled from 1990 to 2015.

The following list summarizes the data within the table:

- 48% of casing leaks occurred in the wells drilled between 1939 and 1969.
- 52% of casing leaks occurred in the wells drilled between 1970 and 2015.
- 47% of all failures occurred in the wells drilled between 1939 and 1969.
- 53% of all failures occurred in the wells drilled between the 1970 and 2015.

- 13 of the 99 failures were reported between surface and 1,000 ft (8 casing leaks, 2 parted casings, 2 tight spots, and 1 other).

The data show no correlation between well age and casing failures.

**Table 31: Number and Types of Casing Failures by Spud Date**

| Spud Date Decade | No. Casing Leaks | No. Tight Spots | No. Parted Casing | Other |
|---|---|---|---|---|
| 1939–1949 | 22 | 11 | 1 | 1 |
| 1950–1959 | 7 | 1 | 1 | 1 |
| 1960–1969 | 1 | 1 | - | - |
| 1970–1979 | 28 | 10 | 1 | - |
| 1980–1989 | 5 | 5 | 1 | 1 |
| 1990–1999 | - | - | - | - |
| 2000–2009 | - | - | - | - |
| 2010–2015 | - | 1 | - | - |

Figure 130 shows that casing leaks represent the majority of the casing failures.

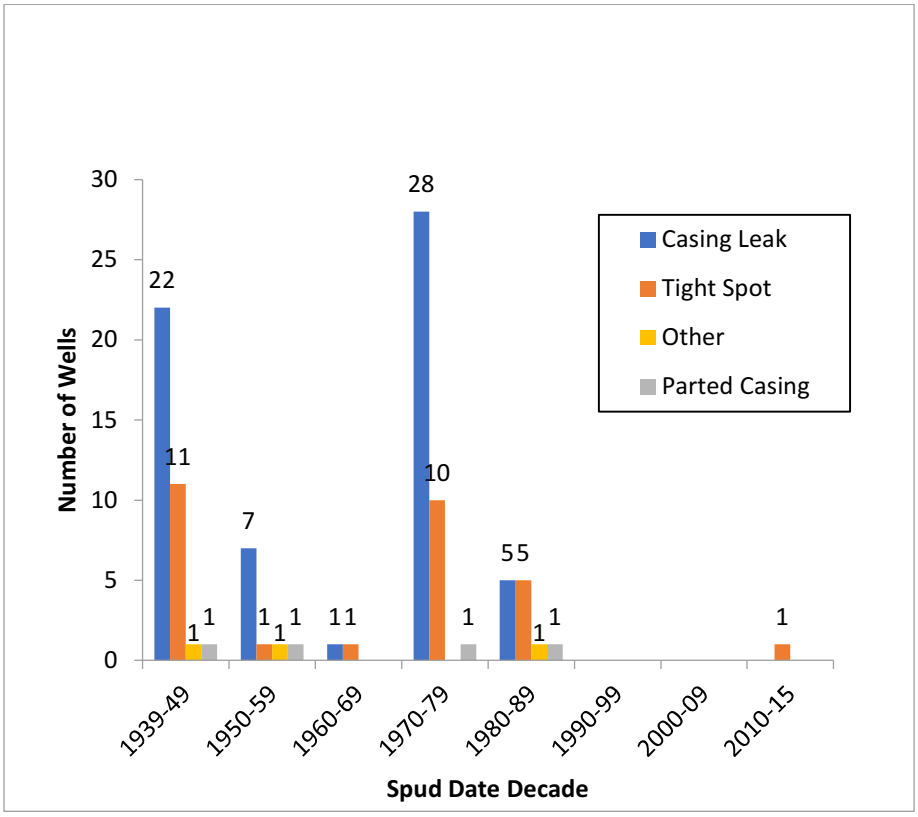


**Figure 130: Number and Types of Casing Failures by Spud Date**

In many cases, we were unable to discern if the failure occurred in the pipe body or in a connection, based on a review of the well records, because no determination or reporting had been made by SoCalGas.

Thirty-seven percent (37 of 99) of the failures occurred in the 7 in. casing and 34% (34 of 99) in the 8 5/8 in. casing (Table 32). These two production casing sizes are the most prevalent ones in the Aliso Canyon field. Photographs and data regarding these failures were not available. The approach was to mitigate the leak and get the well operational. The causes of these leaks or failures were neither understood nor investigated.

**Table 32: Breakdown of Gas storage Wells Casing and Liner Failures by Size**

| Casing OD | 9.625 in. | 8.625 in. | 7 in. | 6.625 in. | 5.5 in. | 5 in. | Total Failures |
|---|---|---|---|---|---|---|---|
| No. of casing Failures by OD | 7 | 34 | 37 | 7 | 3 | 11 | 99 |

### 4.2.2 Parted Casing Analysis

Parted casings were reported in four wells, from 1969 to 1994 (Table 33 including paraphrased comments). The daily reports and log data show that the casings parted in one of the connections in three of the four wells. No records were found regarding whether the parted casing in P-45 was in the connection or pipe body. The reported connection type for P-45 was T&C (threaded and coupled).

The parted 7 in. casing was recovered from SS-12 in 1977. A Speedtite pin was found damaged—it had jumped out of a damaged box. Two more Speedtite connections parted while being pressure tested and after the casing was tied back. The SS-12's 7 in. casing with Speedtite connections was pulled and replaced during the workover in 1977.

The typical repair for shallow parted casings was to pull the upper parted casing and cut and recover a section of the lower casing. The casing was then tied back to the surface with new casing by using a bowl-type casing patch to connect it to the top of the existing casing.

No records of failure analyses were found for any of the parted casings from the four wells. The only documents found were the well operations daily report where on-site rig activities were reported. No evidence of RCA, failure samples collected, lab analysis, photos of failures, or failure analyses reports were found in the wells' files. Consequently, there was no insight into why these failures were happening. Failed casings were recovered from three wells, and samples of the failed casings could and should have been collected and taken for analysis right after they were recovered.

**Table 33: Details of the Parted Casing Failures**

| Well | Casing OD (in.) | Connection Type | Parted Casing Depth (ft) | Repair Year | Comments |
|---|---|---|---|---|---|
| P-45 | 7 | T&C | 177 | 1969 | Recovered parted casing. |
| SS-12 | 7 | Speedtite | 553 | 1977 | Recovered casing with a jumped connection. Connections parted 2 more times during the workover. Pulled all casing with Speedtite connections. |
| P-42B | 8.625 | BTC | 7,488 | 1992 | Connection parted. USIT log indication of a gap in the casing. |
| SS-4-0 | 7 | LTC | 1,445 | 1994 | Earthquake related. Caliper log indication of a gap in the casing. Recovered parted casing. |

### 4.2.3 Casing Leak Analysis by Depth

Figure 131 shows the number of casing leaks by depth range. Our analysis shows that:

- 8 of 61 (13%) casing leaks occurred above 1,000 ft, including the one in SS-25.
- 52% of the leaks were between the surface and 4,000 ft with no trend of leak count vs. depth.
- Leaks in the lower part of the well were more numerous from 7,000 ft to 8,000 ft.
- 63 casing leaks occurred in 41 wells for an average of 1.5 leaks per well.

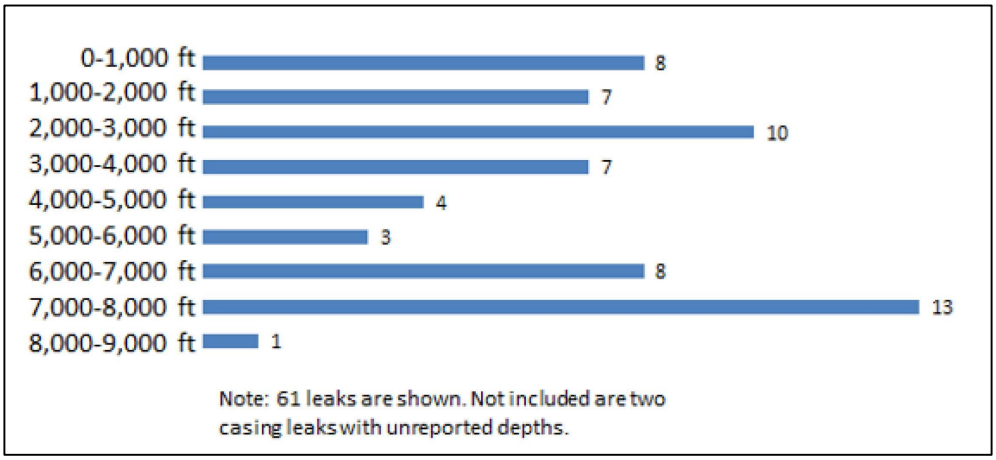


**Figure 131: Casing Leak Count by Depth Range**

### 4.2.4 SoCalGas Casing Leak Evaluation

During a data clarifications meeting on August 24, 2018, Blade learned of a CPUC request to SoCalGas to summarize all the casing leaks associated with gas storage wells at Aliso Canyon. SoCalGas provided a summary table [51] to Blade on September 17, 2018 (Figure 132 and Figure 133).

Figure 132 shows the data from SoCalGas table graphically by leak discovery date on the x-axis and well depth on the y-axis. There are two legends: one for the leak type and a second one for the leak cause. A few trends are visible. What is apparent is that leaks of any type were most prevalent before the mid-1990s. For the casing shoe leak type, all but one leak occurred before 1992, denoted by a green brace. Although not of high importance to the RCA, numerous leaks in stage collars and casing patches (intended to cover the stage collars) are present. Most relevant to the RCA are the casing leaks denoted by red circles. Denoted within each circle are SoCalGas's determinations of the leak cause. The ? symbol denotes unknown causes. About half of the casing leaks are shallower than 2,000 ft and denoted by yellow braces. Most of the shallow casing leaks have unknown causes. There does seem to be a reduction in the number of leaks identified from around 1998 to 2008—denoted by a blue brace. We are not entirely sure why this was the case. There were no changes in the SoCalGas Monitoring Program (Appendix A.1).

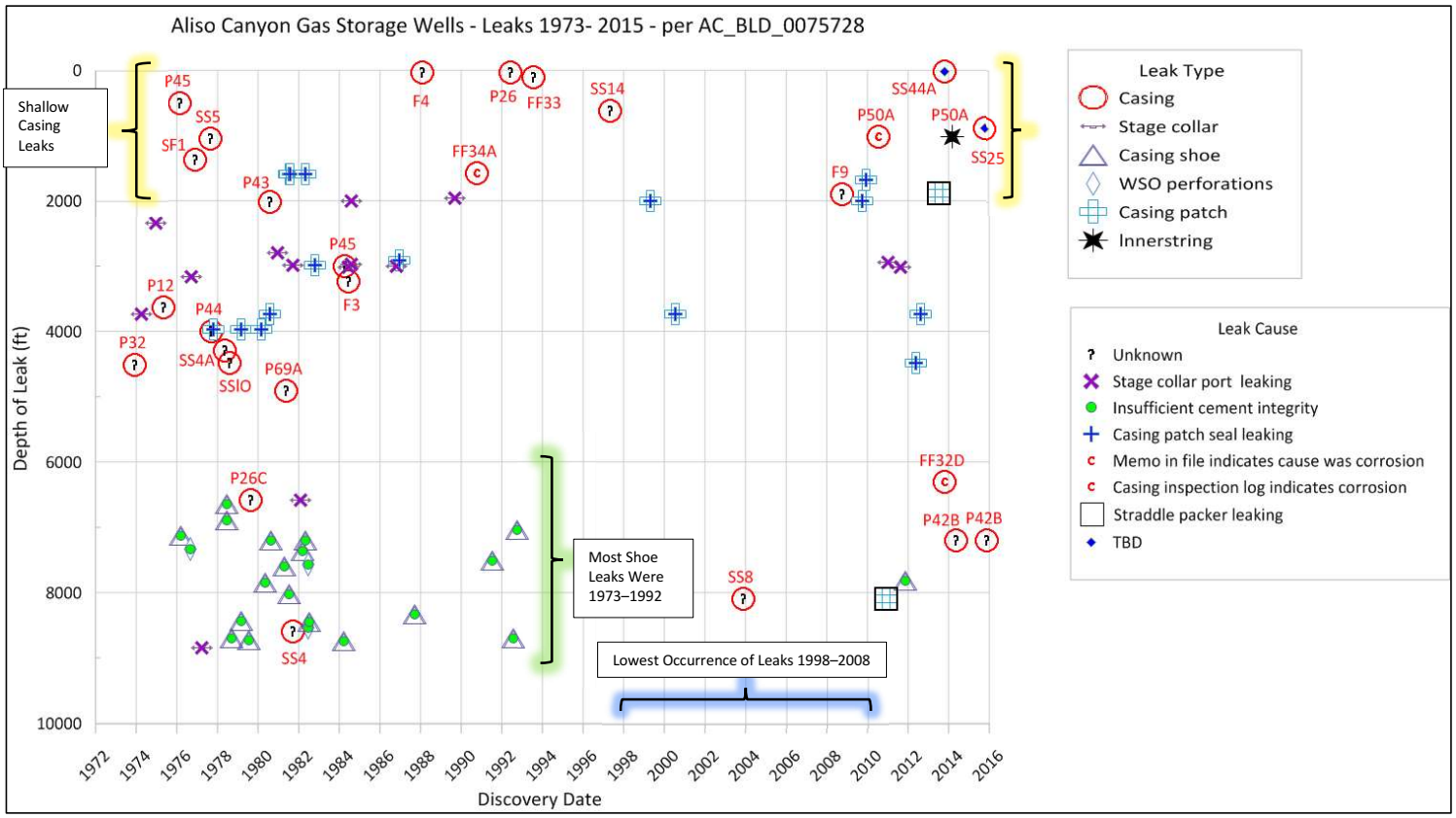


**Figure 132: Leaks per SoCalGas Data [51]**

Figure 133 shows two pie charts: The left one shows the casing leak type and the right one shows the casing leak causes. Of the 81 leaks, 27 are casing leaks. The rest of the leak types are stage collar, casing shoe, water shut off (WSO) perforations, casing patch, and inner string, but these are not of interest to the RCA. The stage collar and casing patch leaks are related because casing patches were run to isolate leaks in the stage collars. Of the 27 casing leaks, 22 are of unknown reasons. Three casing leaks are stated to relate to corrosion, and two casing leaks are to be determined (TBD).

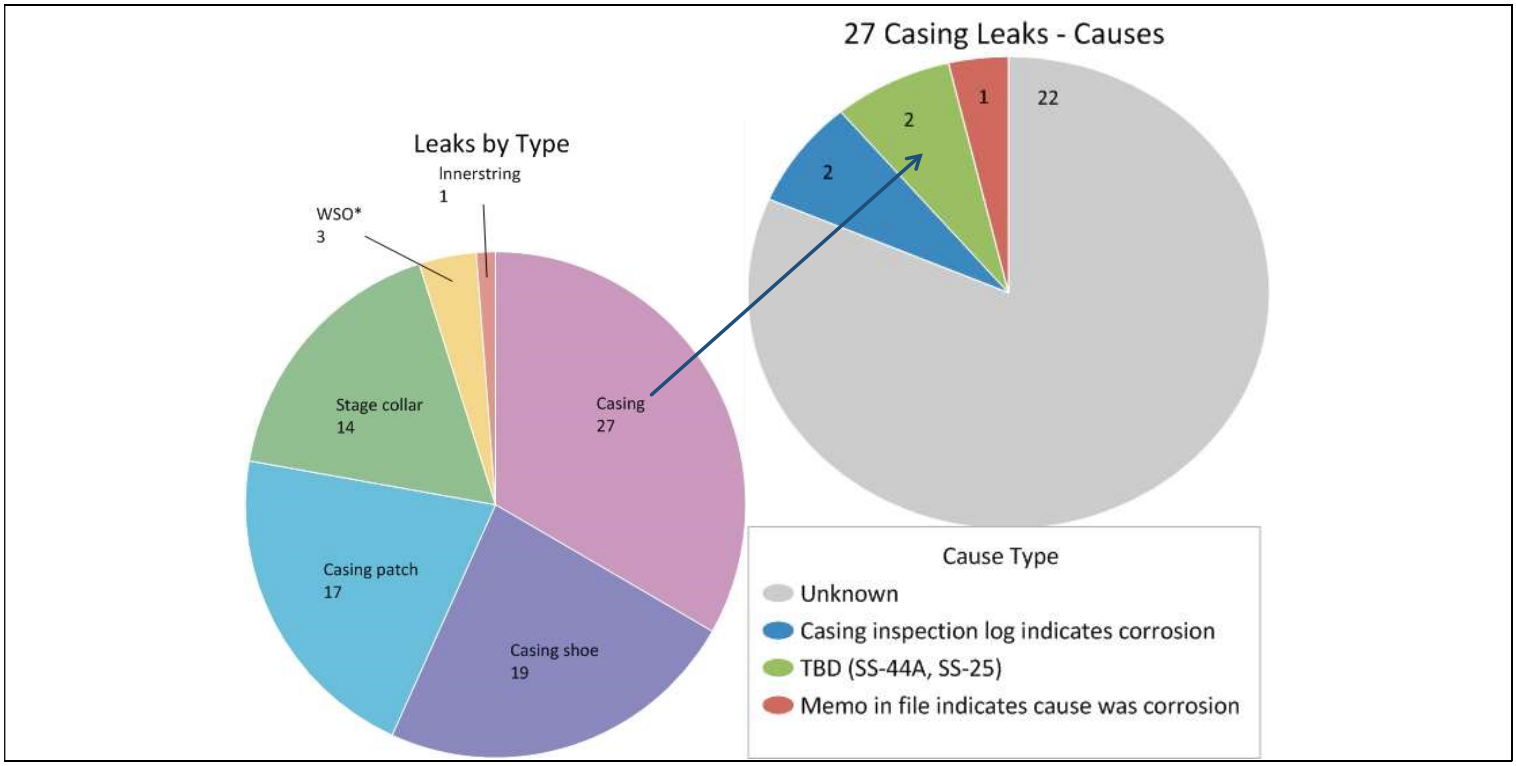


**Figure 133: Leaks by Type per SoCalGas [51]**

The SoCalGas leak data were compared to the Blade analysis of casing failures. The SoCalGas data dates ranged from December 1973 to November 2015, and it is assumed that they are based on the wells that were in service during that time period. Blade analyzed a specific set of 124 Aliso Canyon gas storage wells. It is reasonable to assume that the set of wells analyzed by SoCalGas is different from the set of wells analyzed by Blade. SoCalGas included casing shoe and WSO perforation leaks in their data. Blade excluded these types of leaks because they are not relevant to the RCA. SoCalGas counted leaks multiple times, for example, multiple instances of a casing patch leak in the same well. Blade identified casing leaks and failures and did not double-count failures when they were identified multiple times during the various well operations. A comparison of wells with leaks by both parties showed that some leaks in the SoCalGas list were not identified by Blade, and some leaks in the Blade list were not identified by SoCalGas.

Blade normalized the SoCalGas data to estimate the actual number of wells with leaks and the actual number of leaks. While the SoCalGas and Blade evaluations of casing leaks and failures were done differently, the results are consistent and meaningful and show a significant number of casing leaks. SoCalGas identified 42 casing leaks in 39 wells with failed casing. Blade identified 63 casing leaks in 41 wells.

### 4.2.5 Use of Reduced OD Connections and API Connections in Aliso Canyon

API (American Petroleum Institute) connections include BTC (Buttress Thread Casing), LTC (Long Thread Casing), and STC. These connections are manufactured in such a way that there is a gap between the thread root and crest. The gap is plugged with thread compound to provide a seal when the connection is made up. The gaps are sealed as long as the thread compound is trapped in the gap. Exposure to gas or elevated temperature will dry out the thread compound, which will result in a leak path through the gap in the threads. API connections provide adequate leak resistance for exposure to drilling fluid during the drilling phase of the well. Production casing and production tubing for gas wells where pressure integrity is required usually have metal-to-metal or gas-tight connections for long-term leak resistance.

Standards for connection testing were developed in the mid-1980s because of failures in reduced OD and flush joint connections. Testing found that sealability failures in connections occurred at much lower loads than the ones predicted. This included tension loads and internal pressure loads.

Most of the reduced OD connections that failed in SoCalGas wells were run before 1980 and were manufactured before testing standards were in place; therefore, the connection design and manufacturing quality are uncertain. Reduced OD connections are, by definition, of lower strength, regardless of the quality. Before the 1980s, some manufacturers claimed to have connections with multiple seals. One of the problems with multiple seals is that excess thread compound can be trapped between the seals during makeup. This can lead to excess pressure buildup of the thread compound, and the connection and seal areas are prone to yielding during makeup, resulting in connection leaks caused by the connection makeup.

The assertion that API connections leak gas is supported by SoCalGas data and documentation. Interoffice correspondence dated January 9, 1984 [52], discusses a tracer survey showing connection leaks in 9 5/8 in. 43.5 ppf N80 buttress thread casing (BTC) less than a year after well Porter 50A (P-50A) was drilled. Leaks correlated with the casing tally connection depths were noted at 727 ft, 770 ft, 814 ft, 856 ft, and 898 ft. A leak rate of about 2 Mcf/D was noted in another document [53] for P-50A.

A workover daily report for Frew 4 (F-4) [54] dated September 8, 1988, reported a leak in a 7 in. collar at 32 ft when the casing was tested with nitrogen gas at 875 psi. A noise log detected the leak. The reported casing connection was an 8-round thread, which is an API connection. Because this leak was not confirmed with a pressure test, and the noise log was not located for evaluation, it is not counted in the

analysis. However, the reported leak with nitrogen gas suggests that the research showing that API connections are prone to leak gas is valid.

Problems with 7 in. Speedtite connections were discussed in a SoCalGas interoffice correspondence dated November 25, 1977 [55]. A temperature survey run in SS-5 on September 28, 1977, showed several 8°F cooling anomalies at 150 ft, 300 ft, and 1,300 ft with smaller anomalies in between. The cooling suggested that the connections leaked, and the pressure bled off after the bottom-hole safety valve was closed as discussed in the interoffice correspondence. A Speedtite connection parted in SS-12, and, subsequently, two additional connections parted while being pressure tested during the workover in 1977. The cooling anomalies observed indicate that the Speedtite connection leaked when the reported casing pressure was 2,930 psi.

Forty-nine out of the 124 gas storage wells reviewed had some type of casing failure. All but one of the 49 wells that failed had a reduced OD or an API connection in the production casing or liner that failed[vi]. Reduced OD connections on failed casings and liners included 7 in. Speedtite, 6 5/8 in. FJ (flush joint), 6 5/8 in. AB FL4S, 5 1/2 in. FJ, and 5 in. FJ. The connection types were not reported in some well reports. The remaining failed casings and liners had API connections.

Table 34 shows a breakdown of the production casing connection types used in the 124 SoCalGas wells reviewed. Speedtite and BTC connections were used in half of the wells. T&C are assumed to be API connections (BTC, LTC, or STC). Some wells used more than one connection type for a given casing size.

**Table 34: Breakdown of the Production Casing Connection Types in Gas Storage Wells**

| Casing Connection Type | Speedtite | BTC | LTC | T&C | Not Reported | BTC & LTC | LTC & STC | Hydril 563[a] | Hunting SLGS[a] | Total |
|---|---|---|---|---|---|---|---|---|---|---|
| Well Count | 33 | 29 | 20 | 13 | 10 | 8 | 6 | 3 | 2 | 124 |

[a] The five wells drilled from 2010 to 2015 used Hunting SLGS and Tenaris Hydril 563 connections on the 9 5/8 in. casing. These connections have a metal-to-metal seal and are suitable for gas service.

Table 35 shows a breakdown of the production liner connections used in 102 of the 124 reviewed SoCalGas wells. The remaining wells did not have liners. Flush joint connections were used in many of the wells. The connection type was not reported in 32 wells.

**Table 35: Breakdown of the Production Liner Connection Types**

| Liner Connection Type | Flush Joint (FJ) | Not Reported | LTC | STC | Other[a] | Total |
|---|---|---|---|---|---|---|
| Well Count | 39 | 32 | 16 | 6 | 9 | 102 |

[a] Other includes one of each: FJ & STC, Hydril, Hydril 511, Hydril 513, T&C, TCPC, SLHT, Extreme Line (XL), and BTC.

It was not possible to determine whether each of the failures occurred in the connection or pipe body from the records reviewed. Some well records specifically stated that a pipe body or connection failed,

[vi] A Tenaris Hydril Wedge 563 connection was used on the SS-4B 9 5/8 in. casing run in 2015. This connection is considered a gas-tight connection with a metal-to-metal seal.

while other records were incomplete. Table 36 shows the number of failures (in parentheses) for each connection type and casing size for the production casing and liners.

**Table 36: Count of Connection Types for Casing Failures in Production Casing and Liners**

| Casing and Liner OD | 9.625 in. | 8.625 in. | 7 in. | 6.625 in. | 5.5 in. | 5 in. |
|---|---|---|---|---|---|---|
| Connection Types in Failed Casing | LTC (5 failures)<br>BTC (1)<br>Hydril 563 (1) | BTC (32)<br>LTC (1)<br>Not Reported (1) | Speedtite (18)<br>BTC (6)<br>LTC (5)<br>STC (5)<br>T&C (2)<br>Not reported (1) | FJ (5)<br>T&C (1)<br>AB FL4S (1) | LTC (2)<br>Hydril FJ (1) | FJ (11) |

Seven-inch OD casing with a Speedtite connection was commonly run in the 1940s and 1950s wells. The 7 in. casing in SS-25 had a Speedtite connection, which is an integral joint connection with a swaged-upset box on one end and a swaged-upset pin on the other end. Thirteen wells with 7 in. 23 ppf J55 Speedtite casings had a total of 19 casing failures (Table 37).

As mentioned in Parted Casing Analysis (Section 4.2.2), a notable instance of a 7 in. 23 ppf J55 Speedtite parted casing occurred in well SS-12 in 1977. Well records show that the pin of a Speedtite connection was found damaged—it had jumped out of a damaged box. During the course of the workover to repair the casing, two more Speedtite connections parted; they are not included in the failure data because the parting occurred during the workover.

After cutting the casing at 615 ft and recovering the jumped Speedtite connection, an external casing bowl-type patch was run at 615 ft, and the casing was pressure tested to 4,000 psi with 60,000 lbf tension. The casing was landed in the wellhead with 200,000 lbf tension. A Speedtite connection was found to be parted the next day at 889 ft. After replacing the casing at 1,070 ft, another Speedtite connection parted at 1,224 ft during a pressure test to 3,200 psi. The rest of the 7 in. Speedtite casing was replaced with a 7 in. 23 ppf N80 casing as part of the workover. The 7 in. 23 ppf N80 LTC was cut and pulled in June 2018 as part of the P&A operation. Blade visually inspected the casing as it was pulled. No significant metal loss on the casing OD was observed.

**Table 37: Breakdown of the 7 in. 23 ppf J55 Speedtite Casing Failure Types**

| | No. 7 in. 23 ppf Speedtite Wells Failed | Failure Type and Count | | | | |
|---|---|---|---|---|---|---|
| | | No. Casing Leaks | No. Tight Spots | No. Parted Casing | Other | Total No. Failures |
| Well and Failure Count | 13 | 12 | 4 | 1 | 2 | 19 |

### 4.2.6 Casing Failure Map

Figure 134 shows the Aliso Canyon wells with casing failures. The distribution of casing failures appears to be field-wide and not concentrated in a specific area of the Aliso Canyon Field. SS-25 is located in the western part of the field.

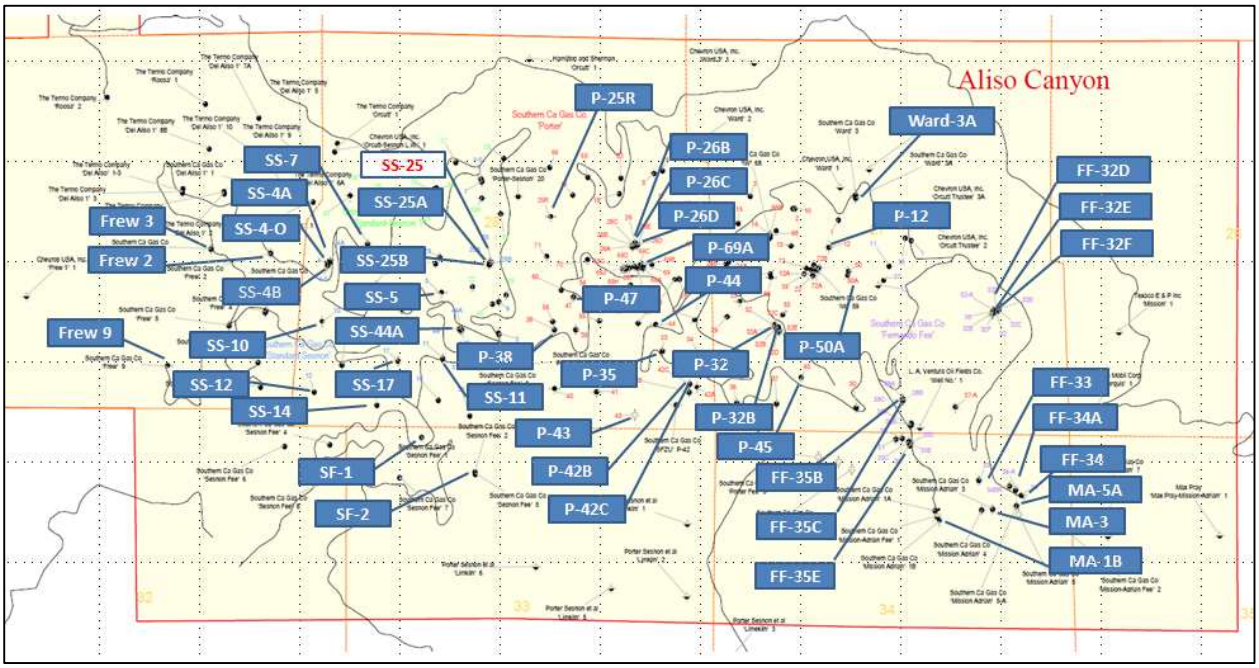


**Figure 134: Map of Aliso Canyon showing Wells with Casing Failures**

### 4.2.7 Casing Failures and Blowouts

The SS-25 blowout in October 2015 is an example of the serious consequences of casing failures. Blade reviewed Aliso Canyon's well records and identified two wells with casing leaks and underground flow: Frew 3 (F-3) in 1984 and FF-34A in 1990. F-3 and FF-34A had leaks at 3,240 ft and 2,093 ft, respectively. SoCalGas killed them within days of discovering the leak by pumping down the tubing. SoCalGas and the well-control company made seven unsuccessful attempts to kill SS-25 by pumping down the tubing and casing. The relief well P-39A was drilled, enabling SS-25 to be successfully killed in February 2016, four months after the leak had started.

The casing leak in SS-25 at 892 ft resulted in a parted 7 in. casing with minimal restriction to flow when compared to the leaks through holes in the pipe body in the other two wells. The shallow parted casing depth, minimum restriction to flow, and high flow rate likely contributed to the difficulty in killing SS-25.

The completion designs for the three wells were similar and consisted of a packer, an annular flow safety system above the packer, and the tubing to the surface. F-3 and FF-34A were completed with Otis annular flow safety systems. The well records showing the internal components of the F-3 safety system were removed prior to the leak. We found no records showing that the internal components of the FF-34A safety system were installed. The Camco annular flow safety system was disabled in SS-25.

Additional details about the F-3 and FF-34A casing leak events can be found in a separate report: *Analysis of Aliso Canyon Gas Storage Wells with Casing Failures* [47].

Additional details on the SS-25 kill attempts can be found in a separate report: *SS-25 Transient Well Kill Analysis* [46].

### 4.2.8 FF-34A Casing Corrosion

A SoCalGas Interoffice correspondence dated August 20, 1991, [1] discussed an 8 5/8 in. casing inspection log showing metal loss and a corrosion protection log run in FF-34A. A recommendation was made to equip FF-34A with cathodic protection (CP). CP was implemented in FF-34A and four other wells according to SoCalGas in response to a February 18, 2018, information request [56]. The documents also states that:

> . . . The possible regional external casing corrosion problem in the southeastern portion of the field will be further studied and a report issued. Additional investigation of well histories and well logs is required before a recommendation can be made as to whether regional CP is necessary. While casing inspection logs show shallow (1000' to 3000' ELM), casing metal loss in FF-35C, MA-1A and MA-5A, there is not enough evidence to substantiate a regional corrosion problem. . . .

In the data provided, Blade was not able to find documentation with results of the proposed study or if the study was done or not.

## 4.3 1988 Candidate Wells for Casing Inspection

SoCalGas made a recommendation in August 1988 to run casing inspection surveys and pressure test the casing in 20 Aliso Canyon wells used as casing flow wells [57] [58]. SS-25 was on the list of wells and was considered a low priority well. Inspection surveys were run in seven of the 20 wells and included all five high priority wells; five of the seven wells showed penetration of up to 60% in. Logs on two of the seven wells have not been located for review. Four of the five wells showed numerous indications of wall loss above the surface casing shoe. Based on the high percentage of wells with significant penetration, the question remains as to why the remaining 13 wells were not inspected in the 2-year period as recommended. The Interoffice correspondence documents and additional details regarding the 20 wells are included in a separate report: *Review of the 1988 Candidate Wells for Casing Inspection* [59].

Figure 135 shows a map of the Aliso Canyon Field with the 20 casing inspection wells flagged.

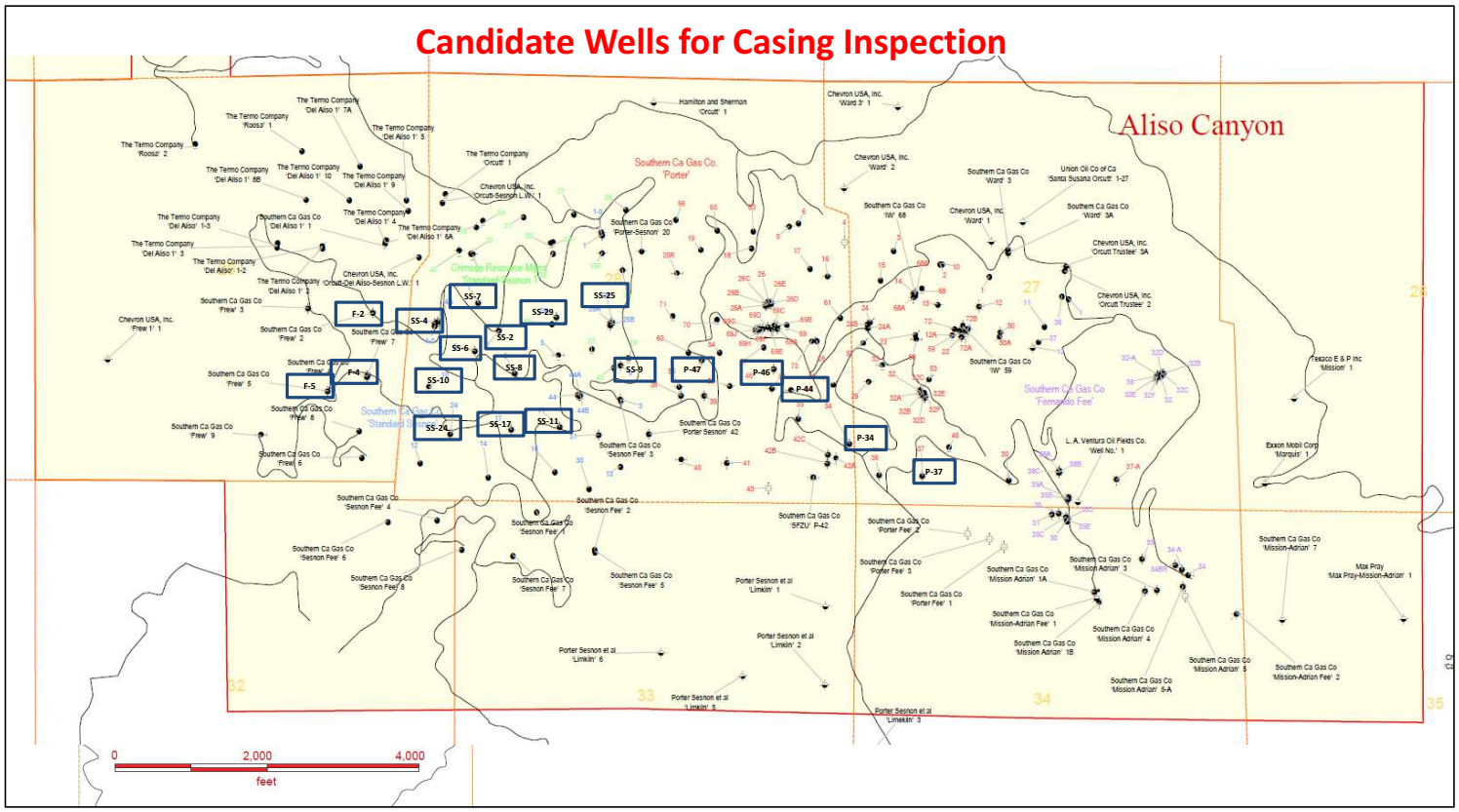


**Figure 135: Aliso Canyon Mapping of the 20 Candidate Wells for Casing Inspection**

Table 38 shows a summary of the list of wells taken from an interoffice correspondence attachment. The priority was based on deliverability, operational history, and the time since the last workover. SS-25 was included in the list as low priority.

Blade reviewed the records of all 20 wells to evaluate subsequent casing inspections and casing problems that occurred in the following years. A number of casing problems were identified. Mitigation for casing problems included running inner casing in some wells in the late 1980s with a packer. Inner casing was run and cemented in some of the 20 wells in 2016–2017 post-SS-25 leak incident. Twelve of the 20 wells are now P&A'd; the remaining eight wells had workovers to mitigate the production casing problems and have passed the required Order 1109 [60] integrity tests.

Blade's interpretation is that SoCalGas's recommendation was for a Vertilog casing inspection to be run to identify damaged intervals and the severity of corrosion. The log analysis and report would have provided a listing of percent wall penetration by casing joint and depth in the well and shown if the defect was internal or external. A casing pipe body can be evaluated by using inspection data to determine if it has the pressure capacity for the expected pressure load. However, Vertilog inspections do not ensure the absence of casing leaks—they inspect the casing body but not the casing connections. (Casing connections interfere with the inspection magnetic field imposed on the casing to identify defects.)

In addition to the recommendation to run a Vertilog casing inspection, a pressure test was also recommended to identify any leaks at the casing collars. A pressure test would confirm the integrity of the casing body and check for small through-wall defects that the Vertilog inspection might have missed.

**Table 38: List of 1988 Casing Flow Wells**

| Lease | Well | Deliverability (MMscf/D) | Priority | Date Logged (within 2 yrs.) | Vertilog Available | Vertilog Summary | Date Logged (Post 2 yrs.) | Log Summary | Notes | Current Status |
|---|---|---|---|---|---|---|---|---|---|---|
| Porter | 34 | 9 | High | Vertilog Nov 2, 1989 | No | N/A | N/A | N/A | Ran 5 1/2 in. inner casing Dec 20, 1989 | P&A 2018 |
| Porter | 37 | 24 | High | Vertilog Oct 11, 1988 | Yes | 4 jts >20% OD Penetration<br>1 jt > 60% OD Penetration | N/A | N/A | Ran 5 1/2 in. inner casing May 12, 1989. Ran and cemented 5 1/2 in. inner casing Nov 14, 2017. | Passed All Tests |
| Porter | 44 | 26 | Low | Not logged within 2 years | N/A | N/A | HRVRT Feb 15, 2016<br><br>USIT Feb 29, 2016 | 1 jt >20% OD Penetration<br>1 jt >80% OD Penetration<br><br>External corrosion on multiple joints and potential casing hole at 4,000 ft | Casing leak between 3,961 ft and 4,010 ft Feb 18, 2016<br>Set casing patch Mar 4, 2016. Set casing patch Mar 5, 2016. | Passed All Tests |
| Porter | 46 | 35 | High | Vertilog Oct 19, 1988 | Yes | 10 jts >20% OD Penetration | USIT Aug 16, 2017 | Indications 3,970–3,984 ft | Ran and cemented 5 1/2 in. inner casing Oct 4, 2017 | Passed All Tests |
| Porter | 47 | 21 | Low | Not logged within 2 years | N/A | N/A | No casing inspection logs found as of Feb 4, 2019 | N/A | Pressure tested 7 in. casing to 1,200 psi for 1 hour, Sep 19, 2016 | P&A 2017 |
| Standard Sesnon | 2 | 16 | Low | Not logged within 2 years | N/A | N/A | No casing inspection logs found as of Feb 4, 2019 | N/A | Pressure tested 7 in. casing to 1,000 psi for 1 hour, Jul 26, 2016 | P&A 2017 |

| Lease | Well | Deliverability (MMscf/D) | Priority | Date Logged (within 2 yrs.) | Vertilog Available | Vertilog Summary | Date Logged (Post 2 yrs.) | Log Summary | Notes | Current Status |
|---|---|---|---|---|---|---|---|---|---|---|
| Standard Sesnon | 4 | 0 | Low | Not logged within 2 years | N/A | N/A | No casing inspection logs found as of Feb 4, 2019 | N/A | N/A | P&A in progress |
| Standard Sesnon | 6 | 10 | Low | Not logged within 2 years | N/A | N/A | USIT Aug 8, 2012 | Questionable log data | Ran and cemented 5 1/2 in. inner casing Jul 17, 2017 | Passed All Tests |
| Standard Sesnon | 7 | 1 | Medium | Not logged within 2 years | N/A | N/A | USIT Nov 1, 2012<br>Noise Jul 6, 2012<br>USIT May 5, 2014 | Indications 1,912–1,927 ft 4,012–4,030 ft<br>Above normal noise activity 3,600–4,200 ft<br>Indications 1,912–1,927 ft 4,010–4,032 ft | N/A | P&A 2014 |
| Standard Sesnon | 8 | 15 | High | Vertilog Jan 17, 1989 | Yes | 28 jts >20% OD Penetration<br>5 jts > 40% OD Penetration | Cast V Apr 28, 2007<br>USIT Apr 24, 2013 | Indications 955–1,080 ft<br>2,276–2,482 ft<br>3,287–3,289 ft<br>8,479–8,482 ft | N/A | Passed All Tests<br>Observation Well |
| Standard Sesnon | 9 | 15 | High | Vertilog Dec 16, 1988 | Yes | 6 jts >20% OD Penetration | N/A | N/A | 5 1/2 in. inner casing 0–8,599 ft<br>(5 1/2 in. USIT log Oct 24, 2018) | Passed All Tests |
| Standard Sesnon | 10 | 25 | Low | Not logged within 2 years | N/A | N/A | USIT Sep 24, 2012 | Indications 2,294–3,246 ft | Ran 7 in. casing patch 4,462–4,524 ft Sep 27, 2012.<br>Ran and cemented 5 1/2 in. inner casing May 17, 2017. | Passed All Tests |

| Lease | Well | Deliverability (MMscf/D) | Priority | Date Logged (within 2 yrs.) | Vertilog Available | Vertilog Summary | Date Logged (Post 2 yrs.) | Log Summary | Notes | Current Status |
|---|---|---|---|---|---|---|---|---|---|---|
| Standard Sesnon | 11 | 9 | Low | Not logged within 2 years | N/A | N/A | No casing inspection logs found as of Feb 4, 2019 | N/A | N/A | P&A in Progress |
| Standard Sesnon | 17 | 7 | Low | Not logged within 2 years | N/A | N/A | No casing inspection logs found as of Feb 4, 2019 | N/A | N/A | P&A 2017 |
| Standard Sesnon | 24 | 11 | Low | Not logged within 2 years | N/A | N/A | HRVRT Feb 11, 2017<br><br>USIT Feb 15, 2017 | 4 jts >20% OD Penetration<br>4 jts >20% ID Penetration<br><br>Daily report USIT comments; External Anomalies 8,406–8,414 ft 2,250–2,920 ft 1,100–1,620 ft<br>8 jts >20% Penetration | N/A | P&A 2017 |

| Lease | Well | Deliverability (MMscf/D) | Priority | Date Logged (within 2 yrs.) | Vertilog Available | Vertilog Summary | Date Logged (Post 2 yrs.) | Log Summary | Notes | Current Status |
|---|---|---|---|---|---|---|---|---|---|---|
| Standard Sesnon | 25 | 38 | Low | Not logged within 2 years | N/A | N/A | HRVRT Dec 2, 2017<br><br>IBC Corrosion Dec 4, 2017 | 4 jts >20% OD Penetration<br>1 Jt > 40% OD Penetration<br><br>Indications of external corrosion 940–980 ft<br>1,525–2,400 ft<br>2,525–2,570 ft | Casing parted at 892 ft Oct 23, 2015.<br><br>The inspection logs were run in the 7 in. casing below 892 ft | P&A 2018 |
| Standard Sesnon | 29 | 22 | Low | Not logged within 2 years | N/A | N/A | USIT Oct 10, 2017<br><br>HRVRT Oct 13, 2017 | 4 jts >20% Penetration<br><br>1 jt >20% OD Penetration<br>3 jts >20% ID Penetration<br>1 jt > 40% ID Penetration | 5 1/2 in. inner casing 0–8,076 ft<br>(5 1/2 in. HRVRT log Dec 26, 2018) | Passed All Tests |

| Lease | Well | Deliverability (MMscf/D) | Priority | Date Logged (within 2 yrs.) | Vertilog Available | Vertilog Summary | Date Logged (Post 2 yrs.) | Log Summary | Notes | Current Status |
|---|---|---|---|---|---|---|---|---|---|---|
| Frew | 2 | 1 | Medium | Vertilog<br>Jan 11, 1990 | No | N/A | USIT Sep 11, 2014<br><br>Vertilog<br>Oct 20, 2014 | Indications<br>600–3,220 ft<br><br>15 jts >20% OD Penetration<br>3 jts >40% OD Penetration<br>5 jts >60% OD Penetration<br>2 jts >80% OD Penetration<br>Possible penetration around 2835 ft | Tight Spot 3,872 ft<br>Tight Spot 8,130 ft<br>Casing leak between 2,949 and 2,969 ft<br>Workover in 2014 | P&A 2017 |
| Frew | 4 | 12 | - | Vertilog<br>Sep 6, 1988 | Yes | 12 jts >20% OD Penetration<br>12 jts > 40% OD Penetration<br>2 jts > 60% OD Penetration | USIT Oct 20, 2016 | Indications<br>764–5,085 ft<br>5,708–5,911 ft<br>6,782–6,788 ft<br>6,908–6,911 ft | N/A | P&A 2018 |
| Frew | 5 | 2 | Medium | Not logged within 2 years | N/A | N/A | Noise Apr 8, 2016 | No casing inspection logs found as of Feb 4, 2019 | Noise detected 1,100-2,200 ft. | P&A 2017 |

Figure 136 summarizes the percent penetration and depths from the Vertilog inspection results for wells P-37, P-46, F-4, and SS-8 production casings above and immediately below the surface casing shoe. The four wells were inspected in 1988 and 1989. The derrick floor elevation (DFE) above sea level is included and shows the significant variation in surface elevations among the wells. All of these wells had OD indications. P-46 had numerous metal loss indications above the shoe; and all of them had indications shallower than 1,000 ft. The behavior in these wells appears similar to SS-25.

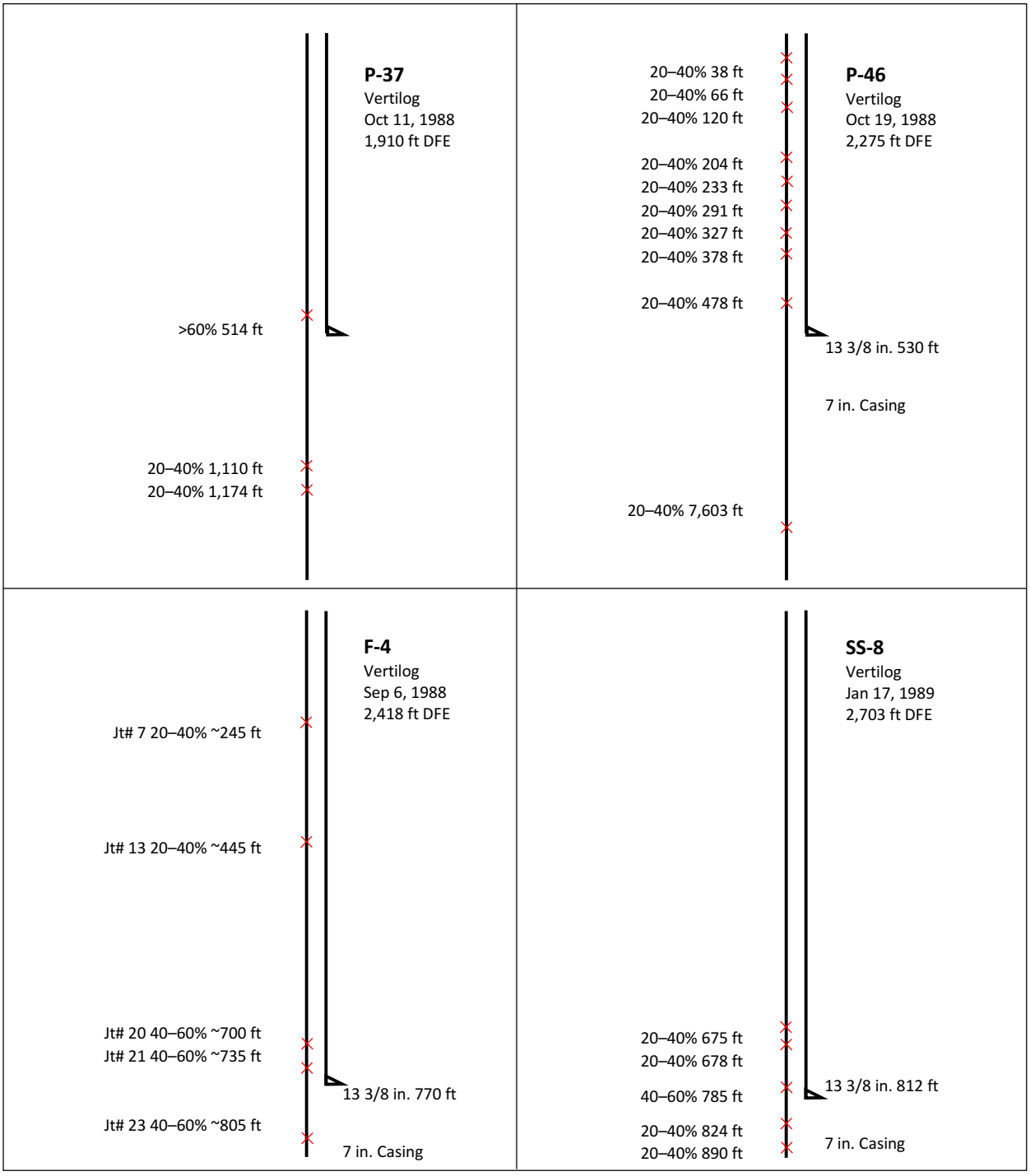


**Figure 136: Wellbore Schematics Showing Vertilog Penetration Data**

## 4.4 Shallow External Corrosion Analysis

Various SoCalGas GRC documents describe their gas storage wells as being affected by aging and deterioration due to the combined effects of corrosion, erosion, and wide variations of pressure and temperature. These documents also discuss the findings of shallow corrosion through the use of casing inspection logs. Blade reviewed recent GRC documents and evaluated casing inspection logs to determine just how prevalent shallow corrosion in the gas storage wells at Aliso Canyon was; the results are presented as follows.

### 4.4.1 General Rate Cases

General rate cases are proceedings in which utility companies submit their operating costs and allocation of these costs for evaluation and approval by the CPUC.

SoCalGas's 2008 GRC: Blade reviewed the 2007 testimony for the 2008 GRC [4]. SoCalGas outlined costs and details related to reservoir engineering studies, additional personnel, technological advances, and well expenses. SoCalGas noted that a 3D geologic model had been created for Aliso Canyon to map the formation tops and provide better field management and continued operational efficiency. Maintenance demands for the aging wells were expected to increase. Additionally, it was cited that the number of gas storage specialists at SoCalGas had reduced, over a 15-year period, from 10 to 4 for unspecified reasons, and the company "experienced a significant decline in its ability to assess the performance of individual wells due to the lack of recent data." Funding for two additional specialists was requested. At the time of the 2007 testimony (2008 GRC), Aliso Canyon was in a period of lowest occurrences of casing leaks (as discussed in the SoCalGas Casing Leak Evaluation in Section 4.2.4).

SoCalGas's 2012 GRC: In 2011 [5] SoCalGas testified that no new replacement wells had been drilled during the 2005–2009 period but that old wells had been upgraded instead. A determination was made to direct new capital spending toward drilling replacement wells and to create a new cost category for replacement wells; funding for two well replacements per year was requested.

SoCalGas's 2016 GRC: It was presented before the CPUC in November 2014 [2]. SoCalGas testified about the required operations and maintenance expenses and capital investments for their underground storage facilities and proposed a new six-year Storage Integrity Management Program (SIMP). The intent was to "proactively identify and mitigate potential storage well safety and/or integrity issues before they result in unsafe conditions for the public or employees." SoCalGas had noted an increasing trend in well integrity repairs, and without the SIMP, operation would have continued in a reactive mode, addressing mainly sudden and major failures and service interruptions. As part of the well repair work from 2008 to 2013, SoCalGas explained that mechanical damage and internal and external corrosion were identified in 15 wells with the use of ultrasonic logs. Also, the external corrosion had been observed at relatively shallow depths in the production casing. SoCalGas cited P-50A, where 400 psi was observed in the casing annulus during routine weekly pressure surveillance in 2008; a footnote provided additional information that a subsequent ultrasonic inspection revealed external production casing corrosion from 450 to 1,050 ft.

Specifically, SoCalGas noted that ". . . two wells were found to have leaks in the production casing at depths adjacent to the shallower oil production sands" and "Ultrasonic surveys conducted in storage wells as part of well repair work from 2008 to 2013 identified internal/external casing corrosion, or mechanical damage in 15 wells." On February 18, 2018, Blade requested the names of the wells in the November 2014 testimony; SoCalGas provided a list with the 17 well names [61]. Six wells in the list were from other

SoCalGas gas storage fields (i.e., not from Aliso Canyon). Including P-50A, there were 12 Aliso Canyon wells.

SoCalGas recognized that production casing leaks related to corrosion could lead to high pressure gas that could migrate to the surface in a matter of hours. Blade's interpretation is that SoCalGas's concern materialized in SS-25 on October 23, 2015. Due to severe external corrosion, the 7 in. production casing ruptured suddenly during gas injection operations; high pressure gas entered the surface casing and was subsequently released to the surface.

The 2007 (2008 GRC) and 2011 (2012 GRC) testimonies presented different views of how to deal with in-service gas storage wells that were 70–80 years old in some cases. In 2007, advanced technologies and additional personnel were discussed, while in 2011, replacement instead of remediation of existing wells was discussed. In both testimonies additional funding was requested. The 2014 testimony (as part of the 2016 General Rate Case) went much further. In 2014 the integrity issues of the gas storage wells were described and funding was requested for a proactive integrity management program—a program that was modeled on their pipeline integrity management programs. No comparable regulations were in place that mandated integrity programs for gas storage wells, and such programs (API RP 1171, September 2015) [62] had not yet become industry recommended practices.

The proposed SIMP program in the 2014 testimony included identifying threats and risk assessments for all wells. The baseline assessments determined the priority of casing inspections and pressure testing. Risk assessments, casing inspection, and pressure testing are now tenets of the 2019 California regulatory requirements for gas storage wells. The risk management approach indicates a shift toward managing the SoCalGas below-ground facilities.

Prior to the incident of October 23, 2015, SoCalGas had recognized that their well integrity program required significant changes, and had developed a plan, timeline, and budget. Considering the age of the wells and the quantity of casing leaks, a well integrity plan was necessary.

### 4.4.2 Casing Inspection Log Analysis

In the public records of 116 Aliso Canyon gas storage wells, Blade found production casing inspection logs for 76 wells. The 116 wells comprised the 114 wells listed under the Comprehensive Safety Review, also known as SIMP, and 2 unique wells from the 2014 Testimony for the 2016 GRC [2]. The objective of the log review was to determine to what degree the shallow external corrosion found at SS-25 was an isolated event. Most of these casing inspection logs were mandated by the March 4, 2016, Order 1109 [60] that was issued by DOGGR to SoCalGas for the Aliso Canyon wells. Amongst other operations, the order stated that SoCalGas shall run a casing inspection log for all wells that were intended for future operations; otherwise the wells shall be plugged and abandoned. Order 1109, within the document itself, is referred to as Comprehensive Safety Review. Status reports for the Aliso Canyon wells were issued by SoCalGas as part of their compliance to Order 1109, and 114 wells were listed. The status report dated February 15, 2019, [63] was used for this work. These casing inspection logs were downloaded from the DOGGR website [64].

Table 39 shows 27 wells that had indications of shallow external corrosion on the production casing out of 76 wells with production casing inspection logs (36%). These 27 wells listed by spud date were the following:

- Frew, two wells
- Standard Sesnon, four wells

- Porter, 14 wells
- Sesnon Fee, one well
- Ward, one well
- Fernando Fee, three wells
- Mission Adrian, two wells

Table 39 shows different columns, and some of them are detailed as follows:

- Column 3 shows the spud dates of the wells ranging from October 19, 1943, to September 20, 1993, a span of nearly 50 years. Figure 137 shows the spud dates of these wells. The two major groups were: first, wells drilled in the 1940s and 1950s by Tidewater, et. al., and second, wells drilled by SoCalGas, about an equal number of wells were from each group; this suggests that the company that drilled the wells was not a factor for shallow corrosion. Although not investigated in detail, the drilling techniques would have been different from 1943 to 1993; this suggests that drilling techniques were not a factor for shallow corrosion either.

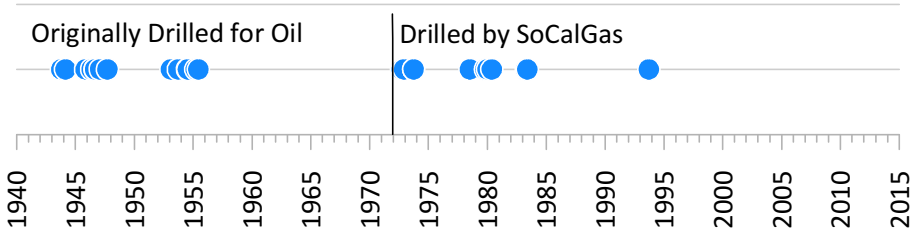


**Figure 137: Range of Spud Dates for Wells with Shallow Corrosion on Production Casing**

- Columns 5 and 6 show the wells that had a casing leak. This information was compiled by using SoCalGas data and Blade analysis, respectively. Aside from SS-25, three unique wells with shallow corrosion were identified on a casing inspection log as having a shallow casing leak: F-4, P-32, and P-50A. Blade reviewed these wells' history. F-4 was identified as having a 7 in. Speedtite connection leak[vii]. P-32 was pressure tested October 27–28, 2016, and at the 654 to 845 ft interval, it was unable to hold pressure; this interval was subsequently cement squeezed and pressure tested. We presumed that the reason for this was the well not being able to hold pressure due to extensive deep external corrosion. P-50A was reported by SoCalGas to have a casing leak at 1,020 ft on July 16, 2010 [51]. This was not the first time SoCalGas reported leaks for this well; P-50A has a complicated history of multiple possible leaks that were determined by noise anomalies, radioactive tracer surveys, shallow gas flow in the surface casing, helium analyses, and anomalous surface casing pressures. The well's reports are from 1983, its completion date. SoCalGas indicated that corrosion was the cause for the casing leak, based on casing inspection logs [51], but no record was found regarding the corrosion mechanism. The gas flowing into the surface casing was analyzed in various years for flow rate and composition. SoCalGas determined that the gas was not storage gas—it was instead from a shallow gas zone; this was determined by low levels of helium [65]. Gas analysis also showed a slightly elevated level of carbon dioxide: around 2 mol% when it was compared to the storage gas. Blade

[vii] Blade did not count F-4 as a leak because the noise log was not located for evaluation and the reported leak with nitrogen was not confirmed with a pressure test.

interpreted that the presence of shallow gas flow containing an elevated level of carbon dioxide and an aqueous environment was the possible cause for the corrosion in P-50A. As with P-32, confirmation of the corrosion mechanism was not possible because the casing was cement squeezed and not recovered.

- Column 7 shows seven wells with shallow external corrosion on the production casing from the wells in the 1988 Candidate Wells for Casing Inspection (Section 4.3) interoffice correspondence. Of the seven wells, three wells had logs from 1988–1990 that showed shallow external corrosion on the production casing; this suggests that shallow corrosion had not been a recent phenomenon.
- Column 8 shows five wells that had shallow external corrosion and were referenced in the 2014 Testimony [2] (as part of the 2016 GRC) or subsequent data request, which included 12 Aliso Canyon gas storage wells. The prevalence of corrosion in these five wells justified the 2014 SIMP plan.
- Columns 9–11 show the production casing details in terms of size, connection, and grade: three casing sizes (7, 8 5/8, and 9 5/8 in.), four connection types (LTC, Speedtite, Buttress, and 8 Round), and three grades (J55, K55, and N80). This variability suggests that the corrosion mechanism was not specific to a single size, connection, or grade.
- Columns 12 and 13 show the depth of the surface casing shoe and the surface elevation of the well. The range of surface casing shoe depths was 501–1660 ft. The average surface casing shoe depth was 812 ft. The average surface elevation was 2,193 ft. SS-25 had the highest elevation: 2,927 ft.

**Table 39: Wells with Shallow External Corrosion Indications on the Production Casing**

| Column 1 | 2 | 3 | 4 | 5 | 6 | 7 | 8 | 9 | 10 | 11 | 12 | 13 |
|---|---|---|---|---|---|---|---|---|---|---|---|---|
| Lease Name | Well # | Spud Date | Years from Spud | Shallow Leak Well [a] | Shallow Leak Well [b] | 1988 Memo Well[c] | 2016 GRC Well[d] | Prod. Casing Size (in.) | Prod. Casing Conn. | Prod. Casing Grade | Surface Casing Depth (ft) | Surface Elevation (ft) |
| Frew | 2 | October 19, 1943 | 76 | No | No | Yes | No | 7 | LTC | N80 | 501 | 2,796 |
| Porter | 46 | February 27, 1944 | 75 | No | No | No | No | 7 | Speedtite | J55 | 533 | 2,255 |
| Porter | 35 | November 8, 1945 | 74 | No | No | No | No | 7 | Speedtite | J55 | 505 | 2,094 |
| Standard Sesnon | 8 | May 14, 1946 | 73 | No | No | Yes | Yes | 7 | Speedtite | J55 | 812 | 2,697 |
| Porter | 37 | August 26, 1946 | 73 | No | No | Yes | Yes | 7 | Speedtite | J55 | 520 | 1,900 |
| Porter | 36 | September 4, 1946 | 73 | No | No | No | No | 7 | Speedtite | J55 | 517 | 1,924 |
| Standard Sesnon | 9 | February 4, 1947 | 72 | No | No | Yes | No | 7 | Speedtite | J55 | 598 | 2,836 |
| Frew | 4 | September 20, 1947 | 72 | Yes | No | Yes | No | 7 | 8 Round | N80 | 770 | 2,420 |
| Standard Sesnon | 24 | February 7, 1953 | 66 | No | No | Yes | No | 7 | LTC | N80 | 1,134 | 2,539 |
| Standard Sesnon | 25 | October 1, 1953 | 66 | Yes | Yes | Yes | No | 7 | Speedtite | J55 | 990 | 2,927 |
| Ward | 3 | July 7, 1954 | 65 | No | No | No | No | 7 | 8 Round | J55 | 1,660 | 2,226 |
| Sesnon Fee | 5 | July 19, 1954 | 65 | No | No | No | No | 7 | LTC | N80 | 837 | 2,439 |
| Porter | 32 | March 21, 1955 | 64 | No | Yes | No | No | 7 | Speedtite | J55 | 522 | 2,079 |
| Mission Adrian | 3 | June 15, 1955 | 64 | No | No | No | No | 7 | 8 Round | N80 | 549 | 2,053 |
| Porter | 32B | September 12, 1972 | 47 | No | No | No | No | 8 5/8 | Buttress | K55 | 694 | 1,995 |
| Fernando Fee | 32F | September 23, 1972 | 47 | No | No | No | Yes | 8 5/8 | Buttress | K55 | 799 | 1,995 |
| Porter | 32F | September 23, 1972 | 47 | No | No | No | No | 8 5/8 | Buttress | K55 | 799 | 1,995 |
| Fernando Fee | 32E | December 6, 1972 | 47 | No | No | No | Yes | 8 5/8 | Buttress | K55 | 717 | 1,995 |
| Porter | 32E | September 25, 1973 | 46 | No | No | No | No | 8 5/8 | Buttress | K55 | 791 | 2,075 |
| Porter | 32D | September 26, 1973 | 46 | No | No | No | No | 8 5/8 | Buttress | K55 | 806 | 2,075 |
| Fernando Fee | 32A | July 6, 1978 | 41 | No | No | No | No | 8 5/8 | LTC | K55 | 990 | 1,995 |
| Mission Adrian | 1A | October 28, 1979 | 40 | No | No | No | No | 8 5/8 | Buttress | N80 | 1,000 | 1,725 |

| Column 1 | 2 | 3 | 4 | 5 | 6 | 7 | 8 | 9 | 10 | 11 | 12 | 13 |
|---|---|---|---|---|---|---|---|---|---|---|---|---|
| Lease Name | Well # | Spud Date | Years from Spud | Shallow Leak Well [a] | Shallow Leak Well [b] | 1988 Memo Well[c] | 2016 GRC Well[d] | Prod. Casing Size (in.) | Prod. Casing Conn. | Prod. Casing Grade | Surface Casing Depth (ft) | Surface Elevation (ft) |
| Porter | 69A | January 3, 1980 | 39 | No | No | No | No | 9 5/8 | Buttress | N80 | 1,002 | 2,365 |
| Porter | 37A | May 17, 1980 | 39 | No | No | No | No | 8 5/8 | Buttress | N80 | 1,024 | 1,898 |
| Porter | 50A | April 15, 1983 | 36 | Yes | Yes | No | Yes | 9 5/8 | Buttress | N80 | 1,025 | 1,936 |
| Porter | 68A | May 23, 1983 | 36 | No | No | No | No | 9 5/8 | Buttress | N80 | 1,015 | 2,080 |
| Porter | 72A | September 20, 1993 | 26 | No | No | No | No | 9 5/8 | LTC | N80 | 814 | 1,909 |
| **Total Wells** | | | **Average** | **Total** | **Total** | **Total** | **Total** | | | | **Average** | **Average** |
| 27 | | | 56.1 | 3 | 3 | 7 | 5 | | | | 812.0 | 2,193.4 |

a – shallow casing leaks identified by SoCalGas [51]
b – shallow casing leaks identified by Blade [47]
c – wells listed in the 1988 Casing Inspection Interoffice Memo [58]
d – wells listed in the SoCalGas response dated March 12, 2018 [61]

Figure 138 shows the locations of the 114 comprehensive safety review wells, also known as the SIMP wells, (upper graphic), and the 27 wells with shallow external corrosion on the production casing (lower graphic). These 27 wells are spread throughout Aliso Canyon with no apparent trends.

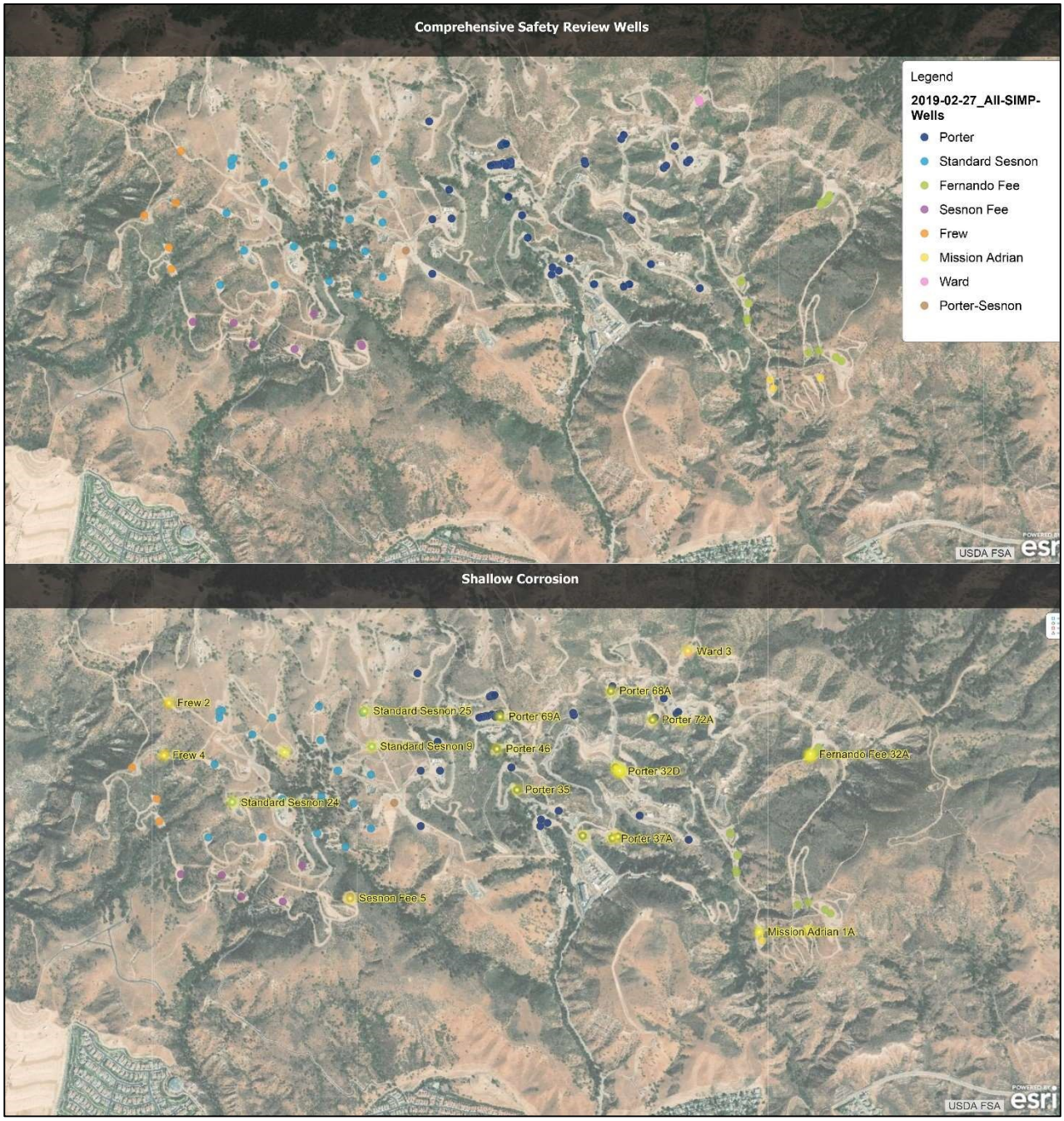


**Figure 138: Well Locations with Shallow External Corrosion on Production Casing Excluding SS-25**

Figure 139 shows the location of the shallow external corrosion on the production casing for 26 wells. Almost all of the wells had production casing external corrosion present just below the surface casing shoe. One well, P-50A, had production casing external corrosion above the surface casing shoe. SS-25 was not included, but it was the only well that showed shallow corrosion above *and* below the surface casing shoe.

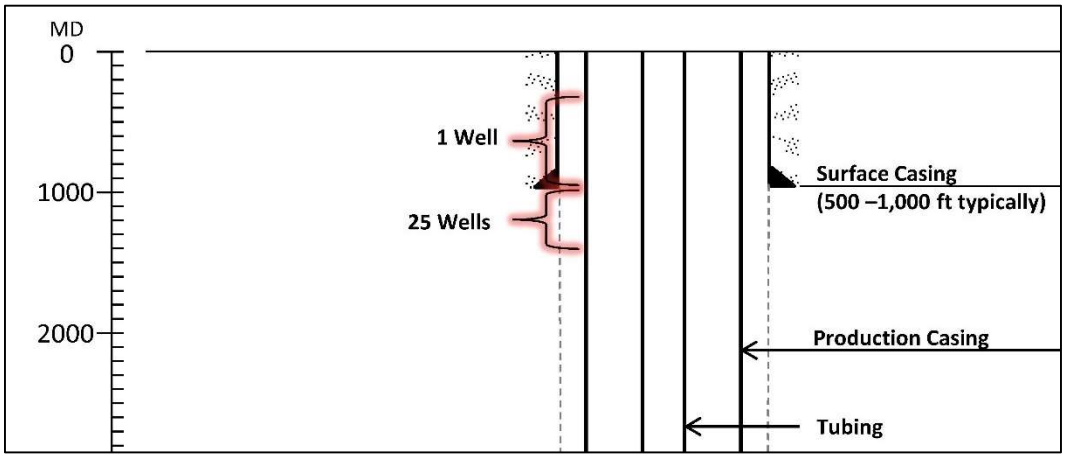


**Figure 139: Location of Shallow External Corrosion on Production Casing Not Including SS-25**

Figure 140 shows a production casing UltraSonic Imager Tool (USIT) log from SF-5 which is a well in the West section of Aliso Canyon. The production casing is 7 in. 23 ppf (0.317 in. wall thickness) N80 LTC. The track titled Minimum of Unflagged Thickness (THMN_RF) is the minimum wall thickness of the production casing measured by the USIT. THMN_RF is denoted by a red line and labeled in red. Above the depth of the surface casing shoe, THMN_RF shows no variability; the production casing has no issues here. Below the depth of the surface casing shoe, THMN_RF drops erratically down to approximately 0.23 in. wall thickness or 27% penetration. Note each division on the THM_RF track is 0.1 in. Blade interprets this production casing metal loss as external corrosion. Some additional observations were evident. The 13 3/8 in. × 7 in. casing annulus is liquid filled to a depth of approximately 400 ft and is labeled “Top of Liquid Column”; this observation of a deep annulus liquid level with gas on top is common to most of the wells reviewed. At the depth of the shoe, the percentage of solids increases; this is also common to most of the wells reviewed. This is denoted by yellow shading in the second from the right track. In some of the wells reviewed, gas is present behind the 7 in. casing adjacent to the casing OD. This is denoted by red shading in the second from the right track.

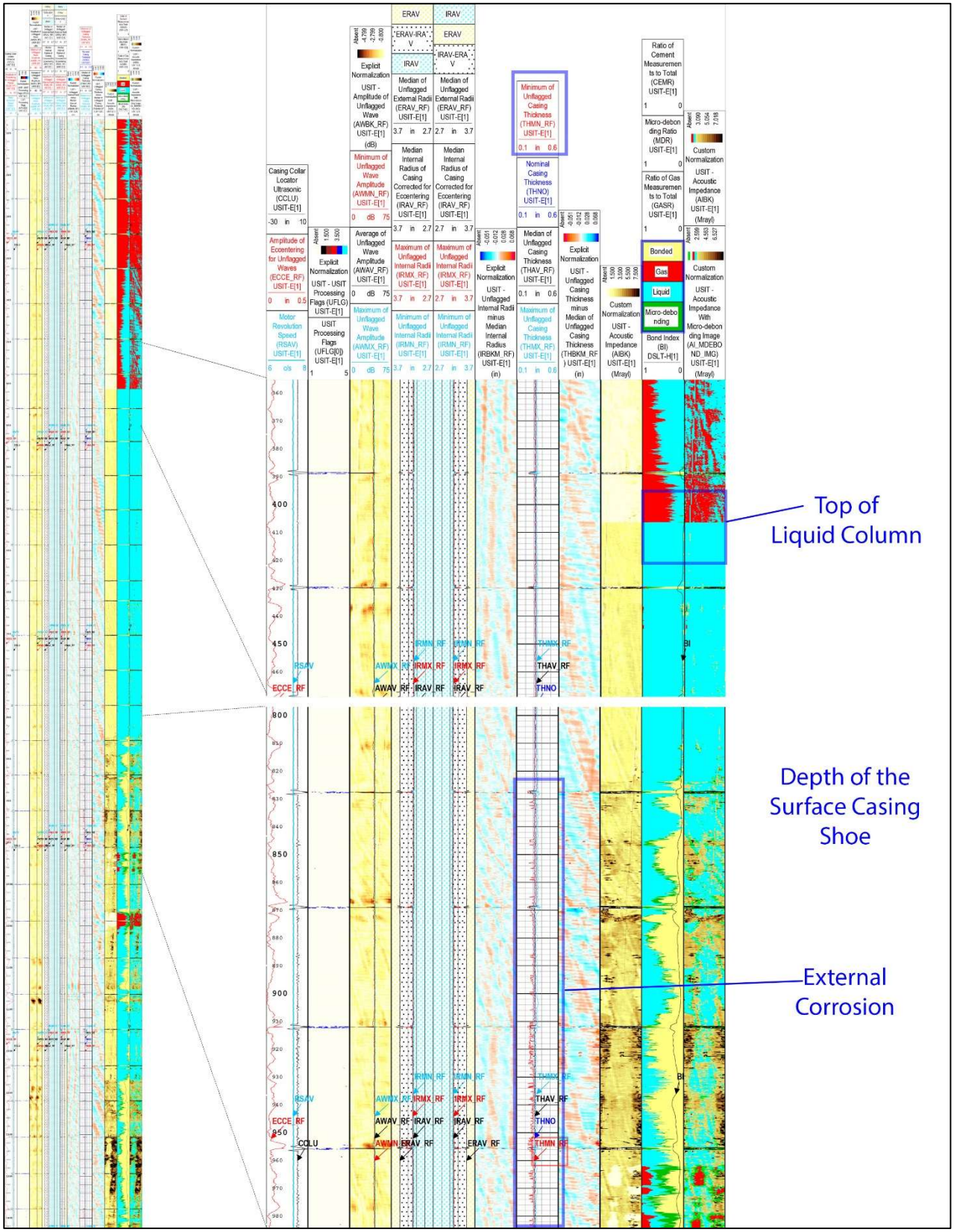


**Figure 140: SF-5 Production Casing USIT Log Example of External Corrosion**

The location and nature of the corrosion in SS-25 including what components led to the corrosive environment have been detailed in this report. But it is still not clear how similar the corrosion mechanisms of SS-25's surface and production casing are to the rest of the Aliso Canyon field. A corrosive environment was or is present in a number of wells and has likely been affecting the production casing at similar depths. Complex processes have interacted to create the corrosive environment. The casing inspection logs provide a snapshot of the deterioration of the casings but do not quantify the corrosion kinetics. Of the 76 casing inspection logs reviewed, 27 showed shallow external corrosion but 49 did not. Furthermore, in many cases, wells adjacent to each other on the same site showed differences in extent, severity, and location of corrosion. Although trends have been identified in this section, additional work, beyond the scope of the RCA, is necessary to investigate the prevalence of SS-25 type corrosion mechanism field wide.

One area of investigation focuses on the location of corrosion near the surface casing shoe. This is common in a number of wells; this suggests a common corrosion mechanism. Figure 141 shows a possible corrosion mechanism supported by some of the observations discussed previously. Using the numbered inset images, the hypothesis is as follows:

1. During the initial cementing operations of the production casing, drilling fluid was circulated and remained in the production casing annulus above the cement. Drilling fluid typically has a high pH and is not likely to cause corrosion.
2. Over time, the drilling fluid in the production casing by surface casing annulus leaked off into the formations below the surface casing shoe. Solids within the fluid settled out, and bridges formed between the production casing OD and the surface casing ID, trapping the drilling fluid. Additionally, the formations below the surface casing shoe may have collapsed and formed a barrier.
3. Over time, groundwater channeled through poor surface casing cement. Groundwater mixed with and displaced the remaining drilling fluid outside the production casing.
4. Over time, gas from seeping production casing connections or gas from a shallow gas formation (e.g., Pliocene Gas Sand) percolated upwards. This gas would have contained carbon dioxide.
5. Corrosion initiated and grew in the aqueous carbon dioxide environment. This process may have been assisted by microbes residing in the groundwater.

The hypothesis described above is consistent with the shallow corrosion observed across the 25 wells. Much of the shallow corrosion, unlike SS-25, was only observed below the surface casing shoe. Further analysis is necessary to develop this hypothesis and appropriately mitigate.

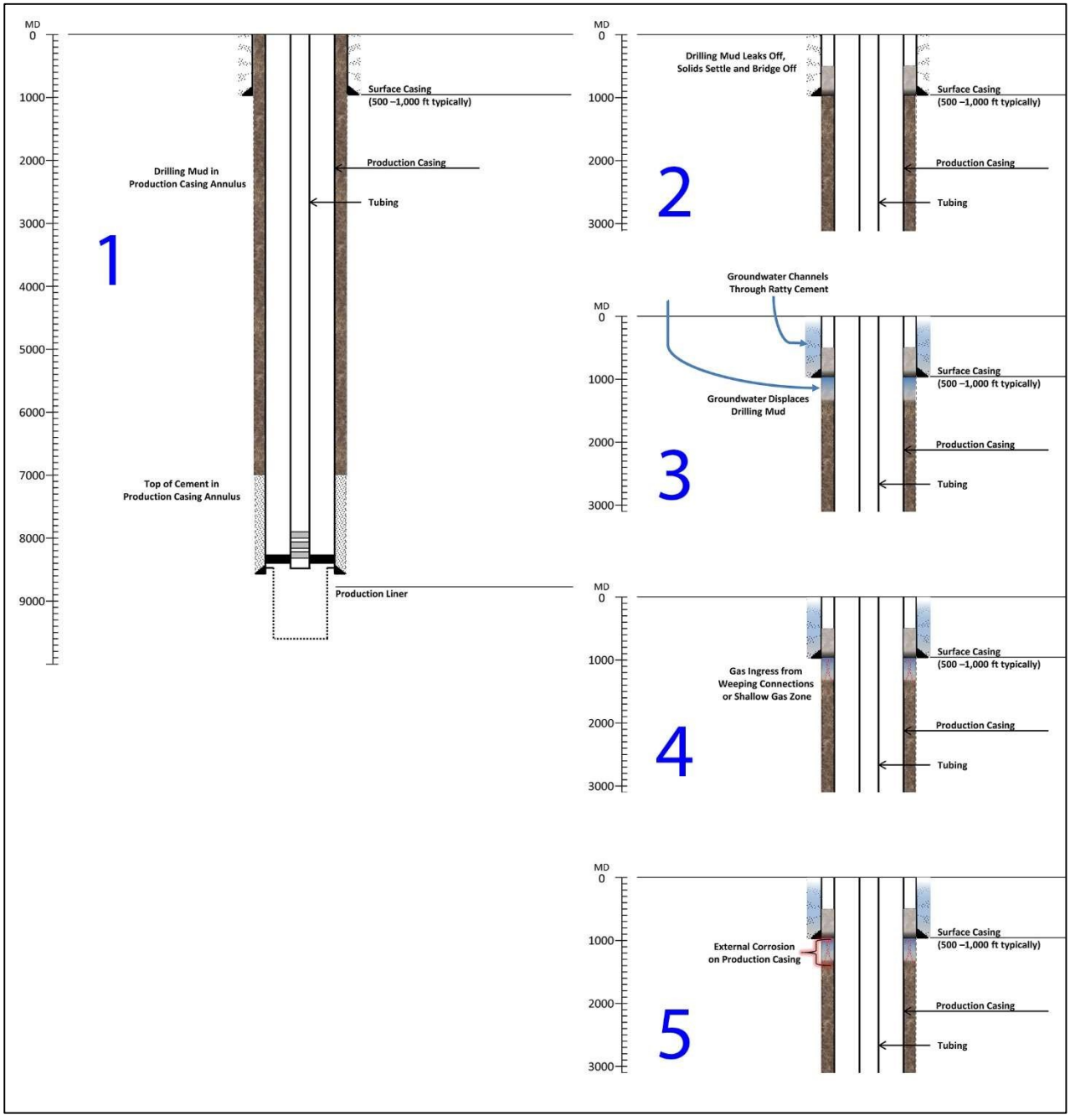


**Figure 141: Hypothesis for the Shallow External Corrosion Mechanism**

## 4.5 Surface Casing Log Analysis

The function of the surface casing is to isolate fresh water sources and also provide a string for drilling the deeper hole for gas storage or oil production. The surface casing is not intended to provide any further barriers to gas or oil. However, in SS-25 the holes in the 11 3/4 in. surface casing played a critical role in allowing escaping gas a low resistance pathway to surface. The kill attempts were made difficult by the surface casing holes.

Blade evaluated the condition of the surface casing in several Aliso Canyon wells for comparison with the surface casing in SS-25. We found significant corrosion in the SS-25 surface casing based on casing evaluation logs run as part of the RCA. The number of wells with surface casing information is limited because inspection logs are run only in some wells on an as-needed basis during the P&A phase of a well's life. Surface casing inspection logs were available on four other wells (F-3, F-9, SF-2, and SS-7) in addition to SS-25. These wells were P&A'd between 2013 and 2018.

Internal corrosion and external corrosion were indicated on inspection logs from the four wells, although they were not as severe as the corrosion in SS-25. SS-25 had the poorest surface casing condition and cement integrity based on the casing evaluation logs of the wells evaluated. The SS-25's 11 3/4 in. surface casing had external corrosion and numerous holes between 134 ft and 300 ft (refer to Section 2.9). A likely reason for the poor casing condition was the poor cement job, which allowed the casing to be exposed to alternating groundwater and air in the vadose zone, depending on the seasonal rainfall. Another difference is that SS-25's surface casing grade is H40, whereas the casing grade for the other wells is J55. The definitive reason for a more severe level of corrosion in SS-25 is not clear. The wall thicknesses for 13 3/8 in. 54.5 ppf, 11 3/4 in. 42 ppf, and 10 3/4 in. 40.5 ppf casings are similar at 0.380 in., 0.333 in., and 0.350 in., respectively.

Figure 142 shows a map with the locations of the wells with surface casing inspection logs. All wells are located in the western part of the Aliso Canyon field.

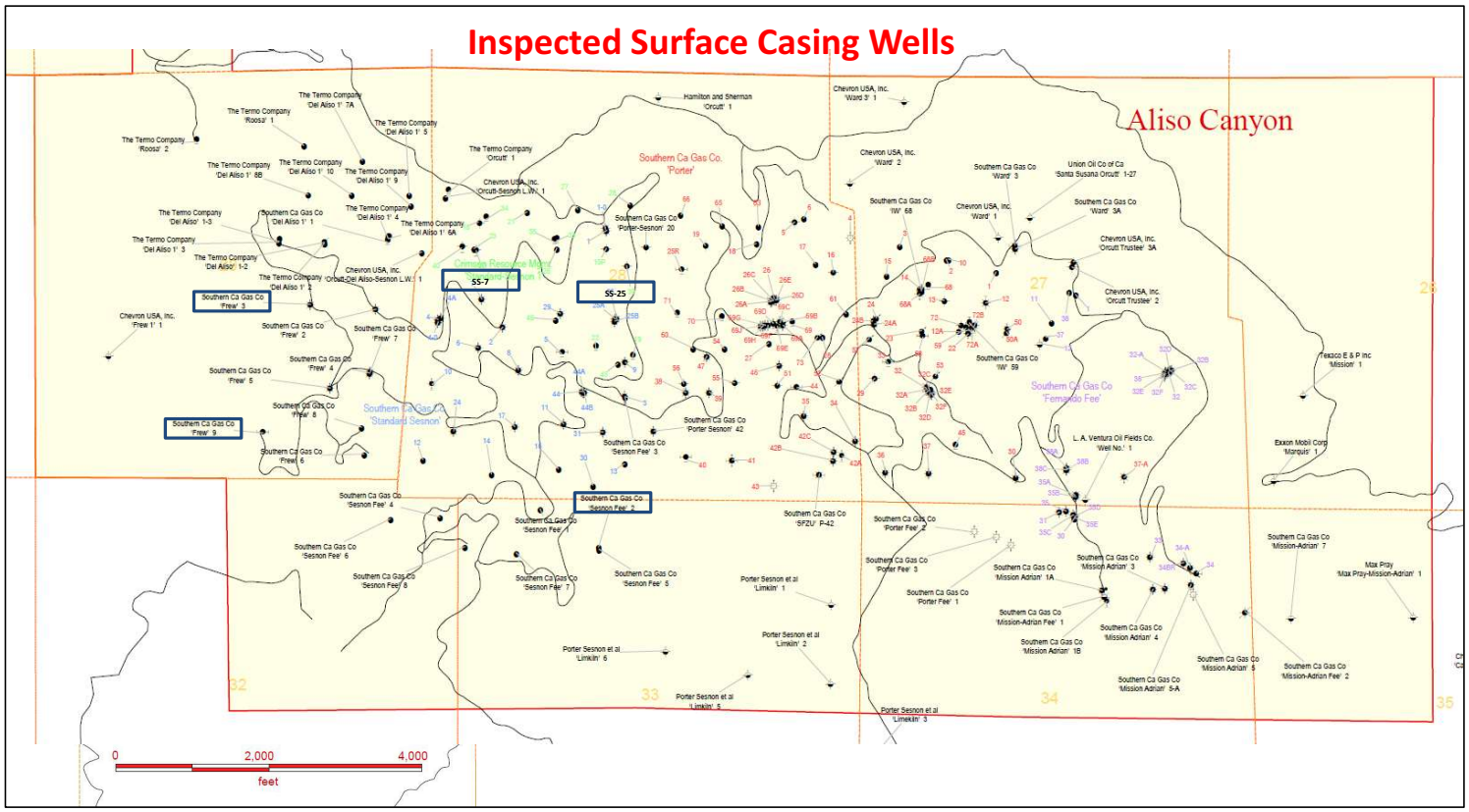


**Figure 142: Map of the Wells with Surface Casing Inspection Logs**

Table 40 shows the wells inspected and a summary of the inspection results. Log results showed casing deformation, internal, and external corrosion.

**Table 40: List of Wells and a Summary of Surface Casing Inspection Log Results**

| Lease | Well | Spud Date | Surface Casing OD (in.) | Grade | Wall Thickness (in.) | Surface Casing Depth (ft) | Inspection Log | Inspection Log Date | Log Summary | Notes | Current Status |
|---|---|---|---|---|---|---|---|---|---|---|---|
| Frew | 3 | September 21, 1944 | 13.375 | J-55 | 0.380 | 1,005 | USIT | August 15, 2013 | Indications of internal and external corrosion surface to 880 ft<br>Log anomalies show casing deformation at approximately 350 ft and 550 ft | A cement retainer stopped at 555 ft and was pulled out | P&A 2013 |
| Frew | 9 | July 26, 1963 | 10.750 | J-55 | 0.350 | 1,500 | USIT | May 12, 2015 | Indications of internal corrosion 130–150 ft, 1,185–1,230 ft, internal and external corrosion 530–540 ft, 570–620 ft, 1230–1,405 ft, external corrosion 960–1,000 ft | N/A | P&A 2015 |
| Sesnon Fee | 2 | April 21, 1953 | 13.375 | J-55 | 0.380<br>0.430 | 1,594 | USIT | December 13, 2017 | Indications of internal corrosion 30–235 ft, 520–540 ft. 590–608 ft, 1,159–1,126 ft, external corrosion 1,112–1,126 ft, 1,208–1,224 ft | 61 ppf casing, the second joint and 570–1,594 ft | P&A 2018 |

| Lease | Well | Spud Date | Surface Casing OD (in.) | Grade | Wall Thickness (in.) | Surface Casing Depth (ft) | Inspection Log | Inspection Log Date | Log Summary | Notes | Current Status |
|---|---|---|---|---|---|---|---|---|---|---|---|
| Standard Sesnon | 7 | October 14, 1945 | 13.375 | J-55 | 0.380 | 1,095 | USIT | May 27, 2014 | Indications of internal corrosion 56–70 ft, 570–610 ft, internal and external corrosion 228–250 ft, 284–294 ft, external corrosion 75–96 ft, 108–134 ft, 500–530 ft, 638–656 ft, 806–814 ft | Processing flags indicating possible aerated fluid near surface Log data may be questionable | P&A 2014 |
| Standard Sesnon | 25 | October 1, 1953 | 11.750 | H-40 | 0.333 | 990 | Two camera runs<br>HRVRT<br>IBC | November 7, 2017<br>August 18, 2018<br>August 12, 2018<br>August 14, 2018 | Camera showed numerous holes in the 11 3/4 in. casing<br>External corrosion and holes 130–320 ft Some internal corrosion 700–950 ft<br>IBC confirms external corrosion 200–540 ft, 625–660 ft, 700–825 ft, and 865–990 ft internal corrosion 200–990 ft | A mechanical Caliper log confirmed holes in the casing<br>The IBC log starts at 200 ft due to the low fluid level | P&A 2018 |

## 4.6 California Gas Storage Well Integrity Regulations

Blade reviewed the 2015 California gas storage well integrity regulations that were in place before the SS-25 leak and the updated November 2018 and January 2019 regulations that were issued after the well leak was stopped. The 2018 and 2019 requirements for underground gas storage projects are the same. Changes in the regulations from October 2015 to January 2019 are significant and address the deficiencies in the 2015 gas storage integrity regulations.

### 4.6.1 2015 Gas Storage Wells Regulations Discussion

Blade reviewed the 2015 California Statutes and Regulations [66] to determine the regulatory requirements for gas storage well integrity at the time of the leak. The following regulations summarize the gas storage well requirements related to well integrity and include commentary related to SS-25:

- Section 1724.10 (g): All injection wells require tubing and a packer, except steam, air, and pipeline-quality gas injection wells.

  Gas withdrawal wells are not mentioned in this regulation. One could assume that gas storage injection and withdrawal wells would be treated the same way. SS-25 was operated as both an injection and withdrawal well. SS-25 qualified for the exemption because pipeline-quality gas was injected and therefore isolation between the tubing and production casing with a packer was not required by the regulation.

- Section 1724.10 (j): A mechanical integrity test (MIT) must be performed on all injection wells to ensure the injected fluid is confined to the approved zones. The MIT consists of two parts.
  - Section 1724.10 (j) (1): MIT Part 1. Prior to commencing injection operations, each injection well must pass a pressure test of the casing-tubing annulus to determine the absence of leaks. Thereafter, the annulus of each well must be tested at least once every five years.

    When SS-25 was converted to a gas storage well in 1973, the 7 in. production casing was pressure tested to 3,400 psi and it was tested to 2,500 psi in 1976, and 1,500 psi in 1979. The pressure tests in 1973, 1976, and 1979 were done with a well service rig on location. No 7 in. casing or 7 in. × 2 7/8 in. annulus pressure tests were reported after 1979[viii].

    The pressure test in 1973 met the requirement for MIT Part 1 because it was done prior to commencing injection operations. The requirement of testing the annulus every five years was not met according to the SS-25 well records.

    The regulatory clarity regarding internal pressure testing of injection wells with regard to gas storage wells was discussed in a DOGGR meeting in May 2006 [67]. The minutes of that meeting reported that because gas storage injection wells do not fall under the federal Underground Injection Control (UIC) program, and should not be subject to federally-imposed internal mechanical integrity testing requirements. The committee considered proposing a change in the regulations to clarify Section 1724.10 (j), but decided not to because section 1724.10 (k) allows for

[viii] SS-25 had a tubing and packer completion at the time of the leak in October 2015; however, there were open ports above the packer so the casing × tubing annulus was not isolated from the tubing. There was a nipple profile below the ports so a wireline plug could have been set to isolate the perforations below the packer and the casing could have been pressure tested.

additional requirements, gas storage injection wells were tested with a static temperature logging tool, and no DOGGR District required casing pressure tests for gas storage wells.

Blade asked SoCalGas for their interpretation of Section 1724.10 (j)'s requirement of casing pressure testing every five years in an information request. SoCalGas responded that their belief and understanding was that the two-part pressure-testing requirement did not apply to gas storage wells based on their correspondence with DOGGR.

SoCalGas proposed to DOGGR in 1994 ". . . the most economical and effective method to monitor casing integrity of gas storage wells is through the use of static temperature surveys [68]." The response to SoCalGas's proposal stated [69] [70]:

> Section 1724.10. (k)(5) in the regulations currently addresses this concern since it acknowledges that additional requirements or modifications of the requirements in Section 1724.10 may be necessary to fit specific circumstances and types of projects. The subsection goes on to list examples of such additional requirements or modifications, including subsection (5), which states that a list of all injection-withdrawal wells in a gas project, showing casing-integrity test methods and dates, the types of safety valves used, may be submitted to the Division annually. Therefore, the monitoring program and static temperature surveys currently used by The Gas Company could be used to satisfy compliance of the requirements for mechanical integrity found in this section.

The casing leak in SS-25 showed that using temperature surveys to confirm mechanical integrity of casing was insufficient. Using a temperature survey assumes that leaks would not be catastrophic, would cause a cooling anomaly, and would be detected in time to allow the well to be controlled quickly and safely. A temperature survey was run in SS-25 on October 21, 2014, a year before the leak on October 23, 2015, and showed no temperature anomalies. The SS-25 incident was unique in one aspect. Small corrosion defects might just result in a hole and leak gas. However, in SS-25 the corrosion patch was large, and more importantly contained a notch like feature due to the microbial nature of corrosion. The large feature along with the notch caused it to be a large axial rupture.

The use of multiple methods to assess well integrity is discussed in the Department of Energy report *Ensuring Safe and Reliable Underground Natural Gas Storage* [71]. Noise and temperature surveys are used to identify leaks, but the sensitivity of the instruments is limited. If no leak is detected, noise and temperature data provide no indication of future integrity problems. Noise and temperature logs are trailing indicators; and by no means sufficient to manage well integrity. Alternatively, casing inspection can identify defects that may be growing with time and can be used to monitor integrity deterioration.

- Section 1724.10 (j) (2): MIT Part 2. The second test of a two-part MIT shall demonstrate that there is no fluid migration behind the casing, tubing, or packer.

  Numerous temperature, noise, and pressure surveys were run in SS-25 between the years of 1974 and 2014, and no major anomalies were found indicating fluid migration.

- Section 1724.3: Well Safety Devices for Critical Wells. Certain wells that meet the definition of *critical* pursuant to Section 1720 (a) and have sufficient pressure to flow to surface shall have safety devices including surface and subsurface safety devices. The definition of a critical well includes a well within 300 ft of any building intended for human occupancy, or an airport runway or is within 100 ft of a public street, highway, railway, navigable body of water, public recreational facility or wildlife preserve.

SS-25 did not qualify as a critical well, so a subsurface safety device was not required. SS-25 was equipped with surface safety valves on the tubing and the 7 in. × 2 7/8 in. annulus.

### 4.6.2 Pressure Surveys

Although SoCalGas performed 41 pressure surveys in 41 years, neither the *DOGGR Project Approval Letter* [72] nor the *SoCalGas Gas Inventory-Monitoring, Verification, and Reporting Company Operations Standard Gas Operations* [73] required pressure surveys. Figure 143 shows the most recent pressure survey on October 21, 2014, to 8,720 ft, in which there seems to be a discrepancy; the title block entry for "Tubing Pressure" (2,659 psi) does not match the graphed data, which appears to be between 2,550–2,600 psi. Despite this discrepancy, no pressure anomalies are observed in the graphed data.

Blade's interpretation of the pressures surveys is that they were not effective in determining the presence or location of a casing leak; small leaks would go undetected. From a casing integrity perspective, pressure surveys differ from pressure tests substantially. In pressure surveys, the well is open to the storage zone, and any gas that escapes into a casing leak is replenished by the storage zone. This is considerably different than a pressure test where all external sources of pressure are isolated. Additionally, the pressures observed during these pressure surveys are the shut-in pressures. The pressure profiles during shut-in are lower than during standard gas injection operations. In other words, pressure surveys are taken at times when the casing is under less pressure than during gas injection.

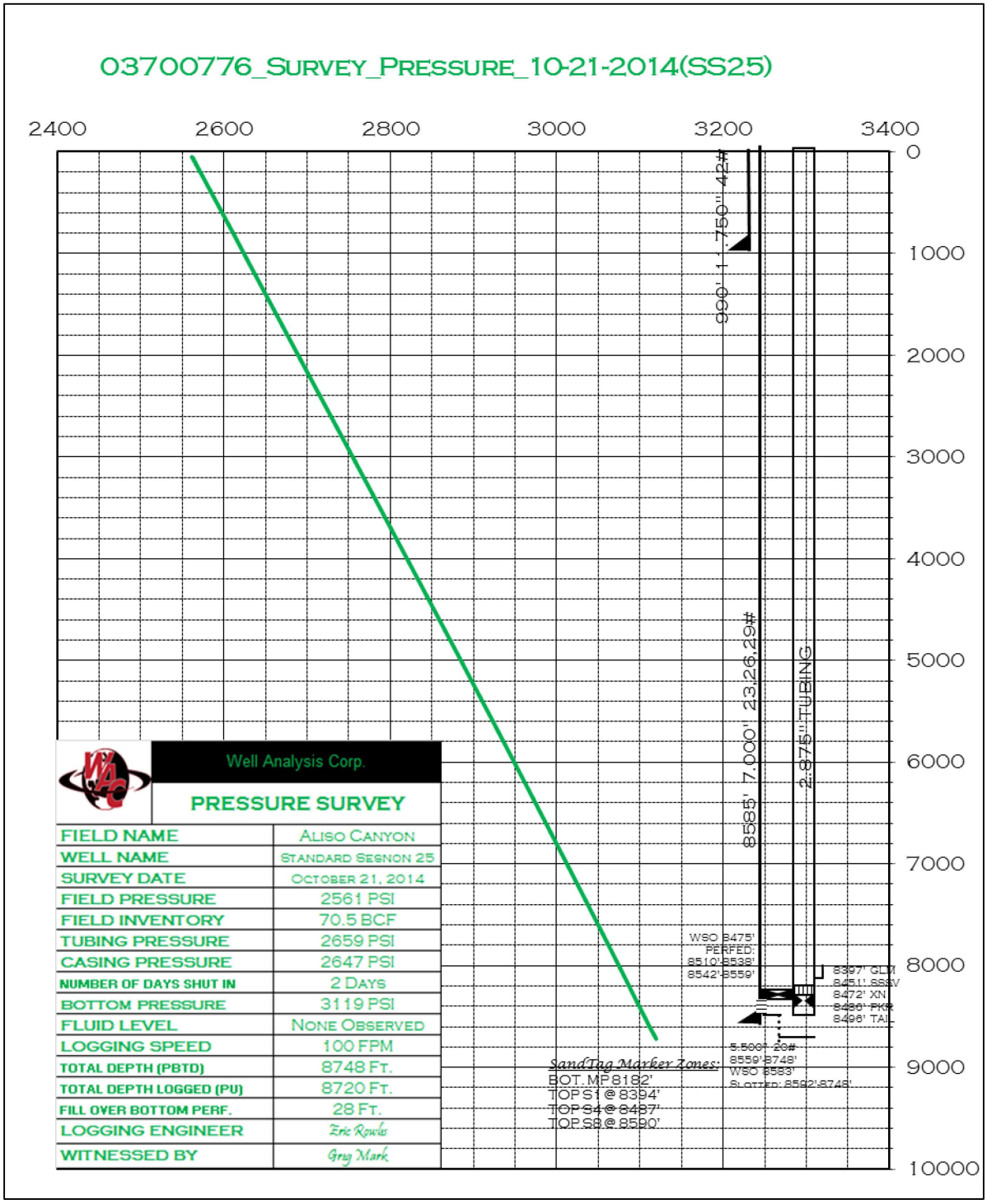


**Figure 143: Most Recent SS-25 Pressure Survey, October 21, 2014**

### 4.6.3 2018 and 2019 Gas Storage Wells Regulations

Blade reviewed the November 2018 California Statutes and Regulations [74], which were revised and issued in November 2018 after the SS-25 casing leak, and the most recent version of the California Statutes and Regulations issued in January 2019 [75]. The requirements for underground gas storage projects are the same in both versions. The 2018 and 2019 regulations for gas storage wells have changed significantly compared to 2015. The following (sometimes paraphrased) regulations summarize the revised gas storage well requirements related to well integrity:

- Section 1726.3: A risk management plan is required for each underground gas storage project that demonstrates that stored gas will be confined to the approved reservoir. The plan shall include protocols for well construction and design standards, evaluating the need for surface and subsurface safety valves, scheduling and demonstration of the mechanical integrity of each well and corrosion and casing pressure monitoring.
- Section 1726.3.1: An emergency response plan is required that addresses leaks, well failures, leakage mitigation approaches, and well-control processes for well failure and full blowout scenarios.
- Section 1726.5: Well construction requirements that ensure that a single point of failure does not pose an immediate threat of loss of control of well fluids and that the well design is appropriate for the expected loads.

  A gas storage well with a primary and secondary mechanical well barrier is a method of meeting these requirements.
- Section 1726.6 Mechanical integrity testing requires a temperature and noise log at least annually and a casing wall thickness inspection and a casing pressure test at least every two years.
- Section 1726.6.1: Pressure testing parameters include a test value of at least 115 percent of the maximum allowable injection pressure. The test shall be continuous for one hour and will be successful if the pressure decline is less than 10 percent in the first 30 minutes and less than 2 percent in the second 30 minutes.
- Section 1726.7: Monitoring for gas pressure in the tubing and tubing by casing annulus at least daily is required.

  No pressure buildup in the tubing by casing annulus confirms that the primary barrier (tubing) has pressure integrity.
- Section 1726.8 Inspection, testing and maintenance of wellheads and valves requires all wellhead valves to be tested at least annually. Surface and subsurface safety valves shall be tested at least every six months.

The gas storage well integrity requirements issued in November 2018 and January 2019 are comprehensive and clear. The likelihood is high of identifying reduced casing wall thickness and taking a well out of service before the casing leaks. The primary and secondary mechanical well barrier requirement is another important step in maintaining well integrity in gas storage wells. Well integrity will be monitored by the periodic casing inspections and pressure tests.

A recommendation for new wells is to protect the production casing from outside corrosion by cementing the casing up to the surface. Cementing technology has advanced to the point that cement to surface is possible by using low-density cement slurry. Cement to surface helps protect the casing from groundwater exposure, resulting in long life gas storage wells.

An additional recommendation is to require an analysis of casing failures that caused loss of pressure integrity, such as, casing leaks and parted casing. The analysis should be documented in a report and include the following as applicable:

- Details of how the failure was identified and located
- Details of the casing OD, weight, grade, and connection
- Photos of the failure if the failure is recovered
- Metallurgical analysis if the failure was recovered
- Analysis and hypothesis of the cause
- Determination of whether the failure was an isolated event or is related to other similar failures
- Recommendations to mitigate future failures

### 4.6.4 SoCalGas Operations Standards

SoCalGas operates the Aliso Canyon facility according to a number of Company Operations Standards. These standards provide policy and scope, definitions, responsibility, and procedures that are required to operate the facility on a day to day basis. An example standard is titled Gas Inventory – Monitoring, Verification and Reporting. Blade reviewed operations standards related to gas storage wells and compared them to standards related to inspections, investigations, and integrity of surface assets. The discussion is included in Appendix A SoCalGas Operations Standards.

## 4.7 Summary of Casing Integrity Analysis

The 2015 regulations regarding well integrity for gas storage wells were insufficient, considering that gas storage wells are long life wells and are exposed to seasonal cyclic pressure loads from high injection pressure to low withdrawal pressure year after year. Gas storage wells are unlike typical oil and gas wells where the pressure starts out high and decreases with time as the reservoir is depleted. No regulations were found that required casing inspections to monitor casing wall defects, corrosion, and remaining wall thickness for the purpose of confirming the pressure capacity of the casing for the expected pressure loads.

SoCalGas proposed to DOGGR in 1994 [68] ". . . the most economical and effective method to monitor casing integrity of gas storage wells is through the use of static temperature surveys." DOGGR approved the use of static temperature surveys to satisfy compliance of the requirements for mechanical integrity.

Blade reviewed SS-25 noise, temperature, and pressure surveys before the incident of October 23, 2015. There were no temperature, pressure, or noise anomalies in the surveys that indicated a preexisting casing failure. Additionally, there were no physical observations from well inspections and weekly pressure measurements that indicated an existing problem. Our interpretation is that SoCalGas complied with the monitoring components of the Operations Standard titled Gas Inventory – Monitoring, Verification and Reporting [73].

The catastrophic SS-25 casing leak showed that using temperature surveys to confirm mechanical integrity of casing was a flawed concept. The concept assumed that leaks would not be catastrophic, would cause a cooling anomaly, and would be detected in time to allow the well to be killed quickly and safely. A temperature survey was run in SS-25 on October 21, 2014, a year before the leak on October 23, 2015, and showed no temperature anomalies.

Allowing an annual temperature survey to meet the requirements of a mechanical integrity test is insufficient for several reasons:

- A leak and cooling must exist to develop a temperature anomaly.
- Lack of an anomaly does not provide any data regarding the future integrity of the casing or remaining wall thickness.
- Temperature change must be within the sensitivity of the tool.
- Interpretation of the survey is subjective.

The revised regulations issued after the leak event are much more comprehensive, requiring periodic casing inspections and pressure tests. The primary and secondary mechanical well barrier requirement is another important step in maintaining well integrity in gas storage wells.

Ninety-nine casing failures were identified in the 124 Aliso Canyon gas storage wells reviewed. The failures included 63 casing leaks, 29 tight spots, 4 parted casings, and 3 other types of failures. Casing leaks include both connection leaks and pipe body leaks. Forty percent of the gas storage wells we reviewed had a casing failure with an average of 2 casing failures per well (99 failures in 49 wells).

A large number of production casing leaks and parted casings have occurred throughout the history of the Aliso Canyon field, with a risk of gas leaks and safety and environmental repercussions. In spite of the possible consequences, no data were provided to demonstrate that measures were taken to understand the root causes of the casing and well failures. The well files and data made available to Blade are mostly void of analyses of the causes of failures. An interoffice memo related to FF-34A [1] stated that "The possible regional external casing corrosion problem in the southeastern portion of the field that was going to be further studied and a report issued"; however, Blade was not able to locate any documentation regarding this study.

SoCalGas has a Company Operations Standard (191.01) for the Investigation of Accidents and Pipeline Failures, but a complementary standard for the investigation of a well failure has not been identified. This implies that more attention was paid to surface equipment and assets failures than to well and downhole failures.

The SIMP program proposed in the 2016 GRC testimony is an indication that perhaps a shift to more focus on below-ground facilities had started. The program included risk assessments for all wells, casing inspections, and pressure testing, which is consistent with the 2019 regulations for gas storage wells.

Serious consequences can result from casing leaks. In the case of the underground flow that was reported for F-3 and FF-34A, the wells were killed by pumping down the tubing. SS-25, though, was a much more serious event where a shallow casing leak broached to surface and a relief well was required to kill the well after several unsuccessful kill attempts were made by pumping down the tubing, resulting in several BCF of gas escaping into the atmosphere.

Most of the casing connections used in the wells that failed were reduced OD or API connections[ix]. However, it was not possible to determine if the failures in most wells occurred in the pipe body or in the

[ix] Wells drilled from 2010 to 2015 did have casing connections that would be considered a gas-tight connection with a metal-to-metal seal.

connection, based on the well reports. There are exceptions where the reports clearly stated the existence of parted connections, e.g., in well SS-12, the 7 in. 23 ppf J55 Speedtite connection parted, and P-50A had connection leaks in the 9 5/8 in. BTC less than a year after drilling. A noise log in 1988 detected a 7 in. 8-round collar leak in F-4 with nitrogen pressured to 875 psi. A temperature survey run in SS-5 in 1977 showed cooling anomalies indicating 7 in. Speedtite connection leaks between 150 ft and 1,300 ft. Many of the reduced OD connections used in Aliso Canyon wells were run prior to 1980. Industry testing in the mid-1980s showed that reduced OD connections were prone to structural failures and internal and external leaks. Nine of the Speedtite connections recovered from SS-25 leaked in an instrumented shop test.

Many of the Aliso Canyon gas storage wells were designed and drilled as oil producers, and the casing and connection designs were not intended for gas exposure and gas storage well loads. The production casing loads for oil and gas wells normally decrease with time due to depletion and reduced reservoir pressure when compared to gas storage wells where the pressure is cyclic depending on the injection and withdrawal cycles. Gas storage wells are pressured up to field operating pressure while injecting gas, and the gas is then withdrawn (produced) usually on an annual cycle. The well pressure is reduced under withdrawal conditions, and the cycle repeats year after year.

Wells with casing failures were distributed throughout the Aliso Canyon Field. Nothing seems unusual regarding the casing failures near SS-25 when comparing them to the casing failures in the rest of the field. The depths of casing failures ranged from the wellhead to below 8,000 ft, and no general pattern is apparent. Thirteen of the 99 failures were reported between surface and 1,000 ft (8 casing leaks, 2 parted casing, 2 tight spots and 1 other).

Most of the failed wells with 7 in. production casings were drilled from 1939 to the mid-1950s as conventional oil and gas wells. The data show that casing failures and casing leaks happened in approximately 50% of these wells. The failed wells with 8 5/8 in. production casing were drilled in the 1970s, and a cement stage collar was run to cement the casing up to the surface, and many of the stage collars leaked. The failure and casing leak rate for the gas storage wells is also around 50%, implying that well age does not correlate with casing failures.

SoCalGas had a two-year plan (1988 memo) to determine the mechanical condition of the casing in 20 casing flow wells, including SS-25, originally completed in the 1940s and 1950s. They prioritized the wells based on gas deliverability, operational history, and length of time since their last workover. SoCalGas logged seven of the 20 wells within two years of the recommendation. Inspection logs showed penetrations greater than 20% to greater than 60% in five of the seven wells logged from 1988 to 1990. Logs in two of the seven wells have not been located; however, a 5 1/2 in. inner casing was run in one of the two wells at the time of the inspection, suggesting the presence of significant penetration. An inner casing string was run in two of the seven wells in 1989. The logs showed numerous indications of metal loss in the production casing above the surface casing shoe in four of five wells and immediately below the shoe in two of the four wells (F-4 and SS-8).

SoCalGas made a recommendation in 1988 to run casing inspection logs in the 20 wells that concerned them at the time, and the opportunity to inspect the casing in SS-25 was missed. It is not possible to determine what an inspection of the SS-25 casing would have shown in 1988, but it is possible that the corrosion was present and detectable, and steps could have been taken to avoid the leak in 2015. SoCalGas logged some of the 13 remaining wells starting in 2007, resulting in a gap from 1990 to 2007 when no inspection logs were run in the 20 wells, according to the available well records.

SoCalGas logged the High Priority wells and found significant penetration. No documentation was found that explained why the remaining wells were not inspected as per the recommendation in 1988. Blade

inquired if SS-25 was inspected based on the 1988 recommendation because it was on the list of 20 wells. SoCalGas responded to an information request dated December 18, 2018, that the high priority wells were logged, and SS-25 was not inspected because the Vertilog technology was less effective at identifying casing leaks than the well diagnostic tests that SoCalGas routinely performed on its underground gas storage wells [76]. However, the 1988 objective was to determine the mechanical condition of the casing and not to identify casing leaks.

There were 76 of 116 wells that had production casing inspection logs available, of which, 27 wells showed indications of shallow external corrosion on the production casing. In almost all of these 27 wells, the external corrosion was below the depth of the surface casing shoe. There were two exceptions, F-4 and P-50A. The shallow corrosion in P-50A was found above the shoe and abruptly stops at the depth of the casing shoe.

Although no well was found with the exact placement and pattern of corrosion as that of SS-25, we conclude that shallow corrosion was a common event that was found field wide, and close to the surface casing shoe. Shallow casing leaks occurred in a number of wells. We found 10 shallow casing leaks in a review of 116 wells. We interpreted that three of these shallow casing leaks could be attributed to shallow corrosion; three were not. There was not enough information to determine if the remaining shallow casing leaks were corrosion related.

Surface casing corrosion was identified in several wells where casing inspection logs were run as part of the P&A operations. The surface casing in SS-25 was the well in the worst condition; logs showed multiple through wall holes in the 11 3/4 in. casing from approximately 134 to 300 ft. The holes in the surface casing likely contributed to the 7 in. production casing corrosion and allowed groundwater and oxygen to enter the 11 3/4 in. × 7 in. annulus.

# 5 Root Cause: Approach and Results

The mechanisms for the failure of the SS-25 wellbore have been discussed in detail. The events that unfolded after the uncontrolled leak and the follow-up efforts to get the well under control were also analyzed. The factors that impacted the ability to control the well have been identified. Finally, the overall Aliso Canyon well integrity issues and the approach to well integrity management have been described. The next step in the process is to integrate all of the data, analyses, reviews, and conclusions from previous sections to get an understanding of all the causes, and in particular, understand the root causes.

This section describes Blade's RCA approach.

## 5.1 RCA Process Background

An RCA is a systematic process used for identifying the root causes of problems or events and defining methods for responding to and preventing them. The goal of an RCA is to analyze problems or events to identify:

- What happened
- How it happened
- Why it happened
- What actions are needed to prevent reoccurrence

There are many different methods and philosophies for conducting an RCA, such as 5-Why's, Fish-Bone Diagram, Fault Tree, Management Oversight, and Risk Tree Analysis depending on the industry and type of problems being investigated. However, most of them use preconceived or pre-defined categories of causes. Blade selected the Apollo Root Cause Analysis (ARCA) approach because it is a structured, evidenced based process that makes no assumptions about possible causes. The ARCA companion RealityCharting software was used to develop a cause-and-effect chart, identify the root causes, and develop solutions. This methodology has been used in the energy, chemical, and aerospace industries.

The ARCA process starts with defining a primary effect, that is, the effect that should be prevented from occurring. The next step is to determine the causes of the primary effect. An *effect* has at least two causes in the form of conditions and actions, and together they become a causal set (Figure 144). Conditional causes are static causes that exist over time prior to the action. Action causes are causes that interact with conditions to cause an effect. In other words, the condition has to already exist for the action to cause the effect, and the condition and the action have to exist at the same time for the effect to occur. For example, think of a fire as an effect. The conditions (i.e. the static causes) for that fire to happen would be a source of oxygen and fuel. The action (i.e., what interacts with the conditions) for that fire to happen would be the addition of heat from a match. The action plus the conditions would result in a fire, and the absence of any of the conditions would not result in a fire regardless of the action.

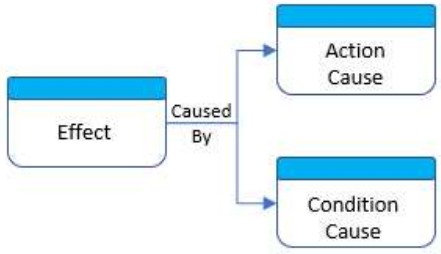


**Figure 144: Causal Set**

Next, the question *what was this caused by?* or *why did this happen?* is asked for each of the action and condition causes. The causes in essence, become effects, and new action and condition causes are determined for each effect. This process of continuously asking what or why and determining causes for each effect is repeated and develops into a cause path until an end point is reached (Figure 145). A valid end point is defined as an effect that is caused by a desired condition (e.g., the pursuit of a goal), a lack of control (e.g., a legal requirement), or some other more relevant or productive cause path. During this process, the evidence supporting each cause has to be identified.

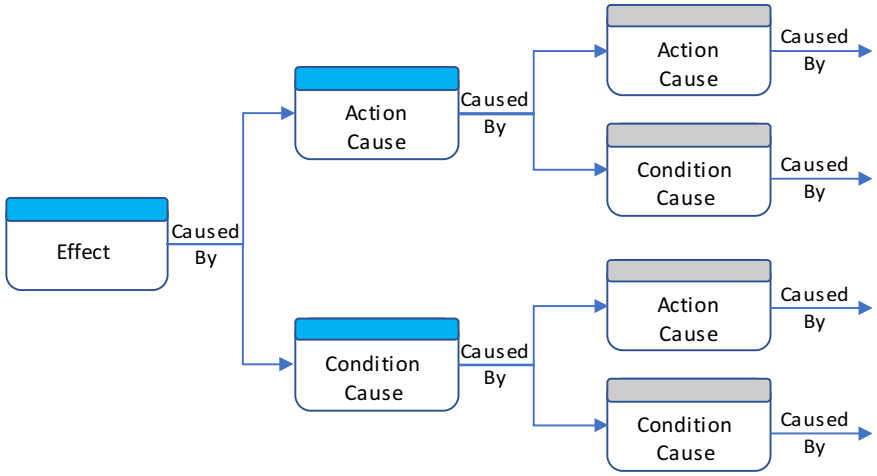


**Figure 145: Casual Flowchart Development**

Once the causal flowchart is complete, the root causes are identified and solutions to mitigate or prevent them are developed. The criteria for developing solutions are:

- Preventing recurrence.
- Being within one's control.
- Meeting one's goals and objectives.
- Not causing other problems.

A team consisting of five Blade investigators involved in all aspects of the RCA project was assembled to execute the structured ARCA. An external facilitator, trained in ARCA was engaged as the process evolved and was being finalized.

## 5.2 Root Cause Analysis Results

The first step in the RCA process was to determine the primary effect of the October 2015 SS-25 incident. As discussed previously, there have been many incidents of casing leaks at Aliso Canyon and two underground blowouts. However, the casing leaks were minor in comparison to SS-25 and were mitigated. The blowouts on the Frew-3 and FF-34A wells in 1984 and 1990 were controlled within several days. In contrast, there were multiple unsuccessful kill attempts and a relief well was necessary to control SS-25. What made the SS-25 incident distinctly different was that there was an uncontrolled release of hydrocarbons, specifically methane gas, to the surface for three and a half months. This is the primary effect.

The RCA effort focused on determining why this primary effect occurred, and what could have been done to have either prevented it or reduced the period of the uncontrolled release. Further, the intent of identifying root causes and implementable solutions is to prevent reoccurrence of similar or other well integrity issues at Aliso Canyon.

There are three causes for the primary effect*:*

- The loss of wellbore integrity, that is, the well was no longer able to contain the pressurized gas inside the wellbore as it had been intended to do. If there had been wellbore integrity, then gas would not have been able to escape from inside the well.
- The wellbore was in direct communication with the gas storage reservoir. This was, in fact, the purpose of the well which served as a conduit to inject gas from the surface down into the reservoir and allowed withdrawal of gas from the reservoir to surface.
- The well-control efforts took 111 days to stop the reservoir gas from leaking to the surface. Seven attempts were made to stop the gas flowing up through the wellbore by pumping kill fluids down into the well from the surface. These top kill attempts were unsuccessful and, ultimately, a relief well had to be drilled to intersect the SS-25 wellbore at 8,534 ft and bring the gas flow to a stop by pumping kill fluid down the relief well to fill SS-25 with kill fluid from the bottom. If, for example, the first top-kill had been successful, the flow of gas to the surface would have been stopped within days. For example, had a successful well kill occurred by October 26, the cumulative volume leaked would have been 0.4 BCF instead of around 6 BCF.

Figure 146 shows the primary effect of the SS-25 incident and the three causes.

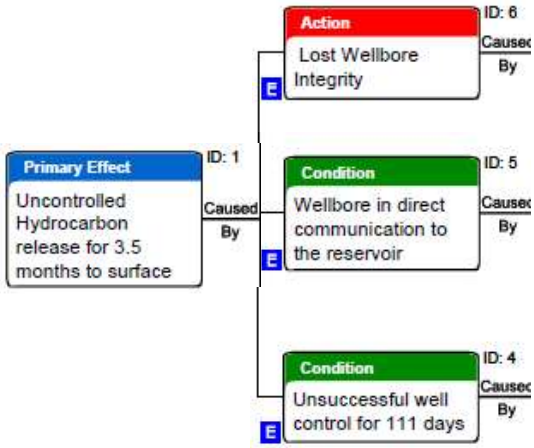


**Figure 146: Causes of the SS-25 Incident**

The next step was to explore the causes for each of the three effects to determine what had caused them and why. This process continued until identification of causes was no longer possible. Figure 147 shows an image of the completed RCA chart, which serves to illustrate the overall structure, and causal branches corresponding to the three causes discussed above. Each of these three branches is discussed in detail in the following sections. (See Appendix A for a larger version of the flowchart.)

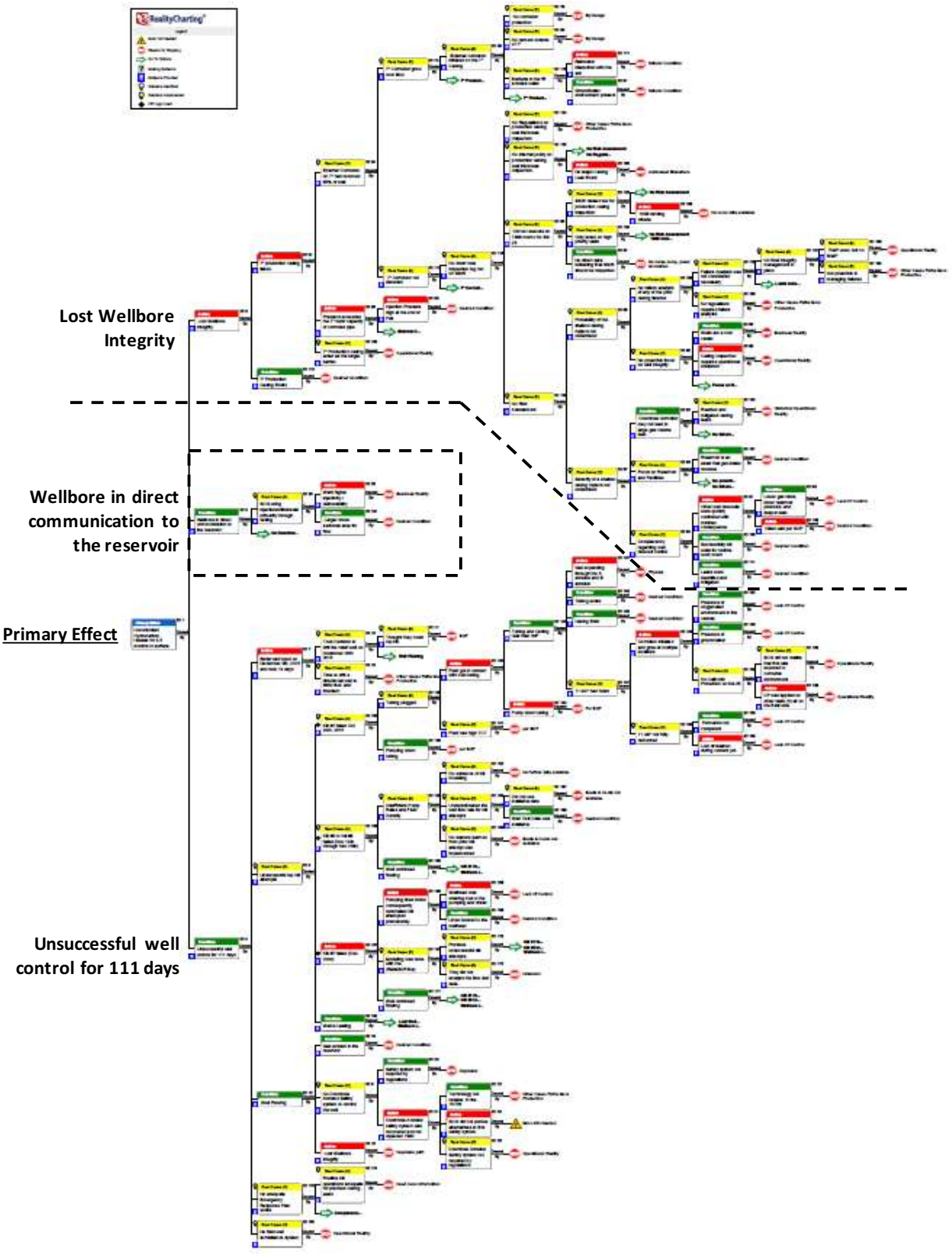


**Figure 147: RealityCharting Root Cause Analysis Flowchart**

### 5.2.1 Wellbore in Direct Communication to the Reservoir

In 1954, SS-25 was drilled and then completed as an oil producing well. Figure 148 shows that a 7 in. production casing string was run from the surface to 8,585 ft, which was approximately 200 ft into the Sesnon oil reservoir. Below the 7 in. casing, a 200 ft 5 1/2 in. production liner was run across the Sesnon formation. This liner had slots cut along its length. A 2 7/8 in. production tubing string was run inside the 7 in. casing. At the bottom of the tubing string, a production packer isolated the annular space between the tubing and the 7 in. casing. During production the oil flowed from the Sesnon through the slots in the liner, up into the tubing, and up the tubing to the surface. The production packer prevented oil from flowing into the 7 in. × 2 7/8 in. annulus. Thus, the wellbore was in direct communication with the reservoir, allowing the oil to be recovered from the reservoir, which was the objective of the well. Note that the reservoir pressure was not high enough to force the oil all the way to surface. Several gas lift valves were therefore installed in the upper section of the tubing string. This allowed gas to be pumped down the 7 in. x 2-7/8 in. annulus, through the gas lift valves and into the tubing. The gas mixed with the oil making it lighter so that it would flow to the surface.

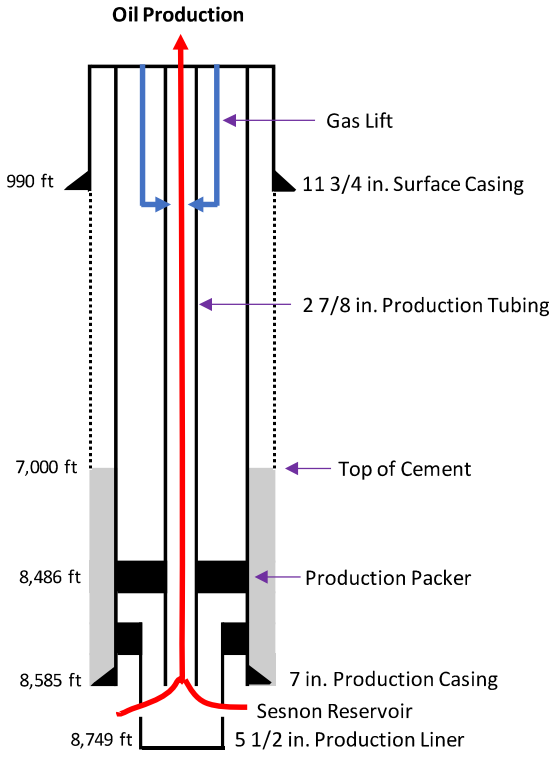


**Figure 148: Well Schematic from When SS-25 Was an Oil Well**

In 1973 the Aliso Canyon Field was depleted, and the Sesnon reservoir was converted to a gas storage reservoir; this allowed gas to be injected into the Sesnon reservoir for temporary storage and withdrawn when it was needed. After 19 years as an oil-producing well, SS-25 was converted to a gas storage well. However, there was one key difference in how the well operated as an oil well compared to a storage well. While oil was produced up through the tubing, gas could be injected and withdrawn through the tubing and through the casing-tubing annulus (7 in. × 2 7/8 in. annulus). This is important because both the tubing and the inside of the casing were exposed to the gas flow.

Having the wellbore in direct communication with the reservoir is a business reality. However, as Figure 149 shows, the effects of the incident were complicated by the fact that the well was configured for injection and withdrawal through the tubing and casing. In the 38 years SS-25 was used as a gas storage well, it was mostly used for injection, and most of that was done through the casing. Injecting gas through the casing allowed higher injection and withdrawal rates because it provided a larger flow area (than just the tubing), and a higher rate of gas could be injected through the casing. Maximizing the injection and withdrawal rates at lower pressures through each well is a business reality, reducing the need for additional storage wells. But this had an adverse impact on the wellbore integrity. Another impact of the well configuration was the absence of a functioning downhole annular flow safety system. Such a system had been initially installed but proved to be unreliable, and it was later removed. This is discussed in more detail in Section 5.2.3.

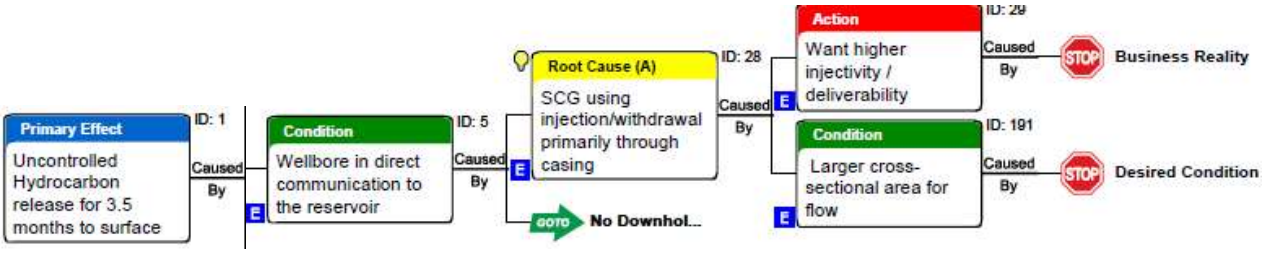


**Figure 149: Causes—Wellbore in Direct Communication with the Wellbore**

## 5.2.2 Lost Wellbore Integrity

The wellbore is defined as the 11 3/4 in. surface casing, the 7 in. production casing and the cement sheath outside of each string, the 2 7/8 in. production tubing, the production packer, and the wellhead. Together, these components act as a system intended to contain the downhole fluids and pressure within the wellbore.

At the time of the incident, gas was being injected into the reservoir. Wellbore integrity was lost when the 7 in. casing (which was being used to provide the conduit between the reservoir and the surface) ruptured and parted, allowing the pressurized gas to escape from the wellbore. Figure 150 shows that the following were the causes of the failure:

- The external corrosion on the 7 in. casing had removed 85% of the wall thickness.
- The pressure inside the 7 in. casing exceeded the burst capacity of the corroded casing.
- The 7 in. casing acted as a single barrier.

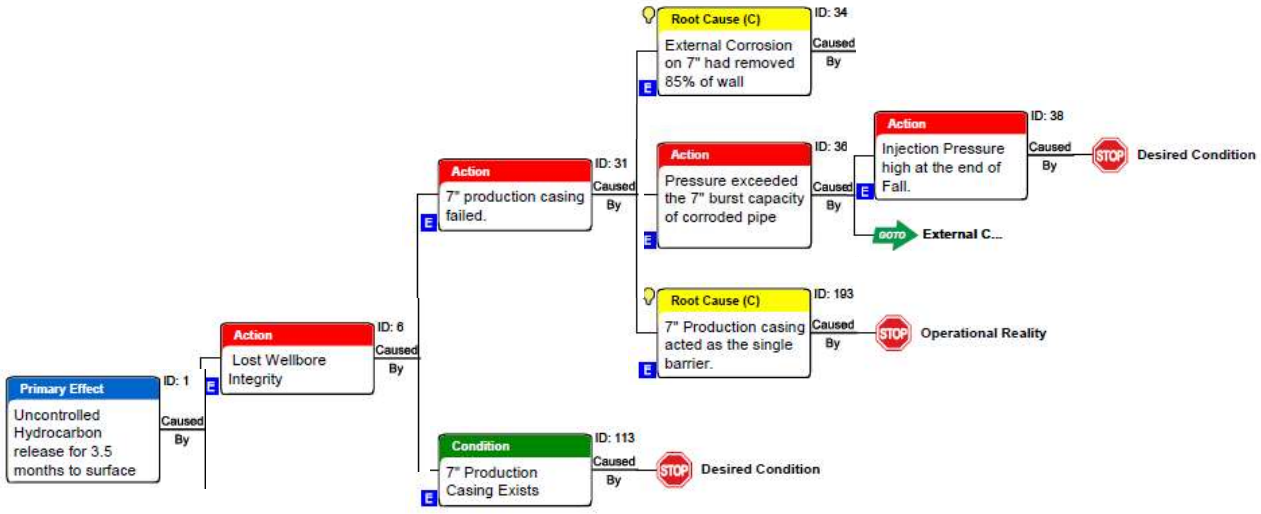


**Figure 150: Causes—Lost Wellbore Integrity**

Rig operations during Phase 3 found that the 7 in. casing had parted at 892 ft. Blade examined the parted sections and found that external corrosion had removed 85% of the wall thickness, which consequently reduced the burst capacity of the 7 in. casing. At the time of the failure, the pressure of the gas being injected into the wellbore was 2,700 psi surface pressure. Blade developed a finite element model of the corroded region where the 7 in. casing failed by using the actual material properties and dimensions of the corroded section. The corroded region included sharp grooves causing a stress concentration that was approximated in the finite element model. The modeling predicted that the corrosion region would fail at a differential pressure between 2,327 and 2,836 psi. This is consistent with an internal pressure of 2,791 psi at the failure location. The surface injection pressure varies throughout the year and was at the highest level for the year. This was normal for the fall months, when more gas is stored for the upcoming winter demand.

Recall that SS-25 was originally designed to be an oil producer in 1954 and was converted to gas storage in 1973, 19 years later. Other wells in Aliso Canyon drilled after 1973 were designed specifically to be gas storage wells. A key difference between the two types of wells is that the reservoir pressure in an oil well decreases gradually over time, whereas the reservoir pressure in a gas storage well does not. An oil well experiences the highest pressures on the first day of production, and pressure then decreases over time. The pressures that gas storage wells are exposed to are cyclic as gas is injected and withdrawn normally on annual cycles (Figure 151). The cyclic pressure levels are approximately the same year after year; the 7 in. casing burst capacity decreased over time because of the effects of wall loss corrosion. A key tenet of ensuring wellbore integrity is that the casing be designed to withstand the pressures it will be exposed to over the complete life of the well.

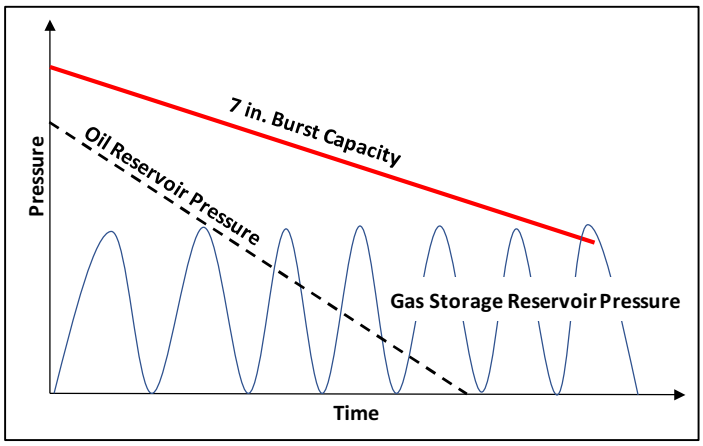


**Figure 151: Oil and Gas Storage Reservoir Pressures Compared**

Typically, oil and gas wells' production occurs only through the tubing string that is run in the production casing. The tubing acts as a primary barrier, containing the produced oil or gas within the wellbore. However, if the tubing fails, the production casing is designed to be a secondary barrier that prevents the production fluids from leaking out of the wellbore, and allows the well to be killed, and the failed tubing string to be removed and replaced. In the case of SS-25, gas injection and withdrawal were done primarily down the casing. Consequently, the 7 in. casing acted only as a single barrier. Outside of the 7 in. casing was the 11 3/4 in. surface casing, set at 990 ft. While it was set below where the 7 in. failed, the 11 3/4 in. casing was not intended or designed to contain the SS-25 injection and withdrawal pressures. Shallow-set surface casing strings are intended to isolate shallow water zones and provide structural support for the rest of the well. When the 7 in. casing failed, nothing else was in place to contain the wellbore pressures.

**What caused the external corrosion to remove 85% of the wall thickness?**

The removal of 85% of the wall thickness was caused by:

- Corrosion growing over time.
- Corrosion going undetected.

Corrosion initiated on the OD of the 7 in. casing and continued to grow over time because there was neither corrosion protection for the OD nor cement outside the casing at 892 ft, and the environment in the 7 in. × 11 3/4 in. annulus was conducive to corrosion (Figure 152). Blade's laboratory analysis of the parted 7 in. casing showed that the wall thickness reduction was caused by microbiologically influenced corrosion (MIC).

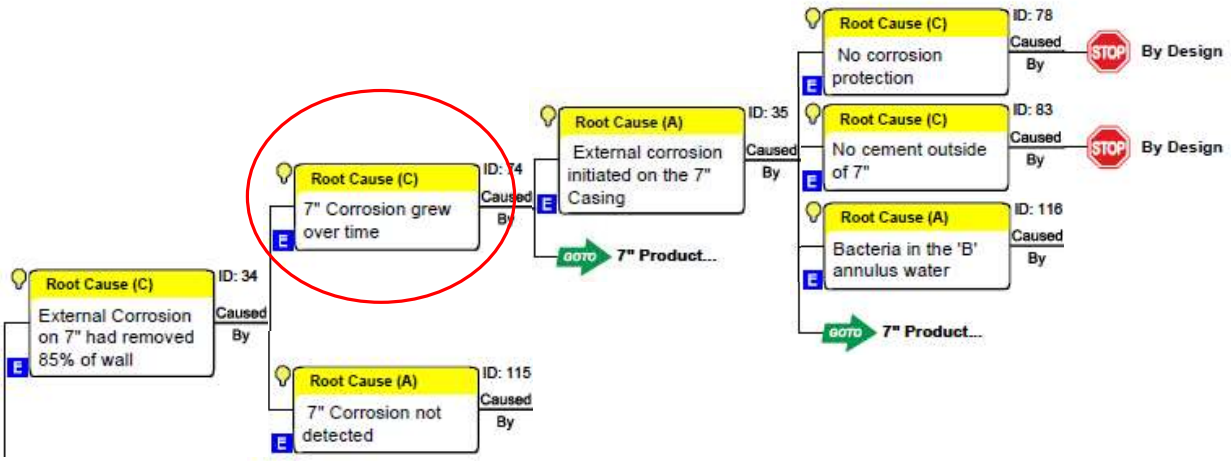


**Figure 152: Causes—Corrosion Growing Over Time**

For the 7 in. casing to have corroded, it must have been in direct contact with an environment that allowed the corrosion mechanism to exist, and a corrosion protection mechanism must have been absent. Cathodic protection systems, for example, are commonly used to protect pipelines from corrosion and are sometimes used on surface casing strings. While a cathodic protection system would have provided corrosion protection to the 11 3/4 in. casing, it would not have protected the 7 in. casing inside the 11 3/4 in. casing. Therefore, the most common method for providing corrosion protection for casing strings is to manage the environment or to modify the casing metallurgy. The presence of bonded cement outside of the 7 in. casing would have mitigated external corrosion. However, there was no cement around the 7 in. casing at 892 ft, because when the well was originally drilled, the cement around the 7 in. casing was intentionally brought up to 7,000 ft and not to surface. The environment outside of the 7 in. casing, above 7,000 ft, would therefore have originally consisted of the drilling fluid used while drilling the well.

In March 2018, two shallow monitoring wells (RBMW-1 and RBMW-2) were drilled from the SS-9 well pad, approximately 600 ft south-southeast of the SS-25 location, which confirmed the presence of groundwater. Two distinct groundwater regimes were found, and the depth of the deeper regime corresponds with the depth of the 11 3/4 in. casing at SS-25. The source of the groundwater is rain. Most of the rain flows on the surface as runoff, while the rest infiltrates into the ground and seeps vertically down. When water encounters permeable (most likely fractured) layers, some of it will enter the layer and move laterally within the permeable layer; for example, the two groundwater regimes noted above. As precipitation varies from month-to-month and year-to-year, the groundwater level will also vary.

The drilling fluid that was left behind the 7 in. casing had a pH ranging from 10 to 12 and would not have caused corrosion. Over time, the drilling fluid leaked off and was displaced by groundwater. The fluid level in the annulus rose and fell with the groundwater level. The groundwater had a microbial environment that resulted in slow corrosion of the OD of the 7 in. production casing (Figure 153).

The metallurgical analyses documented that the failure location had corroded due to MIC. The evidence supporting the interpretation of MIC included metallurgical, scale and corrosion product chemistry, and scale microbial analyses. The metallurgical assessment demonstrated the presence of tunnels, striations and the microbial nature of the corrosion scale. The Raman and XRD analyses demonstrated the predominance of magnetite and modified hematite. The microbial analyses of the scale demonstrated the consistent and predominant presence of methanogen strains that likely caused corrosion. Finally, many of

the 7 in. Speedtite connections exhibited slow leaks, and this seepage of gas likely introduced carbon dioxide, a nutrient for the methanogens.

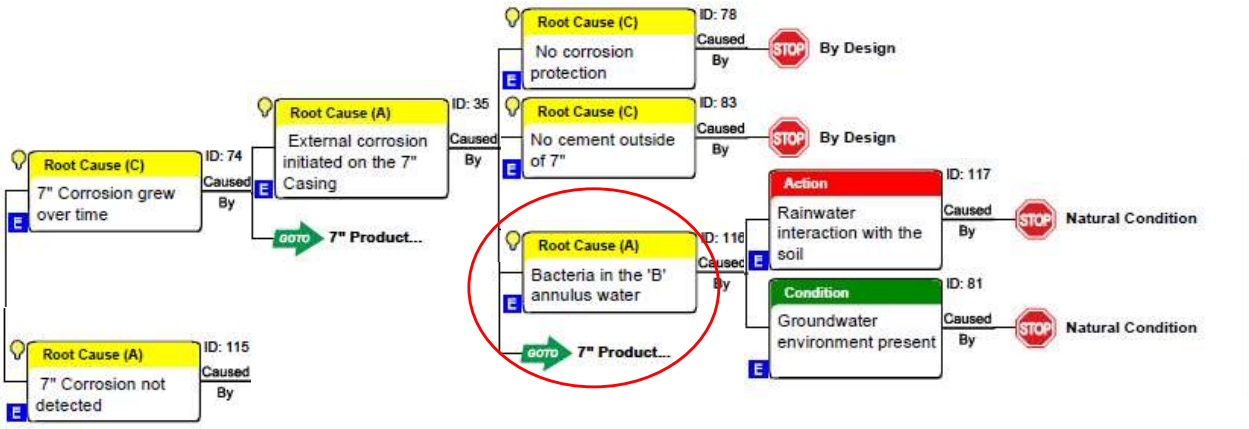


**Figure 153: Causes—Annulus Fluid Corrosion Mechanism**

**Why was the corrosion not detected?**

Corrosion was not detected because the 7 in. casing wall thickness had never been inspected; therefore, the fact that the 7 in. casing was undergoing wall loss corrosion was unknown. Various acoustic and electromagnetic based tools can be run in a well with wireline to measure wall thickness along the entire length of a casing or tubing string. These logs were not run in the 7 in. casing because (Figure 154):

- No regulations were in place requiring them at the time.
- No internal SoCalGas policy addressed wall thickness inspections at the time.
- No action from SoCalGas was taken on a 1988 memo recommending that a wall thickness inspection be done at SS-25.
- No risk assessment was performed.

The 2015 DOGGR regulations required periodic MITs, and annual temperature surveys were approved to meet the MIT requirements. Annual temperature surveys and periodic noise logs were run in SS-25 from 1974 to 2014, and no anomalies were found. This type of monitoring program is not capable of detecting corrosion or the growth of corrosion over time (irrespective of whether it is on the ID or OD). The temperature and noise surveys do not measure wall thickness; they will only detect a leak and are consequently after-the-fact, reactive techniques.

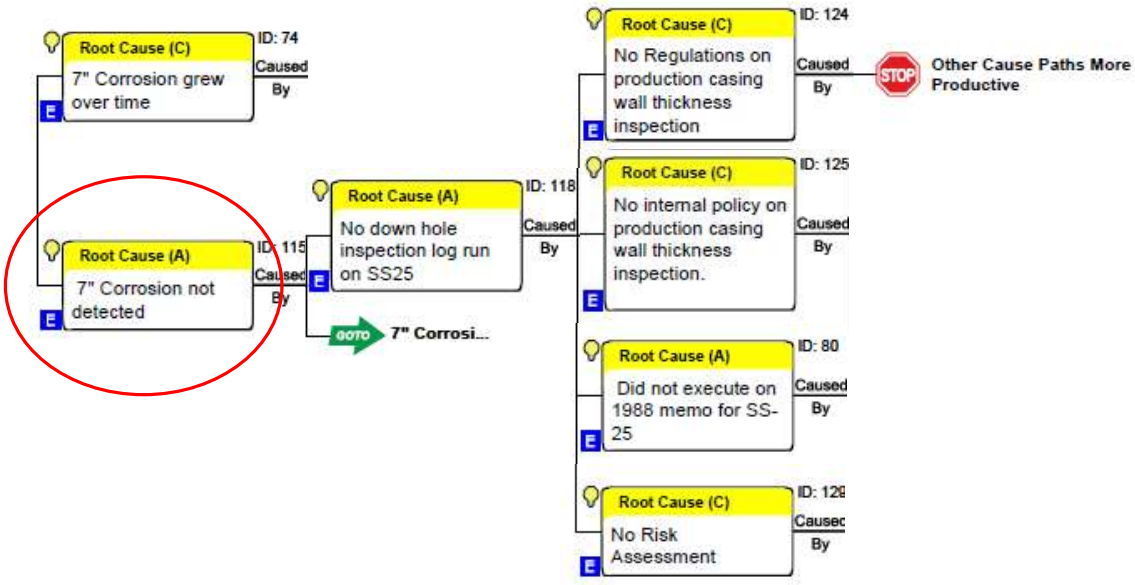


**Figure 154: Causes—Corrosion Not Detected**

In August 1988 an internal SoCalGas memo [57] recommended that a casing inspection survey be run on 20 wells to "determine the mechanical condition of each well casing." The 20 wells were selected on the basis of injection and withdrawal being done through the casing, deliverability, operational history, and how long it had been since their last workover. The well list ranked each well high, medium, or low according to the priority level, and SS-25 was ranked low. The recommendation was approved, but only seven wells were subsequently inspected. Despite the number of casing failures that had occurred in the field, no failure analysis or subsequent risk assessment was done that may have led to an awareness that corrosion was a potential problem.

**Why was there no internal policy on wall thickness inspections?**

The company assumed that regulatory compliance was being adhered to by running annual temperature surveys per the Aliso Canyon Monitoring Plan and the project approval letter dated 1989 requiring an annual MIT. There were no regulatory requirements for wall thickness measurements to be done. The MIT monitoring system did find casing leaks on other wells in the field, which were successfully repaired or remediated. But again, no failure analysis or risk assessment was ever done on previous wells that had leaks or corrosion. In addition, there had not been an event of similar severity to what happened on SS-25 (Figure 155). Further, since no formal risk assessment was conducted regarding well integrity, wall thickness inspection was not identified as a monitoring technique.

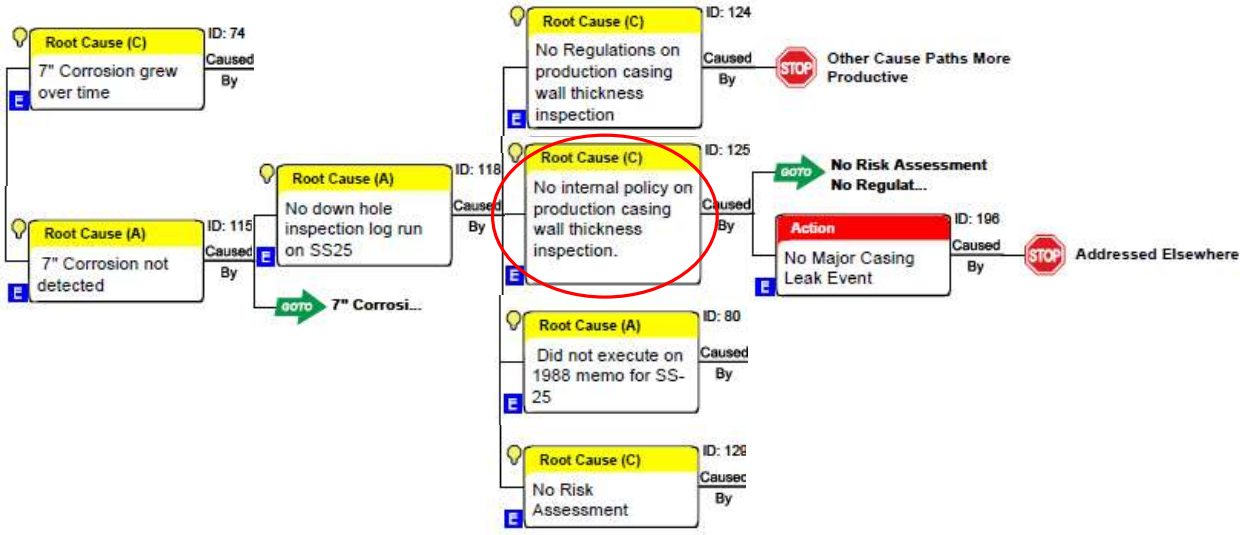


**Figure 155: Causes—No Policy on Wall Thickness Inspections**

**Why did SoCalGas not execute on the 1988 memo?**

The 20 wells recommended for a casing wall thickness inspection were originally oil wells completed between 1944 and 1956. The recommendation was to use a Vertilog inspection tool that used magnetic flux leakage measurements to measure casing wall thickness. The recommendation for conducting the survey was approved with the work to be done over the following two years. During that time, 7 of the 20 wells ended up being inspected (5 were high priority, 1 was medium, and 1 had already been scheduled for a workover). The inspection logs showed metal loss, and an inner casing string was run in some of the wells to mitigate the wall loss. However, 13 of the 20 wells were not inspected within the recommended 2-year window. SoCalGas stated that the remaining 13 wells were not inspected because the Vertilog technology available in 1988 "proved to be less effective at identifying casing leaks than the well diagnostic tests that SoCalGas routinely performed on its underground gas storage wells (e.g. annual temperature surveys, noise logs, etc.) [76]." At the time, there were no anomalies or direct evidence from the noise and temperature log monitoring program that SS-25 needed a wall thickness inspection (Figure 156).

A wall thickness inspection provides a leading indicator of possible casing integrity issues. The noise and temperature logs results are trailing indicators because the leak has to already have happened to be detected. Seven of the wells were inspected, and many of them had OD metal loss indications. There was no follow-up investigation of these anomalies. Further, there was no investigation of why these wells exhibited OD corrosion and why the remaining thirteen wells did not require further analyses (the remaining thirteen wells had been ranked as medium and low priority).

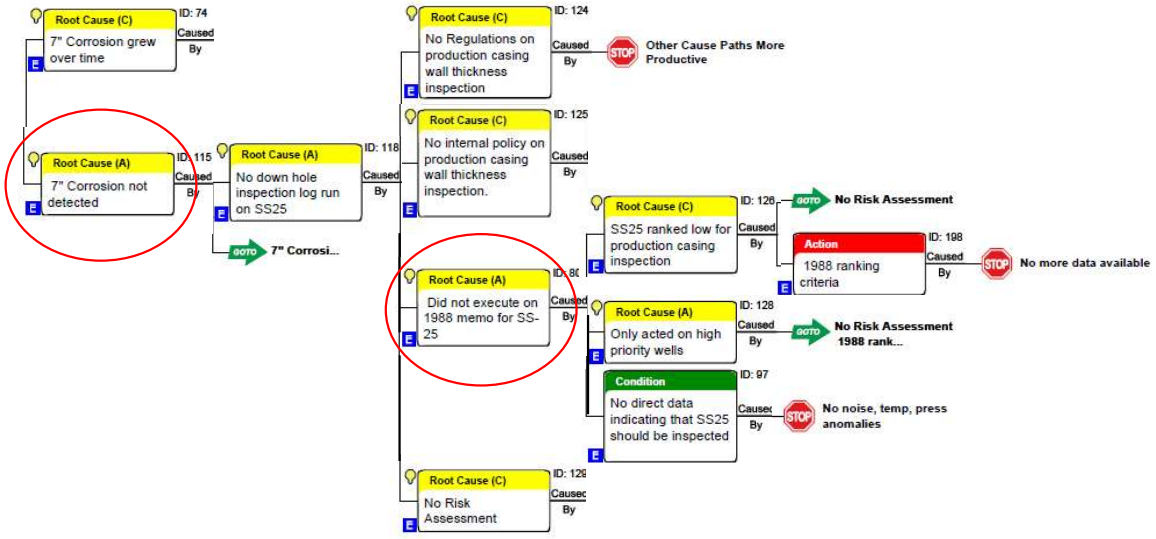


**Figure 156: Causes—Not Executing on the 1988 Memo**

**Why was there no risk assessment?**

When a failure of some component in a system occurs, it is not uncommon to conduct a failure analysis depending on the severity of the failure and its consequences. The purpose of the failure analysis is to determine why it happened, how to prevent its reoccurrence, and, of equal importance, determine if it was because of an isolated problem or if it was a potentially systemic problem. If the problem appears to be systemic, then a risk assessment is commonly done to determine the likelihood of the failure occurring elsewhere, what the potential consequences might be, and how tolerable the risk is. With this understanding of the nature of the problem and potential risks, existing procedures can then be changed or new ones developed to monitor and mitigate the risks.

One hundred and twenty-four wells were designated as gas storage by DOGGR in 2018. Blade's review of the Aliso Canyon well files shows that 40% of the wells had casing failures (leaks, tight spots, parted casing) with an average of 2 failures per well (99 failures in 49 wells). There had been underground blowouts in two wells, Frew-3 in 1984, and FF-34A in 1990. Five of the seven wells that were inspected with the Vertilog tool after the 1988 memo had wall thickness reduction ranging from greater than 20% to greater than 60%. A SoCalGas internal review of casing leaks prepared for CPUC in 2018 listed 81 leaks. Fifty-four of these were related to stage collars, casing shoes, water shut off perforations, casing patches, and inner strings. Of the remaining 27, 3 leaks were related to corrosion, 2 were still being evaluated, and 22 had unknown causes.

Despite this, there is no evidence that SoCalGas conducted a formal failure analysis or follow-up risk assessment on any of the casing failures to determine why they occurred. Nor was there an investigation of the reasons for, and the potential consequences of, the corrosion. It is deduced that the reasons for this are because (Figure 157):

- The probability of a shallow casing rupture was not understood
- The severity of a shallow casing rupture was not understood

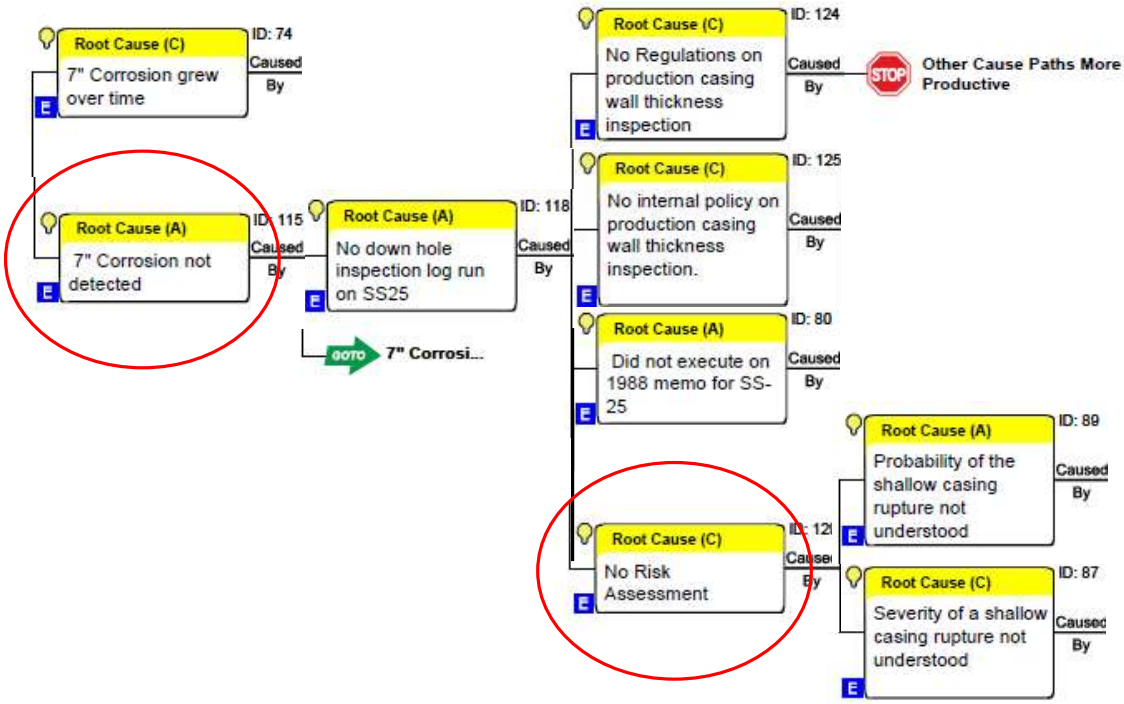


**Figure 157: Causes—No Risk Assessment**

The probability of a shallow casing rupture was likely not understood (Figure 158). A key reason for this was that historically, leaks had been detected and were successfully mitigated, but on an individual well basis. The mitigation efforts appeared to be focused on fixing the problem, getting the well back in operation, and then moving on. Also, no regulations required failure analyses to be done. In 2004, the Federal Pipeline and Hazardous Material Safety Administration (PHMSA) began requiring gas transmission companies, including SoCalGas, to develop and implement a Transmission Integrity Management Program (TIMP). In 2006, PHMSA began requiring distribution companies, including SoCalGas, to develop and implement a Distribution Integrity Management Program (DIMP). The concept of an integrity management system is that it proactively identifies potential problems, determines the associated risks, and then implements actions to prevent the problem from occurring or mitigates the risks. There was no equivalent program that involved well integrity, and the response to casing leaks or well failures was reactive instead of proactive. This is consistent with the view espoused by SoCalGas in their 2014 testimony for the 2016 GRC [2] and the lack of formal or informal investigation of casing leaks.

The severity of a shallow casing rupture was likely not understood because there was complacency with respect to well blowout control (Figure 158). The monitoring program had identified casing leaks, which were successfully mitigated. Wells were top-killed for routine workovers or intervention work. The Frew-3 and FF-34A underground blowouts were quickly controlled with minimal consequences—they occurred with a lower reservoir pressure and flow rate, and leaks were deeper when compared to SS-25's. The Sesnon and Frew reservoir properties are generally benign. The temperature is normal, and the reservoir pressure is sub-hydrostatic, that is, the pressure is less than the hydrostatic pressure of water at an equivalent depth. The reservoir gas is not corrosive and consists predominantly of methane with a small amount of $CO_2$ and no $H_2S$. Under normal conditions, the wells can be killed with water. Complex well-control techniques or high density kill fluids are not required. Kill operations were therefore fairly straightforward and had become a routine standard operating procedure. Wells do not require constant daily maintenance or observation unlike a compressor or other complex machinery. They can be operated

for many years without problems. But wells are mostly underground, so potential problems are much less visible and normally of much less consequence than, for example a transmission pipeline. Nevertheless, well integrity still needs to be effectively monitored with multiple diagnostics methods, and the operating limitations need to be determined and understood because loss of wellbore integrity can be catastrophic as demonstrated by SS-25.

This led to the Aliso Canyon field operating focus directed more at the reservoir and facilities operations and less so on wells. The reservoir is an asset that generates revenue, and wells are cost centers. For instance, running inspection logs requires the well to be taken out of service for the time it takes to kill the well, pull the tubing, run the log, and then rerun the tubing. The implementation and management of TIMP and DIMP programs, mandated by regulation, also require an intensive effort.

It also must be acknowledged that downhole corrosion is not unusual and does not automatically lead to catastrophic failures and large gas volume leaks. If monitored accordingly, corrosion can be managed and mitigated, but the causes and associated risks need to be formally evaluated and understood in order to define safe operating limits of a well.

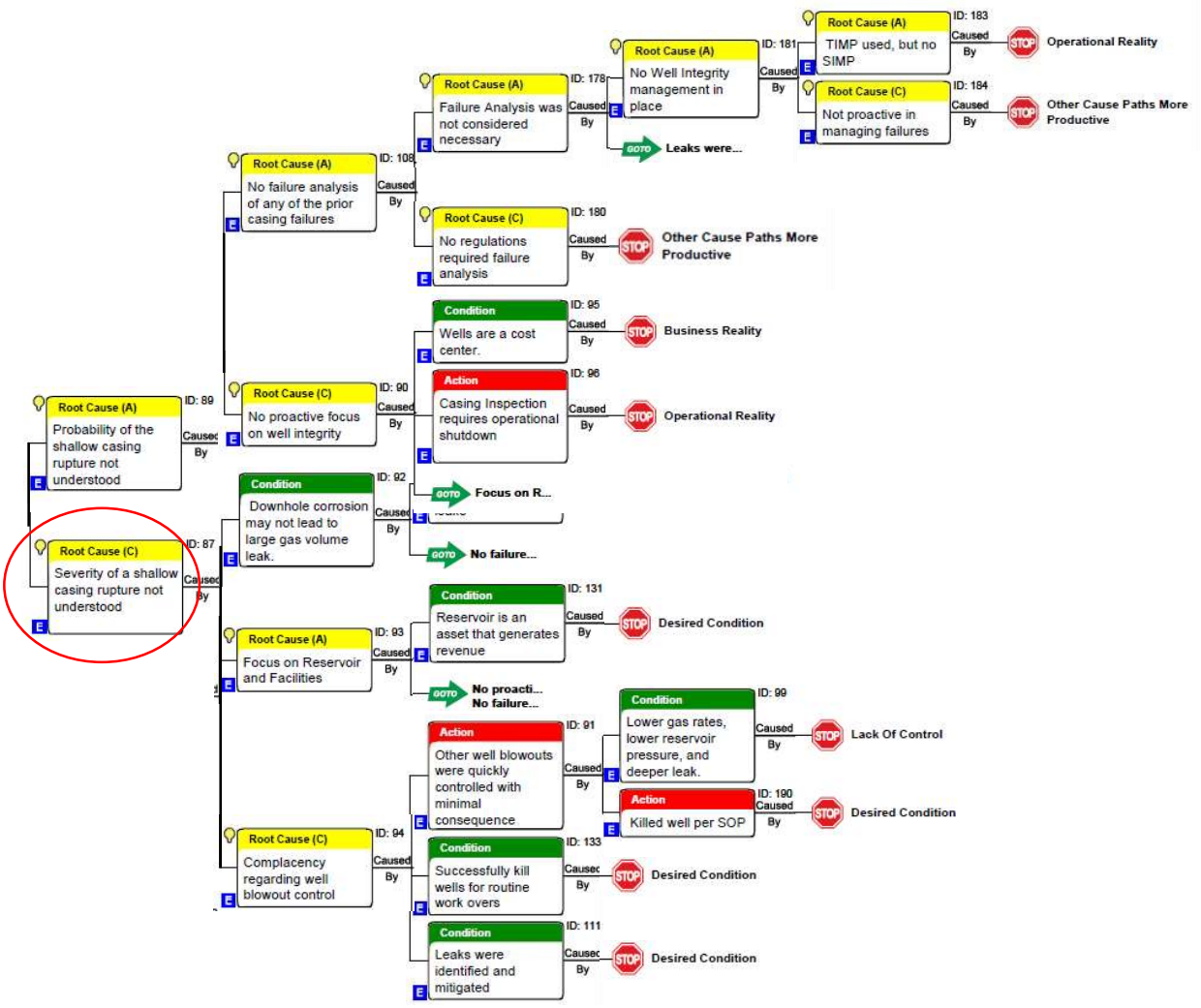


**Figure 158: Causes—Probability and Severity of Shallow Casing Rupture Not Understood**

In November 2014 SoCalGas formally acknowledged the limitations of their normal well monitoring practices. At a General Rate Case meeting for the 2016 budget before the CPUC, SoCalGas requested funding for the implementation of a six-year Storage Integrity Management Program (SIMP). The following is a quote from the GRC testimony describing the basis for a SIMP program [2].

> While we have historically managed risk at our storage facilities by relying on more traditional monitoring activities and identification of potential component failures, we believe that it is critical that we adopt a more proactive and in-depth approach. Historically, safety and risk considerations for wells and their associated valves and piping components have not been addressed in past rate cases to the same extent that distribution and transmission facilities have been under the Distribution and Transmission integrity management programs. As a prudent storage operator, SoCalGas proposes to manage and approach the integrity of its storage well assets, which all fall under the jurisdiction of the California Department of Oil, Gas and Geothermal Resources (DOGGR), in a manner consistent with the approach adopted for distribution and transmission systems. Risk management activities, processes, and procedures for well integrity should have a focus similar to those employed under the Company's pipeline risk mitigation programs.
>
> Accordingly, in this rate case, we propose to establish a highly proactive approach to evaluating and managing risks associated with wells in our storage system through a new SIMP, modeled after the successes of our pipeline integrity management programs (TIMP and DIMP). Through the implementation of the SIMP, better storage well system data will be collected, maintained and modeled to identify the top risks throughout Storage. Comprehensive plans to mitigate those risks will be developed and implemented.

The intent was to "proactively identify and mitigate potential storage well safety and/or integrity issues before they resulted in unsafe conditions for the public or employees." It was noted that their standard monitoring practices only identified problems that already existed, and that there had been an increase in the number of well related issues, such as casing leaks, since 2008. Internal and external corrosion and erosion were identified as the primary well integrity threats.

### 5.2.3 Unsuccessful Well Control for 111 Days

The SS-25 gas leak was detected on October 23, 2015. At the time, gas was being injected through the casing and into the reservoir. Injection was stopped, but gas continued to flow from the well to the surface because wellbore integrity had been lost. On October 24, SoCalGas made the first attempt to kill the well using the same standard top kill procedure that had been in use around the field.

The typical way to top kill a well is to first shut in the well to stop the gas flow, which is done by closing a valve at the surface. When the flow is stopped, the wellbore is full of pressurized gas. The well is then killed by pumping kill fluid into the wellbore and displacing out the gas so that in the end, the wellbore is filled with fluid that provides a hydrostatic pressure greater than the pressure in the reservoir. If the hydrostatic pressure is lower than the reservoir pressure, then the well begins to flow.

In the case of SS-25, the standard top kill procedure was complicated by the fact that the well flow could not be stopped; therefore, the kill attempts had to be done with the well flowing—a sufficient volume of kill fluid had to be pumped at a rate and density to overcome the rate and pressure of the gas flowing out of the wellbore. Another complication was that the leak depth was shallow, which made developing a kill fluid hydrostatic pressure above the leak sufficient enough to kill the well more difficult, compared to a deeper leak.

Seven attempts were made to top kill the well without success. A relief well had to be drilled to intersect SS-25 at 8,534 ft, and kill fluid was pumped down the relief well and into SS-25 from the bottom, which killed the well. It took 111 days to kill the well because (Figure 159):

- The top kill attempts were unsuccessful.
- The well was flowing.
- The emergency response plans were inadequate.
- There was no field well surveillance system.
- The relief well started on December 4, 2015, and took 69 days to complete (74 days including rig up time).

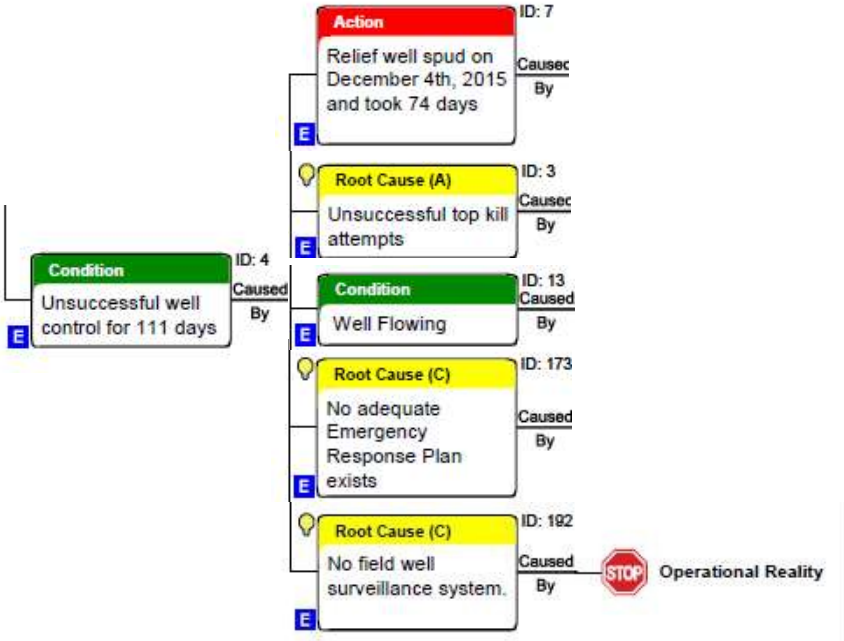


**Figure 159: Causes of Unsuccessful Well Control**

### Why was the well flowing?

The well was flowing because wellbore integrity was lost when the 7 in. casing failed at 892 ft and a downhole annular safety system was not in place to control the well (Figure 160). At the time of the failure, gas was being injected through the casing and into the reservoir. Just after the casing had failed, the injected gas started exiting the well, and gas from the reservoir began flowing up the well and out through the failed casing. Once the leak was discovered, the gas injection was stopped, and the well was shut in at the surface, but gas continued to flow from the reservoir and out the failed area.

A Camco annular flow safety system was installed in SS-25 in July 1976. This system was intended to shut off gas flow in the tubing-casing annulus in the event of a leak in the casing or uncontrolled flow at surface. It was run with the completion tubing and packer and placed deep in the well, above the packer, near the reservoir to provide deep isolation. The safety system was removed and replaced in February 1979. Another attempt was made to repair and test the system in January 1980, when it was concluded that the system did not function as designed. The internal components were then removed, rendering the annular flow safety system inoperable. There are numerous documents in the Aliso Canyon well files indicating problems with this type of safety system. Two systems were tried in various wells in the field; one provided by Camco and the other by Otis. Use of these devices was discontinued in the 1980s,

according to SoCalGas, because they did not work as designed and were unreliable. This is discussed in more detail in the *SS-25 Annular Flow Safety System Review* supplementary report [77].

SoCalGas did not pursue or implement alternatives to the safety system. However, viable deep-set downhole annular safety systems for gas or gas storage wells do not exist even today. Shallow-set systems run in the tubing string that shut off the gas flow in the event of a tubing failure are in common use today, but deep-set annular flow safety systems are not. A shallow-set system would have not prevented SS-25 from flowing either because what failed was the casing and not the tubing. The 2015 regulations did not require a subsurface safety device for non-critical wells.

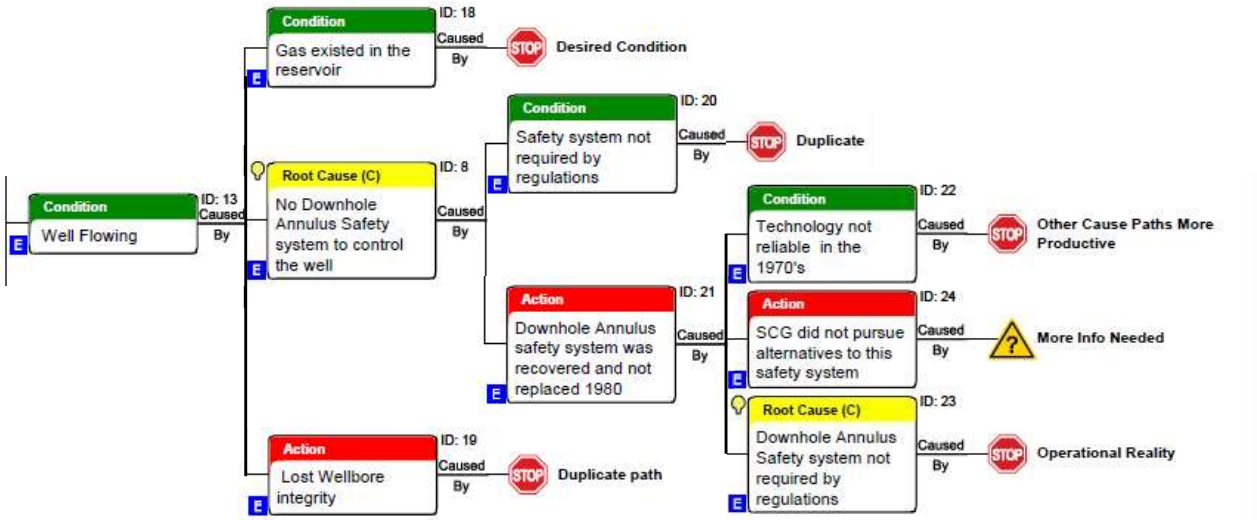


**Figure 160: Causes—Well Flowing**

### Why were the top kill attempts unsuccessful?

The leak was detected on October 23, 2015. The first top kill attempt was made on October 24. Because it was unsuccessful, and the well continued to flow; SoCalGas contracted a well-control company to provide technical and operational support. Over the next 39 days, six other top kill attempts were made, all of which were unsuccessful (Figure 161). Table 41 shows the dates of each kill attempt.

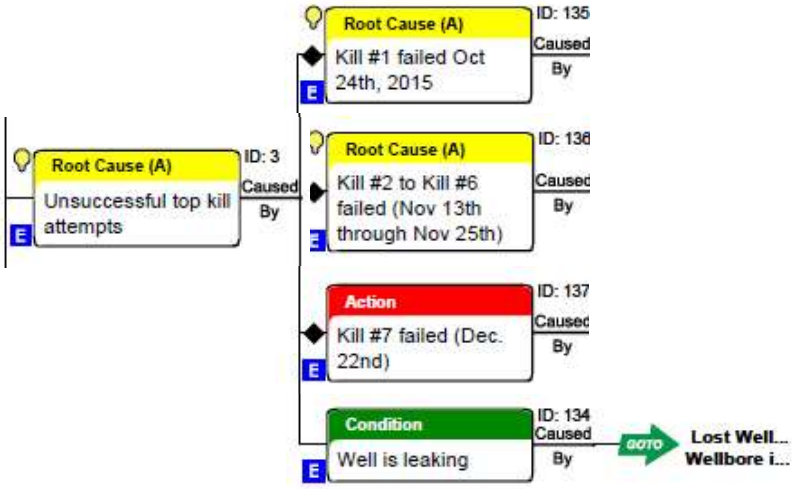


**Figure 161: Causes—Unsuccessful Top-Kill Attempts**

**Table 41: Kill Attempt Dates**

| Kill Attempt | Date |
|---|---|
| #1 | October 24, 2015 |
| #2 | November 13, 2015 |
| #3 | November 15, 2015 |
| #4 | November 18, 2015 |
| #5 | November 24, 2015 |
| #6 | November 25, 2015 |
| #7 | December 22, 2015 |

Initially, the nature and depth of the leak were unknown. The plan for the first kill attempt was to pump 10 ppg polymer brine kill fluid down the tubing to stop the flow of gas and to displace the gas in the 7 in. × 2 7/8 in. annulus with kill fluid to finish killing the well. On October 24, after pumping 11.8 bbl of the polymer brine, the pump pressure jumped to 3,500 psi, and pumping was stopped. During this time the pressure in the 7 in. × 2 7/8 in. annulus remained constant at 290 psi, indicating that there was no communication between the tubing and the annulus, and the tubing was plugged. The pumping was then switched over to the 7 in. × 2 7/8 in. annulus. After pumping 89 bbl of brine, gas started to break through to the surface through cracks in the ground around the well and pumping was stopped. These results suggested a wellhead seal leak or a shallow leak in the 7 in. casing existed.

Because of the Joule-Thomson effect, the flowing gas cooled to approximately 20°F by the time it reached the area where the 7 in. casing parted. The cooling of the gas then cooled the tubing causing the brine being pumped down the tubing to freeze and form a plug in the tubing. The freezing happened because TCT of the brine was higher than the temperature of the tubing. TCT is the temperature at which salt begins to precipitate, causing the brine solution to solidify. The first top-kill attempt was therefore unsuccessful because the tubing became plugged, preventing the kill fluid from being pumped down the tubing (Figure 162).

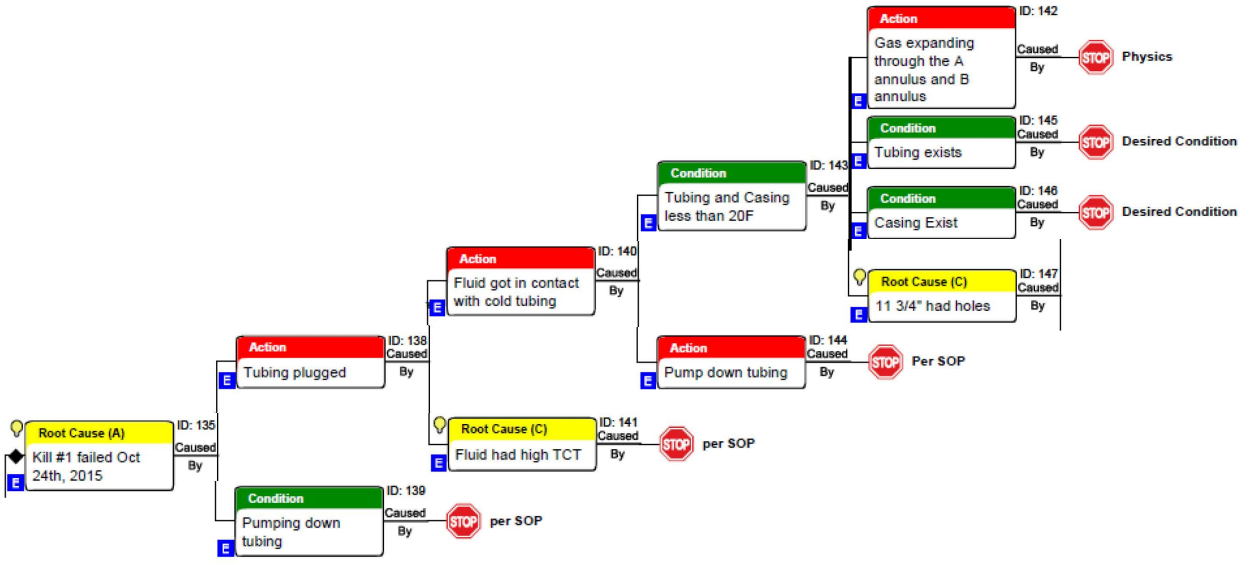


**Figure 162: Causes—Unsuccessful Kill Attempt #1**

During the Phase 3 evaluation of the condition of the 11 3/4 in. surface casing, holes in the casing were found between 134 and 300 ft. These holes were caused by the escaping gas pressure following external corrosion because the casing was neither fully cemented nor cathodically protected leaving the casing exposed to an environment conducive to corrosion (Figure 163). This environment consisted of the undersaturated vadose zone containing air and some water, from surface to 300–400 ft, and then groundwater in the deeper formations.

Lost circulation occurred at 169 ft when the 11 3/4 in. hole section was originally drilled in 1953. This was because the strength of the formations being drilled is low, as is frequently the case in the first several hundred feet in a well. The hydrostatic pressure of the drilling fluid being used exceeded the formation strength, causing lost circulation. Lost circulation also occurred when the 11 3/4 in. was run and was being cemented so that cement was not circulated to surface. Cement was pumped from the surface, and it was assumed that the annulus around the casing had been filled with cement. However, when cement integrity logs were run in the 11 3/4 in. during the Phase 3 operations, fair cement was only found outside the casing from 606 to 660 ft and from 950 to 985 ft, leaving the majority of the casing exposed (Figure 163). Surface casing cathodic protection had been applied to five other wells at Aliso Canyon, but not to SS-25.

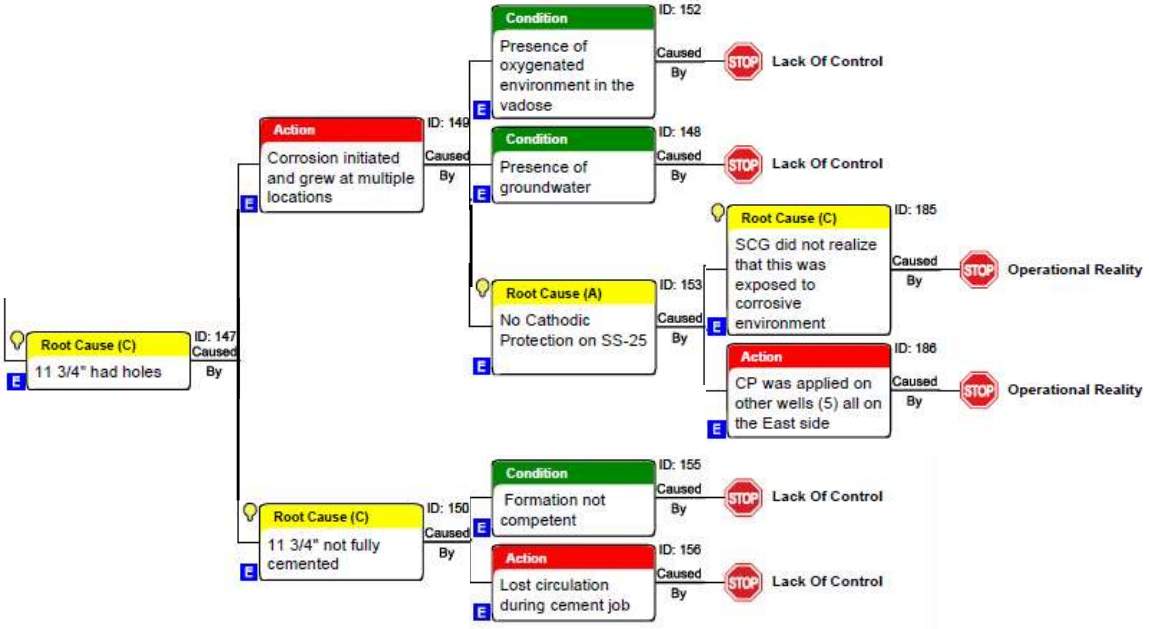


**Figure 163: Causes—Holes in 11 3/4 in. Surface Casing**

The 20 days after the first unsuccessful kill attempt were spent gathering data about the well condition and preparing the site for the subsequent well kill operations. An ice plug in the tubing was found to be at 473 ft. A coil tubing unit was rigged up and used to clear out the plug. Noise, temperature, pressure, and spinner logs were run. Pressure data were recorded. A bridge plug was set in the tubing at 8,393 ft, and holes were punched in the tubing at 8,387 ft to allow circulation down the tubing and into the annulus. Gas continued to flow throughout this time.

At this point the scope of the well-control problem should have been better understood. It was clear that there was a leak in the 7 in. casing at a shallow depth. Gas was flowing from the reservoir up through the 7 in. casing × 2 7/8 in. tubing annulus and then outside of the 7 in. casing at the leak depth. The gas was escaping into the surrounding formation and some was migrating to the surface. The bottomhole

pressure of the reservoir and the tubing and casing pressures at surface were known. Annual flow test data were available for SS-25, and an inflow performance curve could have been generated. These data would have allowed calculation of a reasonable estimate of the gas flow rate.

To kill the well, a column of kill fluid with a hydrostatic pressure higher than the reservoir pressure had to be established in the annulus to stop the gas from flowing; then any gas remaining in the well needed to be displaced out of the well. The height of the column of kill fluid needed would depend on its density. A longer column with a lower density fluid or a shorter column with a higher density fluid would be needed. Kill fluid needed to be pumped down the tubing, out the holes at 8,397 ft, and into the casing where the gas was flowing up the casing. The flowing gas would tend to either blow the kill fluid back up out of the well or dilute it, thereby reducing the fluid density. The right combination of kill fluid density and pump rate and volume would therefore be needed to overcome the effects of the gas flow. Figure 164 shows the well configuration during the top kill attempts.

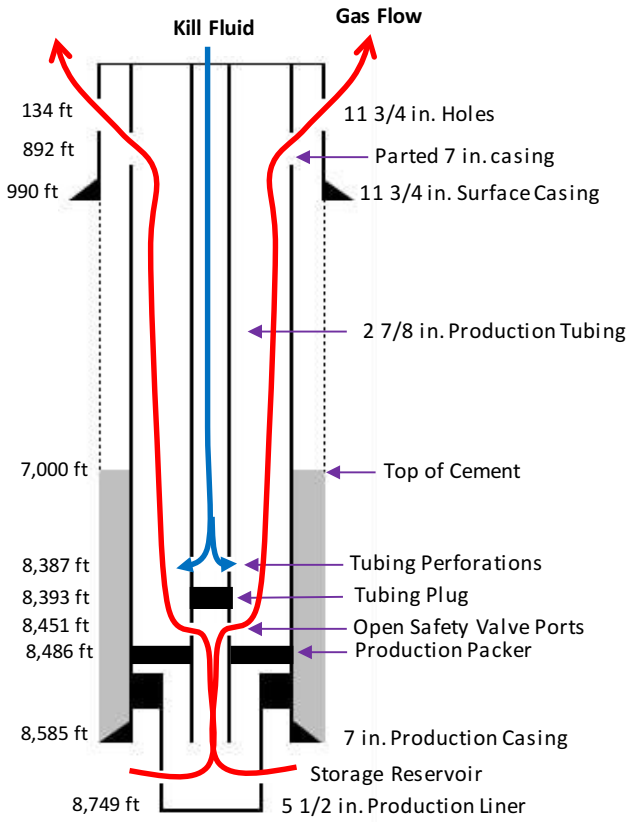


**Figure 164: Top-Kill Well Configuration**

Kill attempts #2 through #6 occurred from November 13 through November 25 and were unsuccessful fundamentally because the pump rates and fluid densities used were insufficient to stop the well from flowing (Figure 165). Various combinations of kill fluid densities and volumes were pumped at various rates without success. Gas, oil, and kill fluid were observed flowing to surface through fissures in the ground, and a large crater began to form around the well. Each kill attempt was a variation of the previous one. It appears that lessons from previously unsuccessful attempts were not applied to refine the future attempts. Gas flow rate leaking from the well appeared to be underestimated, based on later kill modeling. There is no evidence that any kill modeling was done to predict the optimum kill fluid density, volume, and pump rates to design kill operations. Models are estimates and have errors,

depending on how much actual data is available and what assumptions need to be made. However, modeling a well kill is the only way to get a reasonable idea of what would be required to kill the well given the complexity of the fluid and gas flow paths, the high gas flow rate, and the shallow leak depth.

The flow rate data is critical to designing a well kill. For example, during kill attempt #2, the Blade estimated flow rate was 83 MMscf/D. The 9.4 ppg kill density fluid could not kill this well; however, 12 ppg at a flow rate of 9 to 10 bbl/min would have gotten the well under control. There is no documentation to indicate that any modeling or analyses were ever performed for kill attempts #2–6. The decisions appeared to be based on the static reservoir pressure and this would be inadequate and inappropriate for designing kills [3]. SoCalGas-provided information suggested that the well-control company was using 30 MMscf/D as the well flow rate [40]. It is unclear whether this information was ever used in any modeling. Flow rate and kill fluid density have to be designed by using established industry modeling tools before preparing an operational plan to ensure the well is killed.

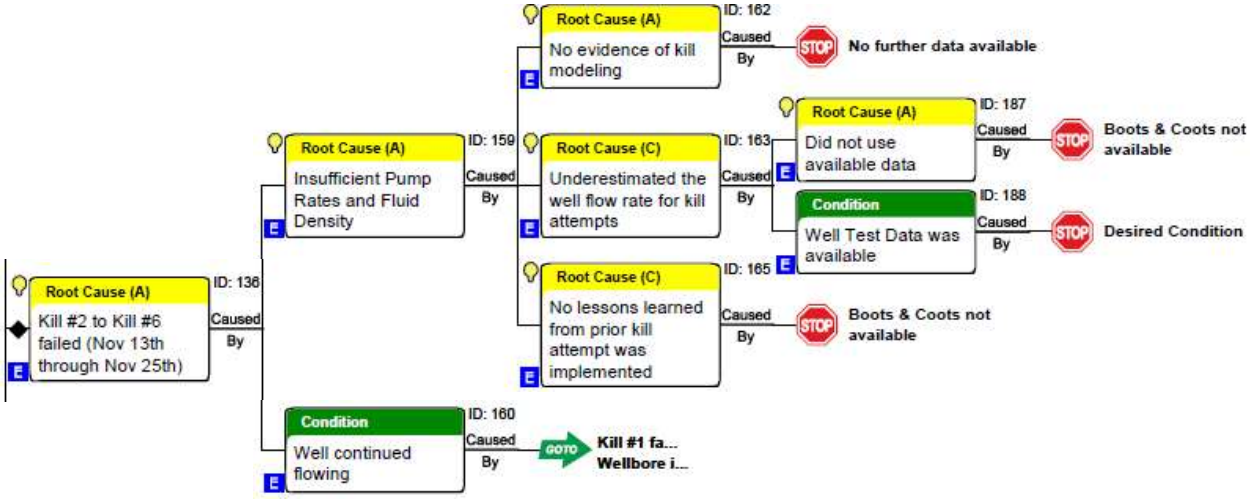


**Figure 165: Causes—Unsuccessful Kill Attempts #2 Through #6**

There is data indicating that the design of kill attempt #7 was modeled ahead of time. The well-control company appeared to assume a gas flow rate of around 25–30 MMscf/D, whereas Blade-estimated flow rate was 60 MMscf/D. However, the annulus pressure dropped to 0 psi for a time indicating that the well had likely been killed, but pumping had to be stopped because of severe vibrations of the wellhead. The wellhead movement caused pumping lines to break off, and operations were stopped to prevent damage to the wellhead itself (Figure 166). The inability to continuously fill the well allowed the production zone to resume flowing. No further attempts were made to top kill the well.

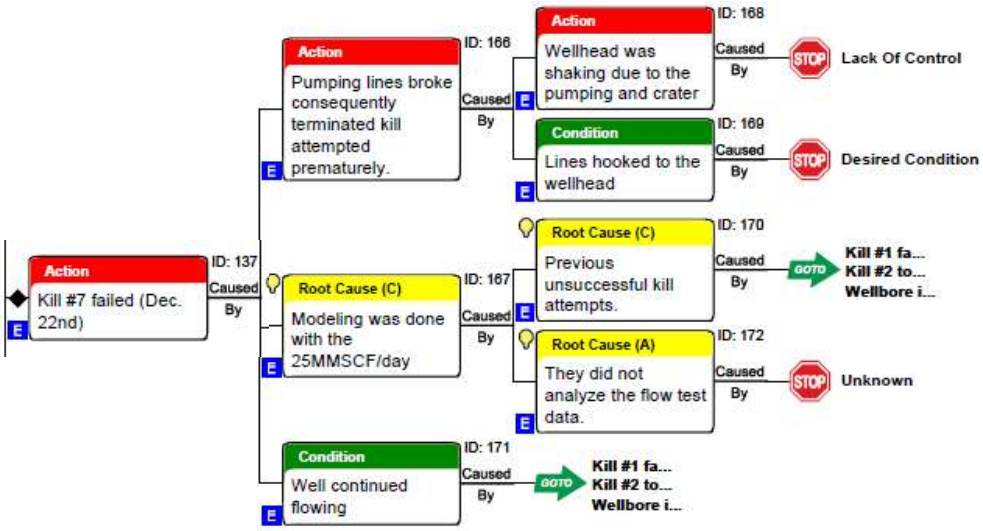


**Figure 166: Causes—Unsuccessful Kill Attempt #7**

The underestimation of the gas flow rate was a deficiency in planning the kill attempts. Flow rate modeling by Add Energy in February 2016 and later by Blade, using the data that were available at the time of the incident, has estimated the gas flow rate to be 80 and 93 MMscf/D, respectively. Records show that the flow rate used for modeling kill attempt #7 was 25 MMscf/D. However, Blade's estimate for kill attempt #7 was a gas flow rate of 60 MMscf/D.

The lack of kill modeling early in the process and the underestimation of the gas flow rate required a number of kill attempts, which resulted in the formation of a large crater around the well. This caused the wellhead and exposed casing to become unstable. The crater became a safety hazard, and the well continued to leak gas to the atmosphere until the well was killed via the relief well in February 2016.

Blade conducted a transient kill simulation study to evaluate the likelihood of success of the actual kill attempts by using the actual field data. According to Blade's modeling, all the SS-25 kill attempts were predicted to be unsuccessful as executed. Kill attempt #7 appeared to be close to killing the well, but it was terminated because of undesirable movement of the wellhead and pump lines that broke during the job.

Furthermore, the simulations showed that a successful kill could have been achieved for all seven kill attempts if 12 ppg or higher density fluid had been pumped at sufficient rates. The required pump rates and pressures were all within the limits of the equipment being used at the time.

The decision to start drilling the relief well was made on November 20, 2015, after four unsuccessful top-kill attempts (Figure 167). The objective of the relief well was to drill down and intersect (i.e., drill into) the SS-25 well at 8,534 ft just below the packer and the top of the 5 1/2 in liner. This would allow kill fluid to be pumped down the P-39A well and into SS-25 near the bottom of the wellbore. The drilling of the P-39A relief well began on December 4, 2015. It took 69 days (74 days including rig up time) to drill down and intersect SS-25. The gas flow was stopped on February 11, 2016, and the well was declared secure on February 18, 2016.

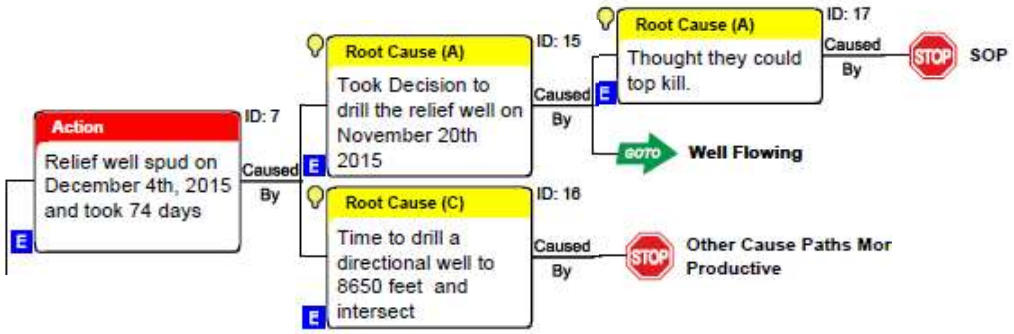


**Figure 167: Causes—Relief Well Drilling**

The top-kill attempts would have been successful if:

- Transient flow modeling of the kill fluid density, pump rates, and pressures had been performed prior to kill attempts #2–6.
- The gas flow rate had been estimated appropriately, which could have been done (1) by using the flow test data and generating the IPR curve, or (2) by using the pressure measurements in the tubing and casing after the well was shut in.

The above observations are supported by the near success of kill attempt #7. The operational issues, such as enlargement of the crater and unstable wellbore, resulted in early termination of kill attempt #7. Proper design and execution of prior kill attempts could have controlled SS-25 earlier.

This suggests that the emergency response plan for this kind of incident was inadequate, and that it was assumed that the routine kill operations were adequate for any scenario (Figure 168). The tubing and casing pressures were measured manually on a weekly basis for all the Aliso Canyon wells. If these pressures had been monitored in real-time with a field surveillance system, then the initial leak in SS-25 would have been detected immediately and injection stopped. This could have prevented the brittle circumferential parting from occurring.

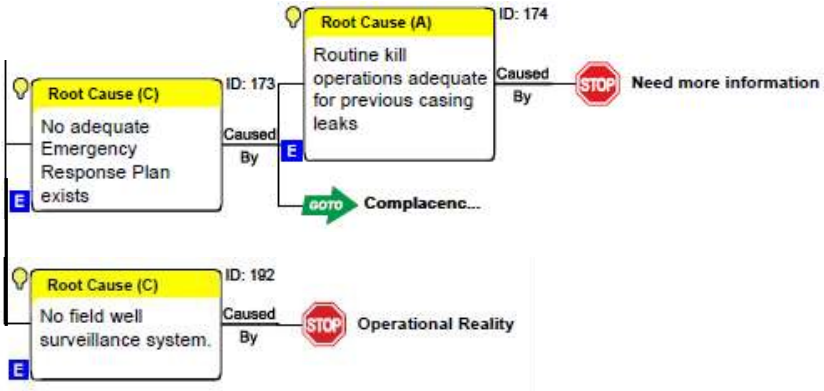


**Figure 168: Causes—Emergency Response Plan and Field Surveillance**

## 5.3 Mitigation Solutions and Root Causes

The ARCA process was taken to completion, and the following solutions and root causes emerged. As discussed previously, the process is highly data-driven and does not have pre-defined causal categories. In

this section, the solutions that the ARCA process identified will be discussed first, and followed by the discussion on root causes.

### 5.3.1 Mitigation Solutions

Twelve solutions were identified that would have mitigated or prevented the primary effect – the uncontrolled release of hydrocarbons for 111 days from SS-25 well.

- **Solution 1: Production Casing Should be Cemented to the Surface**

  Corrosion initiated on the OD of the 7 in. casing because the environment in the annulus around that casing, above 11 3/4 in. casing set at 990 ft, was conducive to corrosion. Cementing the casing to surface changes the environment to one that is not conducive to corrosion, and the cement as a barrier that protects the OD from corrosion.

  This only applies to new wells and not existing wells that may not have originally been cemented to surface. For these wells, the uncemented section needs to be inspected for wall loss and then re-inspected at regular intervals. The fact that there is an uncemented interval does not automatically mean that corrosion will occur, but the casing wall thickness needs to be monitored. The fact that the casing may have wall loss from corrosion also does not automatically mean that the casing is bad or unsafe. Once the amount of wall loss is known, a new burst pressure rating can be calculated to determine whether the well can be safely operated or not. Whether the casing is cemented or not, periodic wall thickness monitoring is a current regulatory requirement [75].

- **Solution 2: Regulations Should Require Wall Thickness Inspections**

  The pre-2015 DOGGR regulations specified a mechanical integrity test program that allowed running a periodic temperature logging tool to meet the regulatory requirements. However, a temperature log does not measure wall thickness. Wall thickness inspections should be included in the mechanical integrity test program since they are a leading indicator of possible casing integrity issues with the wells.

- **Solution 3: Internal Policy Should Require Casing Wall Thickness Inspections**

  SoCalGas's internal well inspection policies should be expanded to include wall thickness inspections. The wells should be prioritized based on risk.

- **Solution 4: A Risk Based Well Integrity Management System Should be Implemented**

  An integrity management system should proactively identify potential problems, determine the associated risks, and then implement actions to prevent the problem from occurring or mitigates the risks. This is similar to the PHMSA required Transmission Integrity Management Program, Distribution Integrity Management Program, and the Storage Integrity Management Program that SoCalGas requested implementation funding for in 2014. Key components of such a system include:

  - A scope that is field-wide.
  - A baseline understanding of well conditions and operating environment.
  - An identification of well integrity risks such as the estimation of corrosion rates and other field wide trends.
  - Well design and operating standards.

- The use of multiple diagnostic methods for integrity testing (e.g., noise, temperature, corrosion inspection, and cement bond logs and pressure tests).
- The establishment of safe operating limits for each well.
- Risk management that evaluates risks and consequences in order to guide well integrity monitoring requirements and development of mitigation plans.
- A data tracking and reporting system.
- Periodic reviews to assess the system effectiveness.

Despite the casing leaks and casing failure history of the Aliso Canyon field, well integrity can be effectively managed with a robust risk management plan that includes probability of failure balanced with consequence of failure. Both aspects have to be addressed, and these wells can be safely operated for a long period of time.

- **Solution 5: Conduct a Casing Corrosion Study**

  Storage wells with good casing and tubing designs can last for long periods and operate safely. Casing corrosion is not uncommon, and its existence does not automatically mean that the casing is going to fail or is unsafe. However, developing an understanding of why corrosion occurs is important for the establishment of corrosion rates and appropriate mitigation plans. The production and surface casing strings should be studied separately. At Aliso Canyon the extent of groundwater and its access to the surface and production casing were not understood before the incident. Detailed investigation, including a study of all forms of corrosion in the field, should be undertaken. The differences in various sectors of the field should be understood and quantified. For example, using cathodic protection should be evaluated for surface casings and applied as needed. Production casings at risk of corrosion should be identified after a detailed assessment of the well design, drilling and completion data, and failure history. Corrosion can be monitored and mitigated. However, the causes and associated risks need to be formally evaluated and understood, and safe operating limits of a well need to be defined.

- **Solution 6: Conduct a Casing Failure Analysis**

  Despite numerous casing failures, no data were provided to indicate that failure causes were investigated. Casing failures need to be formally investigated so that their causes are identified and their implications are understood. Understanding and interpreting failures are critical to defining the propensity or risk of such failures field wide. Such analysis is an important part of any risk assessment. The cause may be straightforward, well specific, and easily mitigated. However, if the cause appears systemic, or the potential consequences are serious, then a more comprehensive investigation is needed to evaluate the potential risks to other wells in the field so that the appropriate mitigation steps are taken. For example, failure investigation of casing OD corrosion in another well might have directed attention to SS-25 and other similar wells. Running an inner string or plugging a well are valid mitigations, but prior to such actions, the cause of the casing leak or failure should be understood. The type of investigation should be commensurate with the risk and consequence of the failure, and should be part of the well integrity management system.

- **Solution 7: Regulations Should Require a Level 1 (Per API RP 585) Analysis of All Failures**

  API RP 585 *Pressure Equipment Integrity Incident Investigation,* discusses failure investigation of pressure equipment. The Aliso Canyon wells are a form of complex pressure vessels. A Level 1 type

analysis of failures, as a minimum requirement, will identify the immediate causes of the failures or near misses and allow operators to understand the implications, if any.

- **Solution 8: Well Specific Detailed Well-control Plan**

  The top-kill attempts were unsuccessful. There were many causes for this that have already been discussed. Every storage well should have the following at a minimum:

  - A well-specific IPR curve. A clear understanding of this deliverability based on pressure.
  - A well specific kill plan based on transient modeling. Plans may be similar; however, a plan should be quantitatively developed for various scenarios (e.g., deep or shallow failure).
  - A relief well plan for each well that considers the surface location and overall approach.

- **Solution 9: Tubing Packer Completion–Dual Barrier System**

  SS-25 was operated so that gas injection and withdrawal was done through the 2 7/8 in. tubing and the 7 in. casing × 2 7/8 in. tubing annulus. As such, the 7 in. casing acted as a single barrier and when it failed, there was nothing behind it to contain the wellbore pressure and fluids. A tubing-packer completion provides two barriers. Gas injection and withdrawal is done only through the tubing. The packer isolates the production casing by tubing annulus from the gas flow. If the tubing fails, the casing acts as a second barrier preventing the wellbore pressure and fluids from escaping the wellbore. This allows the well to be killed and the tubing to be replaced. However, the casing must be designed to withstand the wellbore operating pressures throughout the life of the well.

- **Solution 10: Implement Cathodic Protection as Appropriate**

  Following the corrosion study there should be a good understanding of the groundwater intervals and the associated corrosion risk for existing wells. The surface casings that have inadequate cement isolation should be cathodically protected. This would prevent or stop the shallow corrosion of surface casings that might fail and allow water to enter the surface by production casing annulus causing corrosion on the production casing.

- **Solution 11: Ensure Surface Casings Are Cemented to Surface for New Wells**

  This applies to new wells and is already a regulatory requirement. Surface casing strings are not intended to act as a pressure barrier once the well has been completed. However, a fully cemented surface casing provides protection from corrosion. It will therefore isolate the production casing by surface casing annulus thereby reducing the risk of corrosion on the production casing.

  It is difficult to assess the quality of the surface casing cement on existing wells because the casing is not directly accessible. Wellbore integrity assessments therefore need to focus on the production casing.

- **Solution 12: Well Surveillance Through Surface Pressure (Tubing and Annuli)**

  The lack of real-time pressure measurements prevented the immediate identification of the 7 in. casing failure. The constant monitoring of the tubing, production casing and surface casing pressures will provide better insight into operational deviations in all wells. If this type of system had been installed on SS-25, it would have provided insight into the time of the leak, the opportunity to shut in the well immediately, size of the leak, and the extent of the problem. Furthermore, the information could have used during well-control effort improving the chances of an early success.

Table 42 lists all of the root causes identified during the ARCA process. The twelve solutions discussed address all the root causes. Table 42 also shows which of the solutions have already been addressed by

SoCalGas and by the current DOGGR regulations. Many of the root causes are similar, have been consolidated, and are discussed in detail in Section 5.3.2.

**Table 42: Root Causes and Solutions**

| Root Cause | Solution | Addressed by SoCalGas? | Addressed by Regulation? |
|---|---|---|---|
| • ID78: No corrosion protection<br>• ID83: No cement outside of 7 in. casing<br>• ID116: Bacteria in the "B" annulus water ID35: External corrosion initiated on the 7 in. casing<br>• ID34: External corrosion on 7 in. casing had removed 85% of wall<br>• ID74: 7 in. casing corrosion grew over time | Cement production casing to surface | Unknown (applies to new wells) | Not Required |
| • ID124: No regulations on production casing wall thickness inspection<br>• ID118: No down hole inspection log run on SS-25<br>• ID115: 7 in. casing corrosion not detected<br>• ID34: External corrosion on 7 in. casing had removed 85% of wall<br>• ID74: 7 in. casing corrosion grew over time | Regulations should require casing wall thickness inspection | Yes (Safety Review and SIMP) | Yes (Included in the latest regulations) |
| • ID125: No internal policy on production casing wall thickness inspection<br>• ID118: No down hole inspection log run on SS-25<br>• ID115: 7 in. casing corrosion not detected<br>• ID74:7 in. casing corrosion grew over time<br>• ID34: External corrosion on 7 in. casing had removed 85% of wall | Internal policy should require casing wall thickness inspection | Yes (SIMP) | Not Applicable |
| • ID183: TIMP used, but no SIMP<br>• ID184: Not proactive in managing failures<br>• ID181: No well integrity management in place<br>• ID90: No proactive focus on well integrity<br>• ID102: Reacted and mitigated casing leaks,<br>• ID93: Focus on reservoir and facilities<br>• ID94: Complacency regarding well blowout control<br>• ID126: SS-25 ranked low for production casing inspection<br>• ID128: Only acted on high priority wells<br>• ID89: Probability of the shallow casing rupture not understood<br>• ID87: Severity of a shallow casing rupture not understood<br>• ID80: Did not execute on 1988 memo for SS-25<br>• ID129: No Risk Assessment | Implement a Risk Based Integrity Management Plan | Yes (SIMP) | Yes (Included in the latest regulations) |

| Root Cause | Solution | Addressed by SoCalGas? | Addressed by Regulation? |
|---|---|---|---|
| • ID185: SCG did not realize that this was exposed to corrosive environment<br>• ID102: Reacted and mitigated casing leaks<br>• ID89: Probability of the shallow casing rupture not understood | Conduct casing corrosion study | Unknown (should be part of SIMP) | Yes |
| • ID178: Failure analysis was not considered necessary<br>• ID102: Reacted and mitigated casing leaks<br>• ID108: No failure analysis of any of the prior casing failures<br>• ID184: Not proactive in managing failures<br>• ID89: Probability of the shallow casing rupture not understood | Conduct casing failure analysis | Unknown (should be part of SIMP) | Not Specifically (would be expected to be part of a risk management plan) |
| • ID180: No regulations required failure analysis<br>• ID108: No failure analysis of any of the prior casing failures<br>• ID178: Failure analysis was not considered necessary<br>• ID184: Not proactive in managing failures | Regulations should require a Level 1 (per API 585) analysis of any failure | Not Applicable | Not Specifically |

| Root Cause | Solution | Addressed by SoCalGas? | Addressed by Regulation? |
|---|---|---|---|
| • ID94: Complacency regarding well blowout control<br>• ID187: Did not use available data<br>• ID172: They did not analyze the flow test data<br>• ID141: Fluid had high TCT<br>• ID162: No evidence of kill modeling<br>• ID163: Underestimated the well flow rate for kill attempts<br>• ID3: Unsuccessful top kill attempts<br>• ID165: No lessons learned from prior kill attempt was implemented<br>• ID135: Kill attempt #1 failed October 24, 2015<br>• ID136: Kill attempts #2–6 failed (November 13–25)<br>• ID174: Routine kill operations adequate for previous casing leaks<br>• ID170: Previous unsuccessful kill attempts<br>• ID17: Thought they could top kill<br>• ID159: Insufficient pump rates and fluid density<br>• ID167: Modeling was done with the 25MMscf/D<br>• ID15: Took decision to drill the relief well on November 20, 2015<br>• ID16: Time to drill a directional well to 8650 feet and intersect<br>• ID173: No adequate Emergency Response Plan exists | Well-specific detailed well-control plan | Unknown (should be part of SIMP) | Yes |
| • ID23: Downhole annulus safety system not required by regulations<br>• ID193: 7 in. production casing acted as the single barrier<br>• ID8: No downhole annulus safety system to control the well<br>• ID28: SCG using injection/withdrawal primarily through casing | Tubing packer completion-dual barrier system | Yes | Yes (included in the latest regulations) |
| • ID153: No cathodic protection on SS-25<br>• ID147: 11 3/4 in. had holes | Implement cathodic protection as appropriate | Unknown (should be part of SIMP) | No |
| • ID150: 11 3/4 in. not fully cemented<br>• ID147: 11 3/4 in. had holes | Ensure that the surface casings are fully cemented | Unknown | Yes |

| Root Cause | Solution | Addressed by SoCalGas? | Addressed by Regulation? |
|---|---|---|---|
| • ID163: Underestimated the well flow rate for kill attempts<br>• ID167: Modeling was done with 25MMscf/D<br>• ID192: No field well surveillance system | Well surveillance through surface pressure (tubing plus annuli) | Yes | Yes |

### 5.3.2 Root Causes

The investigation into the SS-25 incident reveals the existence of different causes which can be broadly categorized into two types: Direct causes and Root causes.

- Direct Causes are those that if identified and mitigated, would have prevented the SS-25 incident and would also prevent similar incidents.
- Root Causes are those that if identified and mitigated, would have prevented SS-25 type incidents and other well integrity incidents through the use of procedures, best practices, design, management system, standards, and regulations.

The direct causes for the uncontrolled release of hydrocarbons for 111 days from SS-25 were:

- Axial rupture due to external microbial corrosion on the 7 in. casing OD caused by the groundwater.
  - Groundwater accessed the 11 3/4 in. x 7 in. annulus and provided an environment conducive to microbial corrosion.
  - Carbon dioxide, a component of natural gas, seeped through the 7 in. casing connections and likely was a nutrient for the microbes.
- Unsuccessful top-kills because of insufficient kill fluid density and pump rates.
  - Transient kill modeling was not performed for the first six kill attempts
  - Gas flow rates from the well were not estimated or used in engineering the kill attempts.

The root causes for the uncontrolled release of hydrocarbons for 111 days from SS-25 were:

- The lack of detailed follow-up investigation, failure analyses, or RCA of casing leaks, parted casings, or other failure events in the field in the past. There had been over 60 casing leaks at Aliso Canyon before the SS-25 incident, but no failure investigations were ever conducted. Furthermore, external corrosion on production casing had been identified in several wells. Based on the data reviewed by Blade, no investigation of the causes was performed, and, therefore, the extent and consequences of the corrosion in the other wells were not understood.
- The lack of any form of risk assessment focused on wellbore integrity management. This included assessment of qualitative probability of production casing leaks or failures. By extension, the potential consequences of production casing failures or surface blowouts had not been assessed.
- The lack of a dual mechanical barrier system in the wellbore. The 7 in. OD production casing was the primary barrier to the gas.
- The lack of internal policy or any other regulations that required production casing wall thickness inspections. The existing regulations were inadequate at the time. Annual temperature logging and weekly pressure measurements are adequate to detect leaks and fix them only after an event has

occurred. In SS-25, the corrosion patch was large (around 9.25 in. in length), and due to the microbial nature, there were grooves within the corrosion patch that acted as stress concentration locations. Consequently, when the corrosion region failed, it resulted in a rupture that was about 2 ft long. The trailing indicators of these failures were not adequate to manage the failures. Methodologies such as periodic wall thickness measurements were necessary.

- The lack of a well-specific well-control plan that considered transient kill modeling or well deliverability. There was no quantitative understanding of well deliverability, although data were available, and well-established industry practices existed for such analysis.
- The lack of understanding of groundwater depths relative to the surface casing shoe and production casing, until the two groundwater wells were drilled at SS-9 in 2018.
- The lack of systematic practices of external corrosion protection for surface casing strings. The consequences of corroded surface casing and uncemented production casing were therefore not understood.
- The lack of a real-time, continuous pressure monitoring system for well surveillance. This prevented an immediate identification of the SS-25 leak and accurate estimation of the gas flow rate.

Information about SoCalGas's historical organizational structures and departmental and job function roles and responsibilities was limited. Consequently, the degree to which the organizational structure could have been a cause of the incident could not be evaluated as part of the RCA because of a lack of data and evidence. However, the well histories of 124 gas storage wells, 40% of which had wellbore integrity issues, were analyzed, and the relevant gas storage related operations standards were assessed with respect to wellbore integrity. The integrity procedures were reactive and remained unchanged for decades. They offered no guidance or direction for managing risk or the prevention of well integrity issues. It wasn't until 2014 that the SIMP program, modeled after the TIMP and DIMP programs that went into effect in 2004 and 2006, was proposed to address wellbore integrity concerns. This collectively suggests that the organization was not focused on wellbore integrity, and that the technical and operational resources assigned to addressing wellbore integrity issues were insufficient.

The ISO Technical Specification 16530-1, *Petroleum and Natural Gas Industries - Well Integrity Life Cycle Governance* provides guidance on roles and responsibilities and competencies for well integrity. Four functional roles are discussed—Well Engineering, Production (storage) Operations, Subsurface Engineering (storage/reservoir/geology) and Well Integrity Engineering. The competencies that are listed include: *run and assess corrosion logs, pressure testing, monitor well pressures within envelope, and kill well*.

## 5.4 Interpretation

SS-25 was completed in 1954 as an oil well. The 11 3/4 in surface casing shoe was set at 990 feet. The production casing was cemented up to 7,000 ft. Above 7,000 ft, the production casing annulus contained the drilling fluid that was used while the well was being drilled. SS-25 was completed as a gas-lift oil well, and in 1973 it was converted to an underground gas storage well following a successful pressure test of the 7 in. casing. Injection operations started in the mid-1970s.

Noise and annual temperature logs were run in the SS-25 well, and no anomalous behavior was ever recorded. However, the Aliso Canyon field wells experienced casing leaks, but the causes were never investigated. Some causes identified in the field included connection jump outs and parted casings, but there is no documentation to show that formal or informal investigation was done. In addition, two wells

had underground blowouts from casing leaks: Frew-3 in 1984 and FF-34A in 1990. The wells were successfully killed by pumping down the tubing, but the consequences of a larger leak or a near surface casing rupture was not anticipated until SS-25. These events should have resulted in the development of a formal plan for events with more severe consequences.

In 1988 running a casing wall thickness inspection was recommended for twenty wells based on their deliverability, operational history, and time since last workover. The interoffice memo indicated that all 20 wells would be inspected within two years. SS-25 was on this list but was identified as a low priority. Thirteen of the wells were not inspected including SS-25. Of the seven that were inspected, five had external corrosion on the production casing. Two wells required an inner casing string to be run to isolate the corroding production casing. However, the cause for this corrosion was not investigated. Consequently, any attempt at understanding the potential impact of this issue on a field wide basis was not possible. In addition, had SS-25 been inspected as recommended in the 1988 memo, the external corrosion on the 7 in. casing may have been identified.

Noise and annual temperature logs were run in the gas storage wells to check for casing leaks. These were reactive, trailing indicators of wellbore integrity issues. While they may have been adequate for the detection and mitigation of small leaks, they were inadequate for a leak due to a rupture, such as SS-25's. The limitations of this reactive approach to well integrity management were identified by SoCalGas in 2014 as evidenced by the SIMP proposal in the 2016 General Rate Case submission. OD corrosion on production casing was identified as a threat.

Failure following wall loss due to corrosion would commonly result in a leak incident; however, in SS-25 the size of the corrosion region (9.25 in.) and presence of notches made these corrosion anomalies unique. As the pressure exceeded the burst capacity of the corroded casing, the failure resulted in an axial rupture rather than a leak. Consequently, the traditional method of noise and temperature was inadequate for the SS-25 incident. A leading indicator for rupture could be periodic wall thickness measurements, which are better suited to anticipate and prevent rupture incidents. Noise and temperature logs are adequate for the detection of gas storage reservoir and connection integrity issues but are not suitable for casing integrity.

No records were found that identified the location and nature of the groundwater in and around the SS-25 well site. Consequently, a correlation of the groundwater locations and the depth of surface casing shoes, and an assessment of the potential for surface casing corrosion were not done. The possible corrosion risk to surface casing or production casing was unknown. The corroded surface casing in SS-25 provided an easy pathway for gas to escape to the surface.

Pressures in a conventional oil and gas well reduce over time as it is produced and as the reservoir depletes. Typically, a well experiences the highest pressure on the first day of production. However, the pressure a gas storage well is exposed to is cyclic, and the maximum and minimum pressures are approximately the same year after year. Wellbore integrity therefore remains an issue through a gas storage well's life cycle.

The records indicate that the well was back on injection between 3 and 4 AM on the morning of October 23, 2015. Blade's investigation indicates that the 7 in. casing axial rupture occurred after injection had started that morning. The point in time when the leak started was not known because the well pressures were not monitored in real-time. Stopping the injection to the well immediately may have prevented the cooling at the leak and parting of the 7 in. casing. In addition, immediate availability of information regarding pressures may have provided a prompt understanding of the failure scope.

The SS-25 leak was identified at 3:15 PM on October 23, 2015. SS-25 was shut in at 3:30 PM, and it was realized that the well was still leaking. The estimated flow rate was around 93 MMscf/D after the well was shut in at 3:30 PM and should have been used for designing the well kill.

It appears that the approach to killing the well was based on a static estimation of bottomhole pressure to determine the kill fluid density and concern about pump pressures exceeding the nominal wellhead pressure rating of 5,000 psi. A transient kill model would have revealed that a kill fluid density of 12 ppg or higher at flow rates around 10 bpm would have successfully controlled the well with pump pressures below the wellhead rating. The well could therefore have been top killed earlier. Instead, a variation of the same initial kill attempt was implemented during kill attempts #2–6 with low density kill fluids. Precious time was lost while the location deteriorated with the continued gas flow. External well-control specialists provide necessary experience and expertise; however, underground storage operators should also have personnel with the necessary skills to monitor and manage external specialists, a core skill for the gas storage operator.

Addressing the identified root causes will prevent similar and other well integrity incidents. The SIMP program adopted by SoCalGas and the current DOGGR regulations address most of the root causes. Some of the key changes that have been implemented by SoCalGas include dual barrier, periodic casing wall thickness measurements, well surveillance, and risk assessments.

# 6 Authors

The Blade RCA project was a multi-disciplinary effort that required skills ranging from geology, reservoir, drilling, completion, well control, metallurgy, corrosion to microbiology. This required contributions from many individuals from within Blade Energy Partners and outside.

## Blade Energy Partners (alphabetical order)

Nigel Alvares

Greg Asher

William Bacon

Miodrag Bodganovic

Ismail Ceyhan

Hong Chan

Carol Clayton

Noelle Easter Co

Ming Gao

Ken George

Rudolf Hausler

Shree Krishna

Ravi Krishnamurthy

Ryan Milligan

Randall Rudolf

Eric Sells

Nazia Siddiqui

Jack Soape

Bill Whitney

## Ecolyse

Liz Summer

## GSM Oil Field Services

Jerry Shursen

## Shea Writing & Training Solutions

Marisa Colbert

# 7 Acknowledgements

The Aliso Canyon SS-25 RCA has been a long and complex project which would not have been possible without the support of many individuals and organizations.

We would like to acknowledge CPUC and DOGGR's overall support of Blade's RCA efforts, by facilitating the independence of Blade's investigation, as well as providing guidance for navigating the regulatory, evidentiary and legal requirements. Blade's needs, including operations, data, and witnessing evidence transfer were supported by both CPUC and DOGGR-IT.

We also acknowledge SoCalGas's willing support and cooperation for all aspects of RCA work including providing data for numerous data requests. We also want to acknowledge SoCalGas's support of the independence of this investigation. During the operational phases of the project, Phase I, Phase II, and Phase III, the onsite support at Aliso Canyon was crucial to successful extraction of the tubing and casing. SoCalGas's support for the many complex operational requirements with personnel and other service company resources was essential for a successful investigation.

This RCA project would not have been possible without the unconditional support through the entire period from CPUC, DOGGR, and SoCalGas.

We also acknowledge the more than 23 service companies that provided equipment and expertise for the field operations and services, technical support, data and samples collection, analysis of the downhole data, laboratory testing and analysis, and editorial support.

# 8 References


[1] Southern California Gas Company, "FF-34A Casing Corrosion, Aliso Canyon, Interoffice Correspondence, August 20, 1991, AC_BLD_0033271 (FF-34A Well Documentation from SoCal.pdf, page 183)," 1991.

[2] Southern California Gas Company, "Information Request - 01-28 SIMP.pdf," Chatsworth, 2014.

[3] California Public Utilities Commission, "EUO-06.----------_080818_SEALED.pdf".

[4] Southern California Gas Company, Prepared Direct Testimony, 2008 General Rate Case, "AC_BLD_0008878.pdf," 2007.

[5] Southern California Gas Company, Prepared Direct Testimony, 2012 General Rate Case, "AC_BLD_0009154.pdf," 2011.

[6] Division of Oil, Gas, and Geothermal Resources, "SS-25 Chronology Summary.docx," 2016.

[7] Southern California Gas Company, "Facility Network AC_BLD_0003725".

[8] Southern California Gas Company, SS-25 Well File, "AC_BLD_0000001 - AC_BLD_0001955.pdf," 2016.

[9] Blade Energy Partners, "Phase 1 Summary," 2019.

[10] Blade Energy Partners, "Phase 2 Summary," 2019.

[11] Blade Energy Partners, "SS-25 Phase 3 Tubing, Casing, Wellhead Extraction Protocol (AC-RCA SS25 Phase 3 Tubing Casing Wellhead Extraction Protocol Ver 6 2017-07-14.docx)".

[12] Blade Energy Partners, "Phase 3 Summary Report," 2019.

[13] Blade Energy Partners, "SS-25 Phase 3 Wellsite Tubulars Handling Protocol (AC-RCA Phase 3 Tubulars Handling Protocol Rev 004, 31-July-2017.pdf)".

[14] T. Anderson, Fracture Mechanics, Fundamentals and Applications, 2nd Edition, CRC Press, 2004.

[15] M. Janssen, J. Zuidema and R. Wanhill, Fracture Mechanics, Delft, The Netherlands: VSSD, 2002-2006.

[16] ASM Handbook, Failure Analysis and Prevention, Vol. 11, Materials Park, Ohio, USA: ASM, 2011.

[17] G. M. Boyd, "The Propagation of Fractures in Mild Steel Plates," *Engineering,* vol. 175, no. 16 Jan and 23 Jan, pp. pp 65-69, pp100-102, 1953.

[18] ASM International, Metals Handbook, Volume 12: Fractography (Asm Handbook), ASM, 9th Edition, 1987.

[19] Blade Energy Partners, "SS-25 Casing Failure Analysis," 2019.

[20] SoCalGas, "Temperature Log, Nov 8, 2016, AC_BLD_0018125-AC_BLD_0018136 (SS-25 Completion Profiler Pages.pdf)".

[21] American Petroleum Institute, "Calculating Performance Properties of Pipe Used as Casing or Tubing, API Technical Report 5C3, Seventh Edition, June 2018".

[22] Blade Energy Partners, "SS-25 7 in. Casing Load Analysis," 2019.

[23] Blade Energy Partners, "SS-25 7 in. Speedtite Connection Testing and 11 3/4 in. STC Assessment," 2019.

[24] T. H. Hill and R. C. Money, "Caution: API Gaging Practices Can Be Hazardous To Your Leak

Resistance," Petroleum Engineer International, 1989.

[25] Enertech Engineering and Research Company, "Investigation of Leak Resistance of API 8-Round Connector," 1985.

[26] A. M. Piper, "A Graphic Procedure in the Geochemical Interpretation of Water Analysis," *USGS,* no. 12, 1953.

[27] Geosyntec, Subsurface Assessment Report August 2018, Investigative Order R4-2016-0035, "T10000008175.pdf," 2018.

[28] W. Back and B. B. Hanshaw, Chemical Geohydrology, Washington, D.C.: Geological Survey, U.S. Department of the Interior, 1965.

[29] "CalTopo," [Online]. Available: https://caltopo.com/map.html.

[30] M. Morcillo, B. Chico, J. Alcantara, I. Diaz, R. Wolthuis and D. de la Fuente, "SEM/Micro-Raman Characterization of the Morphologies of Marine Atmospheric Corrosion Products Formed on Mild Steel," *Journal of The Electrochemical Society,* vol. 163, no. 8, pp. C426-C439, 2016.

[31] J. Alcantara, B. Chico, D. Diaz, D. de la Fuente and M. Morcillo, "Airborne Chloride Deposit and Its Effect on Marine Atmospheric Corrosion of Mild Steel," *Corrosion Science,* vol. 97, pp. 74-88, 2015.

[32] M. Morcillo, D. de la Fuente, I. Diaz and y. H. Cano, "Atmospheric Corrosion of Mild Steel," *Revista de Metalurgia,* vol. 47, no. 5, pp. 426-444, 2011.

[33] M. Ueda and H. Takabe, "Effect of Environmental Factor and Microstructure on Morphology of Corrosion Products in CO2 Environments," in *Corrosion*, San Antonio, TX, 1999.

[34] Blade Energy Partners, "SS-25 Analysis of Microbial Organisms on 7 in. Production Casing," Houston, TX, 2019.

[35] M. Siegart, M. D. Yates, D. F. Call, X. Zhu, A. Spormann and B. E. Logan, "Comparison of Nonprecious Metal Cathode Materials for Methane Production by Electromethanogenesis," *ACS Sustain Chem Eng,* vol. 2, no. 4, pp. 910-917, 2014.

[36] H. T. Dinh, J. Kuever, M. Mußmann, A. W. Hassel, M. Stratmann and F. Widdel, "Iron Corrosion by Novel Anaerobic Microorganisms," *Nature,* vol. 427, pp. 829-32, 2004.

[37] T. J. Tidwell, R. De Paula, Z. Broussard and V. V. Keasler, "Mitigation of Severe Pitting Corrosion Caused by MIC in a CDC Biofilm Reactor," in *NACE-2017-9604*, 2017.

[38] T. Zhang, H. H. Fang and B. C. KO, "Methanogen Population in a Marine Biofilm Corrosive to Mild Steel," *Appl Microbiol Biotechnol.,* vol. 63, no. 1, pp. 101-6, 2003.

[39] Southern California Gas Company, "Blade-Follow Up Request_82918_1.pdf," Chatsworth, 2018.

[40] Southern California Gas Company, Supplemental Response to Question 2 of the December 23, 2015 Information Request, "DOGGR -1_Supp Response Q2_ 122815.docx," 2015.

[41] Blade Energy Partners, "SS-25 Nodal Analysis with Uncontrolled Leak Estimation," Houston, TX, 2019.

[42] Blade Energy Partners, "Aliso Canyon Injection Network Deliverability Analysis prior to Uncontrolled Leak," Houston, TX, 2019.

[43] S. Schweikert, J. Wolfersdorf, M. Selzer and H. Hald, "Experimental Investigation on Velocity and Temperature Distributions of Turbulent Cross Flows over Transpiration Cooled C/C Wall Segments," in *5th European Conference for Aeronautics and Space Sciences (EUCASS)*, Munich, 2013.

[44] W. Dahmen, T. Gotzen, S. Muller and M. Rom, "Numerical Simulation of Transpiration Cooling

through Porous Material," *International Journal for Numerical Methods in Fluids,* vol. 76, no. 6, pp. 331-365, 2014.

[45] Blade Energy Partners, "Analysis of the Post-Failure Gas Pathway and Temperature Anomalies at the SS-25 site," 2019.

[46] Blade Energy Partners, "SS-25 Transient Well Kill Analysis," 2019.

[47] Blade Energy Partners, "Analysis of Aliso Canyon Gas Storage Wells with Casing Failures," 2019.

[48] S. Conley, G. Franco, I. Faloona, J. Peischl and D. R. Blake, "Methane Emissions from the 2015 Aliso Canyon Blowout in Los Angeles, CA," *Science,* 25 Feb 2016.

[49] California Air Resources Board, "Determination of Total Methane Emissions from the Aliso Canyon Natural Gas Leak Incident," 21 10 2016. [Online]. Available: https://www.arb.ca.gov/research/aliso_canyon/aliso_canyon_methane_emissions-arb_final.pdf.

[50] Southern California Gas Company, "C039 Blade-02 Supplemental 31516.docx," Chatsworth, 2016.

[51] Southern California Gas Company, "AC_BLD_0075728.pdf," Chatsworth, 2018.

[52] Southern California Gas Company, "Workover Recommendation, Interoffice Correspondence, S., January 9, 1984, AC_BLD_0037665 (P-50A Well History File From SoCalGas.pdf, page 70)," 1984.

[53] Southern California Gas Company, "Investigation of Various Leakage Indications at Aliso Canyon, Interoffice Correspondence, May 22, 1987, AC_BLD_0037626-AC_BLD_0037627 (P-50A Well History File from SoCalGas.pdf, pages 31-32)," 1987.

[54] Division of Oil, Gas, and Geothermal Resources, "History of Oil or Gas Well, Frew 4 September 8, 1988 (Frew-4 03700667 Data_03-20-08.pdf, pages 102-103)".

[55] Southern California Gas Company, "Aliso Canyon - Porter 44 and Standard Sesnon 5 - Second Remedial Operations under G.W.O. 97904-69, Interoffice Correspondence, November 25, 1977, AC_BLD_0121176, AC_BLD_0121177, AC_BLD_0121180".

[56] Southern California Gas Company, *Response to Blade RCA Data Request February 18, 2018 Blade-28.pdf.*

[57] Southern California Gas Company, "Candidate Wells for Casing Inspection, Aliso Canyon Field, Interoffice Correspondence, August 30, 1988 AC_CPUC_0000064-AC_CPUC_0000066 (SS-25 Well Documentation (from SoCalGas)_N.pdf, pages 42-44)," 1988.

[58] Southern California Gas Company, "Candidate Wells for Casing Inspection, Aliso Canyon Field, Interoffice Correspondence, September 2, 1988, AC_CPUC_0000063 (SS-25 Well Documentation (from SoCalGas)_N.pdf, page 41)," 1988.

[59] Blade Energy Partners, "Review of the 1988 Candidate Wells for Casing Inspection," 2019.

[60] Division of Oil, Gas, and Geothermal Resources, "Order To Take Specified Action Re: Aliso Canyon Gas Storage Facility, Order 1109," Sacramento, 2016.

[61] Southern California Gas Company, Response Dated March 12, 2018, "Blade-31.pdf," Chatsworth, 2018.

[62] American Petroleum Institute, "API RP 1171, Functional Integrity of Natural Gas Storage in Depleted Hydrocarbon Reservoirs and Aquifer Reservoirs," Washington, DC, September 2015.

[63] Southern California Gas Company, "Southern CA Gas Report 02.15.19.pdf," Chatsworth, 2019.

[64] Division of Oil, Gas, and Geothermal Resources, "Well Search," [Online]. Available: https://secure.conservation.ca.gov/WellSearch/.

[65] Southern California Gas Company, ""P-50A Well History File from SoCalGas", AC_BLD_0038075–AC_BLD_0038080," Chatsworth, 2016.

[66] State of California, *California Statutes & Regulations for the Division of Oil, Gas, & Geothermal Resources,* 2015.

[67] Division of Oil, Gas, and Geothermal Resources, *ISC Agenda Minutes (2006 ISC Minutes 2006-05-17 GS MIT highlights.pdf),* Santa Maria, California, 2006.

[68] Southern California Gas Company, *Response to proposed amendment to Section 1724.10 (j) and (j)(1), August 22, 1994, to DOGGR (AC_BLD_0124127 - 124128.pdf).*

[69] Southern California Gas Company, "SoCalGas Response Dated April 19, 2019 (Blade-37.pdf)".

[70] Division of Oil, Gas, and Geothermal Resources, "15-Day Public Re-notice of Proposed Rulemaking, May 24, 1995 (AC_BLD_0124129 - 124196.pdf)".

[71] Federal Task Force, "Ensuring Safe and Reliable Underground Natural Gas Storage, Final Report of the Interagency Task Force on Natural Gas Storage Safety," October 2015.

[72] Division of Oil, Gas, and Geothermal Resources, "Gas Storage Project Approval Letter, (SoCalGas GasStorage Project Approval Letter July 26 1989.pdf)".

[73] Southern California Gas Company, "AC_BLD_0026360.pdf," Chatsworth, 2014.

[74] State of California, *California Statutes & Regulations for the Division of Oil, Gas, & Geothermal Resources,* November 2018.

[75] State of California, *California Statutes & Regulations for the Division of Oil, Gas, & Geothermal Resources,* January 2019.

[76] Southern California Gas Company, "Blade-35 Response Files 18 Dec 2018.pdf".

[77] Blade Energy Partners, "SS-25 Annular Flow Safety System Review," 2019.

[78] Southern California Gas Company, "Aliso Canyon Safety Plan (May 2014) - SoCalGas," [Online]. Available: http://www.socalgas.com/documents/safety/aliso-canyon-safety-plan-2014.pdf. [Accessed 26 January 2016].

[79] Southern California Gas Company, Natural Gas System, Operator Safety Plan, "AC_BLD_0011388.pdf," Chatsworth, 2013.

[80] Southern California Gas Company, "AC_BLD_0022648," Chatsworth, 2014.

[81] Southern California Gas Company, "Aliso Canyon Field Annual Review Meeting with the Division of Oil and Gas, 1989," [Online]. Available: ftp://ftp.consrv.ca.gov/pub/oil/Underground%20Gas%20Storage/UGS887Disclosure/AlisoCanyon/0100006/Project%20Reviews/1989%20ALISO%20MEETING%20NOTES.pdf. [Accessed 28 November 2018].

[82] Southern California Gas Company, "AC_BLD_0026308.pdf," Chatsworth, 2012.

# Appendix A SoCalGas Operations Standards

Table 43 shows the SoCalGas Operations Standards related to gas storage wells. Listed are the names of the SoCalGas Operations Standards, document number, and published dates. The language is verbatim from the original content. All of the standards in this table were provided by SoCalGas to Blade, CPUC, and DOGGR through data requests; the file names are in the Reference column. Ten operations standards were related to gas storage wells. The Operations Standards in rows 2 and 10 titled, *Operation of Underground Storage Wells*, and *Gas Inventory - Monitoring, Verification and Reporting*, respectively, will be discussed in Section A.1 and Section A.2.

**Table 43: SoCalGas Operations Standards Related to Gas Storage Wells**

| Row | Company Operations Standard Name | SCG Number | Published Date | Reference |
|---|---|---|---|---|
| 1 | Testing Surface Controlled Subsurface Safety Valve | 224.0000 | February 21, 2014 | AC_BLD_0026280.pdf |
| 2 | Operation of Underground Storage Wells | 224.02 | February 10, 2012 | AC_BLD_0026308.pdf |
| 3 | Blowout Prevention Equipment Configuration, Installation, Testing and Operation | 224.05 | July 29, 2013 | AC_BLD_0026335.pdf |
| 4 | Security and Accounting - Underground Storage Field Production Fluids | 224.0015 | February 5, 2013 | AC_BLD_0026292.pdf |
| 5 | Gas Inventory Verification - Shut In | 224.0020 | March 5, 2014 | AC_BLD_0026301.pdf |
| 6 | Wireline Operations - Wellhead Preparation, Rig-Up and Rig-Down | 224.023 | January 28, 2014 | AC_BLD_0026315.pdf |
| 7 | Well Operations - Well Kill | 224.0030 | February 22, 2011 | AC_BLD_0026303.pdf |
| 8 | Routine Well Kills | 224.045 | August 18, 2014 | AC_BLD_0026325.pdf |
| 9 | Well Operations - Unload and Clean Up | 224.055 | February 25, 2014 | AC_BLD_0026270.pdf |
| 10 | Gas Inventory - Monitoring, Verification and Reporting | 224.070 | November 10, 2014 | AC_BLD_0026360.pdf |

Table 44 shows a select listing of SoCalGas Operations Standards related to inspections, investigations, and integrity [78] [79]. The language is verbatim from the original content. This is not an exhaustive list but rather a selection showing that SoCalGas did have policies (i.e., Operations Standards) related to inspection, investigation, and integrity. We performed a cursory review of these standards and found a robust proactive framework for pipeline integrity. One example of this is in row 8, *Investigation of Failures on Distribution and Transmission Pipeline Facilities* [80], where the purpose of the document was to determine the cause of the pipeline failure and prevent reoccurrence. There was specific guidance on soil and liquid samples to collect, which lab or analysis center to use, what follow-up actions were required, and how long to retain investigation reports. Such guidance was not found in our review of the Gas Storage Operations Standards (Table 43).

*None* of the Operations Standards listed in Table 44 pertain to gas storage wells but instead to pipelines and valves. Proactive procedures for pipeline integrity were clearly visible, whereas well integrity procedures were absent. Our interpretation is that SoCalGas was more focused on surface assets than on downhole assets.

**Table 44: SoCalGas Operations Standards Related to Inspections, Investigations, and Integrity [78] [79]**

| Row | Company Operations Standard Name | SCG Number | Published Date |
|---|---|---|---|
| 1 | In-Line Inspection Surveys Standard | 167.022 | May 23, 2012 |
| 2 | Inspection of Pipelines on Bridges and Spans | 184.12 | December 9, 2013 |
| 3 | Leak Investigation - Distribution | 184.0245 | November 4, 2013 |
| 4 | Investigate Measurement and Regulation Problems - Medium, Large and Above - Standard Pressures MSAs | 185.0342 | March 18, 2014 |
| 5 | Cathodic Protection - Inspection of Exposed Pipe | 186.02 | March 5, 2014 |
| 6 | Investigation of Accidents and Pipeline Failures | 191.01 | November 6, 2012 |
| 7 | Valve Inspections and Maintenance Self-Audit | 203.017 | October 12, 2012 |
| 8 | Investigation of Failures on Distribution and Transmission Pipeline Facilities | 223.003 | October 18, 2012 |
| 9 | Pressure Vessel Inspection | 223.0045 | September 18, 2009 |
| 10 | Pipeline Patrol and Unstable Earth Inspections | 223.0065 | December 12, 2013 |
| 11 | External and Internal Transmission Pipeline Inspection | 223.0095 | October 24, 2012 |
| 12 | Self-Audit Guidelines - Pipeline Integrity Program | 167.0125 | July 27, 2012 |
| 13 | Assessment of Pipeline Integrity Using Guided Wave UT | 167.024 | October 21, 2013 |
| 14 | Leakage Surveys | 223.01 | January 16, 2014 |

## A.1 SCG 224.070: Gas Inventory - Monitoring, Verification and Reporting

The Operations Standard titled Gas Inventory - Monitoring, Verification and Reporting [73] was a key document. It has procedures for:

- Monitoring to confirm the injected gas remained in the storage zone.
- Estimating the gas inventory in the storage zone.
- Reporting gas inventory losses.

Table 45 is a summary of our interpretation of the monitoring requirements of the Storage Zone wells. We focused on the monitoring components of this document because they are related to well integrity.

**Table 45: Monitoring of Storage Zone Wells**

| Monitoring Component | Time Interval | Details |
|---|---|---|
| Storage zone wells—performance review of individual wells and the field | Not explicitly stated: interpreted to be once every two years | • Back pressure curve shifts, changes in deliverability, individual well and reservoir tests, and field performance are investigated. |

| Monitoring Component | Time Interval | Details |
|---|---|---|
| Tubing, production casing × tubing annulus, surface casing × production casing annulus | Weekly readings and plots with monthly reports to DOGGR | • Surface casing × production casing annulus pressure is abnormal when it is high enough to force gas into normally pressured water sands at the shoe or other known surface casing holes or leaks.<br>• Zero pressure is abnormal if that well had a history of annular pressure.<br>• Take diagnostic steps to determine the source of pressure buildup.<br>• Note blowdowns (i.e., bleeding off the annulus pressure) if they occur. |
| Wellhead inspections | Monthly | • Report and correct leaks from wellhead flanges and valves. |
| Subsurface temperature surveys | Annually | • Surveys are done in accordance with DOGGR regulations.<br>• Wells that are killed are not exempt.<br>• Additional surveys will be run if unusual well conditions occur, such as anomalous pressure, surface gas emissions, or other well problems.<br>• Wireline retrievable tubing obstructions are to be removed for temperature surveys.<br>• Ideally, surveys are conducted at high reservoir pressures when shoe leaks are most noticeable.<br>• To investigate anomalies, additional surveys are made such as temperature surveys, noise logs, spinner surveys, and radioactive tracer surveys.<br>• For well casing leaks above the shoe, radioactive tracer surveys are typically used to verify the location of the leak. Additional surveys are used to verify that the leak exists and quantify the leakage rate. |

Figure 169 shows the Summary of the Aliso Canyon Monitoring Plan for Storage Zone Wells from the SoCalGas Annual Review Meeting with DOGGR, 1989 [81]. The components and frequency of the monitoring plan are listed. Industry technology has evolved for real time pressure, temperature, flow, and vibration (noise) monitoring but, surprisingly, there were *no* significant differences in the monitoring plan from 1989 compared to the 2014 SCG 224.070 Operations Standard.

The monitoring program was successful in identifying casing integrity issues, though. Most of the historical casing failures in the Aliso Canyon Field, presented in Historical Casing Failures (Section 4.2), were identified by the program.

These documents fail to mention casing inspection logs, pressure testing wells, real time pressure monitoring, investigation of leaks, and RCA.

TABLE 5
SUMMARY OF THE ALISO CANYON MONITORING PLAN

STORAGE ZONE WELLS

| | ITEM | MINIMUM FREQUENCY OF DATA COLLECTION | PRIMARY RESPONSIBILITY | COMMENTS |
|---|---|---|---|---|
| 1. | Flow tests | Annual | Resident Reservoir Engineer | All wells are flow tested for sand, production and back-pressure curves annually. |
| 2. | Wellhead pressures (including surface casing and annular pressures) | Weekly | Station | Copies to Staff. |
| 3. | Plot of surface casing annular pressures | Weekly | Resident Reservoir Engineer | To be reviewed twice yearly with Underground Storage Staff. |
| 4. | Wellhead inspections | Monthly | Station | To be reported to Underground Storage Staff on daily activity report whenever leakage is found. |
| 5. | Temperature surveys | Annual | Resident Reservoir Engineer | Copies to Staff. |
| 6. | Noise logs | As needed | Resident Reservoir Engineer | Copies maintained in Division and Underground Storage files. |
| 7. | Tracer surveys | As needed | Resident Reservoir Engineer Staff will normally assist | A detailed explanation of methods and results to be prepared by Resident for each well. Copy sent to Underground Storage Staff. |
| 8. | Neutron logs | As needed | Underground Storage Staff | Copy to Division. |
| 9. | Reservoir shut-ins | Annual | Senior Petroleum Engineer | Hysteresis curve and isobaric maps to be updated by Underground Storage Staff. |
| 10. | Annular blowdown | As needed | Resident Reservoir Engineer | To recommend and implement annular blowdown tests and programs to determine corrective action needed, and to prevent fracture of primary cement at surface string shoe. |
| 11. | Annular helium samples | Annual | Engineering Test Center | To monitor gas content in the annular. |

**Figure 169: Summary of Aliso Canyon Monitoring Plan, Storage Zone Wells, 1989 [81]**

## A.2 SCG 224.02: Operation of Underground Storage Wells

The Operations Standard SCG 224.02: Operation of Underground Storage Wells [82] details the following:

- Well signage requirements
- Semi-annual testing and inspection of the following surface safety devices:
  - Automatic fail-close valves
  - High-low pressure sensors (to shut-in the well at high or low pressure conditions)
  - Fire detecting fusible plugs
  - Remote shut-in controls
  - Sacrificial sand probes (to shut-in the well in the case of excessive sand production)
- Wellhead valve configuration
- Critical well criteria and testing and inspection of critical well safety devices
- Record keeping requirements

Figure 170 shows the Well Safety Systems from the Annual Review Meeting with DOGGR, 1989 [81]. The components and frequency of the monitoring plan are listed. There are no significant differences in the monitoring plan from 1989 compared to the SCG 224.02 Operation Standard. There is guidance that if a sacrificial probe should fail, the cause of the failure should be diagnosed and corrected prior to returning the well to service. Like the Gas Inventory – Monitoring, Verification and Reporting Operations Standard, the Operation of Underground Storage Wells Operation Standard [82] fails to mention casing inspection logs, pressure testing wells, investigation of leaks, and RCA.

WELL SAFETY SYSTEMS

All wells at Aliso Canyon are equipped with surface safety systems that are designed to shut the well in to prevent loss of gas and oil in the event of damage to surface piping. The surface safety system consists of fail-close pneumatic operated gate valves that are closed by any of the following:

1. Low pressure pilot - shuts well in if a break in the piping causes pressure to drop below 300 psi.

2. High pressure pilot - shuts well in if pressure in withdrawal line exceeds 710 psi.

3. Sacrificial sand erosion probe - shuts well in if sand erosion wears hole in thin walled probe.

4. Fusible plug - shuts well in if a fire occurs in well cellar.

5. Remote shutdown station - allows well to be shut in manually from no closer than 150 feet away from wellhead.

All surface safety systems are tested twice a year.

**Figure 170: Summary of Aliso Canyon Well Safety Systems, 1989 [81]**

## A.3 SoCalGas Policy Summary

SoCalGas's policies are found in the Company Operation Standards. We reviewed the Gas Storage related Operations Standards in detail and compared them to the Pipeline Integrity Operations Standards. The latter contain proactive, modern, and robust procedures—a stark contrast to the Gas Storage Operations Standards, which contain reactive procedures and offer no guidance for the prevention of reoccurrence of well integrity issues; these Operations Standards hadn't changed in decades. Our interpretation is that SoCalGas was responsible for creating and implementing the monitoring program, and DOGGR had to approve the program and make the data available for review.

# Appendix B RealityCharting Root Cause Analysis Flowchart

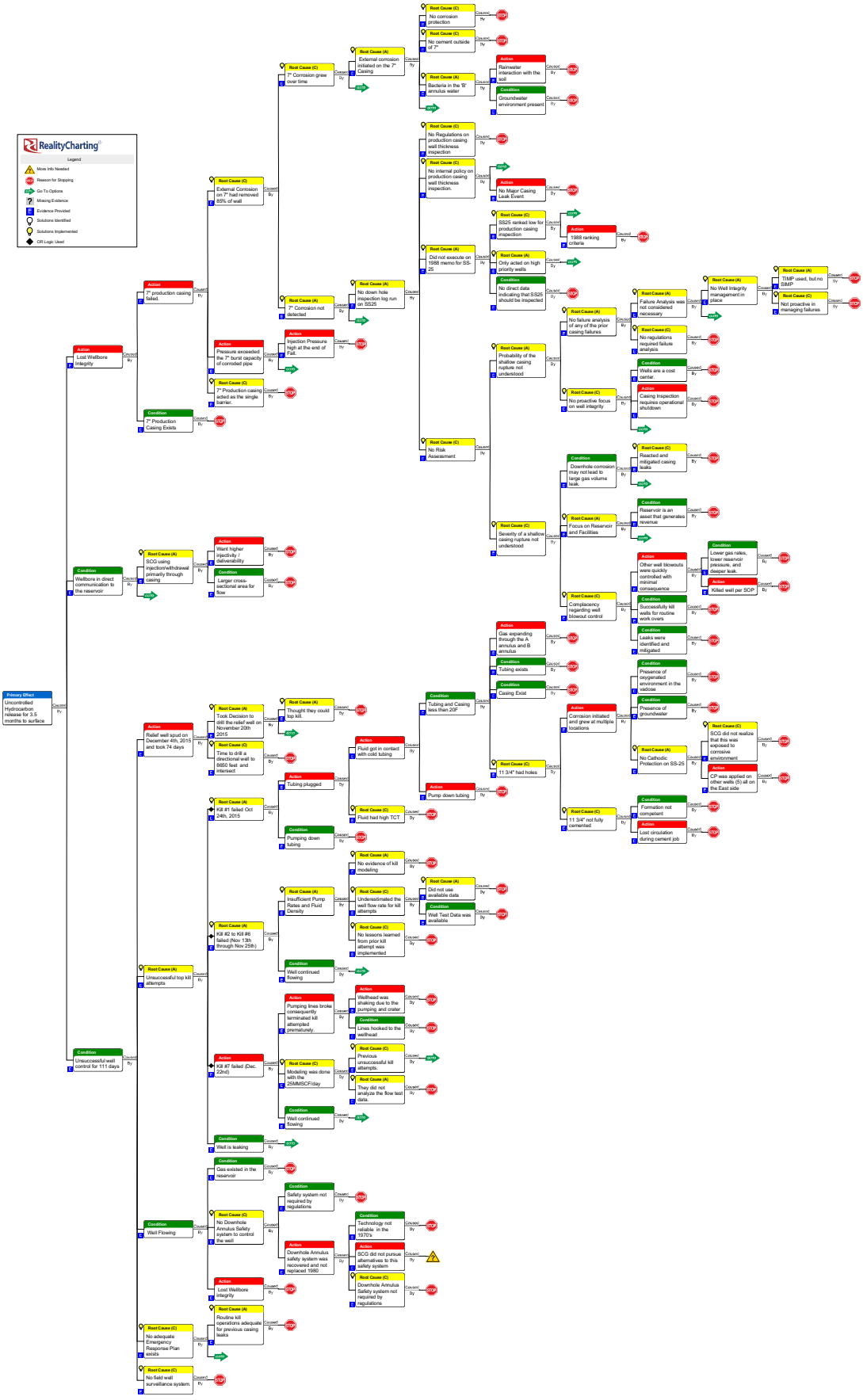
RealityCharting
Legend
More Info Needed
Reason for Stopping
Go To Options
Missing Evidence
Evidence Provided
Solutions Identified
Solutions Implemented
OR-Logic Used
Primary Effect
Uncontrolled Hydrocarbon release for 3.5 months to surface
Caused By
Condition
Unsuccessful well control for 111 days
Condition
Lost Wellbore Integrity
Condition
Wellbore in direct communication to the reservoir
Condition
Well Flowing
Root Cause (C)
No adequate Emergency Response Plan exists
Root Cause (C)
No field well surveillance system.
Unsuccessful top kill attempts
Relief well spud on December 4th, 2015 and took 74 days
Root Cause (A)
Took Decision to drill the relief well on November 20th 2015
Root Cause (C)
Time to drill a directional well to 8650 feet and intersect
Kill #1 failed Oct 24th, 2015
Pumping down tubing
Root Cause (A)
Thought they could No kill.
Root Cause (C)
Fluid had high TCT
Action
Fluid got in contact with cold tubing
Action
Tubing plugged
Kill #2 to Kill #6 failed (Nov 13th through Nov 25th)
Root Cause (A)
Insufficient Pump Rates and Fluid Density
Root Cause (A)
No evidence of kill modeling
Root Cause (C)
Underestimated the well flow rate for kill attempts
Root Cause (C)
No lessons learned from prior kill attempt was implemented
Root Cause (A)
Did not use available data
Condition
Well Test Data was available
Condition
Well continued flowing
Kill #7 failed (Dec. 23rd)
Action
Pumping lines broke consequently terminated kill attempted prematurely.
Root Cause (C)
Modeling was done with the 2MMSCF/day
Action
Wellhead was shaking due to the pumping and crater
Condition
Lines hooked to the wellhead
Root Cause (C)
Previous unsuccessful kill attempts.
Root Cause (A)
They did not analyze the flow test data.
Condition
Well continued flowing
Condition
Well is leaking
Condition
Gas existed in the reservoir
Condition
Safety system not required by regulations
Action
Downhole Annulus safety system was recovered and not replaced 1980
Condition
Technology not reliable in the 1970's
Action
SCG did not pursue alternatives to this safety system
Root Cause (C)
Downhole Annulus Safety system not required by regulations
Action
Lost Wellbore Integrity
Root Cause (A)
Routine kill operations adequate for previous casing leaks
Root Cause (C)
No Downhole Annulus Safety system to control the well
Action
Lost Wellbore Integrity
Root Cause (A)
Routine kill operations adequate for previous casing leaks
Action
7" production casing failed.
Condition
7" Production Casing Exists
Root Cause (A)
SCG using injection/withdrawal primarily through casing
Action
Want higher injectivity / deliverability
Condition
Larger cross-sectional area for flow
Root Cause (C)
External Corrosion on 7" had removed 85% of wall
Action
Pressure exceeded the 7" burst capacity of corroded pipe
Root Cause (C)
7" Production casing acted as the single barrier.
Root Cause (C)
7" Corrosion grew over time
Root Cause (A)
7" Corrosion not detected
Root Cause (A)
No down hole inspection log run on SS25
Action
Injection Pressure high at the end of Fall.
Root Cause (A)
External corrosion initiated on the 7" Casing
Root Cause (A)
Bacteria in the 'S' annulus water
Action
Rainwater interaction with the soil
Condition
Groundwater environment present
Root Cause (C)
No corrosion protection
Root Cause (C)
No cement outside of 7"
Root Cause (C)
No Regulations on production casing wall thickness inspection
Root Cause (C)
No internal policy on production casing wall thickness inspection.
Action
No Major Casing Leak Event
Root Cause (A)
Did not execute on 1998 memo for SS-25
Root Cause (C)
SS25 ranked low for production casing inspection
Action
1988 ranking criteria
Root Cause (A)
Only acted on high priority wells
Condition
No direct data indicating that SS25 should be inspected
Root Cause (C)
No Risk Assessement
Root Cause (A)
Probability of the shallow casing rupture not understood
Root Cause (C)
Severity of a shallow casing rupture not understood
Root Cause (A)
No failure analysis of any of the prior casing failures
Root Cause (C)
No proactive focus on well integrity
Root Cause (A)
Failure Analysis was not considered necessary
Root Cause (C)
No regulations required failure analysis
Root Cause (A)
No Well Integrity management in place
Root Cause (A)
TIMP used, but no SMYP
Root Cause (C)
Not proactive in managing failures
Condition
Wells are a cost center.
Action
Casing Inspection requires operational shutdown
Condition
Downhole corrosion may not lead to large gas volume leak.
Root Cause (A)
Focus on Reservoir and Facilities
Root Cause (C)
Reacted and mitigated casing leaks
Condition
Reservoir is an asset that generates revenue
Root Cause (C)
Complacency regarding well blowout control
Action
Other well blowouts were quickly controlled with minimal consequence
Condition
Lower gas rates, lower reservoir pressure, and deeper leak.
Action
Killed well per SOP
Condition
Successfully kill wells for routine work overs
Condition
Leaks were identified and mitigated
Action
Gas expanding through the A annulus and B annulus
Condition
Tubing exists
Condition
Casing Exist
Root Cause (C)
11 3/4" had holes
Action
Pump down tubing
Condition
Tubing and Casing less than 20F
Action
Corrosion initiated and grew at multiple locations
Root Cause (C)
11 3/4" not fully cemented
Condition
Presence of oxygenated environment in the vadose
Condition
Presence of groundwater
Root Cause (A)
No Cathodic Protection on SS-25
Root Cause (C)
SCG did not realize that this was exposed to corrosive environment
Action
CP was applied on other wells (5) all on the East side
Condition
Formation not competent
Action
Lost circulation during cement job

# Appendix C Abbreviations and Acronyms

| Term | Definition |
|---|---|
| AB FL4S | Atlas Bradford Flushline Quadraseal |
| AMSL | Above Mean Sea Level |
| AOI | Area of Interest |
| API | American Petroleum Institute |
| ARCA | Apollo Root Cause Analysis |
| at% | Atomic Percent |
| BCF | Billion Cubic Feet |
| Blade | Blade Energy Partners |
| Bscf | Billion Standard Cubic Feet |
| BTC | Buttress Thread Casing |
| CARB | California Air Resources Board |
| CHDT | Cased Hole Dynamics Tester |
| CP | Cathodic Protection |
| CPUC | California Public Utilities Commission |
| CVN | Charpy V-Notch |
| DFDI | Ductile Failure Damage Indicator |
| DFE | Derrick Floor Elevation |
| DIMP | Distribution Integrity Management Program |
| DOGGR | Division of Oil, Gas, and Geothermal Resources |
| EDS | Energy Dispersive Spectroscopy |
| F | Frew |
| FBHP | Flowing Bottomhole Pressure |
| FE | Finite Element |
| FEA | Finite Element Analysis |
| FF | Fernando Fee |
| FIB | Focused Ion Beam |
| FJ | Flush Joint |
| FMI | Formation Micro Imager |
| GAP | General Allocation Program |
| GRC | General Rate Case |
| GTC | General Terms and Conditions |
| HHP | Hydraulic Horsepower |
| HRVRT | High Resolution Vertilog |
| IBC | Isolation Scanner |
| IPR | Inflow Performance Relationship |

| Term | Definition |
|---|---|
| JSN | Joint Sequence Number |
| LCM | Lost Circulation Material |
| LIDAR | Light Detection and Ranging |
| LTC | Long Thread Casing |
| mg/L | Milligrams Per Liter |
| MID | Magnetic Imaging Defectoscope |
| MIT | Mechanical Integrity Test |
| MMscf/D | Million Standard Cubic Feet per Day |
| MMstb | Million Standard Barrels |
| MPI | Magnetic Particle Inspection |
| MVC | Microvoid Coalescence |
| MVRT | Micro Vertilog Tool |
| Mcf/D | Thousand Cubic Feet per Day |
| MnS | Manganese Sulfide |
| NDE | Nondestructive Evaluation |
| NMR | Nuclear Magnetic Resonance |
| NOV | National Oilwell Varco |
| OD | Outside Diameter |
| OGR | Oil-to-Gas Ratio |
| P | Porter |
| P&A | Plug and Abandon |
| PHMSA | Pipeline and Hazardous Materials Safety Administration |
| ppf | Pounds Per Foot |
| ppg | Pounds Per Gallon |
| PROSPER | Production and Systems Performance |
| PS | Porter Sesnon |
| qPCR | Quantitative Polymerase Chain Reaction |
| RCA | Root Cause Analysis |
| SCCM | Standard Cubic Centimeters per Minute |
| SEM | Scanning Electron Microscope |
| SIMP | Storage Integrity Management Plan |
| scf/D | Standard Cubic Feet per Day |
| SS | Standard Sesnon |
| STC | Short Thread Casing |
| SoCalGas | Southern California Gas Company |
| T&C | Threaded and Coupled |
| TCT | True Crystallization Temperature |

| Term | Definition |
|---|---|
| TH | Test Hole |
| THMN_RF | Minimum of Unflagged Thickness |
| TIMP | Transmission Integrity Management Program |
| UIC | Underground Injection Control |
| USIT | UltraSonic Imager Tool |
| WBM | Water-Based Mud |
| WGR | Water-to-Gas Ratio |
| WHP | Wellhead Pressure |
| WSO | Water Shut-Off |
| XRD | X-Ray Diffraction |